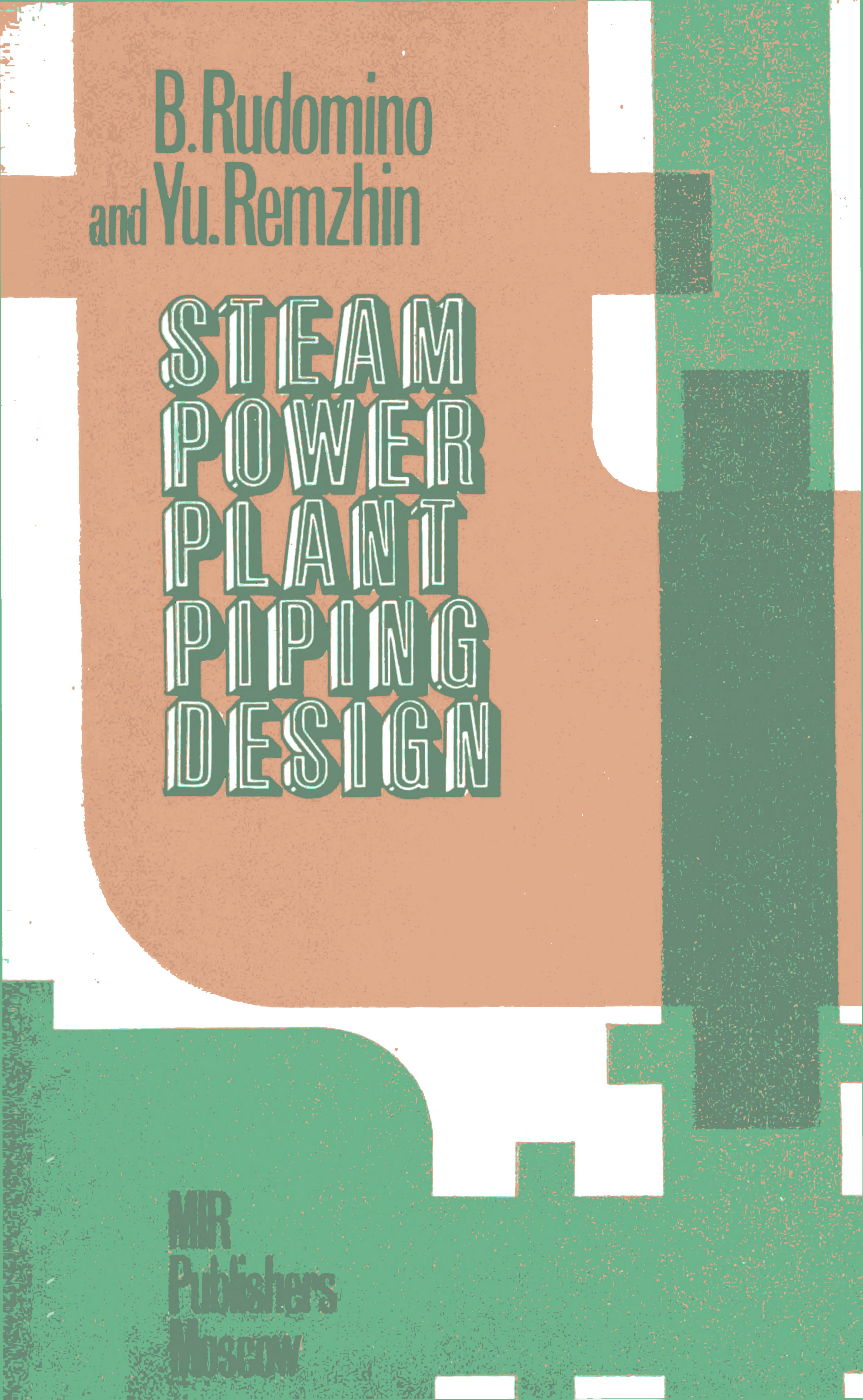

B. Rudomino
and Yu. Remzhin

STEAM POWER PLANT PIPING DESIGN

MIR
Publishers
Moscow

STEAM POWER PLANT PIPING DESIGN

Mir Publishers of Moscow publish Soviet scientific and technical literature in sixteen languages—English, German, French, Italian, Spanish, Portuguese, Czech, Slovak, Serbo-Croat, Hungarian, Mongolian, Arabic, Persian (Farsi), Hindi, Bengal and Tamil. Titles include textbooks for higher technical schools and vocational schools, literature on the natural sciences and medicine, as well as textbooks for medical schools, popular science and science fiction.

The contributors to Mir Publishers' list are leading Soviet scientists and engineers in all fields of science and technology and include more than 40 Members and Corresponding Members of the USSR Academy of Sciences. Skilled translators provide a high standard of translation from the original Russian. Many of the titles already issued by Mir Publishers have been adopted as textbooks and manuals at educational establishments in France, Switzerland, Cuba, Egypt, India, and many other countries.

Mir Publishers' books in foreign languages are exported by V/O "Mezhdunarodnaya Kniga" and can be purchased or ordered through booksellers in your country dealing with V/O "Mezhdunarodnaya Kniga".

Б. В. РУДОМИНО
Ю. Н. РЕМЖИН

ПРОЕКТИРОВАНИЕ ТРУБОПРОВОДОВ ТЕПЛОВЫХ ЭЛЕКТРОСТАНЦИЙ

«ЭНЕРГИЯ»
Ленинградское
отделение

ИЗДАТЕЛЬСТВО
МИР

B. Rudomino
and Yu. Remzhin

STEAM POWER PLANT PIPING DESIGN

Translated from the Russian by
Prem Kumar Dang

Mir Publishers
Moscow

First published 1979

Revised from the 1970 Russian edition

The Russian Alphabet and Transliteration

А а	a	К к	k	Х х	kh
Б б	b	Л л	l	Ц ц	ts
В в	v	М м	m	Ч ч	ch
Г г	g	Н н	n	Ш ш	sh
Д д	d	О о	o	Щ щ	shch
Е е	e	П п	p	Ъ ъ	''
Ё ё	e	Р р	r	Ы ы	y
Ж ж	zh	С с	s	Ь ь	'
З з	z	Т т	t	Э э	e
И и	i	У у	u	Ю ю	yu
Й й	y	Ф ф	f	Я я	ya

The Greek Alphabet

Α α	Alpha	Ι ι	Iota	Ρ ρ	Rho
Β β	Beta	Κ ϰ	Kappa	Σ σ	Sigma
Γ γ	Gamma	Λ λ	Lambda	Τ τ	Tau
Δ δ	Delta	Μ μ	Mu	Υ ϑ	Upsilon
Ε ε	Epsilon	Ν ν	Nu	Φ φ	Phi
Ζ ζ	Zeta	Ξ ξ	Xi	Χ χ	Chi
Η η	Eta	Ο ο	Omicron	Ψ ψ	Psi
Θ θ	Theta	Π π	Pi	Ω ω	Omega

На английском языке

© «Энергия» Ленинградское отделение, 1970

© English translation, Mir Publishers, 1979

Contents

Foreword 7

Chapter One
Piping Layout and Design 9

1.1. Piping Project Design 9

1.2. Layout and Design 12

1.3. Drainage of Pipelines 20

1.4. Pipeline Supports 24

1.5. Application of Pipe Fittings 35

Chapter Two
Hydrodynamic Calculations and Selection of Pipe Diameter 40

2.1. General Information and Formulas 40

2.2. Resistance Coefficients 51

2.3. Hydrodynamic Calculations of Pipelines for Small Specific Volume Changes 59

2.4. Hydrodynamic Calculations of Pipes with Large Steam Specific Volume Variations 66

2.5. Hydrodynamic Calculations of Boiling Water and High-Pressure Saturated Steam Pipelines 88

2.6. Selection of the Most Rational Pipe Size 106

Chapter Three
Pipeline Structural Calculations 117

3.1. General 117

3.2. Basic Properties of Steels Used for Power Station Pipelines 121

3.3. Wall Thickness Calculations 128

3.4. Calculation for Combined Action of Internal Pressure and Additional External Loads 132

3.5. Self-Elongation of Pipelines 138

3.6. Check Calculation of Stresses Caused by Compensating for Thermal Elongations 143

3.7. Flexure in Curved Pipes and Equivalent Stress Ranges 149
3.8. Check Calculation of Elbows for Cyclic Stress Ranges . . 161
3.9. Hydrodynamic Forces in Pipelines 172

Chapter Four
Pipeline Thermal Elongation Compensation and Its Calculation

4.1. Methods of Compensating Thermal Elongations 176
4.2. Self-Compensation Problem and Methods of Its Solution 177
4.3. Coordinate System and Determination of Displacements to Be Compensated 180
4.4. General Theory of Pipeline Calculation for Self-Compensation 186
4.5. Determination of Bending Moments Due to Weight Load 196
4.6. Methods of Calculating Pipelines for Self-Compensation 200
4.7. Bellows-Type Expansion Joints and Their Use as Axial Expansion Joints 215
4.8. Compensation of Pipelines Through the Use of Bellows-Type Expansion Joints as Elastic Hinges 222
4.9. Use of Electronic Digital Computing Machines for Calculating Self-Compensation of Pipelines 230
4.10. Criterion for Calculating the Compensating Capacity of Pipelines 234

Appendices 237
Index 269

Foreword

During the last decade Soviet heat-power engineering has progressed significantly not only in increasing the total and unit capacities of power plants, but also in improving the thermodynamic cycle by using intermediate superheating and raising the initial parameters of the heat cycle. Concurrent with this, the piping layouts have also changed: on the one hand, they have become simpler owing to the change-over to unit systems, but, on the other hand, more complicated because of the use of superheating. The increased steam parameters have required the use of new grades of steel with improved long-term strength at elevated temperatures and especially thick-walled pipes which, in turn, has made it necessary to improve the piping design methods.

Nowadays, strength calculations of pipelines should be made as stipulated by "The Standard Procedures to Calculate Steam Boiler Elements for Strength" [3-1]. Piping design accords with industrial branch standards (OCT) and interbranch standards (MBH) which cover piping elements, fastenings and remote control devices. These standards make it possible to manufacture piping elements on a mass scale despite the fact that the actual piping design work is carried out by different design bodies. They also eliminate the need to describe in detail the methods of calculating for strength various piping elements and fastenings, thus enabling one to restrict oneself to the general principles of strength calculations, the knowledge of which is essential for a piping designer.

The advent of digital computers has considerably improved the piping design. At present, calculations of self-compensating pipelines are made by using computers. Computers have influenced much the piping design, for they have made it possible to calculate complex piping systems with movable inflection points and several anchor points, whose application was previously avoided because of the difficulties in designing them.

Being a special subject computer calculation techniques and programming are outside the scope of this book.

Here we only outline the general theory of computer-aided design of self-compensating pipelines, the knowledge of which is essential for the piping design engineer. In addition, an approximate, simpler calculation procedure assuring adequate accuracy is described. It is suggested that in designing self-compensating pipelines, the deformations of bent ovalled elbows under the action of internal pressure be taken into account, for they may significantly affect the calculation results.

At present, wide application have found sharply bent thin-walled elbows which must be checked for the maximum stress variation range lest they should develop fatigue cracks. Methods for determining the stress variation ranges are described in this book and allowable values given.

A new method is proposed to calculate thermal expansion compensation for pipelines using bellows-type expansion joints as hinges. Along with hydrodynamic calculations for usual pressure drops, methods for calculating piping with large variations in specific volumes are discussed. These methods are necessary to select correctly the size of exhaust pipes and blow-off lines, to calculate the discharge rate of pipelines at large pressure drops, and to analyse the emergency operating conditions under which piping may have to work.

The section dealing with the choice of an economical piping size has been thoroughly revised in accordance with the present-day technical and economic calculation methods used in power engineering.

This book is mainly for engineers engaged in the design of thermal power stations. It may also be used as a textbook for students specializing in steam power plants.

The need for the present edition was long felt, as a book of similar content [3-12] was last published about 20 years ago.

Chapter One

Piping Layout and Design

1.1. Piping Project Design

Piping project design begins with the working out of a draft piping layout on the basis of a detailed heat flow diagram. Questions relating to the use of stand-by equipment (boilers, pumps, etc.) and pipelines to replace the units shut down for repairs are decided upon in the course of the piping layout elaboration. In the last 10-20 years the heat flow diagrams of power plants have become more complex because of the use of intermediate superheating, adoption of higher steam pressures and temperatures, increased unit capacities, improved regenerative cycles, inclusion of turbo-feed pumps in the main turbine cycle, etc.

At the same time the layouts of condensing steam power plants have been considerably simplified by dropping stand-by boilers and pipelines, and by equipping the plants with separate power units not interconnected through main lines.

A considerable improvement in piping reliability has been attained by avoiding flange joints and using flangeless fittings on high-pressure lines, and by improving welding processes and weld inspection methods. This has made it possible to use a single-line feed water piping, without any stand-by pipelines, even for box-header boilers. In modern practice multiline pipings are used only when a single pipeline of maximum size proves incapable of handling the required flow.

Figure 1.1 shows the main steam line layout of a K-200-130 unit in which provision is made for two lines of nominal size $D_n = 250$ mm for fresh steam and six lines of nominal size $D_n = 400$ mm for reheat steam (two lines to the boiler and four from the boiler to the turbine). Heating and power plants, especially those supplying steam for industrial

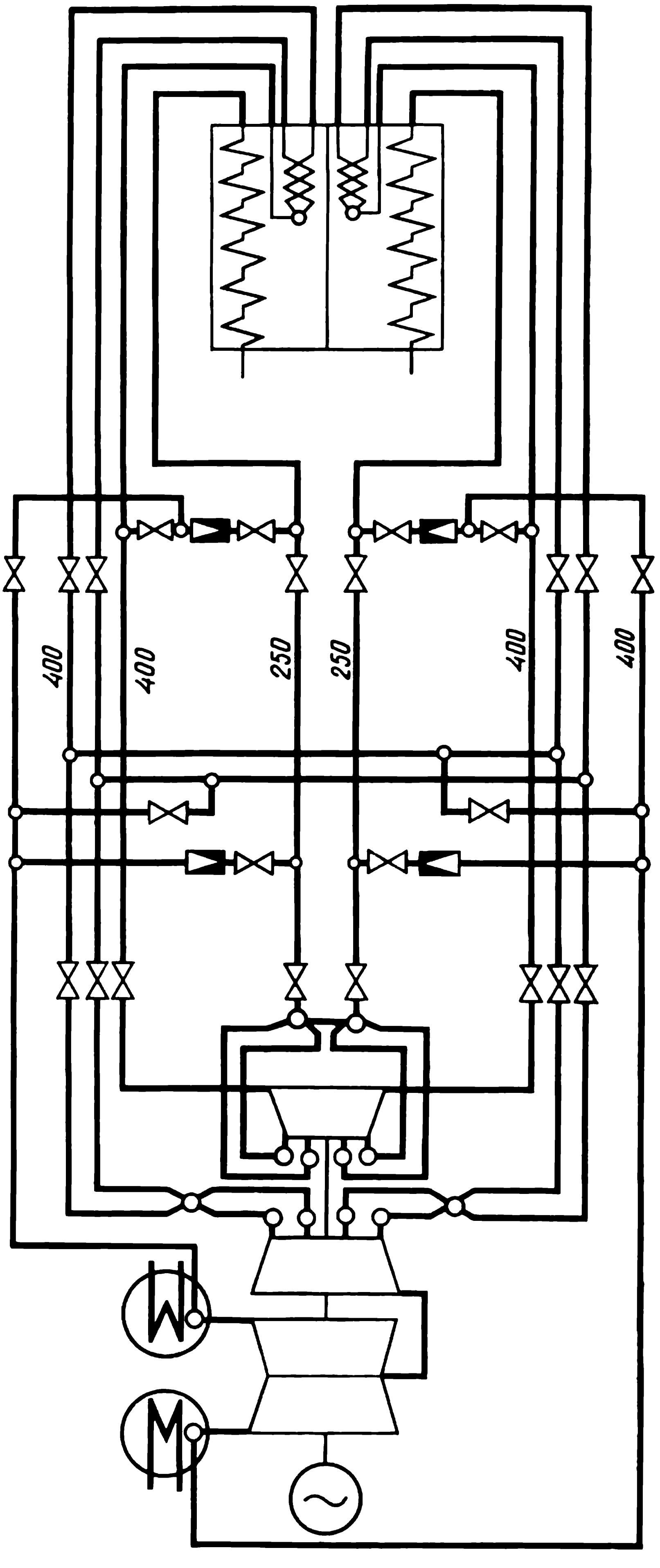

Fig. 1.1. Main steam line diagram of 200-MW unit

purposes, use stand-by boilers. In this case the main steam lines, feedwater lines and condensate lines are equipped with a crossover connection. Such a main steam line layout for a heating and power plant is shown in Fig. 1.2. On disconnecting the boiler-turbine steam lines from the crossover connection, the system changes to a unit-built type,

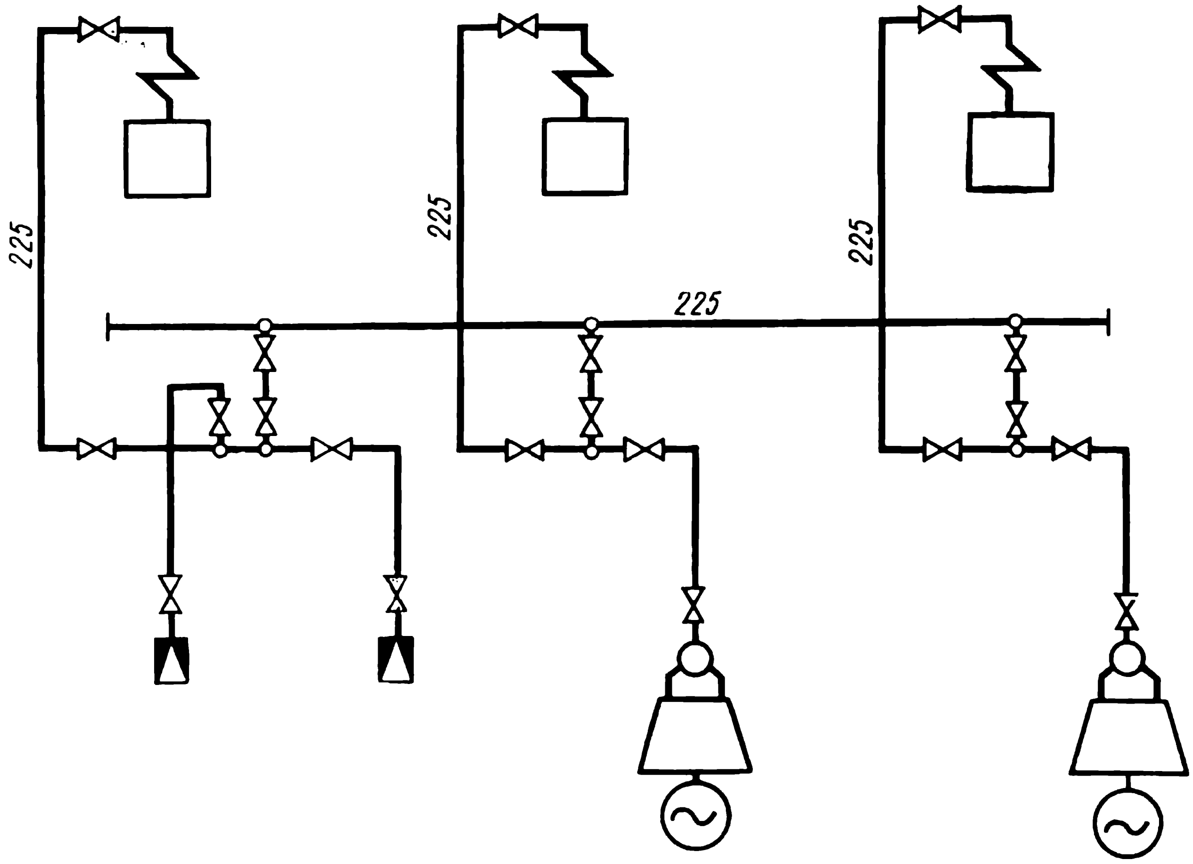

Fig. 1.2. Schematic of steam lines at heat-and-power unit with a cross connector

thus providing for the required redundancy and enabling one to repair the crossover connection. Other sections of the piping system are repaired at the same time as the equipment they serve. To ensure safety, the layout provides for not less than two stop valves to disconnect each piece of the equipment from the pressure lines in case of repair.

High-pressure (more than 22 kg/cm^2) and low-pressure pipings are designed separately. Such a division is dictated by the supply and erection conditions. The design is carried out in accordance with the OCT and MBH standards for the manufacture of the individual components and units of pipelines. The design high-pressure piping plan embraces fresh steam lines, reheat-steam lines, feedwater lines and auxiliary high-pressure pipelines. The low-pressure piping plan involves the following piping assemblies: extraction lines, including steam-supply lines for deaerators, and metered bleed lines; main condensate lines; station tank-system lines; chemically treated water lines; drainage discharge and overflow lines; circulating-water lines; cooling-water systems for bearings and mechanisms; lubrication lines; fuel-oil lines; fuel-gas lines; ash-sluicing systems; compressed air piping; hydrogen, oxygen and acetylene piping systems, and others.

Approximately 50% of the total design and planning work on the thermal and mechanical equipment of a power plant is taken up by the piping. The design and planning of a piping system includes the following stages: (1) working out of a rational piping schematic diagram which would ensure reliable operation of the equipment, its automatic control, starting and heating up; (2) selection of standardized pipe sizes on the basis of technical and economic calculations; (3) elaboration of the piping layout, selection of a thermal expansion compensation system and positioning of anchored and movable fastenings; (4) compilation of·tasks for calculating self-compensating pipelines and spring fastening; (5) computer-aided calculations; (6) analysis of the computerized calculation results; (7) hydrodynamic calculations; (8) development of blow-off and drainage piping systems; (9) breaking down of the piping system into standard factory-supplied units and piping components, with allowances required for welding bosses and nozzles, preparation of working drawings for non-standard components; (10) design of fastenings; (11) design of thermal insulation.

If the calculation results for self-compensating pipelines prove unsatisfactory, the piping layout should be corrected and check calculations made on a computer. The working drawings of the high-pressure units are generally prepared by the manufacturer.

1.2. Layout and Design

The piping layout is predetermined mainly by the arrangement of equipment in the main power-plant building. The arrangement of the equipment, the coordinates of the connecting branch pipes and nozzles of power units and heat exchangers serve as the starting point for elaborating the piping layout versions. Lately, the tendency to select the most convenient and shortest routes for the most important lines has had an ever increasing bearing on the equipment arrangement in the main building. It applies, in particular, to the reheat-steam lines, as it is necessary to ensure a minimum pressure drop in them, and to the main steam lines, because their cost is high. That is why turbines are located with their axes across the machine hall as this reduces the length of the main steam lines compared to the lengths required if the axes were placed longitudinally.

The unit boiler-turbine systems are essential for high-capacity power units with intermediate superheating. The elimination of cross connections between the unit boiler-turbine systems has simplified the piping layout diagrams and alleviated layout problems. At the same time other difficulties arose due to the necessity of routing a large number of boiler-to-turbine steam lines (main and intermediate superheat). For routing boiler-to-turbine pipelines of a 300 MW unit a frontal width of 24 metres is necessary.

At heating and power plants using cross connections a special corridor is provided at the hopper-deaerator level for cross-connection pipelines (main steam cross-over valves, feed-water valves and others) and cross connectors to be mounted. Generally the turbo-sets are arranged longitudinally in the main machine hall. This arrangement provides better compensation of pipelines between the fixed anchor points in the corridor up to the turbine stop valve. Of late, recourse is taken to transverse location of turbo-sets as it is more convenient for the main hall layout.

In general, it should be noted that in a well arranged main hall layout due consideration is always paid to the convenient routing of most important pipelines. This, in particular, applies to the location of feed pumps, economizers, deaerators. Before making a piping layout the economical pipe diameters should be determined. In some cases, final selection of pipe diameters is possible only after the piping route is selected which determines the overall hydrodynamic resistance coefficient for the piping system being designed. In the further examination of layout problems we shall assume the pipe diameter as determined. When developing the piping layout the pipeline routes are indicated with the thermal expansion compensatory methods, location and types of anchors location of fittings, type and location of drives for accessories, slopes of pipes, condensate and air removal points, drainage system, positions and dimensions of service platforms.

A well thoughtover layout should ensure: easy erection, possibly using large units; convenient servicing and repair; good thermal expansion compensation; minimum hydraulic resistance; minimum weight; simple and convenient fastenings; good drainage; accessories of the same type; absence of cast elbows and non-standard components; possibility of plant expansion without piping modification with a minimum shutdown time of earlier installed units for connecting reassembled piping systems.

In certain cases it is difficult to fulfil all the requirements and the task of a piping designer is to find optimum solutions which would satisfy to the maximum extent all given requirements. The modern unit power plants considerably ease the problem. We shall discuss in detail some of the above mentioned requirements.

Primarily, the following operations should be borne in mind, such as: heating, connection and disconnection of pipes, inspection of fittings and maintenance of its packing glands. The fittings should be located at places readily accessible for operation, review, maintenance and repair. The most preferable location of the equipment is on the main working floors of the building.

In case the equipment is located at places inaccessible for direct maintenance from the working levels, then remote controls should be provided for operators at convenient places. Platforms should be designed for inspection and repair of such equipment. Devices for hanging pulley blocks should be provided over the location of heavy equipment.

Steam pipelines at 450°C and above require periodic checking for metal creep rate, condition of welded seams and should be laid at places where their diameters can be easily measured. The main routes of such pipelines should be located at ceiling floors of the building. Service platforms should be provided for the sections of high temperature pipes running at high levels (for example, section from the steam gate valve of the boiler up to the columns of the boiler house).

The pipeline route and the location of rigid anchors should be sufficiently flexible so that self-compensation stresses, forces and moments transmitted by the pipelines to the equipment do not exceed permissible values.

First of all the intrinsic flexibility of a pipe should be used when laying it along its actual path. The flexibility of a pipeline may be increased by artificially lengthening shoulders, by providing additional bends or by cutting in U-shaped expansion joints but only when sufficient thermal expansion compensation is not achieved by placing rigid anchors in the most rational way or by discarding superfluous supports along its actual path. It should be borne in mind that artificial lengthening of a pipeline entails an increase in pipeline's weight and pressure losses.

A simple method to increase the flexibility of a pipeline route and to decrease the forces and moments transmitted to the rigid anchors is to avoid the excessive use of rigid anchors. Objections to such a decision could be: increased pipeline displacements and the consequent difficulties with spring suspensions and increased tendency of a pipeline to vibrate. In such cases different variants of anchors, which limit displacement in one or the other direction, should be examined.

For low pressure pipelines temperature compensation may be achieved by the use of bellows-type expansion joints. These compensators are very effective in hinged diagrams.

The following must be observed to achieve minimum hydrodynamic losses in a pipeline of a given diameter: (a) avoid superfluous bends; use a straight track so that track length and bend angles may be reduced (Fig. 1.3*a*); (b) install tee joints so that the main stream passes straight through the joint (Fig. 1.3*b*); (c) do not use valves of constricting diameter as they have a high resistance coefficient. If such valves are used, straight runs of pipes are necessary before and after the valve (distance of 10-12 diameters before and of 5 diameters after the valve) to avoid abrupt increases of hydrodynamic losses in excess of the value accounted for by the valve resistance coefficient; (d) for high flow rates in pump pressure pipings (up to 5-7 m/sec) a large diameter reducer should be installed immediately after the piping and then a return valve and a gate valve (Fig. 1.3*c*); (e) do not use tee joints as alternatives to elbows, as is sometimes done, when it is necessary to have a rigid anchor close to the bend; (f) when branching a pipe into two pipes of smaller diameter the tee joint size should be assumed equal to the diameter of the supply line.

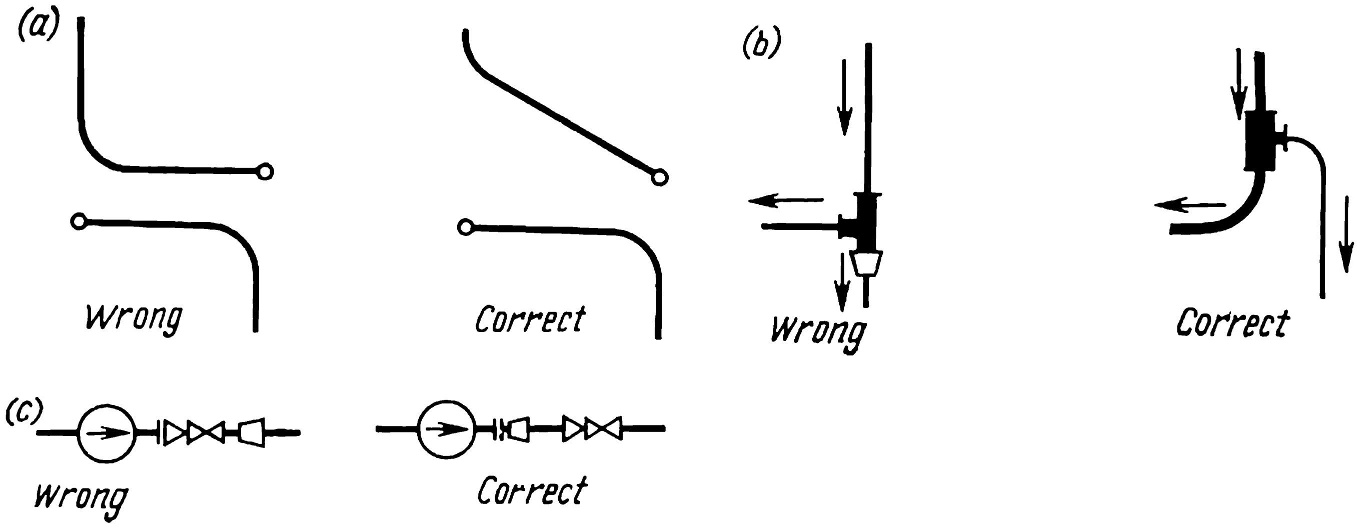

Fig. 1.3. Selection of bends and tees with the aim of reducing hydrodynamic losses

To anchor conveniently pipelines, their routes should be positioned close to columns, along ceiling floors and gangways. While laying small diameter pipelines having permissible spans less than the column spacing special anchor structures should be provided between the columns. When constructing building frameworks the precast reinforced concrete units should contain metallic insertions to which the pipeline supports may be welded.

The routes of pipelines should be so selected as to avoid excessive upper and lower points which would require special drainage devices and air vents. The slopes of pipelines should be selected along the direction of steam flow with due regard to the increase in deflection sag due to metal creep.

While designing pipings it is necessary to strive for the use of similar type of pipeline units as it reduces the number of drawings, calculations, and simplifies the design and manufacture of units at factories. Pipelines connecting similar type of equipment, for example, turbines, boilers, deaerator tanks, feed pumps and heaters should be identical. The layout should begin with pipelines whose design is most difficult as regards layout and self-compensation, say large diameter and high pressure pipelines. Generally, the layout of different pipeline groups has the following sequence: (1) live steam lines; (2) reheat steam lines; (3) high pressure feed lines; (4) low pressure lines of large diameter; (5) other low pressure lines. The erection ties of pipelines, which do not consider lateral bending displacements, due to expansion or cold stretching of pipelines, are indicated on the layout drawings. The erection distances between pipe axes and wall or thermal insulation surfaces of neighbouring pipes should be sufficient to allow thermal insulation works and heat treatment of welded joints. The distances recommended in Appendices 1 and 2 are calculated for a clearance of 120-150 mm from the pipe thermal insulation surface to the wall or the insulated neighbouring pipe and a clearance not less than 200 mm between the surfaces of uninsulated pipes. The distance between the axes of parallel pipelines is determined from appendix 2 as the sum of distances from the pipe axis to the center of the distance between the insulation of neighbouring pipes. If the thermal expansion or cold stretching result in the displacement of a pipeline towards the wall or the neighbouring pipeline then the erection distance should be so taken that at maximum displacement of the pipeline the clearances between the insulation and neighbouring surfaces (walls, heat insulation of neighbouring pipes) are not less than 100 mm. The distances between pipe's axes should be checked with a view to possible mounting supports, hangers and brackets for the pipelines.

When designing pipings the designers should be guided by "Regulations for arrangement and safe operation of steam and hot water pipelines" laid down by the USSR Gosgortekhnadzor (State Commission of the Council of Ministers for Supervision of Industrial Safety and for Mining Inspection). The design of pipeline components and elements are to be selected only according to the Inter-Agency or inter-Branch Standards.

Use of flange joints for stationary pipelines is permitted only in the following cases: (1) for connecting pipelines to equipment manufactured with flanges; (2) for connecting flanged fittings; (3) for installing measuring nipples and diaphragms manufactured with flanges as per MBH; (4) for erection joints of pipelines with linings or anticorrosive coating.

In all other cases the butt welded joints as per MBH should be used. Butt welding of straight pipe pieces should be practised between accessories and moulded or forged components or other parts of fittings. Such pipe pieces are used to protect the ends of moulded and forged components against damage when cutting out the equipment for repairs. The pipe piece length should not be less than 100 mm and should be increased accordingly when it is necessary to carry out ultrasonic flaw detection or heat treatment of welded joints.

At present, quality control of welded cross joints of vital pipelines by the ultrasonic flaw detection method is a must. For this method of inspection the necessary free length of the straight pipe piece (up to the element or bend to be welded to the pipeline) depends on the pipe's wall thickness s and is determined from the following data:

Wall thickness (s) in mm	Minimum length mm
up to 15 inclusive	100
15-30	$5s+25$
30-36	175
over 36	$4s+30$

For heat treatment of welded cross joints a free length not less than

$$l = 1.5\sqrt{(D_n - s)\,s}\text{, mm} \qquad (1.1)$$

should be ensured in every direction from the joint. This length should not be taken less than 100 mm.

Nozzles, drainage pipes and other parts should not be welded to forged or cast components, to longitudinal and cross-sectional welded joints, to the bent pipes within the curved portion.

The distance of welded joints from the bend in curved pipings are specified in MBH. In exceptional cases, however, to suit the piping layout the distance may be decreased to a length of one external pipe diameter but not less than 100 mm. For steep and forged bends the welded joints may be located at the curve beginning, i.e. these components can be manufactured without straight portions at the end.

Assembly tolerances are not given for components or units. To compensate for possible erection inaccuracies and to allow for testing of welded joints provision is made for a spare piece of pipe (of all diameters) in assembly specifications of a pipeline's working drawing. Cold springing, even if given in two or three directions, can be achieved only at one place. For this reason cold spring should be specified on assembly drawings, as shown in Fig. 1.4, indicating its value and direction at the fixed support.

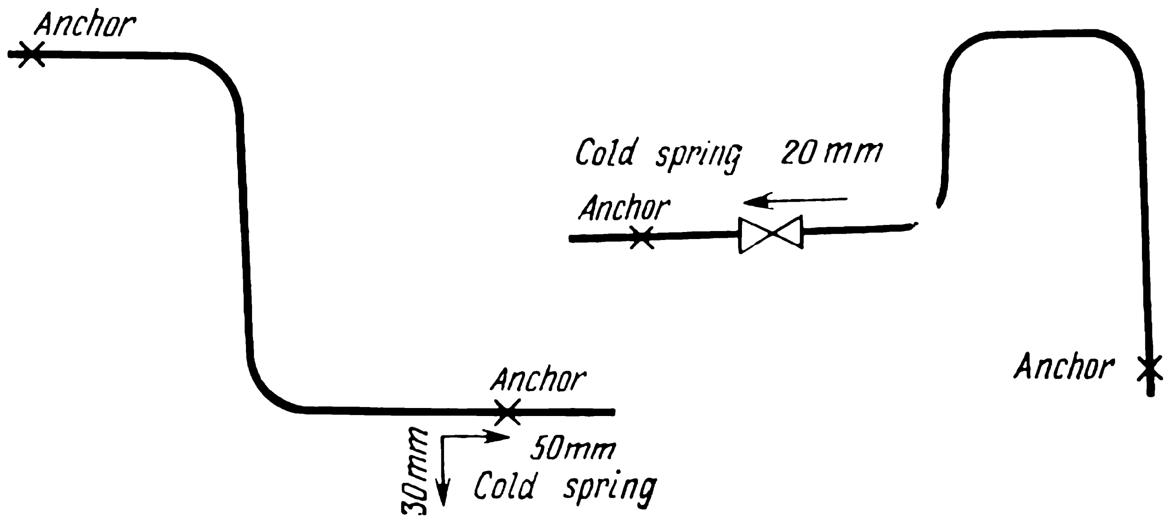

Fig. 1.4. Designation of cold spring on drawings

As per the regulations of ОРГРЭС (State Trust for the Organization and Rationalization of Regional Electric Power Plants and Networks) gauges should be provided for pipelines working at 450°C or more to monitor metal creep. The bench mark to register metal creep should be positioned at the centre of all straight portions longer than 1.5 metres between the welded joints but not near the supports or other bracing belts; the distance from the welded joint or support should not be less than 700 mm. Special check portions 4-5 metres long are provided between the welded joints without supports and the bracing belts to monitor structural changes in metal at high temperatures and stresses in steam pipelines. For the check portions, pipes 300-500 mm longer than the check portions and an additional pipe for replacing pieces cut from the check portions are ordered.

On all steam pipelines of internal diameter 150 mm or more, working at 300°C or higher, indicators should be installed for checking thermal displacements of pipelines and work of supports. On each self-compensation portion 2-3 indicators are installed close to the places of maximum pipe displacements.

1.3. Drainage of Pipelines

The condensate formed during the start up and also during the operation of steam lines should be removed quickly without allowing it to accumulate so as to avoid hydraulic impacts in the pipeline and the equipment connected to it. The drainage of main steam lines should be especially good enough. Sufficient slopes of steam lines in the direction of flow should be provided for better removal of condensate. Drainage points of adequate cross section should be provided before the shut-off valves and at the lowest points of the pipeline.

The drainage blow-off system of steam lines should ensure the following: removal of condensate and wet steam from the steamline portion being heated before its operation (blow-off of steam line, starting drainage); removal of condensate from the steamline already closed (emptying); continuous removal of condensate from the section of pipeline under pressure, if condensate forms in it (continuous drainage); removal of air from steamlines if filling them with water for hydraulic testing; collection and use of condensate and heat of drainage and blow-off water in the heat flow cycle of the power station.

The starting drainage points consist of a nipple and a valve installed in series after it for working pressures up to 22 kg/cm^2. This valve functions simultaneously as a stop and a regulating valve. For working pressures more than 22 kg/cm^2, first a stop valve and then a regulating valve are installed, but for conventional pressures greater than 200 kg/cm^2 a stop valve, a regulating valve and an orifice plate should be installed. In all cases, the regulating valves are installed after the stop valves in order to decrease steam velocity and wear of packing surfaces of stop valves.

For block power stations the drainage of main steamlines is directed, as a rule, to a high pressure steamline drainage expander (one for three-four boilers and turbines). The starting drainages of pipelines at working pressures less than 22 kg/cm^2 are directed, as a rule, to a low pressure drainage expander. For draining steamlines and for drainage of water after hydraulic tests the same blow-off drainage vents are used.

After heating the main steamlines and start up no condensate is formed in the main steamlines (as in other pipelines carrying superheated steam at a temperature higher than the saturation temperature) and devices for continuous removal of condensate are not required. The exceptions are steamlines to the instant-start equipment, for example, stand-by feed pumps, rapid reduction and cooling units. Steamlines to such equipment should remain in the hot condition and under pressure. Before the shut-off valve of such equipment provision should be made for continuous drainage. A continuous drainage system consists of a throttling device (a valve and an orifice plate) through which steam enters into the low pressure steamline (steam reheating pipeline, 6 or 2.5 atm steamline). As a matter of fact, such a system is not meant for drainage but for continuous heating. Continuous drainages of low pressure pipelines are accomplished with the aid of steam traps, and of 1.2-1.5 atm steamlines by the use of hydroseals.

To reduce the number of drainage points the steam lines should be laid out with a continuous slope in the direction of flow avoiding the formation of rapids or risers. In those cases where rapids or risers are unavoidable, for example, in vertical U-shaped expansion joints on the cross connector, a drainage bypass should be provided. There is no need for special drainage devices at points of installation of measuring washers in horizontal pipelines, because flow gauge intake connecting pipes are used for this purpose.

As regards the slopes of steamlines necessary for the drainage of horizontal portions it should be remembered that erection slopes may not be maintained due to the following reasons: (a) vertical displacements of spatial steamlines due to an increase in their temperature causing the slopes of horizontally laid portions to change (Fig. 1.5); (b) appearance of residual deflections which gradually increase in horizontal spans due to metal creep on high temperature pipelines.

A slope $i \geqslant 0.004$ should be provided in those cases where condensate is likely to be formed, i.e. at a saturation temperature t_s corresponding to the steamline working pressure.

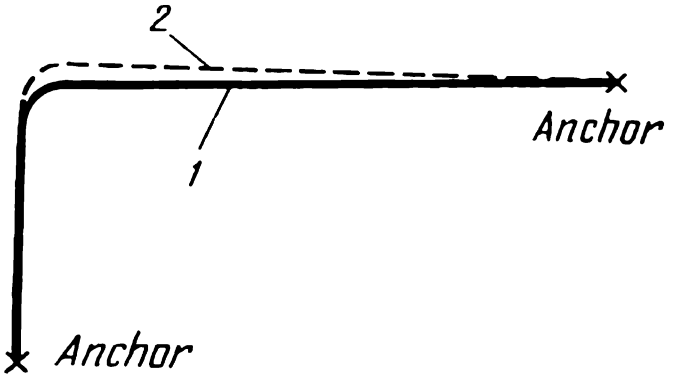

Fig. 1.5. Variation in inclination of horizontal section due to vertical displacement
1—cold pipeline; 2—hot pipeline

It is not difficult to specify the necessary erection slopes, or more exactly the erection levels of a pipeline's axis, because the vertical displacements of a pipeline's axis at the working temperature are determined when calculating for the self-compensation thermal elongation. It is evident that the displacement at the saturation temperature t_s will be

$$h_s = \frac{t_s}{t_{work}} h_{work}$$

where h_{work} is the displacement at the working temperature.

If $h_{work} < 0$, i.e. the pipeline, on heating, is displaced downwards, then the minimum inclination may be taken equal to $i = 0{,}004$. If $h_{work} > 0$, i. e. the pipeline displaces upwards, the required erection levels can therefore be easily calculated graphically. For this (Fig. 1.6) the displacements are laid off on a up-scaled diagram, i.e. a straight line is drawn downwards from the horizontal line and from the beginning of the horizontal section so that it passes through the point ($-h_s$) at which the slope is maximum (in this case, all the remaining displacements will not lie on this line).

Then a line is drawn having a slope 0.004 greater than the previous line which determines the difference in levels of spring supports. In this graphical method the vertical scale should be 20-50 times larger than the horizontal one.

The actual slope varies along the pipeline and depends on the nominal erection slope determined by the difference in support levels and the deflection at the given cross section. To avoid local reverse slopes, the span length should be not more than

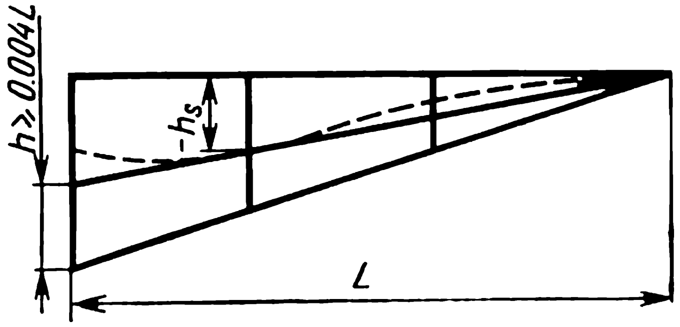

Fig. 1.6. Graphical determination of erection levels of supports for horizontal section

$$l \leqslant \sqrt[3]{\frac{96EIi}{q}}\ \text{m}$$

This condition must be fulfilled when emptying, at the end of discharge. Here, q is the weight of the insulated pipe without water, kg/m, E—modulus of elasticity for the metal in the cold state, kg/cm^2, I—moment of inertia of the pipe's cross section, cm^4. The spans of pipelines given in the MBH standards are specified with due regard for the elastic deflections in the spans at minimum i slopes.

The designed slopes of pipes should be calculated by taking into account their layout and working conditions. In longdistance pipelines, for example carrying steam from a thermal power station to industrial units, slopes more than 0.001-0.002 involve technical difficulties and additional expenditures. Shut down and subsequent start-up of such pipelines are very rare, but their warm-up time is very long, which permits to take a minimum value of heading slope 0.001-0.002 for such pipelines.

For stationary pipelines, having limited length and sufficient, as a rule, difference between the initial and the end levels, it is not difficult to create necessary slopes. At the same time, there is a frequent need for heating of such pipelines, the heating time being limited. Therefore, Regulations for Technical Operation [1-6] specify slopes not less than 0.004 for steamlines.

The erection slopes of horizontal areas of stationary piping designed for other purposes should not be less than: 0.002 for water piping, 0.003 for drainage piping and 0.005 for fuel oil piping.

1.4. Pipeline Supports

An important task when designing a piping system is proper fastening, selection of supports and hangers, and means of adjusting spring hangers. Besides the main function, i.e. transmission of the weight of the piping to the building structures, the movable supports should ensure free movements of the piping and protect the piping from possible vibrations. The rigid supports should ensure the fixed position of the piping and transmit all forces and moments not taken by variable supports to the building structures. Lanes through ceiling floors and walls, and guides for vertical piping, although not taking any load, are classed as supports.

Classes as pipe-supporting devices are: (a) pipe attachments (clamps, cushions, etc.); (b) intermediate elements connecting piping supports to the building (hanger rods, spring supports and others); (c) attachments to building or other structures. The elements to be fastened on a piping system are manufactured with due regard for thickness of the heat insulating layer; their parts which come into contact with the piping become heated to the piping temperature. Elements connected to the piping, and intermediate ones have now been standardized, and separate Inter-branch standards developed for them. Such parts are manufactured as standard parts and are supplied together with the pipes by factories. This way of their manufacture is more economical than their production at the site as previously by old fashioned methods. The following fall mainly into the category of attachments fixed to building structures: different types of brackets, reinforced concrete cushions underneath sliding supports, holes in the ceiling floors with washers for holding hanger rods and sometimes metallic columns. Such attachments are generally designed by civil engineers at the request of design engineers to suit the piping layout.

The rigid supports of a piping system divide it into independent portions as regards temperature compensation. Fastenings to units and assemblies should be regarded as fixed points although these attachments are displaced relative to the building due to heating of equipment. Anchor supports must be strong because, besides the weight of adjacent spans, they take self-compensation forces and moments of adjacent spans having the most unfavourable combinations (including installed valves). These forces and moments should be considered with the full self-elongation of the piping due to relaxation of temperature stresses, the forces and moments from unbalanced spring hanger tensions caused by the weight of the piping. This additional tension can mount up to 15-20% of the total weight of the piping. With sliding supports the dynamic forces caused by hydraulic impacts and frictional forces can mount up to 30% of the total weight of the piping.

For split piping systems (with slip joints, end portions with bellows expansion joints, exhaust piping) the rigid supports should be designed also to take hydraulic pressure forces (in exhaust piping and doubled hydraulic pressure) on the pipe's cross-sectional area. The components of the design loads acting on the variable supports are calculated by the following formula:

for each horizontal direction the component

$$N_H = 1.2\,(P_1 + P_2) + T_{\max} \qquad (1.2)$$

the vertical component

$$N_V = 1.2\,(P_1 + P_2) + 1.2\,(Q_1 + Q_2) + Q \qquad (1.3)$$

where P_1 and P_2 are forces acting on the support due to self-compensation of thermal elongations of adjoining spans; $T_{\max}$ — maximum force of friction transmitted to the support; Q_1 and Q_2—unbalanced tensions of spring supports due to the weight of the piping portion in the cold condition; Q—load on the support (this load is calculated in the same manner as for rigid supports without springs).

In formula (1.2) the larger of the two forces (P_1 or P_2) is taken positive and the sign of the smaller force determined by its direction. In formula (1.3) forces acting downward are taken as positive. If it is not possible to disconnect the second portion from the first (in the absence of a valve) and the erection allowance for both portions is the same (in %), then the reactions P_1 and P_2 and moments due to self-compensation are calculated independently of the given erection allowance issuing from the assumption of complete relaxation of temperature stresses (self-compensation), i.e. as for 100% erection allowance. If the erection allowance for each portion has different values, then it is necessary to determine the forces acting on the support during the initial operation period taking into account the erection allowances, and the rated load is taken as the maximum load. If there is a valve between the portions and the second portion can be disconnected, then the loads acting on the support should be verified in the following cases: (a) if the first portion is hot and the second is cold for the given erection allowances, without taking into account the relaxation temperature stresses (during the initial stage of operation); (b) by taking into account the relaxation temperature stresses when the forces only from the second portion act on the support (all the self-compensation forces will be equal to zero in the first portion because it is hot).

The rated loads should be taken as the maximum ones.

Example: The components of the self-compensation forces due to thermal elongations, acting in the given direction on a rigid support, equal:

	From the side of portion *1*, kg	From the side of portion *2*, kg	Total, kg
In the beginning of operation			
(a) in the hot condition	1200	—800	+400
(b) in the cold condition . . . . . . (due to erection allowance)	—500	+800	+300
After relaxation of temperature stresses in the cold pipeline	—2000	+1800	—200

The direction of the 1200 kg force acting on the support from the side of portion *1* is taken as positive.

If it is not possible to disconnect portion *2*, then the load acting during the hot condition of both portions (assuming $T = 0$) should be taken as the design load, i.e. $N = 1.2$ (1200-800) = 480 kg.

If there is a valve between the two portions, then on closing it a force of 1200 + 800 = 2000 kg will act on the support and after the relaxation of stresses, a force of 1800 kg. In this case the force $N = 1.2\ (1200 + 800) = 2400$ kg should be taken as the design one.

The rigid supports are designed as a metallic base (cushion) (Fig. 1.7*a*) to which the pipe is tightened with clamps or stirrups. To avoid pipe slip due to the clamp loosening as a result of stress relaxation the supports are welded to the pipe.

For the pipings operating under easy conditions at low temperatures welded rigid supports are used. These supports are similar in design to the sliding supports shown in Fig. 1.7*e*, their sliding shoe or guided roller is welded to the base.

The following pipe-supporting devices designed for horizontal displacements are used at thermal power stations: rigid suspensions, roller supports, sliding supports and very occasionally swing supports (Fig. 1.7*d*). At present roller supports are not used as they do not ensure more or less equal distribution of load on the rollers (particularly at the unavoidable bends of pipe's axis in vertical planes) and this leads to support damage and jamming. Rigid hangers are most suitable for horizontal movements owing to their simple design and less resistance to piping displacements. Rigid hangers consist of a clamp, a connecting rod hinged to the clamp and upper bolt (Fig. 1.7*b*), or two connecting rods with a beam and clamp (Fig. 1.7*c*).

When the hanger rod moves away from its vertical position due to displacement of its lower point by a value c (Fig. 1.8) the point raises through a height

$$h = L - \sqrt{L^2 - c^2} \approx \frac{c^2}{2L} \tag{1.4}$$

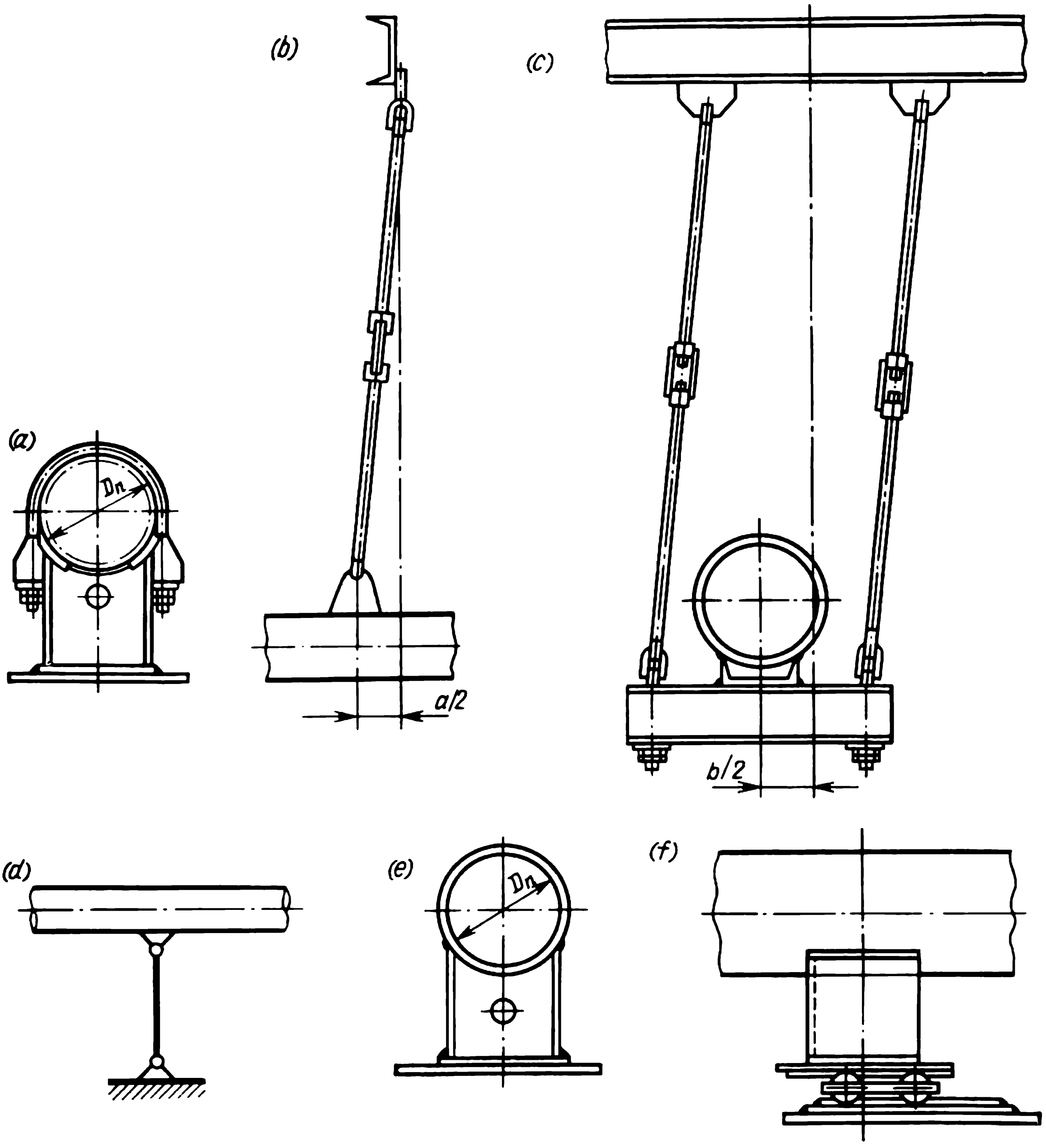

Fig. 1.7. Pipe support types:

(*a*) fixed support; (*b*) rigid single-rod suspended support; (c) rigid, double-rod suspended with hanger's axis displaced in respect to pipe's axis; (*d*) swing support; (*e*) sliding support; (*f*) roller support

where L is the length of the connecting rod, c — horizontal displacement of the pipe at the fastening point. Elevation rise of the fastening point with respect to the neighbouring supports causes load increase on the fastening, additional bending moments in the pipe, variation in slopes and appearance of horizontal force components at the fastening points. For a hanger rod of sufficient length L all the above mentioned phenomena have insignificant values and their effect can be further minimized if during erection the fastening points of the rod to the pipe are displaced by—0.5c (in the direction opposite to the expansion). In this case, at the operating temperature and in the cold condition the vertical level of the hanger does not change, and the load on the support and stresses due to the weight of the piping to be supported and the piping slopes remain equal to the calculated ones. These values are maximum when the piping is heated up to $0.5t_{work}$ and at this temperature the permissible stresses are higher than the stresses at the rated temperature, but in the steamlines the pressure and reduced stresses are less than the calculated ones, and a noticeable increase in stresses from the weight of the piping may be permitted. As proved by the calculations and substitutions, the variation in the piping slope determines the minimum permissible length of a hanger rod for the heated piping. The length of the hanger rod for which the slope decreases no more than 4.10^{-4} should not be less than

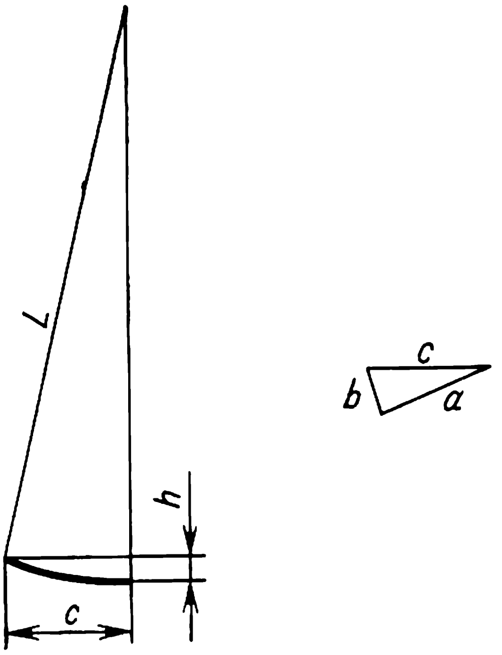

Fig. 1.8. Rise of support point when rigid hanger displaces from its vertical position

L—length of the connecting rod; h—rise of support point; a—longitudinal displacement; b—transverse displacement; c—total displacement

$$L = 12\frac{(0.5c)^2}{l} = 3\frac{c^2}{l} \text{ cm} \tag{1.5}$$

where c is the total horizontal displacement, cm; l—pipe support spacing, m.

This formula is used to calculate the necessary length for the most loaded state, when the hanger is located between two sliding supports.

To avoid bending moments in the horizontal plane, the length of the hanger rod should not be less than

$$L = 10c \text{ cm} \tag{1.6}$$

and the horizontal components of the force then will not exceed 5% of the design weight. Both formulae are true for the displacement of pipe-supporting devices by —0.5*c* as stated in the State Regulations of Gosgortechnadzor; if this requirement is not fulfilled, the length of the hanger rod must be increased four times the value obtained from the formula (1.5) and twice that of requirement (1.6). If necessary, the hanger rods length could be shorter than required (1.6), but in this case the effect of horizontal forces on the flexibility of the piping system should be verified. As regards predisplacement of the suspension point during erection by —0.5*c*, it may be pointed out that when specifying such displacements, designers often forget about lateral displacements of a pipe (perpendicular to its axis) and specify the initial displacement of the clamp only along the axis; meanwhile at many fastening points lateral displacements could be more than the longitudinal ones, say, at the back of a U-shaped expansion joint. This fact should be taken into account for achieving a predisplacement of 0.5*b* in the lateral direction when suspending the pipe on one hanger rod at the given support position to the ceiling floor (displacement of a hole and so on). This can be accomplished with ease during erection when the pipe is supported by two hanger rods (Fig. 1.7*c*) through displacement of the hanger axis with respect to the pipe's axis. Hangers with two connecting rods have the advantage that their design permits the length of connecting rods to be increased by about twice the pipe diameter. The other advantage of using such hangers is that the pipes can be arranged in one single vertical row.

The swing supports (Fig. 1.7*d*) are rarely used, only for arranging the piping at a higher level over the ceiling floor and when the use of a hanger is not possible. Such a support has the same peculiarities as a hanger, i.e. variation in height when the fastening point is moved towards the pipe and appearance of lateral forces. The legs of such supports should be calculated for off-centre compression.

A slide support (Fig. 1.7*e*) is a simple and cheap support. The disadvantage of this support is that it offers sufficient resistance to displacements amounting up to 30% of the load on the support. The longitudinal components of friction forces are transmitted to the fixed supports which should, for this reason, be calculated for substantial loads. The components of friction forces perpendicular to the pipe's axis cause additional bending stresses which may attain significant values. Taking all this into account, the use of sliding supports on important pipelines is avoided and their use is restricted to the points at which the pipeline has smaller transverse displacements. The use of individual sliding supports is expedient as a measure against piping vibration.

Roller supports (Fig. 1.7*f*) have less frictional resistance in the direction perpendicular to the axis of rollers. Their most simple standard design when rollers are arranged perpendicular to the pipe's axis decreases the longitudinal components of friction forces, but does not reduce, compared to sliding supports, the forces of friction acting perpendicular to the pipe's axis (it is precisely these forces of friction that produce additional moments and impair self-compensation). Roller supports with two rows of rollers do not have this disadvantage and offer less resistance to both longitudinal and transverse displacements, but these supports are somewhat complicated in their design and do not resist wind loads.

It would be more rational to use a support with a roller positioned at any given angle to the pipe's axis. Such a support would ensure self-compensation with small resistance to both lateral and longitudinal displacements and at the same time the support would retain its antivibration qualities.

Spring hangers (Fig. 1.9) are the most suitable supports for the piping subjected to vertical movements. Spring hangers of one rod can be made with one, two or three springs arranged in series. Hangers of paired connecting rods can be made respectively with two, four or six springs depending upon the magnitude of vertical movements. Springs with rated compression length up to 70 and 140 mm used for supporting the piping are manufactured in accordance with the interbranch industrial standards. The spring hangers are adjusted so that the spring compression force (or the spring stiffness) balances the weight of the piping under operating conditions. The piping on cooling, depending upon its layout, may move upwards unloading the springs

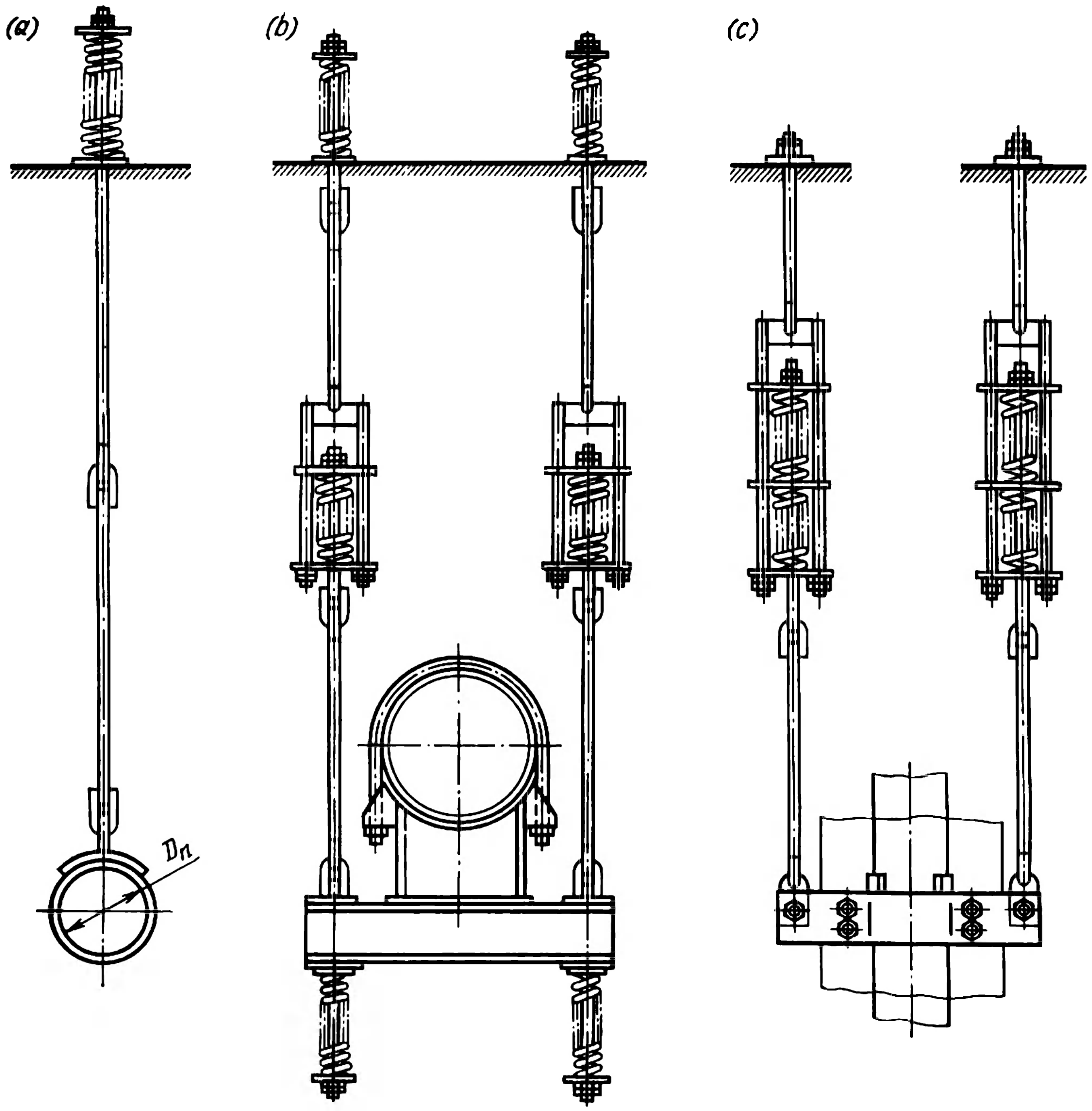

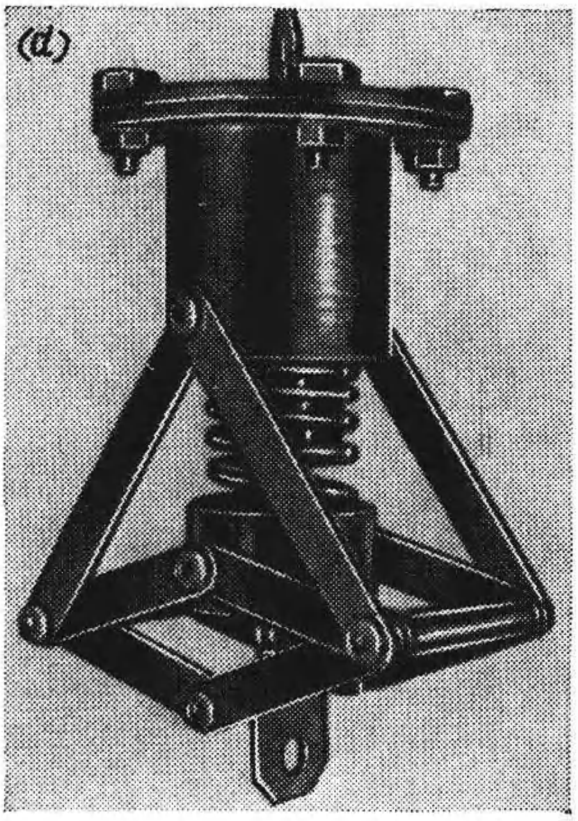

Fig. 1.9. Spring supports

(*a*) single-chain spring hanger for horizontal pipeline; (*b*) double-chain spring hanger with 3 springs each, to horizontal pipeline; (*c*) spring hanger for vertical pipe; (*d*) constant load support

(Fig. 1.10), or downwards compressing the springs. The springs are so selected that the load taken by them in the cold condition differs from the load in the hot condition by not more than 30%.

When the piping is in the cold condition the stresses from spring supports are not balanced by piping weights, and this produces additional forces and moments in the rigid supports and stresses in the cold piping. This proves to be a limiting factor and must be taken into account in structural design calculations of piping systems and the supports in the cold condition. In computer-aided calculations it is possible to take account of all the load factors and the resilience of all spring supports with sufficient accuracy, and to select spring supports for load differences greater than 30% in the hot and cold conditions.

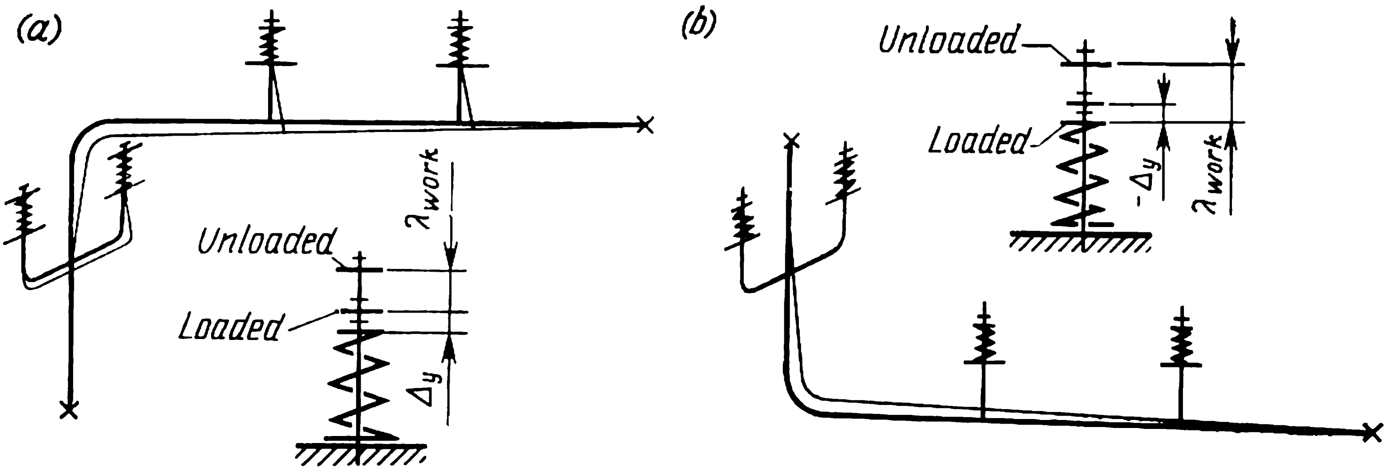

Fig. 1.10. Schematic diagram representing the working of spring supports

(*a*) downward displacement when pipeline is cooled; (*b*) upward displacement when pipeline is cooled

The calculation of springs adjustment becomes somewhat complicated because with the variations in loads taken by the support the elastic deflections of the piping also vary [1-5]. After adding the thermal insulation cover to the piping this problem is solved very easily by adjusting the hangers in two stages: (1) the springs are tightened to a value equal to the weight of the piping span supported by them, then each hanger will bear a load equal to the weight of the corresponding span; (2) the support springs are tightened to a value equal to the thermal shift by making the operative length of the hanger rod equal to the thermal shift (if on heating the pipe shifts upwards, the operative length of the hanger rod should be reduced).

Accordingly the following information is given on the working drawings: (1) the spring rated compression length is H, mm, at the operating load Q, kg; (2) after setting all the pipeline's spring hangers to the operating load the overall length of the hanger rod must be reduced or increased by h, mm.

For large vertical movements constant load spring hangers are sometimes used (Fig. 1.9*d*). But, as proved by tests, the magnitude of the load taken by such a hanger varies significantly with the change in the direction of movement (due to friction in hinges), consequently, the rated load on the support can not be achieved during operation.

In the vertical section of a piping system one hanger is sufficient, because the forces of tension or compression, in this case, are small. The spring hanger clamp should be positioned in the vertical section at a height where the temperature displacement is small. Two or more spring hangers should only be used in the vertical portion when strength requirements of standard hangers demand them (limit loads on springs, clamps) or by the bearing capacity of ceiling floors.

Guiding supports or guides are used to prevent vibrations, ensure normal operation of slip joints and protect cast iron fittings against bending moments produced by self-compensation to accommodate thermal elongation. All types of guiding supports fail to prevent the piping from turning already at 0.01-0.02 radians, and hence, cannot safeguard cast iron fittings (accessories) against the action of bending moments; for this reason not less than two guiding supports located at a distance of a few metres from each other are necessary.

The rated loads for spring supports of steamlines are taken with consideration for the added weight of water used in the hydrostatic testing procedure. For steamlines with outside diameters in excess of 300 mm, attachments which relieve the load from springs during hydrostatic testing are used. The rated loads for fixed supports and hangers should consider overloads due to the uneven load distribution on supports as a result of nonlinearity of the actual pipe axis and errors in mounting supports and piping. The relative increase in load on a support P/ql is proportional to the pipe's rigidity EI and inversely proportional to the span length raised to the fourth power. For normal span lengths recommended in MBH the piping deflections sufficiently provide for more or less even distribution of the loads on supports and the overload coefficient may be taken equal to $K = 1.3$. However, on decreasing the span length the overload coefficient should increase rapidly. Considering the above, for rated loads the weight of the piping with a *normal span* length and coefficient 1.3 should be taken as the rated load irrespective of the actual span length even if it is less than the normal span length.

For calculating loads on supports due to the weight of the exhaust piping the reaction force of discharge into the air directed opposite to the exhaust flow (see Sec. 3.9) should be taken into account.

1.5. Application of Pipe Fittings

The design and calculation problems of pipe fittings are dealt with in special literature [1-1 and 1-2], and are out of the scope of this book. Here, only the use of accessories in stationary piping is considered. At electric power stations many types of pipe fittings are in use: gate and plug valves, control valves, different purpose regulating valves, return valves, safety valves, condensate taps and pots, drains and inspection and measuring equipment.

The fittings are manufactured to nominal inside diameters (GOST 355-67) and for nominal pressures (GOST 356-68). These standards limit the number of different-sized fittings manufactured by industry. Each type of fitting is given a maximum rated temperature of the working medium. The state standard (GOST 356-68) permits manufacture of equipment designed for specific parameters if such equipment is in high demand. The Venyukovsky factory manufactures such equipment, accessories and fittings, for steamlines working at 255 atm and 565°C, and for water pipes at 380 atm and 280°C.

Fittings have butt ends for welding flanges or threaded ends to suit the method of attachment. The most reliable connection is the butt-welded joint which should be used for pipelines withstanding nominal pressures of P_n 64 or higher. Coupled pipe fittings and hand threaded fittings are not used for heat flow pipelines. Steel pipe fittings are usually used at thermal power stations. Cast iron fittings for steamlines and hot water lines are permitted in Regulations of "Gosgortechnadzor" for limited pressures, temperatures and flows provided these fittings are not subjected to bending moments. To avoid bending moments it is necessary to install on straight runs of pipelines in front of cast iron fittings not less than two guiding supports spaced at the maximum possible distance between them on the side on which bending moments act, or a hinged system with bellows-type expansion joints should be used. If it is not possible to effectively protect cast iron fittings from bending stresses, then they should not be used and more costly, though more reliable, steel fittings should be installed. On low-pressure pipelines, when continuous operation is necessary, such as low-pressure feed pipelines steel fittings are obligatory. The application of cast iron fittings at electric power stations is restricted to pressures of 4-5 atm and a temperature of 120°C.

Shut-off accessories are meant only for the interruption of flow, and should remain either fully open or fully closed during pipeline operation. The use of such equipment for throttling or regulating the flow of fluid and pressure results in wear and tear of packing surfaces and loss of tightness. To regulate the steam and water flow at high parameters special regulating valves and taps designed for this purpose are necessary. Such fittings do not ensure total closure or interruption of flow and in front of them shutoff or gate valves must be installed.

To facilitate the opening of valves, which require great effort, and also for heating steamlines bypass valves (bypasses) are installed. The use of bypasses on high-pressure valves relieving the gate from pressure forces when opening the valves, protects the packing surfaces from wear and tear. For high steam parameters if the diagram envisages heating of pipelines through bypass valves, it is necessary to install on the bypass a shut-off valve and a regulating valve in series.

There are full-flow valves and restricting valves. For the full-flow valves the flow diameter of packing rings is equal to the nominal passage diameter. Restricting valves are light in weight and can be opened or closed by applying very little torque. Such valves, however, have a large hydraulic resistance, particularly, when there are no straight runs of pipes up to and after the valve. Gates and valves which can be opened or closed by applying a torque more than 50 kg·m should be equipped with electric drives. Electric drives are also provided for valves operated from a control room and for valves in automated and blocking systems.

Remote control mechanical drives (Fig. 1.11) are manufactured to Inter-Branch Standards.

Hinges allow direction variation but not more than 30°, gear boxes permit a directional variation of 90°. The angles of drive shafts twist should not exceed 0.05 radians (about 3°). For this the moment of inertia (equatorial) for the shaft's cross section should not be less than

$$I = 0.13 M_t l, \text{ cm}^4 \qquad (1.7)$$

where M_{tor} is the torque, kg·m; l—total length of bars from the columns to the fittings, m.

Fittings should be installed at places convenient for maintenance, inspection and repair. In case it is not possible to service fittings from main ceiling floors or service platforms (of boilers, turbines) special service platforms should be designed. Fittings equipped with remote control mechanical drives should be positioned close to rigid supports at places where temperature variations are less. Remote control devices should be designed so that the valve would close in a clockwise direction.

On both sides of heavy equipment (500 kg or more) for easy erection, repair and possible replacement supports or hangers should be attached to the pipeline, and devices for hanging a tackle should be provided over the equipment.

Heavy duty valves should be positioned in horizontal portions. The placing of heavy fittings in vertical portions should be avoided even when permitted by the manufacturer as this complicates erection and repair. Only install heavy

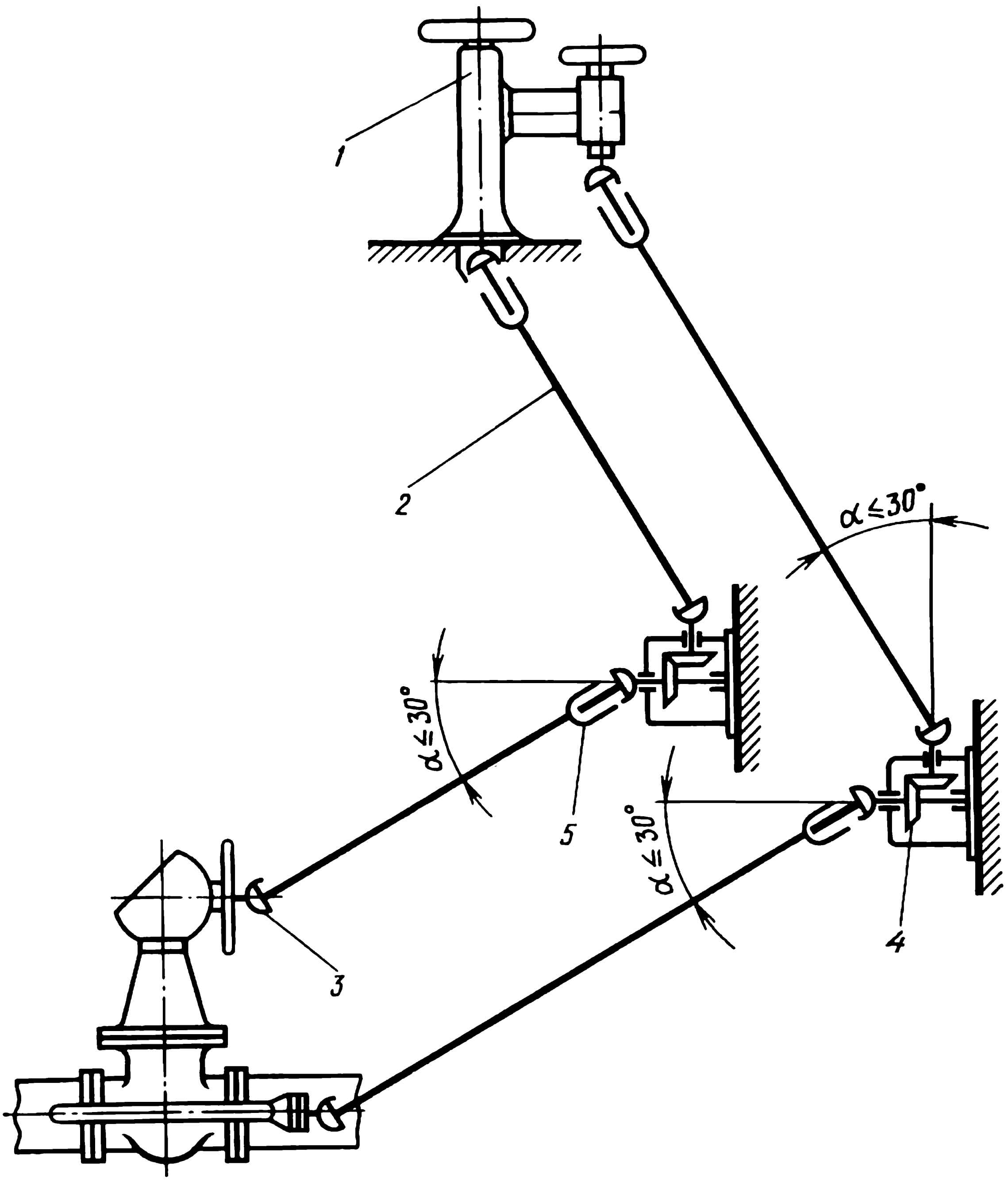

Fig. 1.11. Manual remote control device

1—column; 2—shaft; 3—articulated joint; 4—rotation box; 5—articulated joint with a compensator

fittings in the vertical portions when for horizontal location of the axis of the valve's flow significant elongation is necessary and complications in routing the pipes occur (to build an appropriate horizontal section).

Measuring nipples and diaphragms should be installed on straight runs of pipes at places where their operation is easy. The length of straight sections for obtaining correct readings when pressure is taken by tubular shaped chambers should not be less than: (a) 40 internal pipe diameters aft bend, elbow or tee up to diaphragm or nipple, and after he gate or valve 30 internal pipe diameters; (b) after the diaphragm or nipple 5 internal pipe diameters.

If the layout does not permit to have straight portions of the required length up to the diaphragm or nipple, these engths may be decreased to $10D_i$ (this will lower to some exent the guaranteed accuracy of measurements). The welding of nipples and pockets for thermometers within the straight ections is not permitted.

Chapter Two

Hydrodynamic Calculations and Selection of Pipe Diameter

2.1. General Information and Formulas

The main purpose of hydrodynamic calculations is to determine the loss of pressure in a pipeline for the given rate of flow, its parameters and pipe diameter. Selection of pipe diameter is made on the basis of technical and economic calculations, and is dealt separately (Sec. 2.6). Sometimes, hydrodynamic calculations are made to determine the discharge capacity given the start and end parameters or to select the size of resistances (orifice plate) to regulate the discharge capacity.

The flow of steam through the steam power station piping may be considered as an insulated thermal process, not only because it has thermal insulation, but also due to the limited length of the piping. The basic formula for steady heat insulated flow is

$$-10^4 v\,dp = \frac{w^2}{2g}\,d\xi + \frac{w\,dw}{g} + dH \text{ m} \qquad (2.1)$$

in which v is the specific volume, m^3/kg; p—pressure, kg/cm^2; w—flow rate, m/sec; ξ—coefficient of hydraulic resistance; g—acceleration due to gravity, m/sec^2; H—piezometric height, m.

The left hand side of equation (2.1) represents the work done per kg of mass, the right hand side represents the work done against friction, kinetic energy increment and the work done in changing the piezometric height H also per unit mass. On assuming the last two members of equation (2.1) to be equal to zero the flow will be represented by an isoenthalpic curve (i = const) as it must be for an insulated thermal flow. The work put in is transformed into heat and fully absorbed by the fluid flowing through the piping. The second member of the right hand side of equation (2.1) represents the insulated thermal process of expansion, i.e. adiabatic expansion and takes into account the decrease in enthalpy of the medium due to the change in its velocity.

With a decrease in line pressure the specific volume v and velocity w increase. It is convenient to express the velocity w as mass velocity $m = w/v = Q/F$ kg/(m^2·sec) whose value remain constant in a pipe of constant flow area F; Q, m^3/sec = volume of fluid flowing through the pipe. After substitutions and regrouping the formula becomes

$$\frac{m^2}{2g}\left(d\xi+2\frac{dv}{v}\right)=-10^4\frac{dp}{v}-\frac{dH}{v^2}$$

Integrating this equation, we get the general equation for steady insulated thermal flow

$$\frac{m^2}{2g}\left(\xi+2\ln\frac{v_2}{v_1}\right)=-10^4\int_1^2\frac{dp}{v}-\int_1^2\frac{dH}{v^2}\ \text{kg}^2/\text{m}^5 \qquad (2.2)$$

the limits 1 and 2 correspond to the beginning and the end of a pipe, respectively. Integrals in the right hand side of equation (2.2) should be calculated along the actual curve of the process by taking into account the enthalpy change due to an increment in velocity. For saturated steam the second member on the right may be neglected due to the large specific volumes. In the left hand side of the formula, to the pipe resistance coefficient ξ is added the resistance coefficient $2\ln\frac{v_2}{v_1}$ which takes into account the additional resistance due to an increase in specific volume. For pipelines with small pressure drops, this member may be discarded but must be taken into account for pipelines carrying boiling water, blow-off and exhaust pipes.

Formula (2.2) could be used in its original composition when calculating for hydrodynamics of high pressure boiling water and saturated steam pipelines, whose adiabatic index varies within a wide range.

Since the adiabatic index for superheated steam and gases is constant, formula (2.2) may be reduced to a more convenient form for the hydrodynamic calculations.

The increment in kinetic energy of 1 kg mass of insulated heat flow can be considered as the available useful external work of an adiabatic process when the velocity increases from w_1 to w. Therefore, for constant adiabatic index k the following equalities will hold true

$$\frac{w^2}{2g}-\frac{w_1^2}{2g}=\frac{k}{k-1}(p_1v_1-pv)\cdot 10^4 \tag{2.3}$$

and as a corollary

$$p_0v_0=\left(p_1+\frac{k-1}{k}p_{h1}\right)v_1=\left(p+\frac{k-1}{k}p_h\right)v=\text{const} \tag{2.4}$$

where $p_h=\frac{w^2}{2gv\cdot 10^4}=\frac{m^2v}{2g\cdot 10^4}$ kg/cm^2—hydrodynamic pressure;

p_0v_0—pressure, kg/cm^2 and specific volume, respectively, m^3/kg in the initial state of zero velocity.

Equations (2.3) and (2.4) are modified forms of Bernoulli equation for changing density. The equality (2.4) determines the differential

$$dp=\frac{-p_0v_0}{v^2}dv-\frac{k-1}{k}\cdot\frac{m^2}{2g\cdot 10^4}dv$$

and finds the required integral in the equation (2.2)

$$-\int_1^2\frac{dp}{v}=-\frac{1}{2}p_0v_0\left(\frac{1}{v_2^2}-\frac{1}{v_1^2}\right)+\frac{k-1}{k}\cdot\frac{m^2}{2g\cdot 10^4}\ln\frac{v_2}{v_1} \tag{2.5}$$

On the basis of equation (2.2), after transforming and expressing the first member of the obtained integral through the initial, final and mean parameters, we get the following formulae

$$\left(\frac{p_1}{2p_{h1}}+\frac{k-1}{2k}\right)\left(1-\frac{1}{\beta^2}\right)=\xi+\frac{k+1}{k}\ln\beta \tag{2.6}$$

$$\left(\frac{p_2}{2p_{h_2}}+\frac{k-1}{2k}\right)(\beta^2-1)=\xi+\frac{k+1}{k}\ln\beta \tag{2.7}$$

$$\Delta p=(p_1-p_2)=\frac{m^2}{2g\cdot 10^4}\cdot\frac{2\beta v_1}{1+\beta}(\xi+\sigma) \tag{2.8}$$

in which the ratio of specific volumes is denoted by

$$\beta=v_2/v_1$$

These formulae are for steam and gases, thus the term for change in piezometric height may be discarded. In equation (2.8) value $\frac{2\beta}{1+\beta}v_1=\frac{2v_1v_2}{v_1+v_2}=\frac{2}{\gamma_1+\gamma_2}$ is the mean specific volume and the coefficient σ takes into account the additional resistance due to increase in the specific volume. The coefficient

$$\sigma=\frac{k+1}{k}\ln\beta+\frac{k-1}{2k}\left(\beta-\frac{1}{\beta}\right) \tag{2.9}$$

is the sum of three coefficients:

$$\sigma_\beta=\frac{k+1}{k}\ln\beta-\frac{1}{2k}\left(\beta-\frac{1}{\beta}\right) \tag{2.10}$$

that takes into account the effect of an increase in specific volumes;

$$\sigma=\frac{1+\beta}{2} \tag{2.11}$$

the exit loss of hydrodynamic pressure;

$$\sigma_1=-\frac{1+\beta}{2\beta}$$

and the initial hydrodynamic pressure.

Formulas (2.6) and (2.7) enable the ratio β of the specific volumes to be found from known values (p_1, p_{h1} or p_2, p_{h2}). After finding β the sought pressure (p_2 or p_1) is calculated most easily from the following formulas based on (2.4) and the relationship $p_{h2}=\beta p_{h1}$:

$$p_2=\frac{p_1}{\beta}-\frac{k-1}{k}\left(\beta-\frac{1}{\beta}\right)p_{h1} \tag{2.12}$$

$$p_1=\beta p_2+\frac{k-1}{k}\left(\beta-\frac{1}{\beta}\right)p_{h2} \tag{2.13}$$

Formula (2.6) with formula (2.12) makes it possible to calculate the pipeline's terminal parameters p_2, v_2 from the initial ones. Formulas (2.7) and (2.13) solve the reverse problem. Formula (2.8) is essential for calculating the flow from the given initial and final parameters, and may also be used to calculate the pressure drop for values of β close to 1, In the earlier derived formulas the numerical coefficients depend on the adiabatic index k. For superheated steam, $k = 1.3$, for diatomic gases, $k = 1.4$, and for polyatomic gases, $k = 1.33$. The value of k for saturated and wet steam [2-9] changes over wide limits, as is clear from Fig. 2.1. For dry saturated steam at a pressure up to 25 atm (225°C) the average value of $k = 1.135$ is taken. For pressures up to 100 atm (310°C) the average value $k = 1.08$ is taken for practical purposes. For pressures greater than 100 atm the value k decreases rapidly to 0.38 at critical pressure and formula (2.2) should be used for calculations.

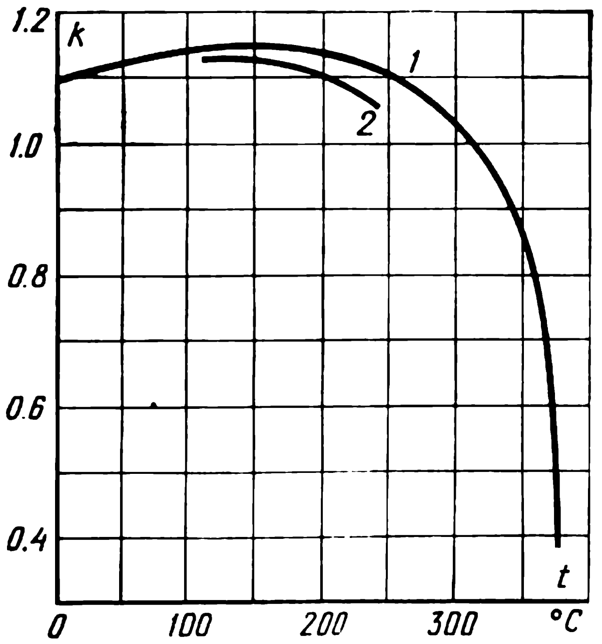

Fig. 2.1. Adiabatic index of saturated steam

1—for degree of dryness $x = 1$; *2*—for degree of dryness $x = 0.9$

Here, we may mention that for dry saturated steam at an initial pressure $p < 40$ atm, expansion takes place in the superheated steam range. With small initial humidity values (1-2%) expansion takes place below the saturation curve and the formulas for saturated steam should be used.

In all the derived formulas it has been assumed that the mass velocity $m = Q/F$ remains constant along the pipeline, i.e. the flow Q and the flow area F of the pipe and other pipe components remain constant. In actual practice local variations in flow area occur in accessories, moulded elbows, tees and changeovers to other diameters (reducers) and flow variations through T-joints. In all cases the change in mass velocity is inversely proportional to the area F and proportional to the flow Q. Hydrodynamic calculations are easy to perform when the mass velocity m_r is constant. The term for this velocity is rated mass velocity. The coefficients of resistance must be simultaneously recalculated by substituting their actual values by values reduced to the rated mass velocity m_r so as to avoid any discrepancy due to replacing m by m_r. Such a value is known as the reduced coefficient of hydrodynamic resistance and is calculated from the following formula

$$\xi_{rd}=\frac{m^2}{m_r^2}\xi=\left(\frac{Q}{Q_r}\right)^2\left(\frac{F_r}{F}\right)^2\xi=a^2\xi \qquad (2.14)$$

where a^2 is the coefficient of hydrodynamic resistance reduced to the rated conditions; $a = m/m_r$—coefficient reduced to the rated mass velocity; F_r—rated passage area; Q_r—rated flow, kg/sec.

The above is valid until the flow velocity at places of constrictions falls lower the critical (sound) velocity. Because of this, while doing similar calculations, it is necessary to verify subsequently the actual constriction velocities—they should not exceed the critical velocity.

In many cases, pipelines have areas through which fluid flows at different mass velocities; the change in mass velocity occurs due to flow bends in tees or a changeover from one diameter to another. If the flow rates through different parts of such a pipeline are known, then hydrodynamic calculations are not very difficult to perform, because the pressures at the end of every portion and at the beginning of the next can be determined subsequently. However, it must be kept in mind that at joints (reducers, tees) the mass velocity and hydrodynamic pressure vary and hence, as per Bernoulli's equation the piezometric pressure will also change.

For convenience the subscript "a" will be used to denote conditions in the pipe approaching the reducer (tee), and the subscript "b" to denote conditions after the reducer, and shall introduce the following dimensionless coefficients:

$c = p_{h.a}/p_a$ = ratio of hydrodynamic pressure and piezometric pressure up to the reducer
$a = m_b/m_a$ = ratio of mass velocities
$\beta = v_b/v_a$ = ratio of specific volumes

It may also be mentioned that pressure losses in local resistance of a reducer ξp_h can be combined with the neighbouring parts. By taking this into account for incompressible liquids the equation can be written as

$$p_b+p_{h.b}=p_a+p_{h.a} \qquad (2.15)$$

where $p_{h.b} = a^2 p_{h.a}$.

For compressible liquids when the values of the coefficient c ($c < 0.05$ at $a < 1$ and $c < 0.03$ at $a > 1$) are small, we can take pv = const and use the following equation to determine hydrodynamic pressure after the reducer

$$p_{h.b} = \frac{a^2 p_{h.a} p_a}{(p_a + p_{h.a}) - p_{h.b}} \tag{2.16}$$

The equation can be easily solved by trial and error method. After solving the equation we find p_b from equation (2.15) and $v_b = 2g \frac{p_{h.b}}{m_b^2} 10^4$.

For $c > 0.03$ to 0.05 the specific volumes v_b and other parameters after the reducer should be calculated with consideration for the change in velocity. Here, we consider the actual process as the sum of two processes—pressure loss in local resistance and expansion (or compression) in an ideal nozzle in which the mass velocity changes from m_a to m_b. Based on equation (2.4), as applied to the accepted designations, we can write

$$p_a v_a + \frac{k-1}{k} p_{h.a} v_a = p_b v_b + \frac{k-1}{k} p_{h.b} v_b$$

Hence, using the above mentioned dimensionless coefficients a, c, β and remembering that $p_b = \beta^{-k} p_a$ for an adiabatic process and after transformation, we get the equation from which the ratio β can be found:

$$a^2 c \beta^2 + \frac{k}{k-1} (\beta^{1-k} - 1) = c \tag{2.17}$$

After finding β all the parameters after the reducer are determined from

$$v_b = \beta v_a; \quad p_b = \beta^{-k} p_a; \quad p_{h.b} = a^2 \beta p_{h.a}$$

After the stagnation of an incompressible fluid ($a < 1$) (assuming $\xi = 0$) the equality

$$\frac{p_b + p_{h.b}}{p_a} = 1 + c$$

holds true. After the stagnation of a compressible fluid this equality does not hold true because of the decrease in specific volumes ($\beta < 1$) and b is introduced. Thus

$$\frac{p_b + p_{h.b}}{p_a} = 1 + c + b > 1 + c$$

in which b is a positive value, becoming greater with increase in the coefficient c and decrease in the coefficient a.

Now we shall take up some hydrodynamic calculation problems at critical velocities. For steam or a gas the critical velocity

$$w_c = \sqrt{2g \frac{k}{k+1} p_0 v_0 \cdot 10^4} = A \sqrt{p_0 v_0} \text{ m/s} \qquad (2.18)$$

or

$$w_c = \sqrt{g k v_c p_c \cdot 10^4} \text{ m/s} \qquad (2.19)$$

in which $A = 333$ for superheated steam and $A = 320$ to 323 for saturated dry steam (at $k = 1.08$ and $k = 1.135$); v_c and p_c are specific volume and pressure, respectively at critical flow velocity. The increase in velocity up to the critical value significantly lowers the enthalpy which for high initial steam parameters becomes 50 kcal/kg.

At critical flow the pressure p_c in the exist section is independent of the pressure p' in the space in which the efflux takes place. This is due to the fact that the velocity of propagation of pressure waves is equal to the velocity of sound. Hence, the critical flow is characterized by the pressure jump $\Delta p = p_c - p'$. Consequently it is not possible to determine the pressure p_c in the exit section of the pipe from p'. It is possible to accelerate the flow in pipes up to the critical velocity in two ways: (1) by efflux through a local contriction (arising slit in the safety valve, a limiting orifice plate, etc.; (2) by increasing the specific volumes of steam (gas) along a pipe of constant section; the flow velocity at the pipe outlet gradually attains its critical value. These ways of accelerating the fluent up to the critical velocity differ substantially from each other. When steam flows through an orifice the pressure p_c is determined only by the initial pressure. For superheated steam, $p_c = 0.546 p_1$

and for dry saturated steam, $p_c = (0.58 \text{ to } 0.59)\, p_1$ (at $k = 1.135$ and $k = 1.08$, respectively).

The actual process of flow through an orifice takes place as per the polytropic curve *1-b* shown in Fig. 2.2. deviating from the theoretical expansion adiabat (*1-a*, Fig. 2.2). Because of this, the actual discharge velocity does not reach the critical velocity but equals $w = \varphi w_c$, where φ = velocity coefficient, less than unity.

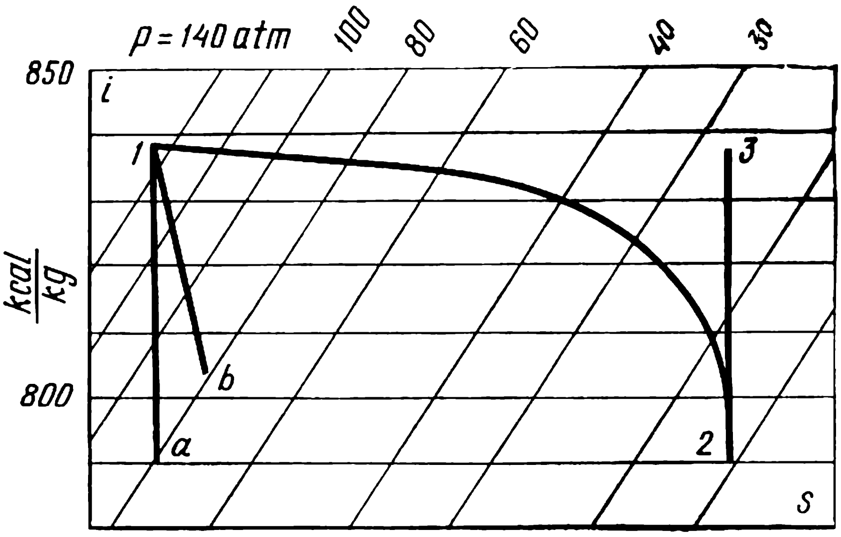

Fig. 2.2. *i-S* diagram representing different processes of increasing steam velocity up to critical velocity

For the critical discharge of saturated steam through an orifice the mass velocity

$$m_c = \frac{Q}{F} = 2.09\mu \sqrt{\frac{p_0}{v_0}} \text{ kg/(m}^2\cdot\text{sec)}$$

where μ is the coefficient of discharge. The curve *1-2* in Fig. 2.2 shows the steam flow acceleration up to the critical velocity at the end of the pipe. The process in the beginning of the pipe is similar to the isoenthalpic one, gradually becomes isoentropic and at the end of the pipe becomes isoentropic. The decrease in pressure during this process may attain any value, but as is seen from the diagram 2.2 this drop is always more than the one for the discharge through an orifice.

The hydrodynamic pressure at the critical discharge rate can be determined from the equality (2.19):

$$p_{h.c} = \frac{w_c^2}{2gv_c \cdot 10^4} = \frac{k}{2}\, p_c \text{ kg/cm}^2 \tag{2.20}$$

This simple relationship between the hydrodynamic and piezometric pressures at the critical discharge rate enables a number of other relationships to be found. Thus, from equations (2.20) and (2.18) the relationship between pressure p_c and mass velocity m_c can be obtained:

$$p_c = \frac{2}{k} p_{h.c} = m_c \frac{A}{\text{kg} \cdot 10^4} \sqrt{p_0 v_0} \ \text{kg/cm}^2 \qquad (2.21)$$

where A has the same value as in formula (2.18).

Substituting the equality (2.20) in equation (2.7), we get an equation that gives the ratio of specific volumes when the discharge rate at the pipe end is critical

$$\beta_c^2 = \frac{2k}{k+1} \xi + 1 + 2 \ln \beta_c \qquad (2.22)$$

This equation indicates that the ratio of critical volumes β_c when the discharge rate at the pipe end is critical depends only on the total coefficient of resistance ξ. The value of ξ in this case should be reduced to the flow area of that section of the pipe in which the velocity is critical (this fact should be taken into account when the pipeline consists of different diameter pipes connected in series). The value β_c is the maximum possible ratio of specific volumes (at known ξ), and, if at given values of p_1, v_1 and ξ it turns out that $\beta > \beta_c$, it indicates that the initial conditions are inconsistent, i.e. at given values of p_1, v_1 and ξ it is not possible to attain the prescribed value of m.

Substitution of (2.20) in equation (2.13) gives the equation for determining p_1 at the end of a pipe when the flow velocity is critical:

$$p_1 = \left(\frac{k+1}{2} \beta_c - \frac{k-1}{2\beta_c} \right) p_c \qquad (2.23)$$

From this formula and formula (2.21) the following relationship between the critical mass velocity m_c and the pressure p_1 at the beginning of the pipeline can be obtained:

$$m_c = \frac{p_1 \cdot 10^4}{\left(\frac{k+1}{2kg} \beta_c - \frac{k-1}{2kg} \cdot \frac{1}{\beta_c} \right) A \sqrt{p_0 v_0}} \ \text{kg/(m}^2 \cdot \text{sec)} \qquad (2.24)$$

in which A has similar values as in formula (2.18). Formula (2.24) is for calculating the flow rate through blow-off pipelines.

The velocity can attain a critical value not only at the end of an exhaust pipe or a pipe connected to a vessel (expander) and also on changing to a large diameter pipe. Formulas (2.18) through (2.24) are also valid for this case, but the increase in pressure due to stagnation (decrease in velocity) must be in accordance with equations (2.15) and (2.16), i.e.:

$$p_b + p_{h.b} \geqslant p_{h.b}\xi_b + p' \qquad (2.25)$$

in which p'—additional head generated due to the resistance offered by subsequent portions of the piping and back pressure at the end of the pipe.

For a decelerating jet of superheated steam flowing out of a pipe at critical velocity, if the deceleration takes place without any losses and the ratio of mass velocities a is less than 0.7, the following ratio is obtained:

$$p_b + p_{h.b} = 1.83 p_a = \frac{1}{0.546} p_a$$

Thus, at total stagnation ($p_{h.b} = 0$) the pressure increases up to the initial pressure when flow takes place through an orifice. The deceleration process is shown in Fig. 2.2 by line *2-3*.

All the obtained formulas take into account the change in enthalpy and specific volumes due to the change in velocity.

In the solution of certain problems one must know how to determine the specific volume v_2 at the end of a pipe employing either the given values of p_1, p_2, v_1, ξ and the unknown m or the given values of p_2, p_0, v_0, m and unknowns p_1, v_1.

In the first case, one must find the ratio of specific volumes $\beta = v_2/v_1$ from the given pressure ratio $\alpha = p_1/p_2$. For α values close to unity, $\beta \approx \alpha$. The ratio α is maximum (at given ξ) when the flow velocity is critical at the end of the pipe.

In this case, as is clear from formula (2.23) $\beta_c \approx \frac{2}{k+1}\alpha_c$. For intermediate values of α it may be assumed that the change takes place as per the square-law, *viz.*

$$\beta=\alpha\left[1-\frac{k-1}{k+1}\left(\frac{\alpha}{\alpha_c}\right)^2\right]=\alpha\left[1-\frac{4(k-1)}{(k+1)^3}\left(\frac{\alpha}{\beta_c}\right)^2\right] \qquad (2.26)$$

This formula is not very exact and gives an error not exceeding 0.5% at $\xi \geqslant 8$; at $\xi = 4$ the error increases to 2% and may be adjusted by making appropriate corrections. It may, however, be kept in mind that the error in determining mass velocity, as is clear from the structure of formula (2.8), is at least four times less than the error in determining β; taking this into account, formula (2.26) may be used for practical calculations when $\xi < 8$ down to $\xi = 2$ to 3.

To solve the second problem of calculating v_2 from the given values of p_2, p_0, v_0 and m one can write on the basis of equality (2.3) and keeping in mind that $v_2 = w_2/m$, the following equation:

$$v_2^2+2g\frac{k}{k-1}10^4\frac{p_2}{m^2}v_2-2g\frac{k}{k-1}10^4\frac{p_0v_0}{m^2}=0 \qquad (2.27)$$

The main disadvantage of this equation for solving practical problems lies in the necessity to find the square root with accuracy up to 4 or 5 numbers.

Equation (2.27), taking into account the equalities (2.18) and (2.21), may be presented as a function of one argument p_2/p_c—the ratio of pressures p_2 and p_c for critical flow velocity at the end of a pipe, *viz*:

$$\left(\frac{w_2}{w_c}\right)^2+\frac{2}{k-1}\cdot\frac{p_2}{p_c}\left(\frac{w_2}{w_c}\right)-\frac{k+1}{k-1}=0 \qquad (2.28)$$

The function in this form was used to plot the graph shown in Fig. 2.9 to obtain the specific volume v_2 from the calculated velocity w_2 and ratio p_2/p_c.

2.2. Resistance Coefficients

Pressure losses are proportional to the product of hydrodynamic pressure $p_h = \frac{w^2}{2gv\cdot 10^4} = \frac{m^2v}{2g\cdot 10^4}$ and the dimensionless coefficient ξ. The two forms of pressure losses are differentiated, one due to friction as the fluid flows through the pipe, and the other due to local resistances from a change in the magnitude and direction of flow velocity.

The friction resistance coefficient is equal to:

$$\xi = \frac{\lambda}{d_r} L \tag{2.29}$$

in which λ is the friction factor as the fluid flows through pipes; L—total length of a pipeline including straight and curved elements, welded elbows and tees, m; d_r—rated internal pipe diameter, m.

The friction factor is the function of the Reynolds number and the relative equivalent roughness of the pipe. The Reynolds number

$$\mathrm{Re} = \frac{wd_r}{\nu} = \frac{md_r}{g\mu} \tag{2.30}$$

is a dimensionless criterion, in which m is the mass-flow rate, kg/(m^2·sec); μ—dynamic viscosity (kg·sec)/m^2; $\nu = g v \mu$—kinematic viscosity, m^2/s.

The viscosity of fluids is given in reference books; for water and water steam in Steam and Water Thermodynamic Tables [2-2]. For steam dynamic viscosity tables are more convenient as the kinematic viscosity sharply changes with variations in pressure and temperature, which makes interpolation difficult.

The value $\varepsilon = \frac{2k_e}{d_r}$ is taken as the relative roughness, but often in calculations the pipe characteristic $\frac{d_r}{k_e}$ is used. Here, d_r is the rated internal pipe diameter, mm; k_e—absolute equivalent roughness, mm. The value of equivalent roughness for stationary installations of steel piping including the resistance of welded joints is taken as 0.2 mm for seamless pipes operating under normal conditions; as 0.3 mm, for welded pipes under normal working conditions and 0.55 to 0.65 mm, for pipes working under the condition of excessive corrosion (exhaust, discharge piping, etc.).

The friction factor λ depends upon the nature of the fluid flow determined by the Reynolds number. In the laminar flow range the Reynolds number is small, and the friction factor varies in inverse proportion to velocity, and therefore, pressure losses increase proportional to the velocity of first degree. With a large Reynolds number the flow is turbulent, the factor λ is independent of velocity and the pressure losses increase proportionally to the square of the velocity. A transition zone exists between these values in which the friction factor λ is determined by a complex function between Re and d_r/k_e. The Reynolds number $\mathrm{Re}_1 = 2300$ separates the laminar flow range from the transition zone. When the Reynolds number is less than 2300, for circular pipes the friction factor λ may be determined from the following:

$$\lambda = \frac{64}{\mathrm{Re}} \tag{2.31}$$

For pipes carrying viscous fluids, such as oil and fuel oil, the Reynolds number is less than 2300.

The Reynolds number for the upper limit of the transition zone is given by

$$\mathrm{Re}_2 = \left(120 \frac{d_r}{k_e}\right)^{1.125} \tag{2.32}$$

When $\mathrm{Re} > \mathrm{Re}_2$ the friction factor λ is independent of the Reynolds number and is determined from the formula

$$\lambda = \frac{1}{\left(1.14 + 2 \log \frac{d_r}{k_e}\right)^2} \tag{2.33}$$

or from the graph shown in Fig. 2.3. In the transition zone when $\mathrm{Re}_1 < \mathrm{Re} < \mathrm{Re}_2$ the factor λ should be taken from the Fig. 2.3.

In the stationary installation piping the flow velocities of steam and water at rated discharge are taken, as a rule, on the basis that the flow is turbulent and formula (2.33) is applicable. Exceptions can be pipelines carrying steam at pressures less than 2 atm or water at low temperatures. Minimum flow velocities for which formula (2.33) is applicable can be determined from the graphs in Figs. 2.4 and 2.5. For velocities less than the velocities indicated on the graphs the Reynolds number and the friction factor λ must be taken from Fig. 2.3.

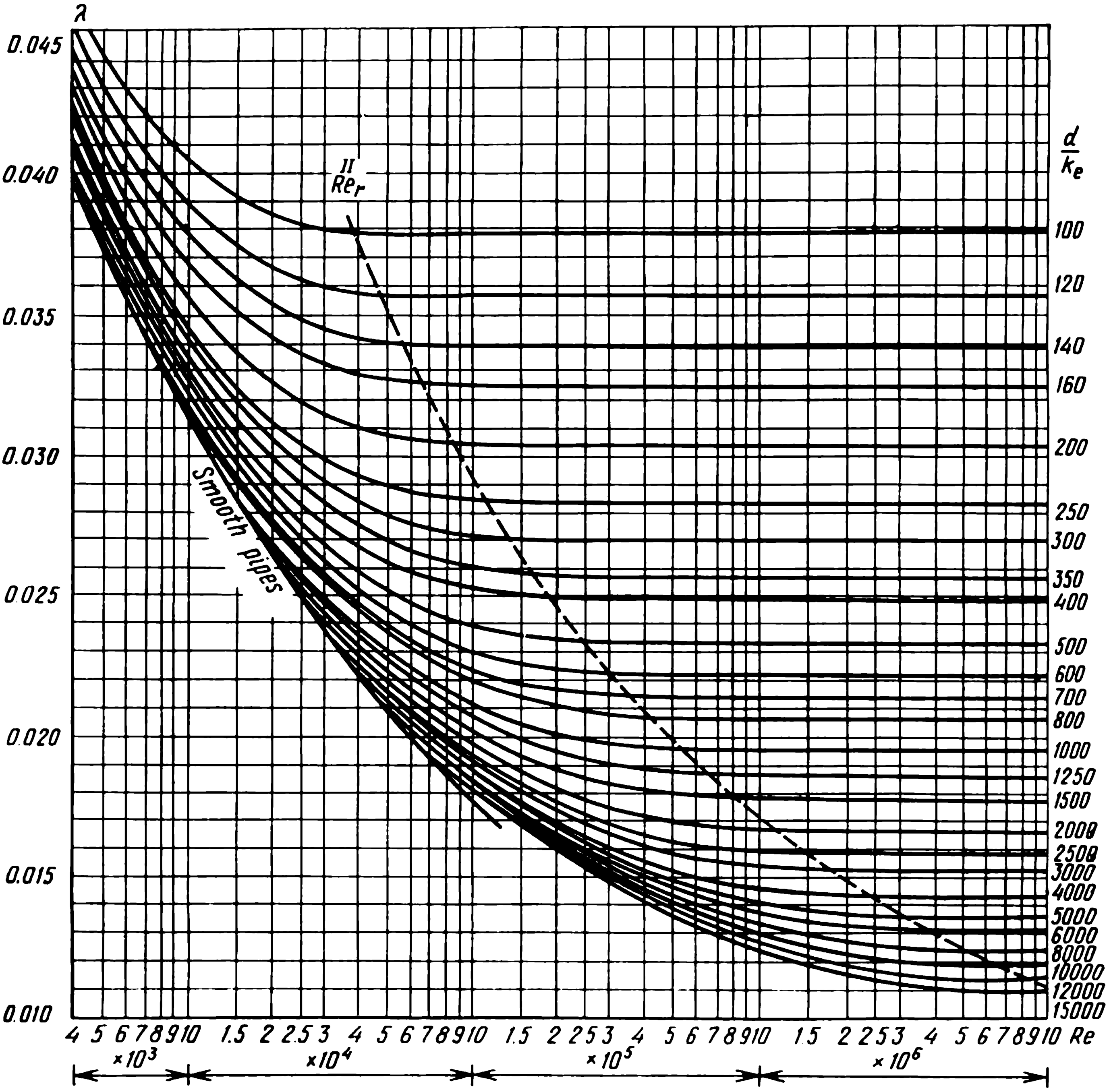

Fig. 2.3. Relation of friction factor λ for steel pipes, Reynolds numbers and pipeline characteristics (Reproduced from data of ВТИ)

Rated pipe diameters d_r and friction factors λ/d_r for a pipe one metre long are given in Appendix 3. In hydrodynamic calculations the design diameter is taken as

$$d_r = \left[D_n - s\left(2 + \frac{\Delta_1 + \Delta_2}{100}\right)\right] \cdot 10^{-3} \text{ m} \qquad (2.34)$$

in which D_n is the nominal external pipe diameter, mm; s—nominal pipe wall thickness, mm; Δ_1, Δ_2—positive and negative allowances for pipe wall thickness ($\Delta_2 < 0$), %.

With symmetrical allowances for pipe wall thickness ($\Delta_1 = -\Delta_2$) the rated diameter is equal to the nominal one. With unsymmetrical allowances ($\Delta_1 = 20\%$ and $\Delta_2 = -5\%$) the formula considers the adjustment limits of tube-rolling mills. For relatively thick-walled high-pressure pipes the rated diameter is decreased relative to the nominal size in steam pipelines with P_n 400 by 2.3 to 2.5% and in steam pipelines operating at 255 atm and 565°C up to 7%. To such diameter changes the losses increase to 13% in the first case and 40% in the second.

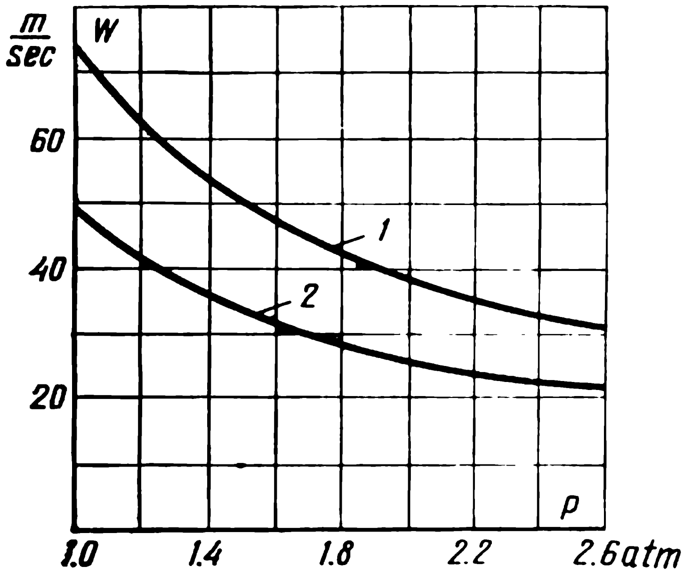

Fig. 2.4. Minimum steam velocities 1-2 atm at (t_s + 20)°C for which the turbulent flow formula is applicable

1—in seamless tubes; 2—in welded tubes

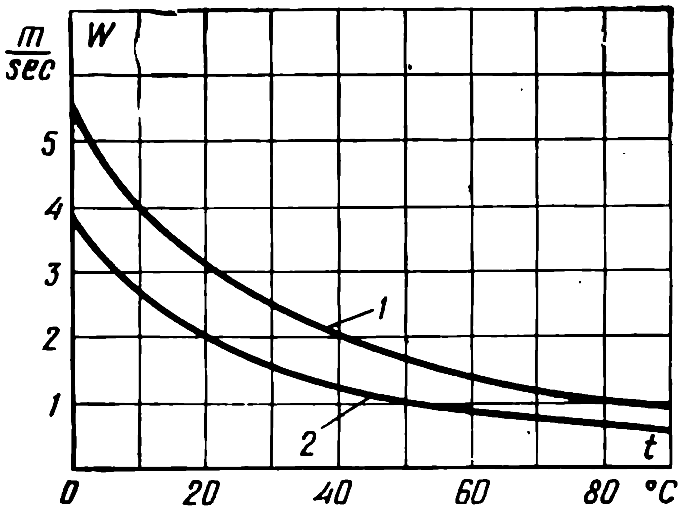

Fig. 2.5. Minimum velocities of cold water for which the turbulent flow formula is applicable

1—in seamless tubes; 2—in welded tubes

The coefficients of local resistances for fittings and valves of a piping system are given in Appendixes 3 through 18.

If fittings or accessories of different passage diameters d_i are installed on a pipeline of given rated diameter d_r, it is necessary to recalculate the coefficient of resistance at the velocity in the fitting relative to the velocity in the rated passage area d_r using the formula

$$\xi_r = \left(\frac{d_r}{d_i}\right)^4 \xi_i \tag{2.35}$$

in which ξ_i is the resistance coefficient for valves or fittings taken from reference books; d_i—actual or nominal diameter of valves or fittings.

Thus, when installing on a pipeline D_n 150 a valve regulating element $D_n = 100$ with a coefficient of resistance $\xi = 6$ its resistance coefficient at rated diameter $d_r = 0.150$ m should be taken equal to

$$\xi_r = \left(\frac{150}{100}\right)^4 \times 6 = 30.4$$

The coefficients of local resistances given in the tables are for level turbulent flows, i.e. in the absence of disturbances from other nearby resistances. Therefore, the use of tabulated data, strictly speaking, is possible only if there are straight portions 8 to 12 diameters long between different elements of resistances. In the absence of such straight portions, total coefficient of two neighbouring elements can be much more than the total coefficient of local resistances listed in the tables. The above mentioned should be taken into consideration when installing accessories or fittings of narrowed passage. The accessories or fittings are designed so that the increased by many times dynamic head in the gate cross section transforms into piezometric pressure in the diffuser and in the straight portion of the pipe; absence of straight portions of sufficient length in the vicinity of such a valve results in dynamic head losses in the neighbouring resistance, i.e. the coefficient of resistance for such fittings will be much more than given in the tables.

About the reference data in the tables on resistance coefficients may be mentioned the following:

Elbows and branch pipes were researched by many authors but their results differed widely, particularly, when evaluating the resistance coefficients of welded elbows. The most reliable results are those of the joint research work carried out by the All Union Scientific and Research Institute for the Pipeline Construction (ВНИИСТ) and of the Hydraulics Department of Moscow Institute of Urban Construction Engineers [2-7]. They studied and tested curved, steep curved and welded elbows of diameters from 75 to 300 mm. These tests revealed that for diameters between 250 and 300 mm the resistance coefficient for the steep curved elbows and for the welded elbows is more than for the normal bends by 15-20%, and 35-40% respectively. At the same time the resistance coefficient of small diameter (75 mm) welded elbows is approximately 3 times more than that of a smooth branch pipe. Data on resistance coefficients of elbows and branch pipes are listed in Appendix 4.

Tees were thoroughly investigated by V. N. Taliev and I. E. Idelchik [2-6 and 2-12]. The resistance coefficients depend on the flow diagram, the ratio between fluid flow in the side branch Q_b and total flow Q_c through the trunk line. The resistance coefficients of bends also depend upon the ratio between the passage areas of the side branch and the trunk line. All the resistance coefficients are reduced to the total (joined) flow velocity w_c. Appendix 5 gives the values of ξ for a number of Q_b/Q_c and F_b/F_c ratios as well as formulas to calculate ξ; these formulas are used for tees in pipelines (right angle between the side branch pipe and the trunk line, the branch pipe diameter is not more than the trunk line diameter).

It should be kept in mind that for small Q_b/Q_c values the resistance coefficient is negative from the side branch pipe to the trunk line, i.e. suction takes place in the trunk line. This is explained by the fact that an increase in hydrodynamic pressure between the side branch pipe and the combined flow in such cases takes place only due to the energy of the straight flowing main flux.

In many cases the passage diameter of a tee is greater or less than the pipe rated diameter d_r (in cast tees and also in welded ones); in such cases, the values of ξ calculated as per tabular data should be reduced to the rated diameter d_r obtained from formula (2.35).

For example, an equal passage tee P_n 400, D_n 200 (Fig. 2.6) (P_n—nominal pressure; D_n—nominal diameter) is manufactured to standard MBH 2601-63 by welding a pipe of passage diameter $d = 257$ mm squeezed at the ends to $d = 204$ mm and nozzle having passage diameter $d = 193$ mm and with its end bored out to $d = 204$ mm for welding. Determine the resistance coefficient when a fluid flows from the branch pipe into the trunk line at an input rate of $Q = 220$ tons/hr and an output rate of 170 tons/hr in section *a-a*.

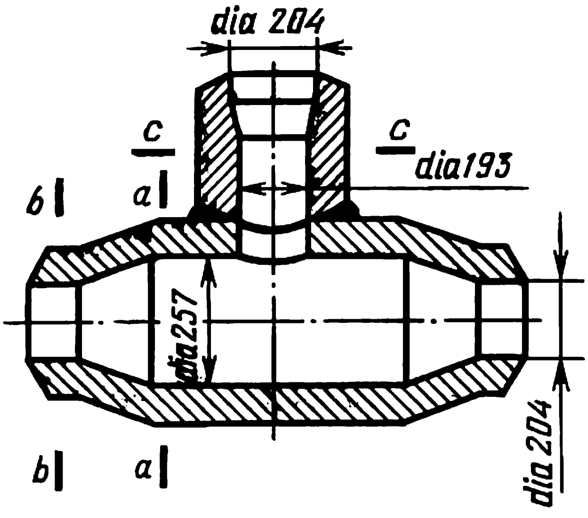

Fig. 2.6. Welded tee P_n 400 D_n 200

The total coefficient of resistance is the sum of resistances of the tee between sections *c-c* and *a-a* and the passage resistance between *a-a* and *b-b*.

From Appendix 5, para 4 the resistance coefficient of a tee is determined as follows:

$$\xi_{c \cdot b} = 1 + 0.3\left(\frac{Q_b d_c^2}{Q_c d_b^2}\right)^2 = 1 + 0.3\left(\frac{170}{220} \times \frac{193^2}{257^2}\right)^2 = 1.06$$

This coefficient is for section *c-c* having a diameter of 193 mm. As the tee is installed in a pipe 273 × 32 of design passage area $d_r = 204.2$ mm, the calculated coefficient of resistance at this diameter will be equal to

$$\xi = 1.06\left(\frac{204.2}{193}\right)^4 = 1.33$$

The conversion factor, from a diameter of 257 to 204 mm, from Appendix 6 is 0.075.

Total resistance $\xi = 1.33 + 0.075 = 1.4$.

When the calculation procedure permits to determine the resistance coefficient not at the combined flow rate, but at the branch pipe (or supply) rate the resistance coefficient should be recalculated from formula

$$\xi_{branch} = \xi_c \left(\frac{d_b}{d_c}\right)^4 \left(\frac{G_c}{G_b}\right)^2 \tag{2.36}$$

in which ξ_{branch} is the resistance coefficient at the branch flow rate; d_c, G_c—passage diameter and flow rate of fluid in the section of the combined flow; d_b, G_b—passage diameter and flow rate of fluid in the section of the branch (supply) flow.

The orifice plate can be calculated from the data given in Appendix 7. The resistance coefficient of orifice plate for steam is higher than that for incompressible liquids. This is because steam expands when it flows through the orifice. The resistance coefficient of orifice plate when steam or gas flows through it is a variable depending on the flow (mass-flow rate) and the adiabatic index.

To determine this coefficient, the well-known flow equation (2.8) and the graph between the irretrievable pressure losses Δp_o and the pressure drop $p_1 - p_2$ at the diaphragm were used. From these equations the following relationship can be obtained

$$\Delta p_o = \frac{\delta}{(\alpha\varepsilon)^2} \left(\frac{D}{d_o}\right)^4 p_{h1} = \xi_1 p_{h1} \text{ kg/cm}^2 \tag{2.37}$$

where ξ_1—resistance coefficient of the orifice plate at the hydrodynamic pressure in front of the washer; p_{h1}—hydrodynamic pressure in front of the orifice plate.

It is clear from (2.37) that coefficient ξ_1 depends on the discharge coefficient α for incompressible liquids, the coefficient of expansion ε, the coefficient of irretrievable losses δ and the ratio between the pipe diameter D and the orifice diameter d_o, the ratio is of the fourth power.

For orifice plate selection the necessary coefficient of resistance ξ_1 and the ratio $\Delta p_o/p_1$ are taken from the graph. An illustrative example is given in Sec. 2.4.

2.3. Hydrodynamic Calculations of Pipelines for Small Specific Volume Changes

To pipelines with small specific volume changes pertain: (1) pipelines carrying liquids at constant specific volume, i.e. effervescence phenomena is absent; (2) steam pipes and gas pipes in which the specific volume variation does not exceed $\beta = 1.6$ or the pressure loss does not exceed 40% of the initial pressure.

Generally, hydrodynamic calculations are made to determine the pressure p_2 at the end of a pipe when the parameters at the beginning and the flow rate are known. The fluid velocity in a pipe is determined from the formula

$$w = 0.354 \frac{Gv}{d_r^2} \text{ m/sec} \tag{2.38}$$

in which G is the flow rate, tons/hr; v—specific volume of liquid, m^3/kg; d_r—rated diameter for the existing assortment, is taken from Appendix 3 or calculated from formula (2.34), m.

The hydrodynamic pressure at the beginning of a pipe is determined from formula

$$p_{h1} = \frac{w_1^2}{2gv_1 \cdot 10^4} \text{ kg/cm}^2 \tag{2.39}$$

The pressure p_2 at the end of a constant diameter pipe carrying incompressible liquid is determined from the formula

$$p_2 = p_1 - p_{h1}\xi - \frac{1}{v \cdot 10^4}(H_2 - H_1) \tag{2.40}$$

in which p_1 is the pressure at the beginning of the pipe; $H_2 - H_1$—difference in the start and end levels of the pipe, m; ξ—total resistance coefficient. This is equal to $\xi = \frac{\lambda}{d_r} L + \sum \xi_l$.

Here, λ/d_r is the frictional coefficient of a pipe 1 m long; L—total length of the piping route including elbows, bends and other fittings, m; $\sum \xi_l$—total coefficient of local resistances.

Since the hydrodynamic pressure along a pipeline does not change (w and v are constant), in formula (2.40) it is not necessary to take into account neither the hydrodynamic pressure of the incoming fluid nor losses due to exit velocity (i.e. the coefficient $\xi = 1$, which takes into account exit losses, should not be included in the total coefficient of resistance).

The resistance coefficients of measuring orifice plates and nozzles are determined based on irrecoverable pressure losses in accordance with known contraction dimensions. For preliminary calculations when the measuring devices are yet to be selected

$$\xi_o = \frac{0.3}{p_{h.r}}$$

in which $p_{h.r}$ is the hydrodynamic pressure for the rated (maximum) flow.

Steam pipelines and gas pipelines are calculated from the following simplified formulas obtained from equations (2.6), (2.7) and (2.12), (2.13):

$$p_2 = p_1 \sqrt{1 - 2\frac{p_{h1}}{p_1}\xi\left(1 + 2.5\frac{p_{h1}}{p_1}\right)} \text{ kg/cm}^2 \quad (2.41)$$

$$p_1 = p_2 \sqrt{1 + 2\frac{p_{h2}}{p_2}\xi\left(1 + \frac{p_{h2}}{p_2}\right)} \text{ kg/cm}^2 \quad (2.42)$$

$$\beta = \alpha - n\alpha(\alpha^2 - 1)\frac{p_{h1}}{p_1} = \alpha - n\left(\alpha - \frac{1}{\alpha}\right)\frac{p_{h2}}{p_2} \quad (2.43)$$

in which p_{h1} and p_{h2} is the hydrodynamic pressure in the beginning and end of the pipe, kg/cm^2; $\alpha = p_1/p_2$, $\beta = v_2/v_1$—ratios of pressures and specific volumes; $n = \frac{k-1}{k}$ —coefficient which depends on the adiabatic index k, for superheated steam $n = 0.23$, for saturated steam $n = 0.12$, for multiatomic gases $n = 0.25$ and for air $n = 0.285$.

The remaining notations are as in formula (2.40). The hydrodynamic pressure p_{h1} is calculated from formula (2.39), and $p_{h2} = \beta p_{h1}$.

Formulas (2.41), (2.42) and (2.43) give sufficiently correct results (error less than 0.5%) down to the ratio $\alpha = 2$ for the ratios p_{h1}/p_1 or $p_{h2}/p_2 < 0.03$, this far exceeds the maximum ratios used in actual practice.

For common velocities and pressure losses $p_{h1}/p_1 < 0.01$ and $\alpha < 1.2$, therefore may be taken $\beta = \alpha$.

In the case, when $\frac{p_{h1}}{p_1}\xi < (0.03 \text{ to } 0.04)$ take

$$p_2 = p_1 - p_{h1}\xi \quad (2.44)$$

When calculating steam pipelines it is convenient to use mass-flow rate

$$m = 0.354\frac{G}{d_r^2} = \frac{w}{v}\ \text{kg/(m}^2\cdot\text{sec)} \tag{2.45}$$

which keeps constant with a change in pressure.

The above listed design formulas hold true for a constant value of m. Many pipelines, even in block units, consist of portions joined in series having different mass-flow rates m, i.e. has sections of different diameters and different flow rates. Such pipelines are calculated by sections. In doing so the pressure at the beginning of every subsequent section should be taken with regard to the changes of dynamic pressures in reducers and tees, i.e.

$$p_{b1} = p_{a2} + p_{h.a2} - p_{h.b1} - \xi p_h \tag{2.46}$$

in which p_{b1}, $p_{h.b1}$ are piezometric and hydrodynamic pressures respectively at the beginning of section b (after the reducer, tee); p_{a2}, $p_{h.a2}$—piezometric and hydrodynamic pressures respectively at the end of the previous section a (up to the reducer); ξp_h—pressure drop in the reducer or tee.

Formula (2.46) is applicable for steam also when the dynamic pressures are 1 to 2% of pressure p_{a2}. An example of such a calculation is given below.

In certain cases, it is necessary to determine flows of fluids in parallel pipelines. The flow distribution is determined from the formula

$$\frac{G_1}{G_2} = \sqrt{\frac{\xi_2}{\xi_1}} \tag{2.47}$$

where ξ_1 and ξ_2—resistance coefficients of the first and the second sections, respectively, reduced to one rated diameter according to formula (2.35).

The flow distribution problem is solved by the method of successive approximations as it is necessary to correct the resistance coefficients of tees whose values depend upon the flow distribution pattern.

According to their function, pipelines with small specific volume variations pertain to those for which the designed flow rate is known beforehand. Therefore, it is not necessary

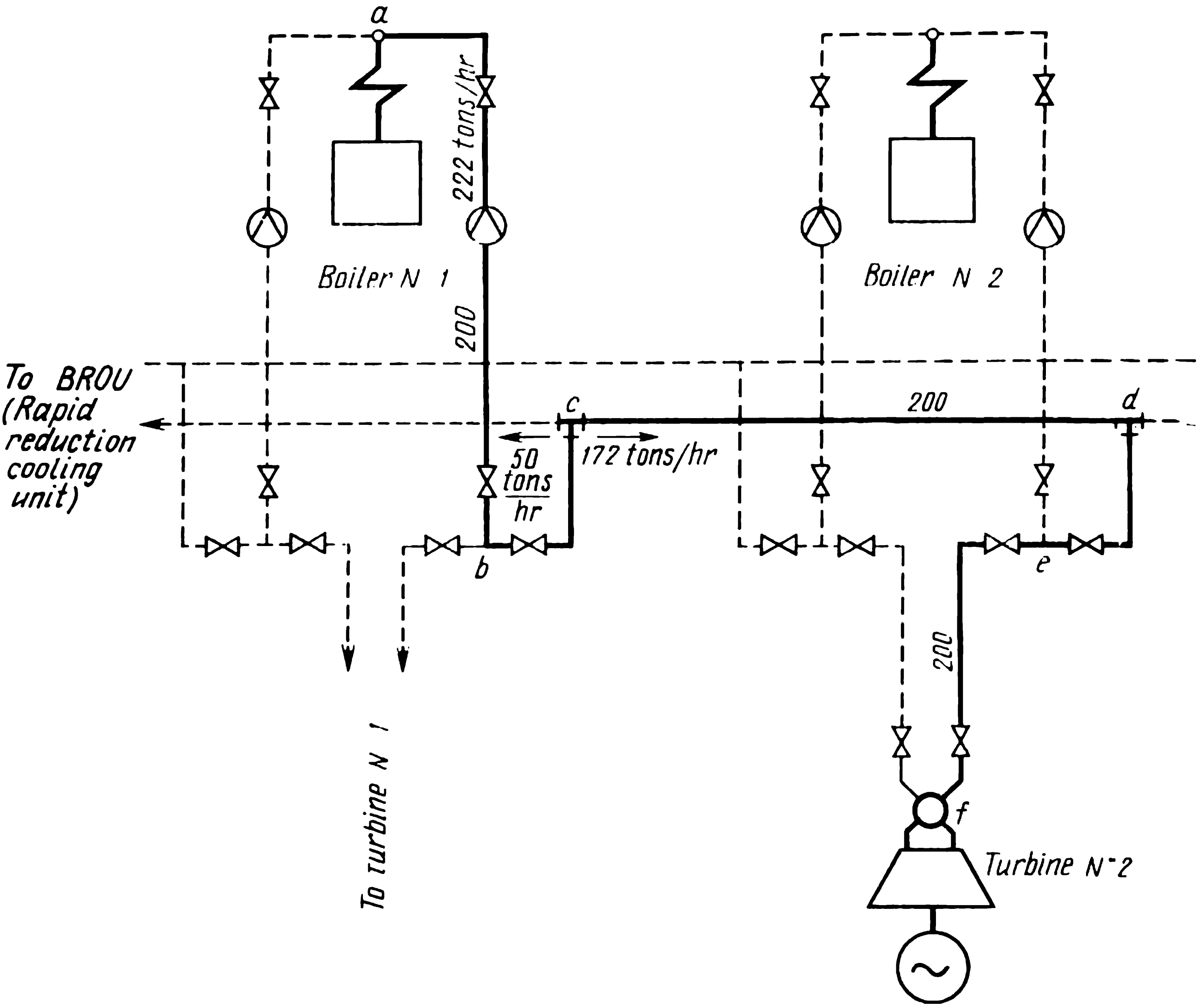

Fig. 2.7. Schematic of main steam line used for hydrodynamic calculation

to determine the flow-carrying capability of such pipes with reference to normal regimes, but a need may arise when investigating the work of pipelines and equipment in emergencies. However, in such cases either the fluid initial or the end parameters change significantly, and the pipeline is recalculated as a pipe with large specific volume changes of the flowing fluid.

Example 1. Hydrodynamic calculations of the main steamline for a heating and power plant.

Determine the pressure drop in the steamline with 140 atm 570°C when feeding turbine No. 2 from boiler No. 1 through a cross connector. The flow diagram is shown in Fig. 2.7. The rate of steam flow in the section *a-b-c* is 222 tons/hr, from tee-bend to turbine—172 tons/hr. The piping system is made from 273 × 32 mm pipes.

The design passage diameter from Appendix 3 is 0.2042 m.

The tees *b*, *c*, *d* are welded tees (Fig. 2.6). Their resistance coefficients are obtained from Appendix 5 as the example given in Sec. 2.2. The flow rate ratio $Q_b/Q_c = 1$ for tees *a* and *b*, and 0.78 for the tee *c*.

The resistance coefficients are given in Table 2.1.

Table 2.1

Piping elements	Coefficient of resistance for one element	Portion *a-b-c*		Portion *c-d-e-f*	
		Number of elements	Total coefficient of resistance	Number of elements	Total coefficient of resistance
90° elbow	0.2	9	1.80	11	2.20
60° elbow	0.15	1	0.15	—	—
45° elbow	0.12	1	0.12	—	—
Gate valve BA3 B-310	0.4	3	1.20	3	1.20
Tee	1.5	1	1.50	—	—
Tee	1.38	1	1.38	—	—
Tee	1.54	—	—	1	1.54
Tee (in the passage) . .	0.11	—	—	2	0.22
Reducer 257/204	0.075	—	—	1	0.08
Measuring devices . . .	—	1	0.64	1	0.74
Pipe (1 m long)	0.0956	82.1	7.85	86	8.22
Total	—	—	14.64	—	14.20

The resistance coefficient of measuring devices has been based on irrecoverable losses of 0.3 kg/cm², and the hydrodynamic pressure p_{h1} in the section *a-b-c* of 0.472 kg/cm² for the flow rate of 222 tons/hr; for section *c-d-e* it is based on the hydrodynamic pressure of 0.41 kg/cm² for the flow rate of 200 tons/hr and parameters 130 atm, 565°C.

Calculation of section *a-b-c*.

According to (2.45)

$$m = 0.354 \frac{222}{0.2042^2} \approx 1884 \text{ kg/(m}^2\cdot\text{sec)}$$

Specific volume $v_1 = 0.02609$ m³/kg.

Hydrodynamic pressure at the beginning of the pipe, according to (2.39), is

$$p_{h1}=\frac{1884^2\times 0.02609}{19.62\times 10^4}=0.472\ \text{kg/cm}^2$$

The ratio p_h/p_1 = 0.472:140 = 0.00338, and according to (2.41), we get

$$p_2=140\sqrt{1-2\times 0.00338\times 14.64\,(1+2.5\times 0.00338)}=$$
$$=132.86\ \text{atm}$$

Since $p_{h1}/p_1<0.01$, $\alpha<1.2$, we get

$$\beta=\alpha=\frac{140}{132.86}=1.054$$

The steam velocity at the pipe end is

$$w_2=\beta mv_1=1.054\times 1884\times 0.02609=$$
$$=1.054\times 49.2=51.8\ \text{m/sec}$$

and the hydrodynamic pressure equals

$$p_{h2}=\beta p_{h1}=1.054\times 0.472=0.498\ \text{kg/cm}^2$$

The specific volume at the end is v_2 = 1.054·0.02609 = = 0.0275 m^3/kg.

The flow rate for the section *c-d-e-f* is 172 tons/hr, therefore,

$$m=\frac{0.354\times 172}{0.2042^2}=1460\ \text{kg/(m}^2\cdot\text{sec)}$$

The hydrodynamic pressure p_{h1} can be determined from formula (2.16) at the ratio of mass velocities a = 1460:1884 = = 0.775

$$p_{h1}=\frac{0.775^2\times 0.498\times 132.86}{(132.86+0.498)-p_{h1}}=0.298\ \text{kg/cm}^2$$

and the pressure at the beginning of the section, from formula (2.46), will be

$$p_1=132.86+0.498-0.298=133.06\ \text{kg/cm}^2$$

The further calculations are as in the previous example, and β = 1.034 and p_2 = 128.8 kg/cm^2.

2.4. Hydrodynamic Calculations of Pipes with Large Steam Specific Volume Variations

Typical examples of hydrodynamic calculations of steam pipes with large specific volume variations of steam and large pressure drops can be the calculations of exhaust steam pipes from safety valves and expanders, calculations of the discharge capacity of steam pipes from the turbine to deaerators, calculations of the discharge capacity of blow-off steam pipes, calculations of restricting orifice used to reduce the discharge capacity.

For the great majority of such examples the critical flow velocity has to be considered. Hydrodynamic calculations have some particular features dealt with in Sec. 2.1. A definite value of the ratio $p_{h.c}/p_c$ for critical flow simplifies calculation formulas which are more convenient in use than the general ones. Because of this, the summary below contains both the general and special formulas for cases when the flow from the end of the pipe is critical. The following will serve as criteria to ascertain whether for a given case the flow is critical: (1) ratio of specific volumes $\beta = v_2/v_1$; (2) ratio of pressures $\alpha = p_1/p_2$; (3) pressure p_c of critical flow from the end of the pipe corresponding to known values of ξ and m.

The maximum possible values of β and α are the ratios β_c and α_c conforming to critical flow for a given value of ξ (formulas (2.22) and (2.23)). If the value β (or α) determined for the stipulated conditions of a problem turns out to be more than that of β_c (or α_c, respectively), it will indicate that at the end of the pipe the pressure $p_2 = p_c$ is more than the rated pressure $p_2 = p'$. The curves of coefficients β_c and α_c, which are the functions of the total coefficient of resistance ξ, are presented in Fig. 2.8.

The value of critical pressure p_c, as follows from (2.21), is a function of parameters m, p_0 and v_0; if the critical pressure calculated for given conditions is less than the pressure p' in the portion to whch the pipe end is fixed, then the flow will be subcritical; if $p_c > p'$, then the flow is a critical one. The use of any flow criteria (β_c, α_c, p_c) is made depending upon the conditions of a given problem.

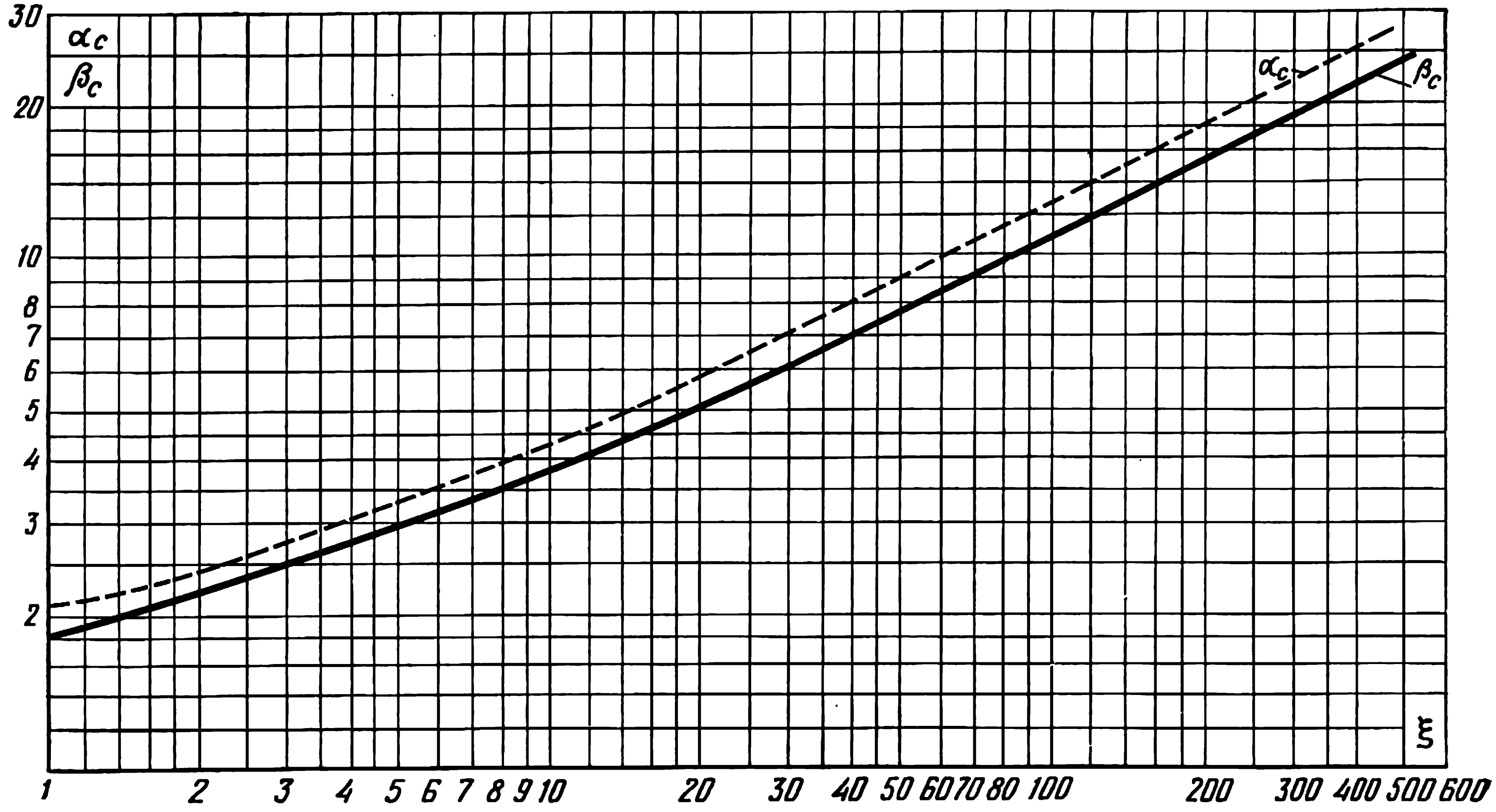

Fig. 2.8. Critical ratios of pressures $\alpha_c = p_1/p_2$ *vs* volumes $\beta_c = v_2/v_1$ with total pipe resistance coefficient ξ as parameter

Formulas for superheated steam with adiabatic index $k = 1.3$ are given below. It should be noted that the use of formulas for superheated or saturated steam is dictated not by initial steam parameters, but by the range of parameters within which steam flows. Thus, for dry saturated steam with initial pressure less than 30 atm the flow process line in the *i-s* diagram lies above the saturation curve, and such pipelines should be calculated using the formula for superheated steam. Calculation of saturated steam pipelines with large pressure drops is so rare that we shall not give formulas used for their calculations. Should the need arise, they can be derived from general formulas by substituting the appropriate adiabatic index.

Now we consider general cases of calculations, and formulas for superheated steam ($k = 1.3$). Here, as before, i_1, p_1, v_1 denote the parameters at the pipe beginning, and i_2, p_2, v_2 — parameters at the pipe end; i_0, p_0, v_0 — parameters when the velocity is close to zero, m — mass velocity, kg/(m^2·sec); p' — pressure in the portion to which the pipe end is fixed; pressure is measured in kg/cm^2 and specific volume in m^3/kg.

1. Formulas for determining p_1, v_1 at given values of m, ξ, p_0, v_0 and p'.

To determine the nature of flow the pressure p_c corresponding to the critical flow from the pipe end is calculated as follows:

$$p_c = 26.1 \times 10^{-4} m \sqrt{p_0 v_0} \text{ atm} \qquad (2.48)$$

Case 1. $p_c < p'$, therefore, pressure at the end of a pipe is $p_2 = p'$.

The specific volume is determined from the equation

$$v_2^2 + 84.8 \cdot 10^4 \frac{p_2}{m^2} v_2 - 84.8 \cdot 10^4 \frac{p_0 v_0}{m^2} = 0 \qquad (2.49)$$

or from the formula

$$v_2 = \frac{w_c}{m} \left(\frac{p_c}{p_2} + f \right) \text{ m}^3\text{/kg} \qquad (2.50)$$

in which w_c is calculated from formula (2.18), and f is determined from the graph shown in Fig. 2.9.

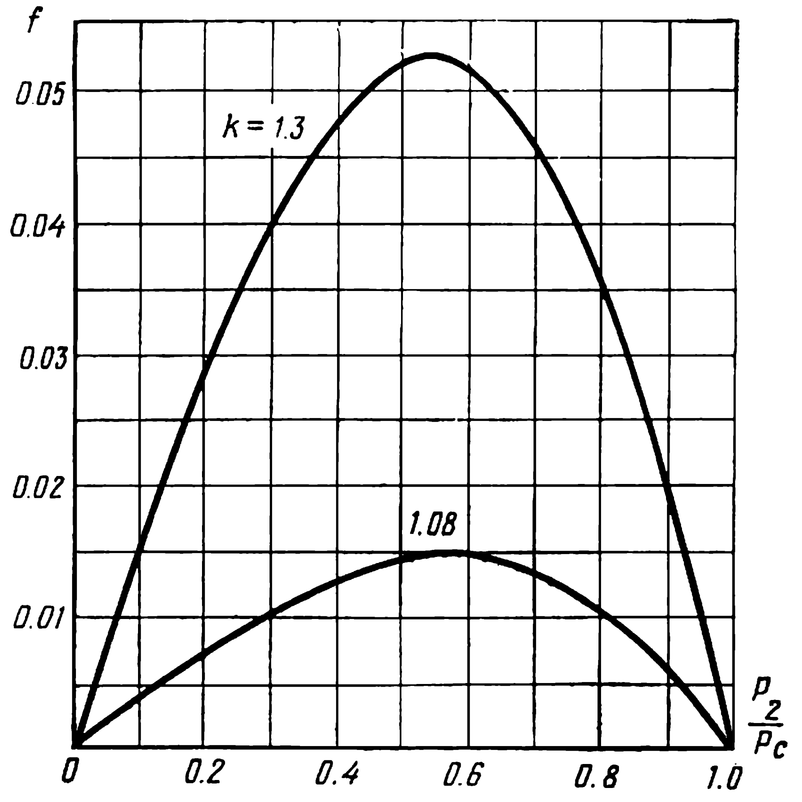

Fig. 2.9. Graph for determining coefficient f appearing in formula (2.50)

The hydrodynamic pressure is calculated as follows:

$$p_{h2}=\frac{m^2 v_2}{2g \cdot 10^4}\ \text{kg/cm}^2 \qquad (2.51)$$

and thereafter the ratio of specific volumes $\beta = v_2/v_1$ is determined from the equation

$$\left(\frac{p_2}{2p_{h2}}+0.115\right)(\beta^2-1)=\xi+4.07\log\beta \qquad (2.52)$$

and the parameters at the beginning of the pipe are found as

$$v_1=\frac{v_2}{\beta};\quad p_1=\beta p_2+0.23\left(\beta-\frac{1}{\beta}\right)p_{h2}\ \text{kg/cm}^2 \qquad (2.53)$$

Case 2. $p_c \geqslant p'$, pressure at the pipe end should be taken as $p_2 = p_c$.

The ratios α_c and β_c are determined from the graph shown in Fig. 2.8. and then

$$p_1=\alpha_c p_c; \qquad v_1=\frac{v_2}{\beta_c}$$

are calculated.

The values of these ratios can be found from the following formulas:

$$\beta_c^2 = 1.13\xi + 1 + 4.6 \log \beta_c \tag{2.54}$$

$$\alpha_c = 1.15\beta_c - \frac{0.15}{\beta_c} \tag{2.55}$$

II. Formulas for determining p_2, v_2 from the given values of p_1, v_1, m, ξ.

The ratio of specific volumes β is calculated from the following formula:

$$\left(\frac{p_1}{2p_{h1}} + 0.115\right)\left(1 - \frac{1}{\beta^2}\right) = \xi + 4.07 \log \beta \tag{2.56}$$

and is compared with the critical ratio β_c determined from the graph presented in Fig. 2.8 or calculated from formula (2.54).

Case 1. $\beta < \beta_c$—the flow is subcritical and the parameters at the end of a pipe are calculated from the formula

$$p_2 = \frac{p_1}{\beta} - 0.23\left(\beta - \frac{1}{\beta}\right) p_{h1} \text{ kg/cm}^2 \tag{2.57}$$

Case 2. $\beta = \beta_c$—the flow is critical and, in this case, $p_2 = p_c$ is determined from formula (2.48);

$$p_{h2} = 0.65 p_c \tag{2.58}$$

Case 3. $\beta > \beta_c$—the task is not possible, since at the given parameters p_1, v_1 and ξ the given mass velocity m can not be attained.

III. Formulas for determining m from the given values of p_1, v_1, i_1, ξ and pressure p'.

The given ratio of pressures $\alpha' = p_1/p'$ is compared with the critical pressure ratio α_c which is determined from Fig. 2.8 or calculated through the use of formulas (2.54) and (2.55).

Case 1. $\alpha' < \alpha_c$, therefore, the pressure at the end is more than the critical one, $p_2 = p'$ and $\alpha' = p_1/p'$.

Value of β is determined from the approximate formula

$$\beta = \alpha\left[1 - 0.1\left(\frac{\alpha}{\beta_c}\right)^2\right] \tag{2.59}$$

where the value of β_c is taken from the graph (Fig. 2.8).

The mass velocity is determined from the formula

$$m=\sqrt{\frac{(p_1-p_2)(1+\beta)\,g\cdot 10^4}{(\xi+\sigma)\,\beta v_1}}\ \text{kg/(m}^2\cdot\text{sec)} \tag{2.60}$$

in which

$$\sigma=0.115\left(\beta-\frac{1}{\beta}\right)+4.07\log\beta \tag{2.61}$$

takes into account the difference in the coefficients of hydrodynamic pressures at the entrance and exit, the coefficients are reduced to the mean velocity.

Having determined m the specific volume v_2 is verified through the use of formula (2.49) or (2.50) and the value of β checked.

Case 2. $\alpha' > \alpha_c$, therefore, the pressure at the end is critical: $p_2 = p_c > p'$. Here,

$$m=\frac{p_1\cdot 10^4}{\left(30\beta_c-\frac{3.9}{\beta_c}\right)\sqrt{p_0v_0}}\ \text{kg/(m}^2\cdot\text{sec)} \tag{2.62}$$

where β_c is found from Fig. 2.8 or formula (2.54).

The calculation of pressure drop in a pipeline with different mass velocities in different sections is carried out section by section, assuming the mass velocity m to be constant. In this case, the steam parameters at the beginning of the next section (after a reducer or tee) should be determined based on equations (2.15), (2.16), and (2.17). For superheated steam ($k = 1.3$) these equations become

$$a^2c\beta^2+4.333\,(\beta^{-0.3}-1)=c \tag{2.63}$$

$$p_b=\beta^{-1.3}p_a \tag{2.64}$$

in which $a^2=\left(\frac{m_b}{m_a}\right)^2$; $c=\frac{p_{ha}}{p_a}$; m_a and m_b —mass velocities in cross sections a and b; p_a and $p_{h\cdot a}$—given piezometric and hydrodynamic pressures in cross section a; $p_{h\cdot b} = a^2\beta p_{h\cdot a} = a^2\beta c\, p_a$—hydrodynamic pressure in cross section b; p_b—piezometric pressure in the cross sections b; $\beta = v_b/v_a$—ratio of specific volumes in cross section a and b. The index "a" corresponds to the parameters of that cross section in which they are known, and the index "b" to the cross section where the parameters are to be determined, Equations (2.63) and (2.64), which do not take into account pressure losses due to the hydrodynamic resistance of the reducer, are used to determine parameters after and before the reducer, as well as to solve the inverse problem.

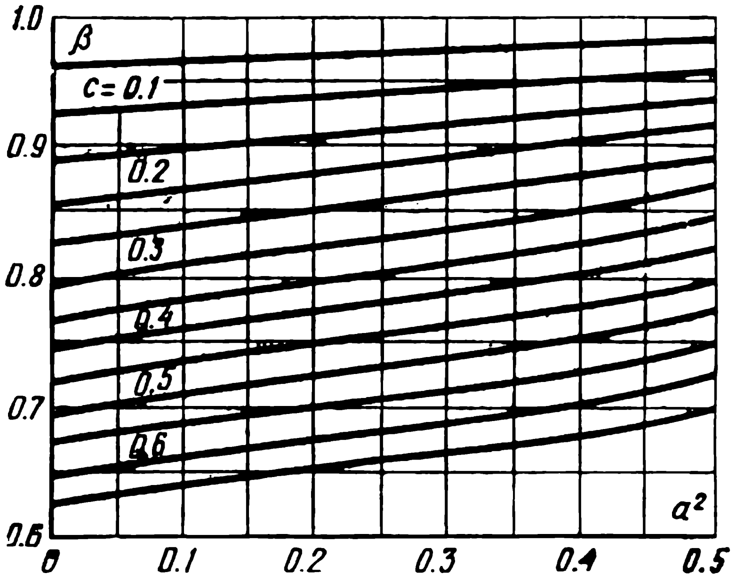

Fig. 2.10. Relation of volume ratio β, ratio of mass velocities $a < 1$ and relative pressure $c = p_{h-a}/p_a$ $(k = 1.3)$

To simplify the calculation curves are given in Fig. 2.10 for determining β for $\alpha < 1$, and in Fig. 2.11 for superheated steam when $\alpha > 1$.

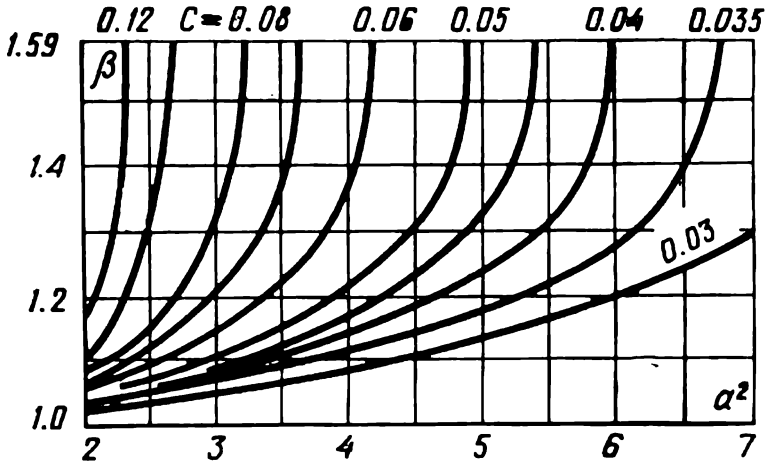

Fig. 2.11. Relation of volume ratio β, ratio of mass velocities $a > 1$ and relative hydraulic pressure $c = p_{h-a}/p_a$ $(k = 1.3)$

Hydrodynamic pressure in a reducer or a tee varies proportionally not only to $a^2 = (m_b/m_a)^2$, but also to the ratio $\beta = v_b/v_a$. When experimentally determining local resistance coefficients the specific volumes change insignificantly and the coefficient β is close to unity, in this case β can also differ significantly from unity as is clear from Figs. 2.10 and 2.11. For this reason the pressure decrease caused by local resistance should be determined from the mean specific volume. This can be done if half of the reducer's resistance coefficient (or of tee) is included in the total resistance coefficient of the previous section, and by adding half of the resistance coefficient to the sum of resistance coefficients of the section after the reducer (tee). It is self-evident that in this case the reduced coefficient of resistance calculated from formula (2.14) should be considered.

Example 1. A 150/205 mm reducer is installed in an exhaust pipeline. The coefficient of resistance reduced to $d_r = 0.150$ m is equal to $\xi_{rd} = 0.06$.

The steam parameters before the reducer are $p_a = 4.00$ atm and the hydrodynamic pressure $p_{h.a} = 1.0$ kg/cm².

In the total coefficient of resistance of the pipe nominal size $D_n = 150$ was included 50% of the reducer's resistance coefficient. Thus, it equals $\xi_{rd} = 0.5 \times 0.06 = 0.03$ (if this had not been done the rated pressure before the 150/205 reducer would have been more by $0.03 \times 1.0 = 0.03$ atm, i.e. it would have equalled 4.03 atm).

The dimensionless parameters of the reducer are:

$$c = \frac{p_{h.a}}{p_a} = \frac{1.0}{4.0} = 0.25 \quad \text{and} \quad a^2 = \left(\frac{150}{205}\right)^4 = 0.285$$

From Fig. 2.10, $\beta = 0.862$ and accordingly the parameters beyond the reducer will be:

$$p_b = \beta^{-1.3} p_a = 0.862^{-1.3} \times 4 = 4.86 \text{ atm}$$

and

$$p_{h.b} = a^2 \beta p_{h.a} = 0.285 \times 0.862 \times 1.0 = 0.246 \text{ kg/cm}^2$$

The reducer's coefficient of resistance should be included in the total resistance coefficient of the pipe D_n 200

$$0.5\xi_{rd} \cdot \frac{1}{a^2} = 0.5 \times 0.06 \frac{1}{0.285} = 0.105$$

Pressure losses caused by this resistance are equal to $0.105 \times 0.246 = 0.026$ kg/cm² and will be taken into account in the hydrodynamic calculations of the pipe D_n 200.

Thus, for the above mentioned conditions the pressure in the reducer increases from $4.00 + 0.03 = 4.03$ atm to $4.86—0.026 = 4.834$ atm, i.e. by 0.804 kg/cm^2.

Example 2. In the exhaust pipeline assuming its end is open to the atmosphere the pressure beyond the 150/205 mm reducer was found equal to 4.86 atm (including the pressure caused by the reducer's resistance, which is equal to $0.5\xi\,\frac{1}{a^2} = 0.105$) and the hydrodynamic pressure at the beginning of the D_n 200 pipe was 0.246 kg/cm^2.

The section after the reducer we shall call a, and hence $p_a = 4.86$ atm, $p_{h.a} = 0.246$ kg/cm^2.

$$c = \frac{0.246}{4.86} = 0.0505; \qquad a^2 = \left(\frac{205}{150}\right)^4 = 3.5$$

From Fig. 2.11, $\beta = 1.155$ and the parameters up to the reducer are

$$p_b = \beta^{-1.3} p_a = 1.155^{-1.3} \times 4.86 = 4.02 \text{ atm}$$

$$p_{h \cdot b} = a^2 \beta p_{h.a} = 3.5 \times 1.155 \times 0.246 = 1.00 \text{ atm}$$

The ratio (2.25) is the critical flow condition from the end of the pipe when changing to a large diameter. This condition may be expressed as follows when the diameter increases by more than 25%:

for superheated steam

$$1.83 p_c \geqslant p_{h.b} \xi_b + p' \qquad (2.65)$$

for saturated steam

$$1.73 p_c \geqslant p_{h.b} \xi_b + p'$$

where p_c is the critical pressure at the end of the pipe of smaller size; $p_{h.b}$—hydrodynamic pressure at the beginning of the pipe of larger size; ξ_b—hydrodynamic resistance coefficient of a reducer (tee) calculated for a larger size; p'—additional pressure produced due to the resistance offered by subsequent sections and the back pressure at their ends.

The conditions for critical flow when changing from one pipe size to another are clearly seen from the graphs for determining β at $a > 1$; maximum possible value of β is 1.59, as per Fig. 2.11 and corresponds to the critical flow of superheated steam.

Example 3. The hydrodynamic pressure beyond the 150/205 mm reducer is 0.08 of the piezometric one. Find the parameters up to the reducer. The coefficients are $c = 0.08$, $a^2 = \left(\frac{205}{150}\right)^4 = 3.5$. From Fig. 2.11 it is clear that when $a_2 = 3.5$ the flow is already critical at $c = 0.074 < 0.08$. Therefore, in this case critical flow occurs and a pressure jump is possible. The pressure up to the reducer is determined from formula (2.48).

Special attention should be paid to the discharge capacity calculations of pipelines consisting of in series-connected sections with different passage areas. If the passage area of the first section $F_1 = \frac{1}{a_1} F_r$ and the last section $F_n = \frac{1}{a_n} F_r$, then the difference in dynamic pressures at the inlet and outlet will be determined by the following coefficient reduced to the mean velocity:

$$\sigma_{i/o} + \sigma_1 = a_n^2 \frac{1+\beta}{2} - a_1^2 \frac{1+\beta}{2\beta} \tag{2.66}$$

The exact value of the reduced resistance coefficient $\sigma_\beta = a_1^2 \sigma_{\beta 1} + a_2^2 \sigma_{\beta 2} + \ldots$ can not be predetermined, since the ratio of specific volumes β for each section should be found first which depend upon the unknown m. Because of this, an approximate value of the reduced coefficient $\sigma'_{rd} = a_\beta \sigma_\beta$ is taken for calculation purposes, in which

$$a_\beta = \frac{\sum a_i^2 (a_i^2 \xi_i)}{\sum a_i^2 \xi_i} \tag{2.67}$$

and σ'_β is determined from the ratio $\beta = \frac{v_{n+1}}{v_1}$ between the specific volumes at the end of the last section and the beginning of the first one.

The value of the total additional coefficient σ in formula (2.60) for superheated steam ($k = 1.3$) is determined from

$$\sigma'_{rd} = a_\beta \left[4.07 \log \beta - 0.385 \left(\beta - \frac{1}{\beta}\right)\right] + \\ + a_n^2 \frac{1+\beta}{2} - a_1^2 \frac{1+\beta}{2\beta} \tag{2.69}$$

Should the need arise the calculation may be verified by successive approximations. For this, it is necessary to perform hydrodynamic calculations of the sections in succession and determine the parameters p_2' and β' after substituting the approximate value of σ_{rd}' in the formula and calculating the mass velocity m'. Thereafter the resistance of the pipeline is verified from the formula

$$\xi_{rd}+\sigma_{rd}=\frac{(p_1-p_2')\,(1+\beta')\,g\cdot 10^4}{(m')^2\,\beta' v'} \qquad (2.70)$$

and the calculation is done with the exact value of the reduced resistance coefficient $\xi_{rd}+\sigma_{rd}$.

The hydraulic resistance coefficient of such a pipeline should be related to the passage area of the exit section, i.e. should be calculated from formula (2.14) taking $F_{rd}=F_n$ and finding the critical ratio of the specific volumes β_c, which corresponds to the known value of ξ_{rd} determined from (2.70). Further, the calculation is made by formulas (2.60) and (2.62) depending upon the given values of β.

While determining the discharge capacity of a pipeline consisting of sections with different passage area, it is necessary to assume that the flow may be critical at all places of transition to a larger size. Taking this into consideration determine the discharge through the first section and then through the first two (and relating at that the resistance coefficient of the first section to the passage area of the second one), and then through the first three sections (relating the reduced resistance coefficient of the first two sections to the passage area of the third one) and so on. The minimum value from the obtained ones should be taken as the provisional discharge capacity of a pipeline as a whole. Then check calculations should be done section by section at the assumed value of m so as to adjust the resistance coefficients depending upon m and the specific volume ratio β for the different sections.

The following examples illustrating the application of the above obtained formulas explain the hydrodynamic calculation procedure for exhaust pipings from safety valves. These calculations are performed to check the pressure after the safety valve and in its body. The relieving capacity of safety valves is determined by the manufacturers based on critical flow conditions through the gap between the valve seat and disc; for this it is necessary that the pressure in the outlet chamber of impulse safety valves should not be more than $0.5p_0$, where p_0—maximum permissible pressure below the valve. To ensure the rated relieving capacity in gravity and spring-loaded safety valves the pressure in the valve body should be less, not more than $0.3p_0$.

The pressure in the valve body is determined by the additional pressure created by the exhaust pipe because of pressure jumps when the steam flow is critical. The calculation begins from the end of the exhaust pipe. The pressure at the end of the pipe when the steam flow velocity is less than the critical one, is equal to the atmospheric one, and at the critical velocity is determined from formula (2.48) as it depends upon the mass velocity. Other examples given below explain the procedure for calculating the discharge capacity of steamlines at subcritical and critical steam velocities.

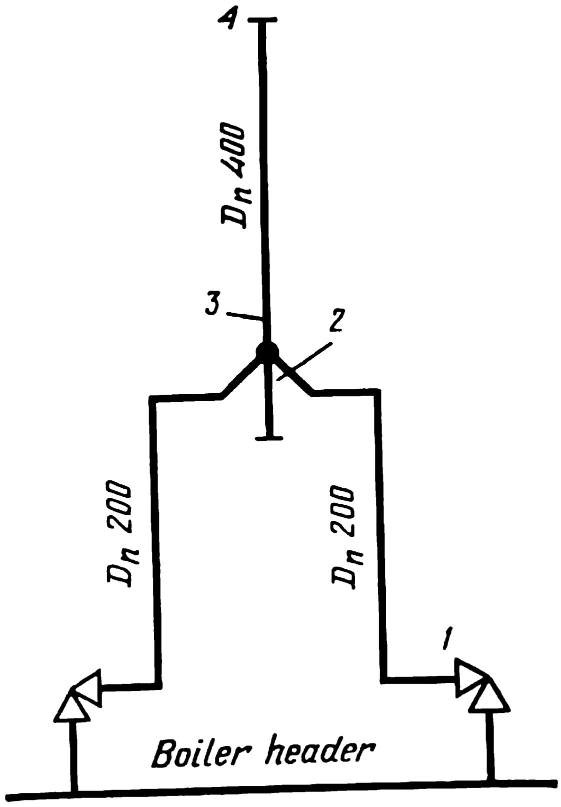

Fig. 2.12. Schematic of exhaust pipeline

Example 4. Calculation of exhaust pipes at critical steam velocities.

A boiler with 140 atm 570°C and 420 tons/hr steam rating is equipped with four safety valves. Every two valves are connected by 219 × 7 mm pipes to a common exhaust 426 × 11 mm pipe (Fig. 2.12). The nominal size D_n 200 pipes are connected to a common exhaust pipe in the form of a skewed pipe cross welded joint whose resistance coefficient for the D_n 400 pipe area (section of the combined flow) is $\xi = 2.5$. The resistance of this pipe cross for the D_n 200 pipe cross section is

$$\xi = \left(\frac{455}{885}\right)^2 \times 2.5 = 0.66$$

where 455 and 885 kg/(m^2·sec) are the mass velocities in D_n 400 and D_n 200 pipes, respectively (Table 2.2).

Table 2.2

	Parameters	Section *1-2*	Section *3-4*
1	Rated diameter d_r, m	0.205	0.404
2	Characteristic $\frac{d_r}{k_e} \cdot 10^3$	342	675
3	Friction factor λ (from Fig. 2.3) . . .	0.026	0.0215
4	Friction factor per 1 m of pipe λ/d_r, 1/m	0.1266	0.532
5	Pipe route length L, m	17	17
6	Friction factor for the pipe route length $\lambda/d_r L$	2.15	0.90
7	Local resistances (entry to the pipe, elbows, tees)	1.13	1.25
8	Total friction factor	3.28	2.15
9	Design flow rate of steam G, tons/hr	105	210
10	Mass velocity m, kg/(m^2·sec)	885	455

The equivalent pipe roughness is taken as $k_e = 0.6$ mm.

Let us denote the beginning and end of the D_n 200 pipe by indices *1* and *2*, and that of D_n 400 pipe by *3* and *4*.

The rated characteristics of the pipe's sections are given in Table 2.2. In this table under item 7 the resistance of the four pipe joint in the sections *1-2* and *3-4* has been taken into account as being $0.5 \times 0.66 = 0.33$ and $0.5 \times 2.5 = 1.25$, respectively.

The starting point for the hydrodynamic calculation is the end of pipe *4*.

The pressure at which the critical velocity develops at the end of pipe *4* (formula 2.48) equals

$$p_{c4} = 26.1 \times 10^{-4} m \sqrt{p_0 v_0} = 26.1 \times 10^{-4} \times 455 \times \times \sqrt{140 \times 0.0261} = 2.27 \text{ atm}$$

The pressure p_{c4} is more than the atmospheric one and hence for the given flow rate of steam the critical velocity will be established at $p_4 = p_{c4} = 2.27$ atm. As per formula (2.58) the hydrodynamic pressure equals

$$p_{h4} = 0.65 p_{c4} = 0.65 \times 2.27 = 1.475 \text{ kg/cm}^2$$

The ratios of pressures α_{34} and volumes β_{34} for the section *3-4* can be determined from the graph shown in Fig. 2.8 or from equations (2.54) and (2.55) as follows:

$$\beta_{34}^2 = 1.13 \times 2.15 + 1 + 4.6 \log \beta_{34}$$

$$\alpha_{34} = \left(1.15\beta_{34} - \frac{0.15}{\beta_{34}}\right)$$

whence $\beta_{34} = 2.25$ and $\alpha_{34} = 2.525$, and in accordance with this

$$p_3' = 2.525 \times 2.27 = 5.73 \text{ atm} \quad \text{and} \quad p_{h3} = \frac{p_{h4}}{\beta_{34}} = \frac{1.475}{2.25} = 0.66 \text{ kg/cm}^2$$

The pressure p_3' is marked with a stroke since it is considered as a back pressure in relation to cross section *2*.

The steam parameters in cross section *2* should be obtained from equations (2.63) and (2.64), and the section *3* should be considered as section *a* in the given formulas. The dimensionless coefficients are:

$$c = \frac{0.66}{5.73} = 0.115 \quad \text{and} \quad a^2 = \left(\frac{885}{455}\right)^2 = 3.77$$

From Fig. 2.11 it is clear that for $a^2 = 3.77$ the flow velocity attains critical value even when $c = 0.065$, and therefore, in this case for $c = 0.115 > 0.065$ steam will enter D_n400 pipe at its critical velocity.

The pressure p_2 at the end of D_n200 pipe can be determined from the formula

$$p_2 = 26.1 \times 10^{-4} \times 885 \sqrt{140 \times 0.0261} = 4.40 \text{ atm}$$

$$p_{h2} = 0.65 \times 4.40 = 2.86 \text{ kg/cm}^2$$

The ratios of pressures α_{12} and volumes β_{12} can be found from Fig. 2.8, and they are:

$$\alpha_{12} = 2.9; \quad \beta_{21} = 2.57, \text{ hence}$$

$$p_1 = 2.9 \times 4.40 = 12.75 \text{ atm}$$

$$p_{h1} = \frac{2.86}{2.57} = 1.11 \text{ kg/cm}^2$$

The pressure in the valve body $p_1 = 12.75$ atm is many times less than the permissible pressure $0.5 \times 140 = 70$ atm at which the rated discharge capacity of the safety valve is ensured.

The results show that the maximum pressure for which the $D_n 200$ pipes should be calculated do not exceed 11.75 atm gauge. The critical flow velocity of steam in cross sections *2* and *4* equals $w_c = 333\sqrt{140 \times 0.0261} = 638$ m/sec. The velocity of steam at point *1* is $w_1 = \frac{w_c}{\beta_{12}} = \frac{638}{2.57} = 248$ m/sec and the enthalpy $i = 841.3 - \left(\frac{248}{91.5}\right)^2 = 834.0$ kcal/kg and correspondingly the temperature is about 507°C.

In conclusion it may be said that the pressure of the decelerated jet of steam in cross section *2* mounts up to $1.83p_2 = 1.83 \times 4.40 = 8.05$ atm and exceeds the sum of pressures in cross section *3* which equals $5.73 + 0.66 = 6.39$ atm.

Example 5. Calculation of an exhaust pipe at a subcritical steam velocity.

An impulse safety valve is installed in the pipe serving the deaerator to guard it against excessive pressure. The steam parameters when the valve is in operation are: $p_0 = 7.0$ atm, $t = 281$°C, $v_0 = 0.3727$ m³/kg, $i = 726.4$ kcal/kg. The discharge capacity of the valve $G = 67$ tons/hr. The resistance coefficient of 377 × 5 mm exhaust pipe $\xi = 1.76$. The rated pipe diameter $d_r = 0.367$ m.

The mass velocity

$$m = 0.354, \quad \frac{G}{d_r^2} = 0.354 \times \frac{67}{0.367^2} = 176.0 \text{ kg/(m}^2\cdot\text{sec)}$$

The critical flow pressure for the given mass velocity

$$p_c = 26.1 \times 10^{-4} \times 176\sqrt{7.0 \times 0.3727} = 0.741 \text{ atm}$$

Since this pressure is less than atmospheric, critical flow does not occur and the pressure at the pipe end should be taken as $p_2 = 1.0$ atm.

The critical velocity of steam

$$w_c = 333\sqrt{7 \times 0.3727} = 538 \text{ m/sec}$$

The specific volume of steam is obtained from formula (2.50) and Fig. 2.9.

$$v_2=\frac{w_c}{m}\left(\frac{p_c}{p_2}+f\right)=\frac{538}{176}\left(\frac{0.741}{1}+0.043\right)=2.40\ \mathrm{m^3/kg}$$

The hydrodynamic pressure at the pipe end

$$p_{h2}=\frac{176^2\times 2.40}{19.6\times 10^4}=0.378\ \mathrm{kg/cm^2}$$

The ratio of specific volumes is determined from equation (2.52):

$$\left(\frac{1.0}{2\times 0.378}+0.115\right)(\beta^2-1)=1.76+4.07\log\beta$$

or

$$\beta^2=2.222+2.83\log\beta$$

whence $\beta = 1.696$.

As per equation (2.53)

$$p_1=1.696\times 1.0+0.23\left(1.696-\frac{1}{1.696}\right)0.378=1.79\ \mathrm{atm}$$

and

$$p_{h1}=\frac{p_{h2}}{\beta}=\frac{0.378}{1.696}=0.223\ \mathrm{atm}$$

The resistance of the exhaust part of the safety valve body should not be more than $\xi = 3$ and the pressure in the body should be no more than

$$p=1.79+0.223\times 3=2.46\ \mathrm{atm}$$

The exhaust pipe satisfies the condition

$$p=2.38<0.5p_0=3.5\ \mathrm{atm}$$

Example 6. Calculation of steam pipe's discharge capacity at subcritical velocity.

When selecting excessive pressure relief devices for deaerators it is essential to determine the maximum possible discharge capacity of the pipeline connecting the second extraction of the K-100-90 turbine to the deaerator. Steam flow will be maximum when the regenerative preheater fed from the second extraction is off, and when the pressure regulators located ahead of the deaerator are full open.

The steam pressure in the turbine extraction is $p_1 = 14.4$ atm. The pipeline (Fig. 2.13) consists of three sections: (1) main—D_n200 pipe (common for the preheater and deaerator), (2) second—D_n150 pipe extending up to the deaerator room, and (3) third—two D_n150 pipes, each feeding its own deaerator. The passage area of the third section, which equals $2 \times 176.9 = 353.8$ cm^2, is taken as rated passage area. The pipeline characteristics are listed in Table 2.3.

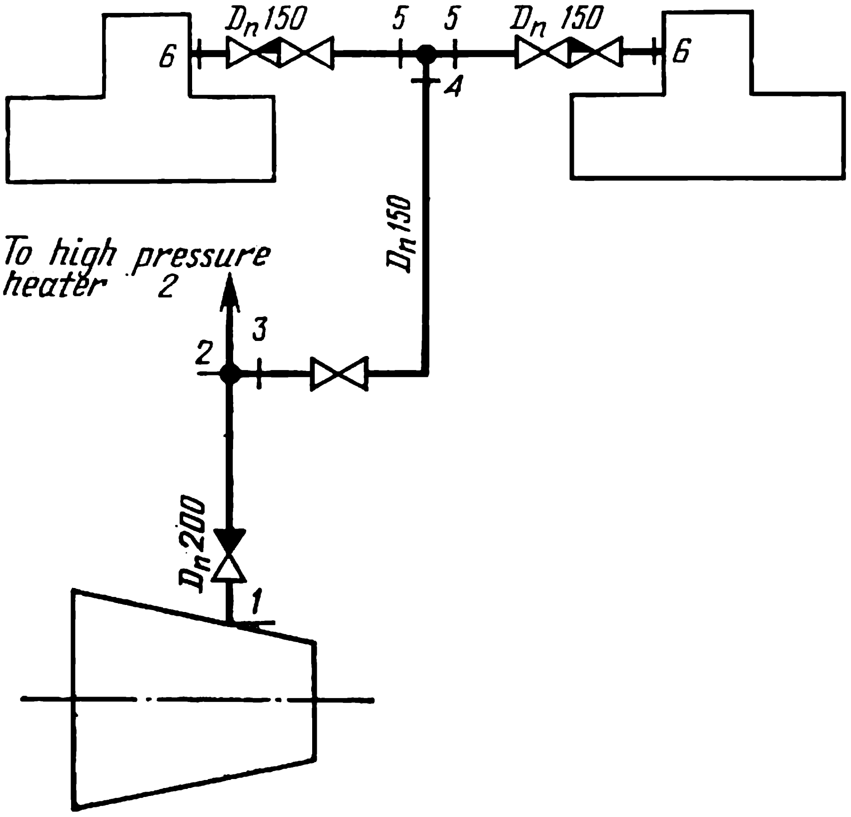

Fig. 2.13. Schematic of steam supply line from turbine extraction to deaerator

The critical ratios (as may be seen from Fig. 2.8) relating to $\xi = 68.5$ are the same for pressures $\alpha_c = 10.45$ and for specific volumes $\beta_c = 9.1$. As the given ratio of pressures $\alpha = \frac{14.4}{6} = 2.4 < \alpha_c = 10.45$, the flow will not be critical.

The design ratio of specific volumes are derived from formula (2.59):

$$\beta = 2.40\left[1 - 0.1\left(\frac{2.4}{9.1}\right)^2\right] = 2.38$$

Table 2.3

Parameters	Section			Total
	1-2	*3-4*	*5-6*	
Nominal diameter D_n, mm	200	150	2×150	—
Passage area F_i, cm^2 . . .	330.5	176.9	353.8	—
Reduction coefficient $a^2=(F_r/F_i)^2$	1.15	4.0	1.0	—
Total resistance coefficient ξ of the section	7.98	11.75	12.34	—
Reduced resistance coefficient $a^2\xi$	9.16	47.0	12.34	68.5
Product $a^2(a^2\xi)$	10.54	188.0	12.34	210.88

The approximate value of the additional coefficient σ_{rd} in accordance with formula (2.69)

$$\sigma_{rd}=3.08\left[4.07\log 2.38-0.385\left(2.38-\frac{1}{2.38}\right)\right]+$$

$$+1\,\frac{1+2.38}{2}-1.15\,\frac{1+2.38}{2\times 2.38}=3.27$$

Here, the reduction coefficient $a_\beta=\frac{210.88}{68.5}=3.08$ and the coefficients $\alpha_n=1$ and $\alpha_1=1.15$.

The approximate mass velocity calculated from formula (2.60)

$$m'=\sqrt{\frac{(14.4-6)(1+2.38)\,9.81\times 10^4}{(68.5+3.27)\,2.38\times 0.1752}}=305\ \text{kg/(m}^2\cdot\text{sec)}$$

The steam flow rate

$$Q=305\times 353.8\times 10^{-4}=10.80\ \text{kg/sec}$$

The hydrodynamic calculation of the steam pipeline for the steam flow rate of 10.80 kg/sec determined the parameters at point 6: $p_6=5.76$ atm and $v_6=0.439$ m^3/kg.

The ratio β at the rated mass velocity $m_r=305$ kg/(m^2·sec)

$$\beta=\frac{v_6}{v_1}=\frac{0.439}{0.1752}=2.50$$

The exact value of resistance from formula (2.70)

$$\xi_{rd} + \sigma_{rd} = \frac{(14.40 - 5.76)\,(1 + 2.50)\,9.81 \times 10^4}{305^2 \times 2.50 \times 0.1752} = 72.8$$

and the exact mass velocity

$$m = \sqrt{\frac{(14.4 - 6)\,(1 + 2.38)\,9.81 \times 10^4}{72.8 \times 2.38 \times 0.1752}} = 303 \text{ kg/(m}^2\cdot\text{sec)}$$

Steam flow rate per hour

$$G = 3.6 \times 353.8 \times 10^{-4} \times 303 = 38.6 \text{ tons/hr}$$

The precalculated flow rate proved to be, in this case, more than the exact flow rate by 1%.

Example 7. Calculation of the steam pipeline's discharge capacity at critical velocities.

The blow-off piping of the steam line 140 atm 570°C consists of two sections: (1) section *1-2* made of $D_n 20$ pipes, $F = F_2 = 3.35$ cm^2, line resistance coefficient $\xi = 40$; (2) section *3-4* made of $D_n 50$ pipes, $F = F_4 = 19.7$ cm^2, line resistance coefficient $\xi = 18$.

The blow-off piping is connected to the expander in which the pressure is not more than 2.0 atm.

To begin with let us explain the nature of flow at the end of the pipe. The resistance coefficient of the whole line reduced to the passage area $F_4 = 19.7$ cm^2

$$\xi_{rd\,4} = \left(\frac{19.7}{3.35}\right)^2 \times 40 + 18 = 1380 + 18 = 1398$$

The critical ratio of specific volumes is obtained from equation (2.54)

$$\beta_{c4}^2 = 1 + 1.13 \times 1398 + 4.6 \log \beta_{c4} = 1581 + 4.6 \log \beta_{c4}$$

whence

$$\beta_{c4} = 39.9$$

This value conforms to the critical ratio of pressures (in accordance with formula 2.55):

$$\alpha_{c4} = \frac{p_1}{p_{c4}} = 1.15\beta_{c4} - \frac{0.15}{\beta_{c4}} = 1.15 \times 39.9 - \frac{0.15}{39.9} = 45.9$$

For the given pressure ratio $\alpha = \frac{140}{2} = 70 > \alpha_{c4} = 45.9$ the flow from the pipe end should occur at the critical velocity. The discharge capacity of the pipe at the end of section *3-4* is determined from formula (2.62):

$$m_4 = \frac{140 \times 10^4}{\left(30 \cdot 39.9 - \frac{3.9}{39.9}\right) \sqrt{140 \times 0.02609}} = 610 \text{ kg/(m}^2 \cdot \text{sec)}$$

or

$$Q_4 = m_4 F_4 = 610 \times 19.7 \times 10^{-4} = 1.20 \text{ kg/sec}$$

Let us check the discharge capacity of the section *1-2*

$$\beta_{c2}^2 = 1 + 1.13 \times 40 + 4.6 \log \beta_{c2} = 46.2 + 4.6 \log \beta_{c2}$$

whence $\beta_{c2} = 7.09$ and

$$m_2 = \frac{140 \times 10^4}{\left(30 \times 7.09 - \frac{3.9}{7.09}\right) \sqrt{140 \times 0.02609}} = 3440 \text{ kg/(m}^2 \cdot \text{sec)}$$

or

$$Q = m_2 F_2 = 3440 \times 3.35 \times 10^{-4} = 1.15 \text{ kg/sec}$$

Thus, the discharge capacity of the whole pipeline is determined by the critical flow conditions at the end of section *1-2* of D_n20 pipe, i.e. $Q = 1.15$ kg/sec.

The mass velocity at the end of section *3-4* for the above mentioned flow rate

$$m_4 = \frac{1.15}{19.7 \times 10^{-4}} = 583 \text{ kg/(m}^2 \cdot \text{sec)}$$

For this value, as per formula (2.48) the steam pressure at the end of section *3-4*

$$p_4 = 26.1 \times 10^{-4}\, 583 \sqrt{140 \times 0.02609} = 2.93 \text{ atm} > 2 \text{ atm}$$

Thus, in this cross section the critical flow occurs for $m_4 = 583$ kg/(m^2·sec).

The pressure at the end of section *1-2*

$$p_2 = \frac{m_2}{m_4} p_4 = \frac{3420}{583} \times 2.93 = 17.2 \text{ atm}$$

The pressure at the beginning of the section *3-4* is determined by the additional pressure $p_4 = 2.93$ atm and the resistance of the section *3-4*.

For $\xi = 18$, as is obvious from the graph in Fig. 2.8, $\alpha_c = 5.68$, therefore,

$$p_3 = \alpha_c p_4 = 5.68 \times 2.93 = 16.6 \text{ atm}$$

This pressure is appreciably lower than the one generated at the end of section *1-2* by the decelerating steam jet, which approximates 1.83 × 17.2 = 31 atm.

Example 8. Calculation of a flow regulating orifice. The maximum permissible steam flow rate to the deaerator is 36 tons/hr or 10 kg/sec.

The steam parameters at the beginning of the pipeline are: $p_1 = 14.4$ atm, $v_1 = 0.1752$ m^3/kg, and at the end (with allowance for steam velocity) $p_4 = 7.25$ atm, $v_2 = 0.350$ m^3/kg.

The coefficients of hydrodynamic resistance of a steamline reduced to the passage area $F_{rd} = 176.9 \times 10^{-4}$ m^2 are: for section *1-2* from the beginning of pipeline up to the orifice installed position $\xi_{12} = 3.23$, for portion *3-4* from the orifice up to the deaerator $\xi_{34} = 11.33$.

To calculate the orifice the steam parameters p_2 and v_2 before the orifice plate (from the given values of m, p_1, v_1, ξ_{12}) and p_3, v_3 after the orifice (from the given values of m, p_4, v_4, ξ_{34}) are obtained. Thereafter the necessary coefficients of resistance for the orifice are determined.

The given mass velocity

$$m = \frac{Q}{F} = \frac{10.0}{176.9 \times 10^{-4}} = 565 \text{ kg/(m}^2\cdot\text{sec)}$$

The hydrodynamic pressure

$$p_{h1} = \frac{565^2 \times 0.1752}{19.6 \times 10^4} = 0.285 \text{ kg/cm}^2$$

Since $p_{h1} \cdot \xi_{12} = 0.285 \times 3.23 = 0.9$ kg/cm² is 7% less than the initial pressure 14.4 atm, for calculation purposes we use equation (2.41)

$$p_2 = 14.4 \sqrt{1 - 2 \times \frac{0.285}{14.4} \times 3.23 \left(1 + 2.5 \frac{0.285}{14.4}\right)} = $$
$$= 13.38 \text{ atm}$$

$$\beta_{12} \approx \alpha_{12} = \frac{14.4}{13.38} = 1.074$$

$$p_{h2} = 1.074 \times 0.285 = 0.306 \text{ kg/cm}^2$$

The hydrodynamic pressure at the end of pipeline

$$p_{h4} = \frac{565^2 \times 0.350}{19.6 \times 10^4} = 0.570 \text{ kg/cm}^2$$

The ratio β_{34} is found from equation (2.52)

$$\left(\frac{7.25}{2 \times 0.570} + 0.115\right) (\beta_{34}^2 - 1) = 11.33 + 4.07 \log \beta_{34}$$

or

$$\beta_{34}^2 = 2.752 + 0.63 \log \beta_{34}$$

hence, $\beta_{34} = 1.70$ and from formula (2.53)

$$p_3 = 1.70 \times 7.25 + 0.23 \left(1.70 - \frac{1}{1.70}\right) 0.570 = 12.48 \text{ atm}$$

$$p_{h3} = \frac{0.570}{1.70} = 0.335 \text{ kg/cm}^2$$

The pressure loss in the orifice

$$\Delta p_o = 13.38 - 12.48 = 0.900 \text{ kg/cm}^2$$

The required coefficient of resistance

$$\xi_1 = \frac{\Delta p_o}{p_{h2}} = \frac{0.900}{0.306} = 2.94$$

The relative pressure drop in the orifice

$$\frac{\Delta p_o}{p_2} = \frac{0.900}{13.38} = 0.067$$

From the graph shown in Appendix 7: $\left(\frac{d_0}{D}\right)^2 = 0.56$

$$d_0 = \sqrt{0.56}D = \sqrt{0.56} \times 150 = 112 \text{ mm}$$

2.5. Hydrodynamic Calculations of Boiling Water and High-Pressure Saturated Steam Pipelines

This section deals with hydrodynamic calculations of fluids whose adiabatic indexes are not constant. These include pipelines carrying saturated steam at pressures more than 100 atm when their pressure losses are large, and pipelines transmitting hot water which evaporates as pressure decreases along the pipeline. In both cases the specific volume of the fluid increases. Equation (2.2) is used for hydrodynamic calculations of such pipelines. The values of integrals used in equation (2.2) are determined by the numerical integration method using Steam and Water Tables, Thermodynamic Properties [2-2], which automatically takes into account the variation in adiabatic index.

The only task involved in calculating the above mentioned pipelines is the determination of their discharge capacity at the beginning of the pipeline (p_1, i_1) and its coefficient of resistance. The end of pipeline is generally connected to the expander (separator) or condenser which has a known pressure p'. As a rule, the pressure p_2 at the end of pipeline is more than the pressure p' and conditions for critical flow from the end of pipeline are created. Pressure p_2 depends upon the mass velocity m and is unknown. Thus, to solve the problem it is necessary to determine two unknown values p_2 and m. With this aim in view the following equations may be used:

1. The equation that expresses relationship between the mass velocity and the coefficient of line resistance ξ and pressure p_2 at the end. It evolves directly from the equality (2.2)

$$\sqrt{\frac{2g}{\xi+4.6\log\beta}\left(-10^4\int_1^2 \gamma\,dp - \int_1^2 \gamma^2\,dH\right)} \text{ kg/(m}^2\cdot\text{sec)} \tag{2.71}$$

where p is the pressure, kg/cm^2; $\gamma = 1/v$—specific volume, kg/m^3; $\beta = v_2/v_1$—ratio of specific volumes; v_2—volume at the end of pipeline; v_1—volume at the beginning of pipeline; dH—variation in the geodetic level of pipeline's axis, m.

2. The equation expressing relationship between the mass velocity m_c and the pressure $p_2 = p_c$ at the end of pipeline when the flow is critical

$$m_c = q p_c \text{ kg/(m}^2\cdot\text{sec)} \tag{2.72}$$

The coefficient q depends upon the ratio between the critical pressure p_c and the saturation pressure p_s, but varies within a relatively small range.

Now we consider the methods used for calculating the values appearing in formula (2.71). These methods are common to saturated steam and boiling water.

To determine the integral—$\int_1^2 \gamma\, dp$ the pressure range $(p_1 - p_2)$ is divided into a sufficiently large number of intervals and for each pressure stage p_n the degree of dryness (steam content) is expressed as:

$$x_n = \frac{i_0 - i'_n}{r_n}$$

where i_0 is the initial enthalpy, kcal/kg; i'_n and r_n—enthalpy of liquid and heat of evaporation at pressure p_n; n—interval number; then the specific volume is found $v_n = x_n (v''_n - v'_n) + v'_n$ and $\gamma_n = 1/v_n$.

Any of the formulas given below can be used for numerical integration, e.g.:

$$10^4 \int_2^1 \gamma\, dp = 10^4 \sum_1^2 (p_n - p_{n+1}) \left(\frac{\gamma_n + \gamma_{n+1}}{2}\right) \text{ kg}^2/\text{m}^5$$

or Simpson's rule:

$$10^4 \int_2^1 \gamma\, dp = 10^4 \sum_1^2 \frac{p_n - p_{n+1}}{6} (\gamma_n + 4\gamma_m + \gamma_{n+1}) \text{ kg}^2/\text{m}^5$$

where γ_m is determined for $p_m = \frac{1}{2}(p_n + p_{n+1})$.

For convenience greater intervals may be taken when calculating by Simpson's rule. For saturated steam the results are sufficiently correct even at three points:

$$\left(p_n = p_1; \quad p_m = \frac{p_1 + p_2}{2}; \quad p_{n+1} = p_2\right)$$

The values thus obtained do not take into account the enthalpy decrease $\Delta i = \left(\frac{mv}{91.5}\right)^2$ due to the increase in velocity. The inclusion of this correction raises the $\int\limits_2^1 \gamma \, dp$ value, and hence, also the rated mass velocity m. Calculation of this correction requires predetermined values of m and p_2. The specific weight correction which takes into account the velocity

$$\Delta\gamma = \frac{1}{v + \Delta v} - \frac{1}{v} \approx \frac{-\Delta v}{v^2} = \frac{-\Delta x\,(v'' - v')}{v^2} = \left(\frac{m}{91.5}\right)^2 \frac{v'' - v'}{r}$$

The integral correction may be derived from Simpson's rule

$$10^4 \int\limits_2^1 \Delta\gamma \, dp = 0.2\,(p_1 - p_2)\, m^2 \left(\frac{v_2'' - v_2'}{r_2} + 4\,\frac{v_m'' - v_m'}{r_m} + \frac{v_1'' - v_1'}{r_1}\right) \text{ kg}^2/\text{m}^5 \qquad (2.73)$$

where index 1 corresponds to parameters at the beginning of pipeline and index 2 to the parameters at the end of pipeline, and the index m to the parameters at mean pressure, i.e. $0.5\,(p_1 + p_2)$, kg/cm^2.

The numerical coefficient in formula (2.73) represents a value of $\frac{1}{6} \times \frac{10^4}{91.5^2} = 0.2$. The velocity correction may be neglected for velocities $w_2 = mv_2 < 120 \div 150$ m/sec.

To facilitate practical calculations, given in Figs. 2.14 and 2.15 are graphs for determining $10^4 \int\limits_2^1 \gamma \, dp$ and

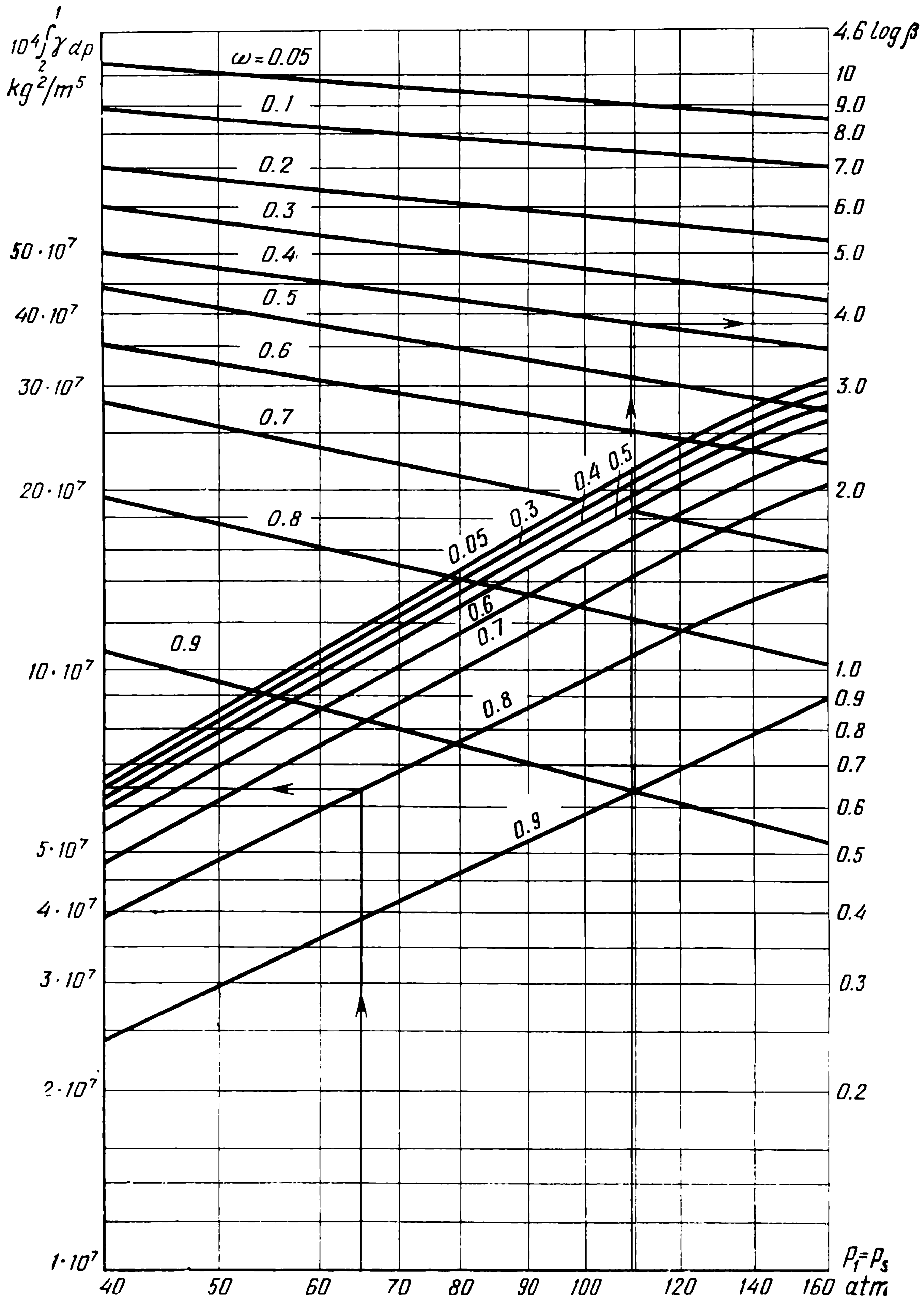

Fig. 2.14. Chart for determining $10^4 \int_2^1 \gamma\,dp$ and 4.6 log β for condensate at initial pressure p_s between 40 and 160 atm; $\omega = p_2/p_s$

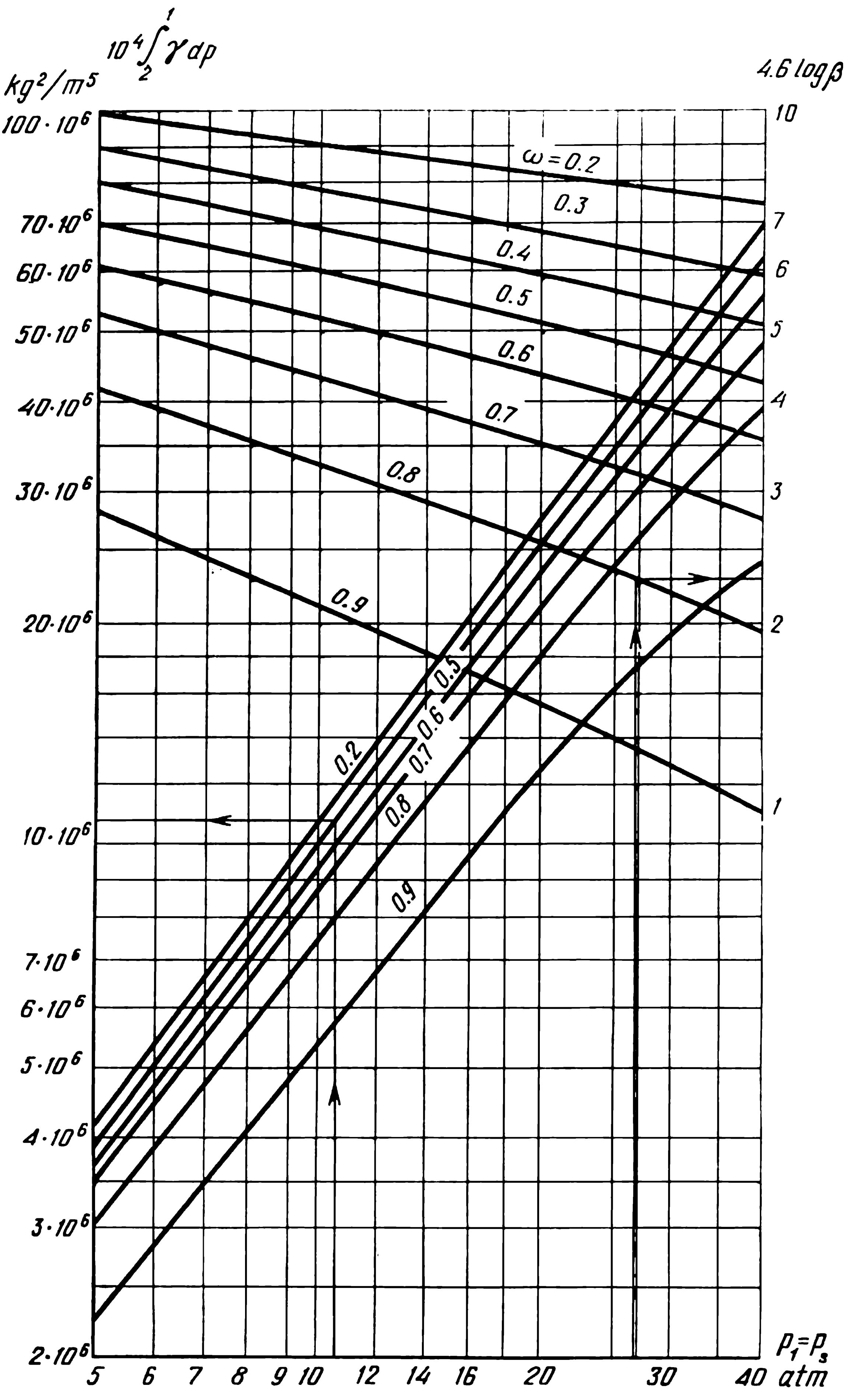

Fig. 2.15. Chart for determining $10^4 \int_2^1 \gamma\, dp$ and $4.6 \log \beta$ for condensate at initial pressure p_s between 5 and 40 atm; $\omega = p_2/p_s$

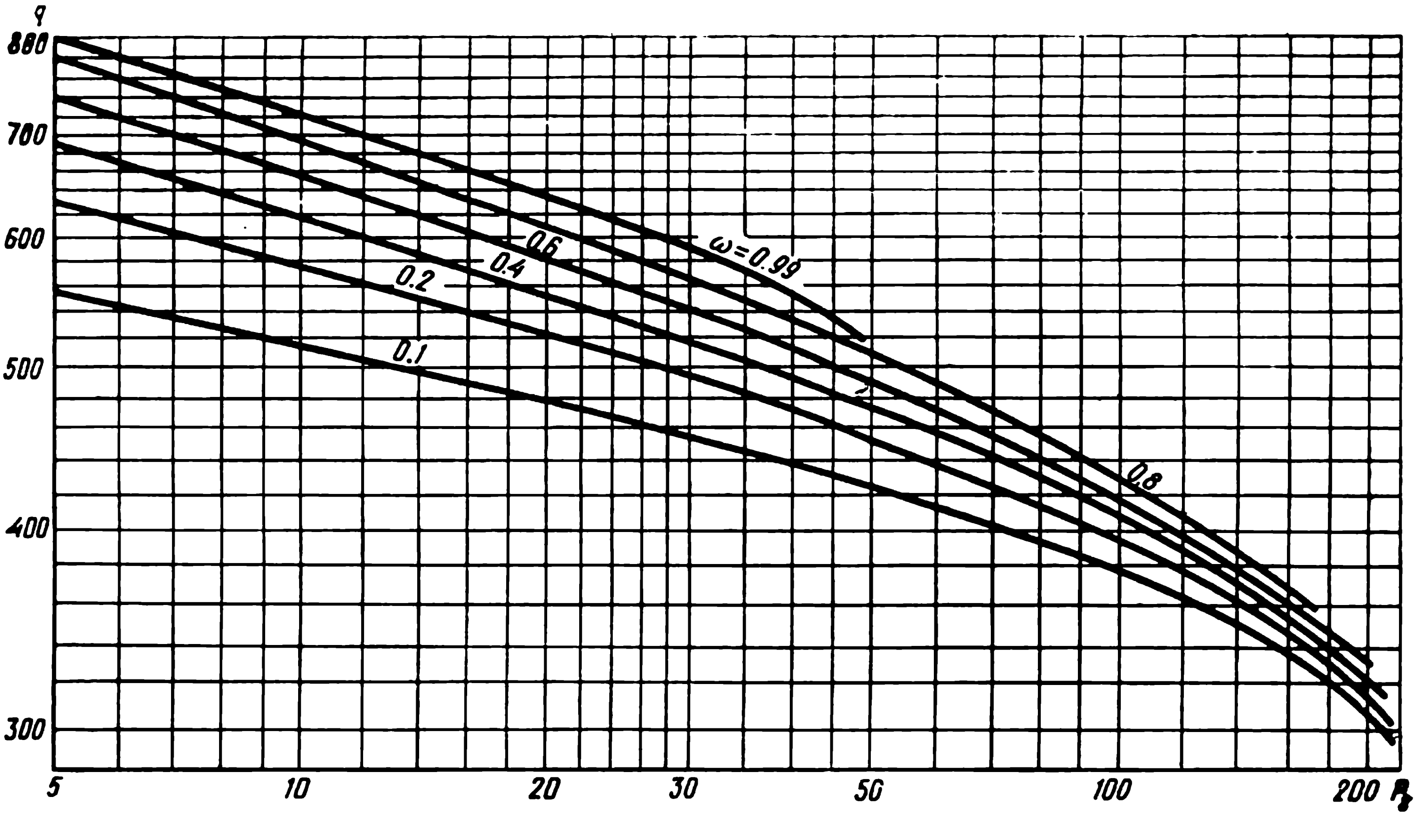

Fig. 2.16. Chart for determining coefficient $q = \frac{m_c}{p_c}$ when condensate expands from p_s to p_c; $\omega = p_c/p_s$

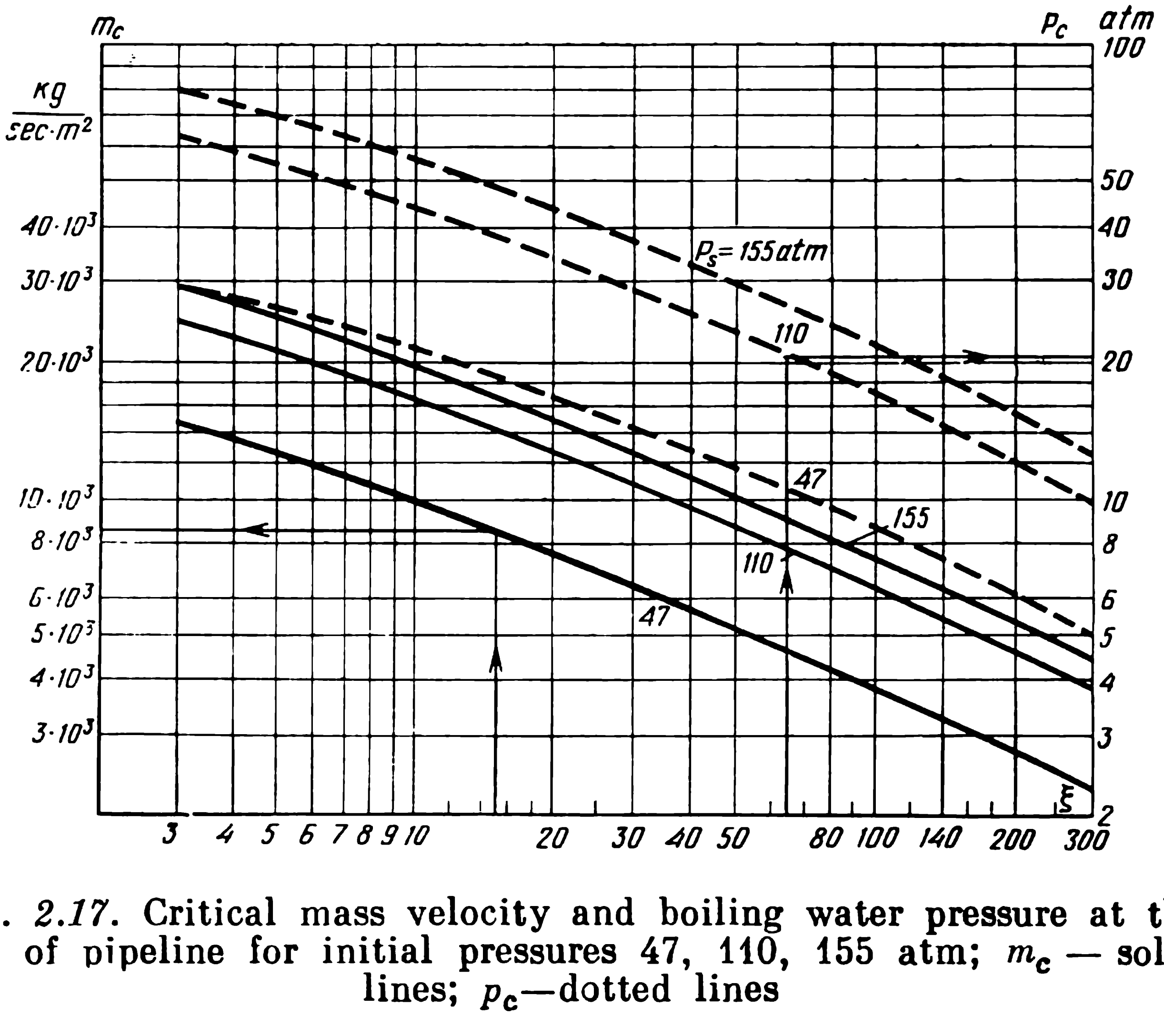

Fig. 2.17. Critical mass velocity and boiling water pressure at the end of pipeline for initial pressures 47, 110, 155 atm; m_c — solid lines; p_c—dotted lines

$4.6 \log \beta$ for boiling water depending upon $p_1 = p_s$ and the ratio $\omega = p_2/p_s$. These graphs do not take into account the effect of decrease in enthalpy due to increase in velocity.

The value $\int_2^1 \gamma^2\, dH$ appearing in equation (2.71) should be taken into account when calculating boiling water pipelines and may not be considered in calculations of saturated steam pipelines. The value of this integral depends upon the pressure at the beginning and end of every vertical section of the pipeline, and can be calculated only after m has been determined. For initial approximation the value m may be found from equations (2.71) and (2.72) and Fig. 2.16 or taken from the graph in Fig. 2.17 in which the relationship between m_c and the coefficient of resistance ξ of the pipe track is given for standard boiler pressures, i.e. 47, 110 and 155 atm. The mean specific weight of boiling water in standpipes located in the main part of the pipe track may be taken for preliminary calculations as $\gamma_{mean} = 0.85\gamma_1'$ for pressures $p_1 \geqslant 100$ atm and as $\gamma_{mean} = \gamma_1'$ for pressures less than 10 atm.

For a more exact solution the pressure at the beginning and end of a vertical section of a pipeline should be calculated after the preliminary determination of m. To accomplish this, equation (2.2) is used which may be written as:

$$\frac{m^2}{2g}\left(\xi_y + 4.6 \log \frac{\gamma_1}{\gamma_y}\right) = 10^4 \int_y^1 \gamma\, dp + \int_y^1 \gamma^2\, dH \qquad (2.74)$$

where y is the cross section in the vertical part of the pipeline (at the beginning or end of the pipeline); p_y—pressure in the cross section y, kg/cm^2; γ_y—specific weight at pressure p_y, kg/m^3; ξ_y—coefficient of resistance of pipeline from its beginning up to the cross section y.

The unknown value in this formula is γ_y or p_y, i.e. the lower limit of integrals on the right-hand side. This equation is very easily solved graphically as the intersection of lines representing the functions (of pressure p_y) on the right- and left-hand side of the formula. Without significant error, in this case, it may be taken

$$\int_y^1 \gamma^2 dH = \frac{H_1 - H_2}{2} (\gamma_1^2 + \gamma_y^2)$$

The example given below is chosen as a means of demonstrating how to perform calculations and to solve the equation (2.74) concerning the discharge capacity of an emergency drainage pipeline serving the boiler.

At high initial pressure, the value $\int_2^1 \gamma^2 dH$ is relatively small (as compared with $\int_2^1 \gamma \, dp$) and its inherent inaccuracy does not introduce significant errors. On the other hand, at low initial pressures the value $\int_2^1 \gamma^2 \, dH$ may exceed significantly $\int_2^1 \gamma \, dp$ and, in this case, it should be more accurately determined.

Now we take up the problems of determining the critical mass velocity for a two phase medium. A great number of scientific papers [2-4, 2-5, 2-11] have been devoted to the study of sound velocity in a two phase medium. The research work is based on different assumptions—both in the absence of heat transfer between the steam and liquid phases when sound wave passes through them and also for complete and partial heat transfer between the phases.

In the first case, as shown in [2-4], the velocity of sound in a mixture can be determined from the following approximate formula (it is assumed that for steam $pv'' = \text{const}$ and the sound velocity in a liquid $a' = \infty$):

$$a = a'' \left(\sqrt{x} + \frac{1 - v}{\sqrt{x}} \cdot \frac{v'}{v''} \right) \text{ m/sec} \qquad (2.75)$$

where x is the degree of dryness; a'—velocity of sound in dry saturated steam.

This formula agrees very well with the experimental data used for the determination of velocity of sound wave caused by hydraulic shock. Thus, as shown by the experiments, when the sound wave passes through a medium there is no time for heat transfer between the liquid and steam phases to occur.

For such conditions, the variation in sound velocity depending upon x is shown in Fig. 2.18 by dashed lines. With a decrease in the degree of dryness the velocity of sound decreases from $a = a''$ to the minimum, but for values of x close to zero it again rises and for $x = 0$ it is as great as the velocity of sound in a liquid phase $a' = \infty$. However, when a liquid flows through a pipeline, quickly fluctuating pressure waves do not occur therein but a gradual increase in velocity and smooth variation in the parameters along the pipeline take place, and hence it may be expected that there should be time for the heat transfer between the phases to occur. That is why the Laplace formula based on thermodynamic theory holds true for the critical velocity

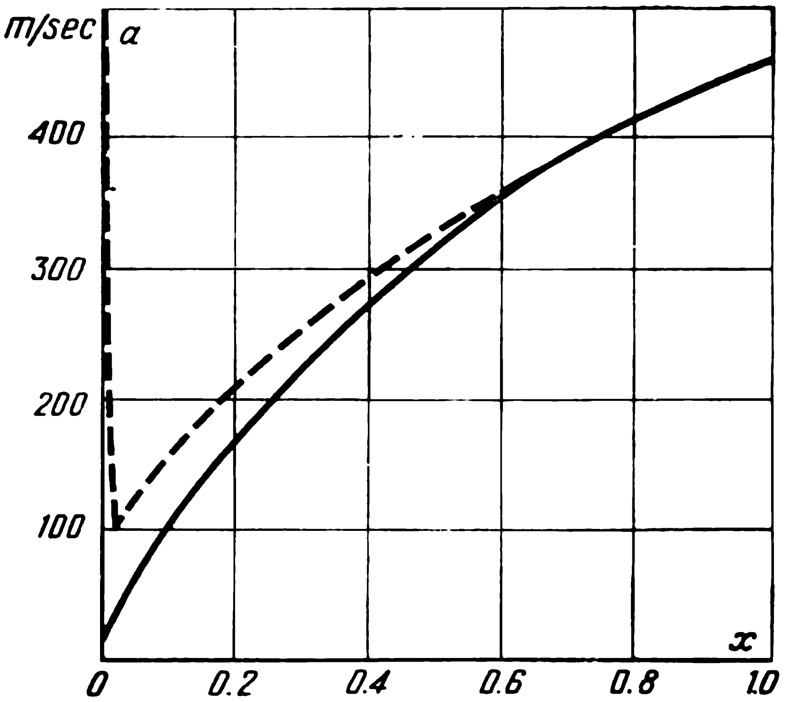

Fig. 2.18. Variation of sound velocity in a two phase medium (steam—water) *versus* degree of dryness x

solid line—when heat exchange takes place between phases; dotted line—when no heat exchange takes place between phases

$$w_c = \sqrt{-v^2 g \left(\frac{\partial p}{\partial v}\right)_s 10^4} \text{ m/sec} \qquad (2.76)$$

The relationship between the critical velocity and x is shown in Fig. 2.18 by thick line. With a decrease in x the critical velocity decreases down to an insignificant value (10 m per second) when x is close to zero. However, when $x = 0$ the critical velocity is, evidently, equal to the velocity of sound in a liquid. It is essential to assume that in this case when x is very small the elastic properties of the mixture begin to come closer to the properties of liquid, the sound velocity increases quickly up to the sound velocity in water $a' \geqslant 1400$ m/sec when $x = 0$.

The flow of boiling condensate from the high pressure reservoir to the low pressure one through a 4″ pipe was investigated by Benjamin and Miller [2-14]. From a series of experiments, in four cases the velocity at the end of the condensate flow pipe attained the critical value. Data from these experiments are given in Table 2.4. The values of the

Table 2.4

Parameters	Experiment No.			
	2a	5a	7	14
Passage area, cm^2	82.2	82.2	82.2	82.2
Pressure, kg/cm^2:				
(a) in the high pressure receiver	3.01	2.60	2.67	2.92
(b) in the low pressure receiver	0.74	0.457	0.917	0.490
(c) at the end of pipeline	1.82	1.28	1.36	1.55
Specific volume at the end of pipeline, m^3/kg	0.0266	0.0562	0.052	0.0439
Flow rate, kg/sec	11.47	8.25	8.68	10.06
Velocity at the end of pipeline, m/sec	37.2	56.3	54.8	53.9
Degree of dryness at the end of pipeline	0.0312	0.041	0.0395	0.0382
Mass velocity, $kg/(m^2 \cdot sec)$				
(a) as per experimental data	1400	1005	1055	1230
(b) as per formula (2.77)	1450	1005	1070	1240
(c) as per formula (2.75)	3072	1730	1840	2290

critical mass velocity $m_c = w_c/v_c$ calculated experimentally and with formulas (2.75) and (2.76) are also listed in this table. From these values it is clear that (1) formula (2.75) gives too high discharge capacity; (2) experiments provide support for the correctness of calculation of pipe's discharge capacity as per formula

$$m_c = 100\sqrt{g\left(-\frac{\partial p}{\partial v}\right)_s} \approx 100\sqrt{g\left(-\frac{\Delta p}{\Delta v}\right)_s} \qquad (2.77)$$

This is based on Laplace's formula.

When calculating mass velocity from Steam and Water Thermodynamic Properties Tables [2-2] the change in pressure—Δp is taken equal to one or two stages allowed for in these tables (2-5% of p_c).

It is convenient to calculate the increase in specific volume from the formula

$$\Delta v = (v''_\Delta - v'')\,x + (v''_\Delta - v'_\Delta)\,\Delta x - (1 - x)\,(v' - v'_\Delta)$$

where v'_Δ and v'_Δ—specific volumes of steam and water at pressure $p_c - \Delta p$; Δx—variation in the dryness coefficient of steam for isoentropic expansion and is expressed as:

$$\Delta x = \frac{(s'' - s')\,x + s' - s''_\Delta}{s''_\Delta - s'_\Delta} - x$$

where s'', s'—entropy of steam and water respectively at pressure p_c; s''_Δ, s'_Δ—entropy of steam and water respectively at pressure $p_c - \Delta p$.

The degree of dryness x at pressure p_c is determined with allowance made for the decrease in enthalpy due to an increase in velocity, i.e. from formula

$$\left(\frac{m}{91.5}\right)^2 (v'' - v')^2 x^2 + \left[r + 2\left(\frac{m}{91.5}\right)^2 (v'' - v')\,v'\right] x - {} \\ - (i_0 - i') = 0$$

For practical calculations, the graph in Fig. 2.16 may be used to find coefficient q and then the critical mass velocity $m_c = qp_c$.

The nature of relations between the flow rate of boiling water and pressure p_2, expressed by equations (2.71) and (2.72), is shown in Fig. 2.19. The m_1 curve is plotted for

$p_1 = p_s = 7$ atm, $\xi = 10$ for a geodetic level difference of 1.25 m and the m_2 curve for a height difference of 20 m. Point *2* on the intersection of m_1 and m_c curves corresponds to 4.1 atm pressure which for the given conditions is the minimum possible pressure at the end of the pipeline. With the decrease in pressure p' of the space to which the end of the pipeline is connected below 4.1 atm the pressure at the end of the pipeline remains at the same level $p_2 = p_c = 4.1$ atm $> p'$ and the mass velocity will remain critical 2900 kg/(m^2·sec); and if pressure p' exceeds 4.1 atm, then the mass velocity decreases. Thus, the mass velocity depending upon p' varies along the line *1-2-3*.

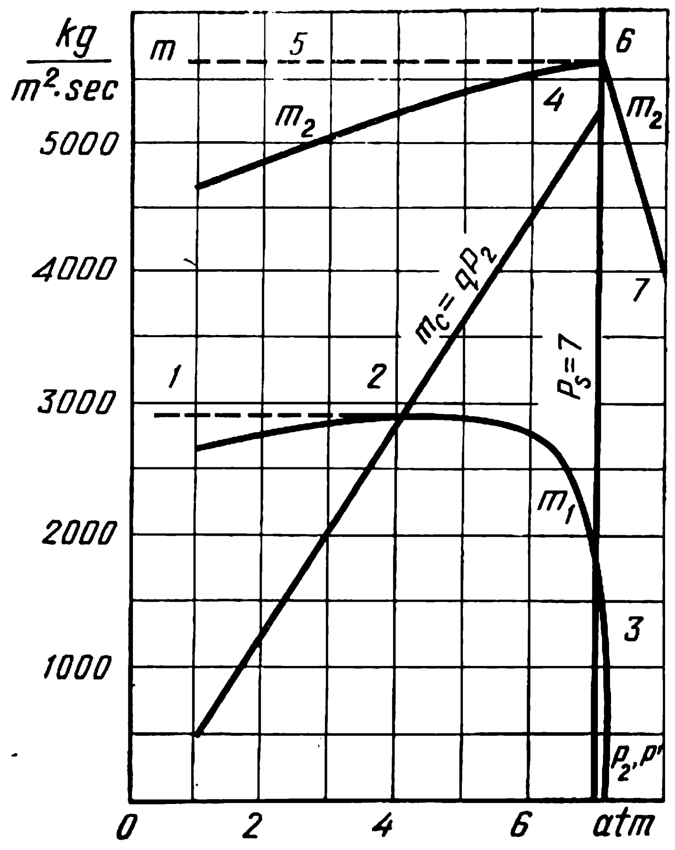

Fig. 2.19. Variation in condensate flow rate at $p_1 = p_s =$ 7 atm, for pipeline track resistance $\xi = 10$ and for 1.25 and 20 m long vertical sections

For a very large gravitational head (curve m_2) the mass velocity m, which is determined from equation (2.71), may exceed the maximum critical mass velocity m_c found from formula (2.77) for a two phase liquid (point *4* in Fig. 2.19). However, as shown earlier, for pressure p_2 very close to p_s

the critical mass velocity should increase (within the limit, for $p_2 = p_s$, up to the sound velocity in water). Taking this into consideration, when the flow rate curve m exceeds the critical mass velocity m_c at pressure $p_2 = 0.99\ p_s$ the flow rate m of the medium at pressure $p_2 = p_s$ should be taken as critical mass velocity (i.e. point *6* in Fig. 2.19). It is easy to note that this flow rate is the maximum possible for the given conditions. When the atmospheric pressure $p' < p_s$ the pressure at the end of the pipeline remains equal to $p_2 = p_s$, and the flow rate is maximum corresponding to point *6*. The relationship between the mass velocity and pressure p' is shown by line *5-6-7*.

In many practical cases it is sufficient to determine the approximate discharge capacity. For standard boiler pressures, i.e. 47, 110, 115 atm the use may be made of the graph in Fig. 2.17, which immediately shows the discharge capacity of a pipeline depending upon the total coefficient of resistance of the line ξ (reduced to the exit cross section). This graph does not take into account the gravitational head, i.e. it gives the minimum discharge capacity only. If this data is taken as the basis for selecting expanders and their evaporator pipe sizes, the discharge capacity determined from graph in Fig. 2.17 should be increased by 8 to 10% for pressure 47 atm, 3 to 4% for pressure 110 atm and by 2 to 3% for pressure 155 atm.

Example 1. Determine the discharge capacity of the emergency drainage pipe serving 140 atm boiler.

Initial data. The parameters of water in the boiler drum are: $p_s = 155$ atm, $\gamma_1 = 600$ kg/m^3, $i'_1 = 386.5$ kcal/kg. The pipeline 86 m long consists of 133×11 mm pipes. The coefficient of resistance per 1 m pipe $\lambda/d_r = 0.21$. Total coefficient of resistance of the line including all local resistances and discharge velocity losses $\xi = 22.1$. The difference between the levels of the drain cone in the boiler drum and inlet to the expander $H_1 - H_2 = 42$ m. The coefficient of resistance of the vertical portion $\xi_v = 11.5$. The rated pressure for the expander is 1.5 kg/cm^2 (2.5 atm).

Calculation: The mass velocity for $p_1 = p_s = 155$ atm and $\xi = 22.1$, in accordance with the graph shown in Fig. 2.17, is 14800 kg/(m^2·sec). With allowance made for the gravitational head, we provisionally take $m = 1.025 \times 14800 =$

$= 15200$ kg/(m^2·sec). The pressure at the end determined from the same graph $p_2 = 42$ atm.

Now we check these preliminary results by direct calculation. In doing so we take into consideration the gravitational component and the velocity correction factor. The numerical values of $\int_2^1 \gamma^2\,dH$ and $\frac{m^2}{2g}\,(\xi + 4.6 \log \beta)$ are given in Table 2.5 for three values of pressure, i.e. for 134, 128

Table 2.5

Parameters	Pressure, atm		
	134	128	122
Enthalpy of water i_1', kcal/kg . . .	367.1	361.5	355.8
Decrease in the enthalpy of water $\Delta i' = 386.5 - i'$, kcal/kg	19.4	25.0	30.7
Heat of evaporation r, kcal/kg . . .	268.0	276.9	285.7
Degree of dryness $x = \frac{\Delta i'}{r}$	0.0725	0.0902	0.1075
Specific volumes, (m^3/kg)·10^3:			
$(v'' - v')\cdot 10^3$	11.02	11.87	13.10
$x\,(v'' - v')\cdot 10^3$	0.798	1.070	1.408
$v'\cdot 10^3$	1.574	1.550	1.528
$v\cdot 10^3 = x\,(v'' - v')\cdot 10^3 + v'\cdot 10^3$	2.372	2.620	2.936
Specific weight $\gamma_y = \frac{1000}{v\cdot 10^3}$, kg/m^3	422	382	341
$\frac{H_1 - H_2}{2}\gamma_y^2 = 21\gamma_y^2$, kg/m^5	$3.73\cdot 10^6$	$3.06\cdot 10^6$	$2.44\cdot 10^6$
$\int_2^1 \gamma^2 dH = 21\,(600^2 + \gamma_y^2) = 7.56 \times \times 10^6 + 21\gamma_y^2$, kg^2/m^5	$11.29\cdot 10^6$	$10.62\cdot 10^6$	$10.00\cdot 10^5$
Ratio of specific volumes $\beta = \frac{600}{\gamma_y}$	1.42	1.57	1.78
$\xi + 4.6 \log \beta = 11.5 + 4.6 \log \beta$ . . .	12.19	12.40	12.65
$\frac{m^2}{2g}(\xi + 4.6 \log \beta) = 11.78 \times 10^6 \times \times (11.5 + 4.6 \log \beta)$	$143.8\cdot 10^6$	$146.2\cdot 10^6$	$149\cdot 10^6$

and 122 atm. These points are premarked on the basis of tentative mean specific weight $\gamma_1 = 0.85 \times 600 = 510$ kg/m³ and the corresponding value of $\int_2^1 = \gamma^2\, dH = 42 \times 510^2 = 10.9 \times 10^6$ kg²/m⁵.

In Fig. 2.20 shown are the lines $A = \int_2^1 \gamma\, dp$, $B = A + \int_2^1 \gamma^2\, dH$, $C = \frac{m^2}{2g} \times (\xi + 4.6 \log \beta)$. The intersection point of lines B and C determines the nominal pressure $p_n = 126$ atm at the end of the vertical section. The interpolation of data given in Table 2.5 gives $\gamma_n = 368$ kg/m³ and, hence

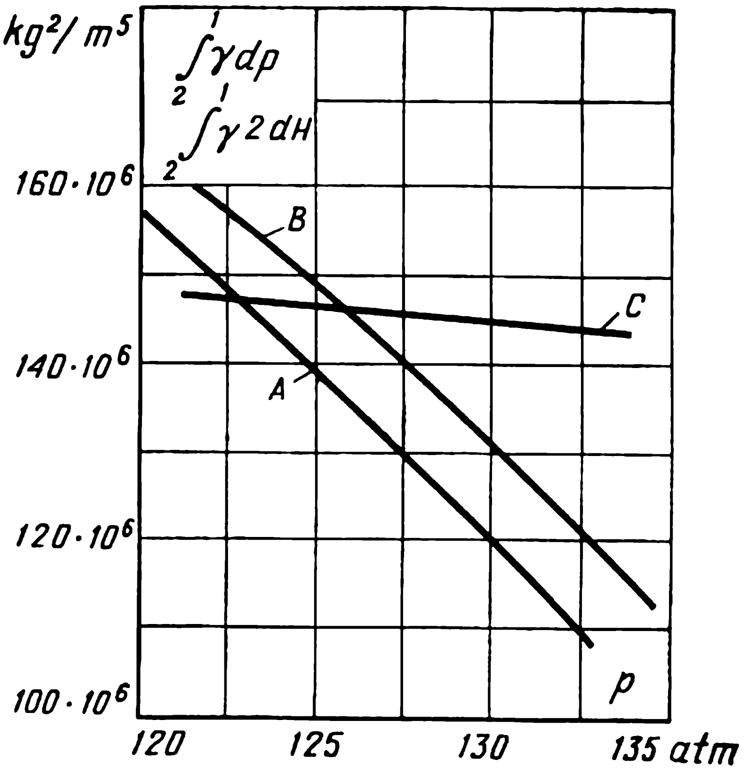

Fig. 2.20. Determination of pressure at the end of vertical section of pipeline carrying boiling condensate

$$\int_2^1 \gamma^2 dH = \frac{42}{2}(600^2 + 368^2) = 10.4 \times 10^6 \text{ kg}^2/\text{m}^5$$

The velocity correction Δ for $p_1 = 155$ atm, $p_2 = 42$ atm, $p_m = 0.5\,(155 + 42) = 98.5$ atm calculated as per formula (2.73)

$$\Delta = 0.2\,(155-42) \times 15.2^2 \times 10^6 \left(\frac{0.04702}{407} + 4\,\frac{0.01736}{319.6} + \frac{0.00847}{235.8}\right) = 1.92 \times 10^6 \text{ kg}^2/\text{m}^5$$

From the graph shown in Fig. 2.14, we calculate for $p_1 = 155$ atm and $\omega = \frac{42}{155} = 0.27$ the value of $\int_2^1 \gamma\,dp = 29.5 \times 10^7$ kg²/m⁵; for the same parameters, $4.6 \log \beta = 4.5$. Substitution of the calculated results in formula (2.71) gives

$$m = \sqrt{\frac{19.62\,(295 + 1.92 + 10.4) \times 10^6}{22.1 + 4.5}} = 15060 \text{ kg/(m}^2\cdot\text{sec)}$$

From the graph in Fig. 2.16 for $p_s = 155$ atm and $\omega = 0.27$, we get $q = 358$ and the critical mass velocity $m_c = qp_2 = 358 \times 42 = 15050$ kg/(m²·sec).

Thus, the mass velocity about 15050 kg/(m²·sec) satisfies simultaneously both conditions: pressure drop in the pipeline and critical flow conditions.

A comparison of the obtained results with approximate ones found through the graph in Fig. 2.17 shows that the error from using the graph is about 1%.

The specific volume of the steam water mixture at the end of pipeline for $p_2 = 42$ atm

$$v_2 = \frac{i_1' - i_2'}{r}\,(v_2'' - v_2') + v' = \frac{386.5 - 261.8}{407.0}\,0.04702 + 0.00126 = 0.01566 \text{ m}^3/\text{kg}$$

Accordingly the critical velocity

$$w_c = v_2 m_c = 0.01566 \times 15050 = 236 \text{ m/sec}$$

For $v_1 = 0.001668$ m³/kg, the velocity at the beginning of pipeline

$$w_1 = 25.1 \text{ m/sec}$$

Example 2. Calculation of the discharge capacity of the overflow pipeline serving the 7 atm deaerator.

The overflow line 65 m long consists of D_n 200 pipes ($d_r = 0.205$ m) and four elbows.

A gate valve with $\xi = 1.63$ operated by electronic level regulator is used as a shut-off device.

The overflow device cone is positioned at 23.0 m, the expander entry at 3.2 m, the top part of the pipe track is vertical.

Determine the discharge capacity of the overflow device after it has been in service for a long period, the equivalent roughness being $k_e = 0.6$, and during the initial operation period when $k_e = 0.2$ (the latter to verify the required discharge capacity of the evaporate pipe serving the expander).

Here, the line resistance coefficients are:

equivalent roughness, mm	0.6	0.2
resistance coefficient per 1 m pipe	0.127	0.095
resistance coefficient of 65 m long pipe	8.25	6.17
local resistance including discharge velocity losses	3.83	3.83
total resistance coefficient for the line	12.08	10.00

Because of the small intake water velocity in the overflow discharge cone the coefficient accounting for exit velocity losses is taken equal to unity. First we shall calculate for $\xi = 12.08$. Taking $p_2 = 0.8$, $p_s = 0.8 \times 7 = 5.6$ atm, from the graph shown in Fig. 2.15 we find that

$$\int_{5.6}^{7.0} \gamma\, dp = 4.64 \times 10^6 \text{ kg}^2/\text{m}^5 \quad \text{and} \quad 4.6 \log \beta = 3.84$$

We take the specific weight of the medium in the vertical portion as equal to the specific weight of water at $t = 164.2$°C assuming that water is not boiling $\left(\frac{\Delta p}{H} < \frac{\gamma}{10^6}\right)$.

Therefore, $\int_2^1 \gamma^2 dH - \int_{3.2}^{23} 903^2\, dH = 16.2 \times 10^6$ kg^2/m^5 and the discharge capacity at $p_2 = 5.6$ atm

$$m=\sqrt{\frac{19.62\,(4.64+16.2)\times 10^6}{12.08+3.84}}=5070\ \text{kg/(m}^2\cdot\text{sec)}$$

To calculate the critical velocity we use Fig. 2.17; for $p_s = 7$ atm and $p_2/p_s = 0.8$, we find $q = 732$. Hence,

$$m_c=732\times 5.6=4100\ \text{kg/(m}^2\cdot\text{sec)}$$

The obtained results indicate that pressure p_2 should be more than 5.6 atm.

Taking $p_2 = 0.99$, $p_s = 6.93$ atm, from the graphs we get

$$10^4\int_2^1 \gamma\,dp=0.6\times 10^6\ \text{kg/m},\quad 4.6\log\beta=0.4\ \text{ and }\ q=760$$

Therefore,

$$m=\sqrt{\frac{19.62\,(0.6+16.2)\times 10^6}{12.08+0.4}}=5140\ \text{kg/(m}^2\cdot\text{sec)}$$

$$m_c=760\times 6.93=5270\ \text{kg/(m}^2\cdot\text{sec)}$$

These results show that pressure p_2 should be less than 6.93 atm.

By interpolation, we find that common solution of the equations is satisfied for $p_2 = 6.76$ atm, when $m = 5120$ kg/(m^2·sec) and $G = \frac{md_r^2}{0.354} = \frac{5120\times 0.205^2}{0.354} = 607$ tons/hr.

The pressure losses per 1 m pipe when $k_e = 0.6$ are:

$$\frac{m^2 v}{2g\,10^4}\,\frac{\lambda}{d_r}=\frac{5120^2\times 0.001107}{19.62\times 10^4}\,0.127=0.0188\ \text{kg/cm}^2$$

which is almost five times less than the gravitational head caused by the fluid with specific weight $\gamma = 903$ kg/m^3, it being $\frac{1\cdot\gamma}{10^4} = 0.0903$ kg/cm^2. This confirms the earlier assumption that there is no boilling in the vertical section of the pipeline.

For new pipelines the total coefficient of resistance $\xi = 10$ will be a little less and the discharge capacity more than in the case considered. Assuming $p_2 = 7.0$ atm and correspondingly $\int \gamma\, dp = 0$, we get

$$m = \sqrt{\frac{19.62 \times 16.2 \times 10^6}{10}} = 5640 > 760 \times 7 = 5320 \text{ kg/(m}^2\cdot\text{sec)}$$

As is shown, in this case $m_c = 5640$ kg/(m^2·sec) should be taken as the critical mass velocity. The decrease in discharge capacity due to increased roughness will be about 10%.

Example 3. Determine the discharge capacity of the continuous blow-off pipeline serving a boiler 140 atm. The continuous blow-off line is made from D_n20 (28 × 2.5) pipes, $d_r = 0.0227$ m, $F = 4.06$ cm^2, pipeline's length 60 m. Two stop valves are installed in the line, one of them is a regulating gate valve of passage area 80 mm^2 and the other a throttle piping with orifice dia 10 mm.

Total coefficient of the line resistance including the coefficient of resistance at the exit ($\xi = 1$) is equal to 276. The line discharge capacity is determined from Fig. 2.17. The critical mass velocity in the pipeline is $m_c = 4.6 \times 10^3$ kg (m^2·sec) (critical pressure at the pipeline end is $p_c = 13$ atm).

The line discharge capacity $G = 3.6 \cdot F \cdot 10^4 \cdot m_c = 3.6 \times 4.06 \times 10^{-4} \times 4.6 \times 10^3 = 6.72$ tons/hr.

2.6. Selection of the Most Rational Pipe Size

In many cases due emphasis is not placed on the technical and economic study of pipe diameters. The weight and cost of pipelines for modern power units is fairly high; the total weight of pipelines for a 300 MW unit exceeds 1000 tons and the cost approaches 1.5 million roubles.

A decrease in pipe diameter lowers its erection and maintenance cost but increases the hydrodynamic resistance and causes additional expense due to greater energy losses and higher consumption of electricity to drive pumps. Thus, when selecting a pipeline's diameter both the capital investment and annual running costs must be considered, the latter to a certain extent are related to the consumption of electricity and energy losses and increases due to decreased capital investments. The criterion of economy therefore is the reduced expenses which take into account the operational cost and a part of the capital investment.

Annual equivalent expenses are determined for one-time investment (construction time up to 1 year) from the formula:

$$S = pK + I, \text{ roubles/year} \tag{2.78}$$

in which K is the one-time capital investment, roubles; p—equivalent coefficient (standard coefficient of effectiveness) 1/year; I—expenditure during normal operation (operational cost), roubles/year.

At present the coefficient p for electric power stations is taken equal to 0.125-0.15.

The selection of most advantageous pipe diameter is restricted by the manufactured assortment of sizes. For pressures P_n100 and less the pipe assortment includes pipe nominal passage diameters for their major types only (for which accessories are manufactured). Manufacture of intermediate nominal sizes (175, 225 mm, etc.) for these pressures is not envisaged in the assortment. The diameter ratios for adjacent sizes in a series are, as a rule, 1.25:1 or 1.20:1, but for passage diametrs greater than D_n300 the ratios decrease to 1.15:1. The hydrodynamic resistance of pipes, including local resistances, varies approximately proportionally to $D_{\text{in}}^{4.5}$ and on changing to the next size the pressure drop in the pipeline at once varies by 1.9 to 2.8 times.

For each parameter of thick-walled high-pressure pipelines a separate size assortment is developed whose passages suit the unit steam rating of boilers. But, after the assortment specification has been fixed the selection of possible pipe sizes when designing pipelines is very limited, i.e. the piping designer has only two or three size versions and sometimes only one at his disposal, and the question of selecting a pipe size loses its significance. It does not mean that the selection of pipe diameter should be done without any technical and economic calculations. Optimum pipe diameters depend upon fuel cost which varies widely, i.e. from 2 to 21 roubles per ton of reference standard fuel. Thus, the feasibility study becomes indispensable, but it should be carried out, rather when developing the assortment for parameters of steam in question, than when the power station is being designed.

The assortment being worked out should consider the cost of two or three grades of fuel; after adopting the assortment specification the limits of fuel cost and the steam flow rates should be defined within which it is advantageous to use this or that pipe diameter. For modern power stations constructed according to a modular system such a task can be easily accomplished. From the point of economic feasibility the given pipe size assortment may be supplemented with additional pipe diameters. This would make technical and economic studies for selection of pipes as a practical factor and save time for piping designers.

The selection of pipe size is closely related to the choice of pumps with a suitable pump head. Powerful pumps used at power stations (feed-water and circulating pumps) can regulate the developed pressure (by use of pipelines, hydraulic couplings, rotating blades in axial pumps) and reduced losses in pipelines give sufficient economy in power consumption with allowances made for control devices. The pressure at a given discharge rate in centrifugal pumps without control devices can be decreased by reducing the size of the wheel to suitable dimensions and, hence, the power consumed by the pump is reduced. Thus, in this case also, economy can be achieved by selecting the pipe diameter correctly. Unfortunately, very often this problem is solved in a very primitive manner: the pipe diameter is selected based on established in actual practice velocities of water, i.e. 2 to 3.5 m/sec, the pipeline's resistance is calculated and from the calculated flow rate G_{cal} and pressure H_{cal} a pump is selected with parameters equal to or more than the parameters given in the catalogue, i.e. $Q_{cat} > Q_{cal}$, $H_{cat} \geqslant H_{cal}$. In this case, it is exigent to throttle the excess pressure with a gate valve after the pump because for Q_{cal} the pressure head H would increase additionally above the value given in catalogue. Such a primitive decision involves useless consumption of electricity.

The internal diameter of a pipe as parameter to be investigated should not be changed smoothly, but in a step-like manner, since one can give only definite values corresponding to standard outside pipe diameter and wall thicknesses used in calculations for strength. For a step-like variation in the parameter the most suitable is version [2-3] for which the total equivalent cost is less than for other neighbouring values of the parameter, i.e.

$$S_{n-1} > S_n < S_{n+1}$$

in which the index n corresponds to the most optimum parameter.

From this inequality it follows that the most optimal pipe diameter for a given flow rate Q depends, particularly, on the ratio of neighbouring values of pipe diameters envisaged by the assortment.

To find the most advantageous pipe diameter it is necessary to compare choices characterized by different power station outputs and different rates of power consumption for station needs. For correct comparison, the choices should be reduced to similar power outputs, i.e. to equal capacity and same electric power available at the busbars. For this reason in the versions when less power is available at station busbars additional cost for the installation and operation of some additional capacity, known as replaceable capacity (power), is taken into account. In those versions when heat economy is very low the appropriate expenditure on fuel must be considered.

All the technical and economic characteristics of compared versions should correspond to the same level of technical development and costs.

When comparing the versions the following should be considered:

A. Capital investment costs of: (1) piping erection; (2) pump sets; (3) the replaceable capacity in power system.

B. Annual expenditures: (1) on amortization and routine repair and maintenance of pipelines; (2) on additional fuel cost due to (a) heat losses in pipelines, (b) deterioration of steam parameters ahead of the turbine, (c) power consumption by pumps; (3) maintenance and operation of replaceable capacity in the power system.

The capital investment costs on pipelines can be calculated from the data given in Appendix 9.

The capital costs of pumps can be taken from current price lists. To this must be added the installation cost of stand-by units. In most cases the same type of pump is taken when different versions are compared, but with different power of electric drives. In the last case, for rough calculations the additional rate of the installed motor can be taken as 10 roubles/kW.

The capital expenses on replaceable capacity provided in power systems, at present, should be taken on the basis of the experience gained in operating large power stations with 300 MW units. The specific capital investment for the main industrially developed area can be taken as 88 roubles per kW of the installed capacity. To the cost of replaceable capacity must be added the cost of the reserve power and the power consumed by the station proper. Taking 12% as reserve power and 4.2% for station needs for a 300 MW unit the specific capital investments are:

$$\frac{1.12}{1-0.042}88=103 \text{ roubles/kW}$$

The power consumed by pumps, in each case, is determined from the characteristic of pumps or from the pumps trial data with allowances made for pressure regulation, and for centrifugal unregulated pumps—with the possibility of decreasing the pump pressure up to the required value (by grinding the wheel). The required pump head should be determined from the hydraulic calculations performed for each version.

In those cases, when the pressure at the end of a pipeline is very high more exact results are given by directly calculating the additional power needed to propel the fluid through the line:

$$\Delta N=\frac{Q_p v_p g \Delta p 10^4}{\eta 10^3} \text{ kW} \tag{2.79}$$

in which Q_p is the rated supply of pump, kg/ses; v_p —specific volume of the pumped liquid, m^3/kg; Δp—pressure loss (additional) in the pipeline, kg/cm^2; η—pump's efficiency factor.

At power stations where the main steam lines are fitted with a changeover connector, cases are known when the pressure losses in different turbines were so large that the turbines could not generate even their nominal power. In such cases, the costs to increase the discharge capacity of pipelines are compensated for by the economy in erection cost of new turbines. Such calculations, however, are more correct when made on the basis of the maximum, not the rated, output of turbosets which they can generate with normal steam parameters and design vacuum (turbines are calculated for rated output in somewhat lower vacuum during summer and in winter in a normal vacuum they are capable of developing maximum power from 5 to 10% over the nominal one. Certain turbines permit prolonged increase in pressure before the turbine (for example, the K-200-130 turbine permits an increase up to 135 kg/cm^2), and if such an increase in pressure under some definite conditions can enhance the available turbine power, then this fact should also be taken into account when selecting the pipeline diameter.

The annual expenses on piping include: depreciation, routine maintenance and expenses incurred by metal creep control, structural changes of metals and condition of welded joints. These expenses can be determined as percentage against piping cost in the following rate:

Pipeline	Annual expenses	Including depreciation
Steam lines at $t > 500°C$	11%	8%
Same at $t > 400°C$	10%	8%
Same at $t < 400°C$	8%	7%
Feed water pipelines . .	10%	8%
Heating pipelines . . .	4%	3.5%
Circulating water pipelines	4%	3.5%

The annual expenses on fuel are assessed from the total fuel cost in a particular region. These data on different types of fuels are listed in Appendix 10.

The amount of fuel needed to overcome heat losses is determined from the formula

$$B = (0.044t \sqrt{D_o}) L \frac{\tau \varepsilon_r}{\eta_{nb} 7 \cdot 10^6} \text{ tons/year} \qquad (2.80)$$

in which $(0.044t\sqrt{D_0})$—heat losses in a unit length of insulated pipeline, kcal/(hr·m); t—temperature of heat-transfer agent, °C; D_0—outside pipe diameter, mm; L—length of pipeline, m; τ—number of annual operation hours for the pipeline; η_{nb}—net efficiency of boiler (with allowances for the heat equivalent of electric power consumed); 7×10^6—calorific value of fuel, kcal/ton $\varepsilon_r = 1 - z_r \dfrac{i''_c - i'_c}{i''_e - i''_c + \Delta i''_{i-r}}$ — coefficient of steam heat value obtained from the turbine extraction r;

$$z_r = \frac{i''_e - i''_r + \Delta i''_{i\text{-}r}}{i''_r - i'_r}$$

i''_e, i''_r, i''_c—enthalpy of steam before the turbine, in extraction r and in condenser, respectively; i'_r, i'_c — enthalpy of condensate after the heater and condenser; Δi_{i-r}—increment in steam enthalpy in the reheater (installed before extraction r).

The coefficient ε_r should be considered when determining the cost of heat losses both in the steam and water pipelines; in the latter case ε_r is taken for the water heater installed at the end of the water pipeline. For feed water pipelines after the last high-pressure heater and for main steam pipelines $z_r = 0$ and $\varepsilon_r = 1$.

For approximate calculations $\eta_{n.b} = 0.85$.

The additional amount of fuel required (or economy gained) due to the increase (or decrease) in steam pressure before entering the turbine may be taken from Table 2.6. This table is based on the data collected by ОРГРЭС (State Trust for

Table 2.6

Turbine type	Maximum output capacity, MW	Steam pressure ahead of the stop valve, atm		Variation in specific heat consumption, %	
		Nominal	Maximum pressure during prolonged operation	Pressure increased by 1 atm	Pressure decreased by 1 atm
K-200-130	210	130	135	—0.06	+0.068
K-160-130	165	130	135	—0.3	+0.3
K-100-90	110	90	95	—0.9	+0.9
K-50-90	55	90	95	—0.9	+0.8

the Organization and Rationalization of Regional Electric Power Plants and Net Works). The additional amount of fuel required to cover pressure losses in steam pipelines of the intermediate steam reheat system is calculated specially. The amount of reference fuel required for 1 kW·hour of power consumed by pumps supplying water to the thermal system is determined from the formula

$$b = b_{r.c.s}(1 + z_r\eta_{e.m.p}\eta_{e.m.t}) - 0.123\,\frac{\eta_{e.m.p}}{\eta_{nb}}(1 + z_r) \qquad (2.81)$$

in which $b_{r.c.s}$ is the specific reference fuel consumption for a replaceable condensing steam power station, kg/kW·hour; $\eta_{e.m.p}$—electro-mechanical efficiency factor of pump (this takes into account the losses in electric motor and friction in pump's bearings); $\eta_{e.m.t}$—electro-mechanical efficiency of a turbo-set; $\eta_{n.b}$ and z_r—see formula (2.80).

Formula (2.81) takes into account the increase in enthalpy of water due to hydraulic losses in the pump and pipelines and the subsequent decrease in steam intake from the turbine extraction r and the amount of fuel burnt in the boiler.

For feed water pipelines installed beyond the last high-pressure heater $z_r = 0$ and $b = b_{r.c.s}$—0.12. For circulating, ash handling and bearing cooling pumps $b = b_{r.c.s}$. At present the value of $b_{r.c.s}$ is generally taken equal to 0.36 kg of reference fuel for 1 kW·hour.

The operational charges for replaceable capacity in a power system include: depreciation, routine repair, salary of operation staff and miscellaneous charges and are taken as 11% of the capital investment on replaceable capacity.

Before we conclude, we shall discuss one more methodical problem. Very often, while finding the economical pipe diameter the inside diameter is considered as a continuously varying factor and the minimum annual reduced expenses are found which also, in this case, are a continuous function. In this solution of the problem one can define, for example, that for the power unit K-200-130 the inside diameters of the main steam pipelines should be:

When the fuel cost is, roubles/ton *r.f.*	Inside diameter, mm
5	200
10	250
15	268

However, we immediately face a difficulty, because the passage diameters available in the assortment are 209, 249 and 287 out of which only one, the 249 mm, coincides with the passage calculated one as per the above mentioned procedure. One cannot forecast passage diameter when the fuel cost is 8 roubles per ton of reference fuel—209 or 249 mm.

The proper approach to this problem, apparently, is to find the border costs of fuel for which it is advantageous to use a pipe of bigger diameter. With this correct approach it will immediately become clear that apart from the fuel cost, the ratio of the adjacent and the nearest maximum and minimum pipe diameters has effect upon the economical pipe size.

An example of determining the economical diameter of a feed water line serving a double chest boiler of a power unit with a K-200-130 turbine.

The rated feed water supply to each chest of the boiler is 320 tons per hour or 377 m^3/hr when the specific volume $v = 1.18 \times 10^{-3}$ m^3/kg, pressure 230 atm, temperature 230°C.

The length of the pipeline feeding one chest of the boiler is 100 m and the other 125 m and the necessary value of the pump head is determined based on resistance offered by the line serving the second chest. Total coefficient of local resistances for each pipeline equals 8.5. Assumed in the calculation are: 7000 working hours for the unit in a year, annual feed pump operation hours 6300, average yearly temperature of feed water 220°C. The capital investment on pipelines of bulk supply is calculated based on 1320 roubles per ton. Capital investment on replaceable electric power is 103 roubles/kW.

The operational charges are taken as 10% of the capital investment for pipelines and 11% for replaceable capacity. The standard coefficient of effectiveness is 0.125.

The fuel consumption of a feed pump is calculated at a pump efficiency of 0.7. The amount of fuel necessary to cover heat losses through insulation is based on a net boiler efficiency of 0.85 and a fuel heat evaluation coefficient $\varepsilon_r = 1$. The calculation is given in Table 2.7. For the accepted cost of reference fuel, i.e. 10 roubles/ton the most advantageous version is the second (velocity of water 3.91 m/sec). To solve the problem in a general way the relationship between

Table 2.7

Parametres	Versions		
	1	2	3
Pipe size, mm	245 × 18	219 × 16	194 × 15
Weight of pipeline, ton	27.8	22.0	18.2
Velocity of water, m/sec	3.14	3.91	5.10
Total coefficient of hydrodynamic resistance including accessories	20.55	22.10	23.60
Pressure drop in pipeline, kg/cm^2	0.875	1.462	2.65
Power consumed by pumps, kW	28.2	47.2	85.5
Annual power consumption, MW·hour	178	297	538
Consumption of reference fuel to overcome pipeline resistance, tons per year	42.7	71.3	129.2
Consumption of reference fuel to cover heat losses in pipelines, tons/year	40.1	37.9	35.7
Total consumption of reference fuel, tons/year	82.8	109.2	164.9
Capital investment, in thousand roubles:			
(a) on pipelines	36.7	29.1	24.0
(b) on replaceable capacity	2.9	4.9	8.8
(c) total costs	39.6	34.0	32.8
Annual expenses, in thousand roubles:			
(a) maintenance and depreciation of pipelines	3.67	2.91	2.40
(b) operational costs of replaceable capacity	0.32	0.54	0.97
(c) depreciation (0.125) of capital investment	4.95	4.25	4.10
Fuel cost at the rate of 10 roubles per ton of reference fuel	0.83	1.09	1.65
Annual reduced expenses	9.77	8.79	9.12

the annual reduced cost and the cost of reference fuel x should be determined for each of the three versions: $S_1 = 8.94 + 0.0828\ x$; $S_2 = 7.70 + 0.1092\ x$; $S_3 = 7.47 + 0.1595\ x$.

The cost of reference fuel, for which the versions (1) and (2) are equally economical, is determined by the equality $S_1 = S_2$, whence $x \approx 46$ roubles/ton, the versions (2) and (3) are equally economical when $S_2 = S_3$, whence $x = 4.1$ roubles per ton.

The rated cost of fuel in all parts of the Soviet Union ranges between 4.5 and 21 roubles per ton of reference fuel (Appendix 10), and the most economical under these conditions is version No. 2 (pipes 219 × 16 mm). Exceptions are brown coal mined in Eastern Siberia whose low cost (two roubles per ton of reference fuel) decides on somewhat better economy of version No. 3.

Chapter Three

Pipeline Structural Calculations

3.1. General

According to their origin loads acting on any structure can be divided into two categories: (a) loads due to applied forces (hydrodynamic pressure, weight, etc.); (b) loads caused by deformations at different stages, i.e. during manufacturing, assembly, erection, temperature variations. The effect produced by these categories of loads is very significant and should be taken into account in strength calculations.

The external (applied) forces acting on a structure do not decrease in magnitude because of the deformations appearing in the structure; an increase in loads of the first category beyond a certain limit increases deformation and may lead to structural failure. The loads of the second category caused by deformations of earlier restricted dimensions can not bring an increase in deformation or cause structural failure as the structure is made of a ductile material. The above pertains wholly to pipelines at thermal power stations. These pipelines are made of low carbon content steel of high ductility. The pipelines for thermal power stations are calculated as per the standards for structural design of steam boiler elements [3-1]. The methods of calculation listed in the standards are based on the principle of evaluating strength from maximum load-carrying capacity (limit load).

In all components, in which stresses get unevenly distributed along the cross section (during bending, torsion) or exist peaks of local stresses (at holes, etc.), as the load acting on a component approaches the limit value a relative redistribution of stresses takes place and they become uniform throughout the cross section due to plastic deformations. The load-carrying capacity method accounts for this redistribution of stresses and, because of this, ensures maximum economy of metal.

When calculating pipelines it becomes necessary to replace limit and rated loads with the stresses proportional to these loads, because only such a replacement enables one to take into account the combined action of loads, different in their nature, and also use the same method for calculating pipelines made of different steels. Under limit loads, due to plastic deformations, the distribution of stresses in the structure may be completely different than it would have been at the working (rated) load, when the deformations, as a rule, remain elastic. For this reason the stress diagrams for limit and rated loads are not similar (see Fig. 3.1).

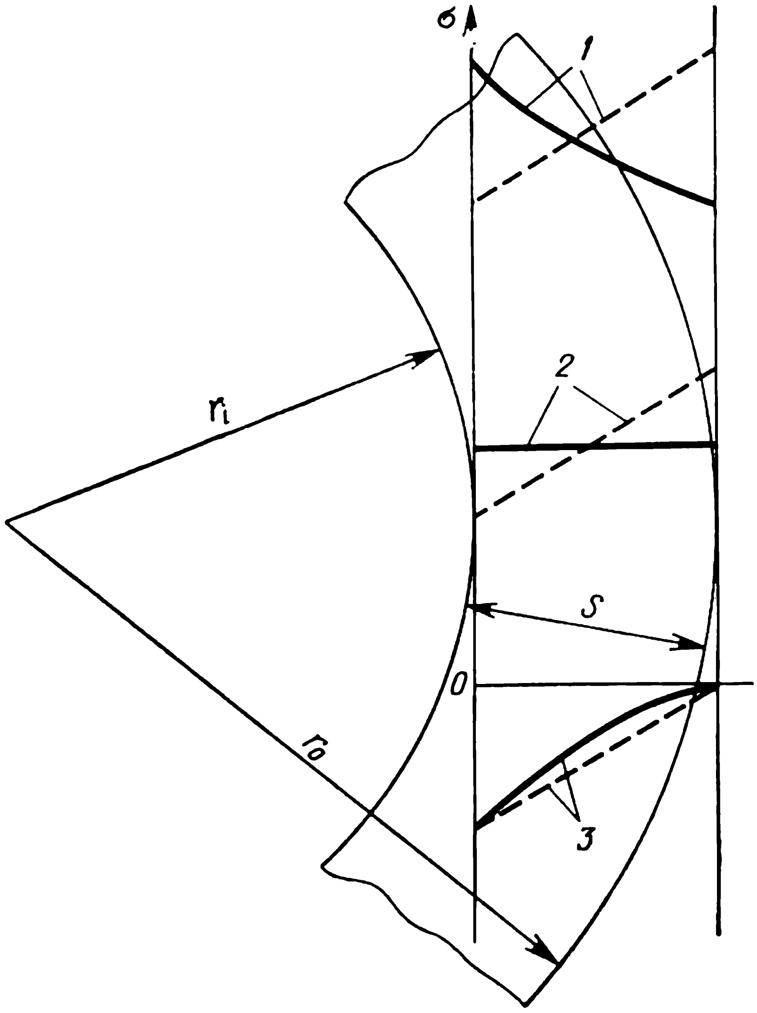

Fig. 3.1. Stresses in pipe wall due to internal pressure
1—circumferential; *2*—tensile; *3*—radial; thick lines—stresses at the rated pressure; dotted lines — at the limit pressure

In calculations performed in accordance with the limit load method the design stresses are taken *k* times less than the stresses in the limiting condition, where k is the ratio of actual (rated) load to the limiting one. One may mention that the bending stresses in a pipe wall caused by irregularities in its cross section (ovality) do not decrease the limit load, for the reason that with the onset of plastic state in pipe walls the ovality disappears. When the wall thickness is different the strength is determined by the minimum wall thickness. To calculate elements working at high temperatures and in a multiaxial stressed state, the standards list formulas, depending on the theoretical and experimental data, which determine the load-carrying capacity by using the long-term strength parameter instead of the yield point.

Where there is a metal creep the difference between stresses, which are caused by external loads and elastic deformations, is completely maintained. Presence of small creep deformations do not, practically, change the magnitude of the external (applied) loads in a pipeline. Since creep deformations are plastic ones, redistribution and the slow levelling of stresses caused by these loads take place in the pipeline. Stresses caused by different types of plastic deformations relax after some time and disappear as the elastic deformations change into plastic ones.

The working pressure is taken as basic load by which the wall thickness of a pipe and piping elements should be calculated.

When taking into account the combined action of different types of loads (internal pressure, weight) one should proceed from the limiting condition of the element for simultaneous combination of loads. Therefore, formulas taking into account bending stresses must also consider plastic bending stresses (plasticity hinge) in the walls of the pipeline under the limiting pressure for the given combination of loads. Experiments conducted by the ЦКТИ (I. I. Polzunov's Central Scientific Research, Planning and Design Boiler and Turbine Institute) [3-6] proved the following: (1) for the combined action of internal hydraulic pressure and bending moment the limit load (appearance of plastic state) is accurately determined from the Mises-Huber plasticity condition; (2) presence of bending moments including moments which cause plastic bending has little effect on the destructive hydraulic pressure; (3) the cross welded joints, which have a decreased plasticity, were affected by bending stresses.

Using these criteria the Standards for evaluating the effect of bending moments and torque have taken into account formulas deduced for the limiting condition from the Mises plasticity condition. After adding main stresses caused by internal pressure to the corresponding stresses produced by additional loads and simplifications, the limiting state condition can be reduced to:

$$\sigma_s^2 = \sigma_{rd}^2 + (\sigma_t + 0.8\sigma_b)^2 + 3\tau^2$$

in which σ_{rd} is the reduced stress caused by internal hydraulic pressure; σ_t and σ_b—additional axial tensile and bending stresses; τ—additional shear stress.

The coefficient 0.8 for σ_b takes into account plastic bending (an increase in the moment of resistance of pipe's cross section by 27% during plastic bending as compared to elastic bending).

The decreased resistivity of welded joints to bending is taken into account, when determining bending stresses, by introducing the coefficient of strength for welded joints in bending φ_b.

The above mentioned condition with different safety factors is used as the basis for formulas which determine permissible stresses due to external loads and temperature stresses. The weight and other external loads pertain to additional external loads. The limiting permissible values of constant external loads are taken from the Standards. These values have been determined based on the decrease in the safety factor by 9.5% with respect to the limiting state.

The additional weight loads (moments) appearing due to faulty erection (elevation and subsidence of supports, inaccuracy in hanger adjustment) are not accounted for in calculations, because at the limit load these additional loads disappear.

Stresses caused by self-compensation of thermal expansion are the result of plastic deformations appearing in a pipeline. For this reason these stresses can not result in pipeline failure. The appearance of multiple bending and torsion plastic deformations is undesirable for a number of reasons, including the risk of failure due to fatigue cracks. The self-compensation stresses are restricted by the Standards, but the safety factor decreases, in this case, to the minimum, $1.5/\sqrt{2} = 1.06$, with respect to the limiting condition. This minimum value of the safety factor is sufficient to ensure reliability relative to cyclic stresses (change-over from the inoperative to the operative condition and vice versa) appearing in straight and curved pipelines of normal radius which do not have significant ovality. For small radii of curvature and small relative wall thickness of elbows, it is necessary to consider the large tangential bending stresses in walls appearing as a result of flexible flatting of cross section of curved pipes. In steep bent elbows of radius (1-1.5) D_n, the intensification coefficient of tangential bending stresses amounts to 5-7, and in welded elbows it reaches 15. For this reason it becomes necessary to check such elbows for fatigue after a limited number of cycles.

To the category of stresses which cause deformations may be grouped stresses due to resilient elongations and also stresses caused by the decrease in the central angle of curved elbows with ovality. This and the other type of deformation increase pipeline length (in its free state) and should be compensated for along with temperature expansion of pipeline.

Nominal allowable stresses are not considered by the Standards as a limit for local stresses even if such stresses are caused by the main load. Thus, for example, stresses at the internal surface of a pipe's wall for $(s\text{-}c)\colon D_n = 0.25$ can amount to $1.54\sigma_{allowable}$. This is one of the peculiarities of the method of calculation as per limiting loads. This method has been accepted in the Standards. Therein, restrictions aimed at eliminating significant plastic deformations have been listed. They limit the ratio between pipe wall thickness and diameter to 0.25, thus limiting self-compensation stresses.

3.2. Basic Properties of Steels Used for Power Station Pipelines

In the Standards the following principal characteristics of steels at the design temperature t have been listed: σ_u^t — tensile strength (ultimate tensile strength); σ_s^t —proof stress

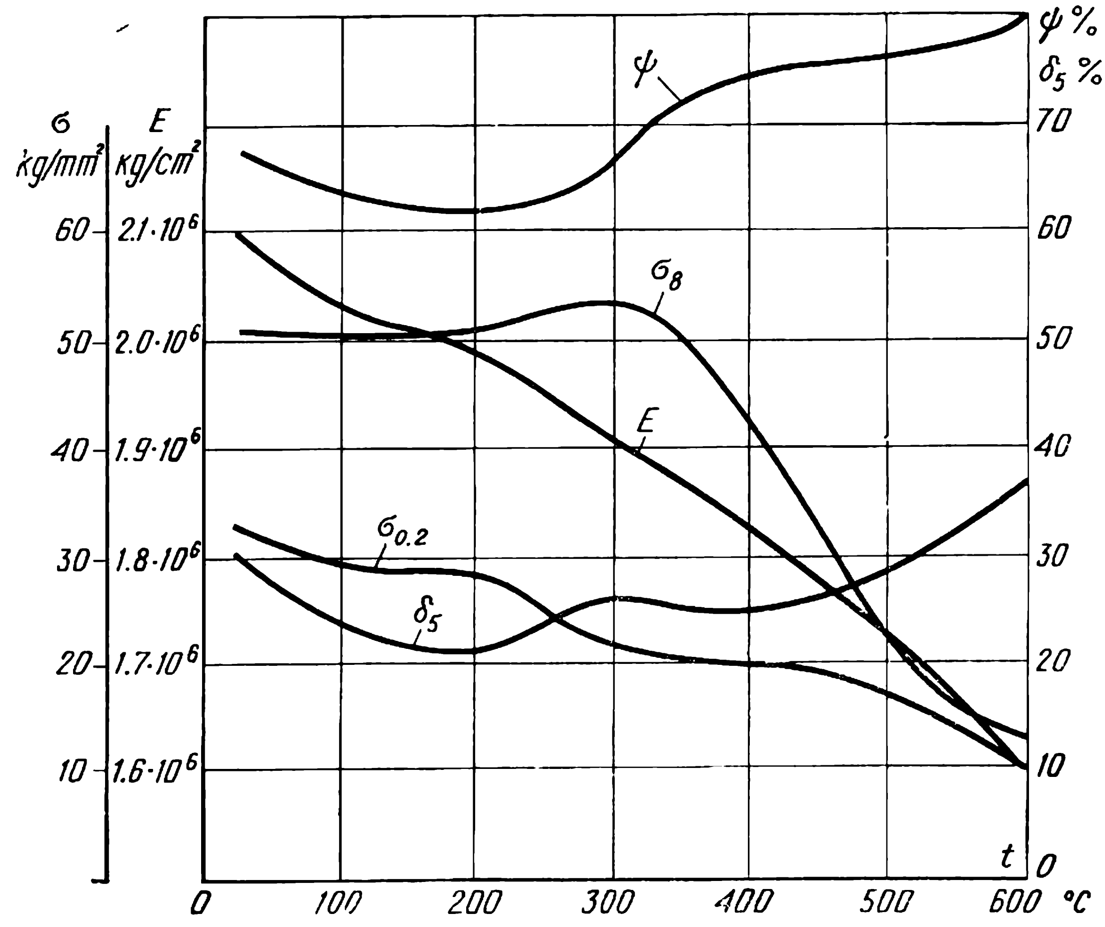

Fig. 3.2. Mechanical properties of steel Grade 20 at different temperatures

(for residual deformation 0.2%) in elongation; σ_r^t—rupture stress in elongation (the stress causing failure after 100,000 hours).

The minimum value out of the three given below has been taken in the standards as the allowable stress σ_{al} at the working temperature:

$$\sigma_{al} \leqslant \frac{\sigma_u^t}{2.6}\,; \quad \sigma_{al} \leqslant \frac{\sigma_s^t}{1.5}\,; \quad \sigma_{al} \leqslant \frac{\sigma_r^t}{1.5}$$

The mechanical properties of steels, i.e. tensile strength σ_u, yield point σ_s and also the relative elongation δ (per cent) and the reduction in area ψ (per cent) are determined by common methods. These methods are stipulated in the State Standard, GOST 1497-61.

The yield point of a steel can be increased through plastic deformation (work hardening). But, cold hardening worsens the resistivity to corrosion, lowers plastic properties and toughness, and to avoid this cold worked steel is subjected to heat treatment.

Temperature significantly effects strength and plasticity factors as seen from Fig. 3.2. On increasing the temperature the tensile strength at first increases, becomes maximum in the range from 250 to 300°C, but thereafter quickly decreases with further increases in temperature. The plasticity factors, on the contrary, at first decrease, becoming a minimum at 250-300°C and increase with further rise in temperature. Thus, for carbon steels maximum tensile strength corresponds to the minimum plasticity. The yield point and the proportionality limit decrease smoothly as the temperature increases. In low-carbon steels the yield point occurs at a temperature of up to 250°C, but is not discovered at high temperatures.

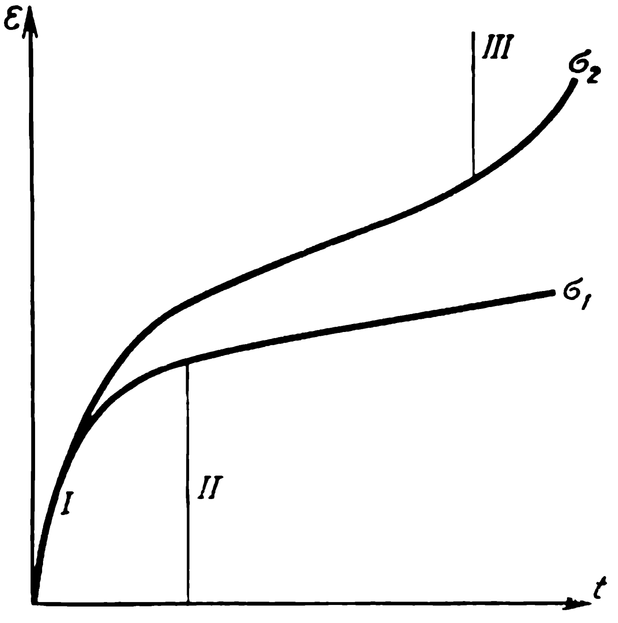

Fig. 3.3. Creep curves at different tensile stresses

At elevated temperatures, continuous plastic deformation takes place in steels subject to constant loads, and this phenomenon is called creep. Elongation *vs* time curves (creep curves) are shown in Fig. 3.3. There are three stages in creep: stage I on creep curves (Fig. 3.3) corresponds to a nonuniform rate of creep. In stage II the rate of creep is uniform and the stage III refers to the final state (failure). In stage I, the metal is elongated at a decreasing rate of creep, asymptotically approaching the steady rate of creep. The metal in this stage may remain for a few hundred hours. With the lapse of time, if the elongation stresses and temperature are fairly large, the rate of creep increases and, finally, the rupture of the specimen takes place. The stress to fracture the specimen, at a given temperature and time, is known as rupture stress. Here, it may be mentioned that total elongation due to creep, at which a material fails, is not very large and amounts to 5-10% in mild steels, and 1-2% in alloy steels highly resistant to creep. For this reason, it is not correct to fix permissible stresses in pipelines based on a certain creep velocity, similar for every grade of steel. The more so, an increase in pipe diameter, caused by creep, itself does not restrict further use of the pipeline. It is more correct to determine allowable stresses on the basis of rupture stress (the values of allowable stresses recommended in the standards are calculated based on rupture stress). The creep rate for the recommended allowable stresses does not exceed, as a rule, 10^{-7} mm/(mm·hr) or 1% in 100,000 working hours of steam pipelines.

To determine the rupture stress, i.e. the maximum stress that may be applied for a long period of time, say 100,000 hours, a number of specimens are tested under different loads and stress *vs* time to fracture the specimen curves are plotted for each specimen (Fig. 3.4). The curves drawn for tests, which are carried on to the failure of the specimen, are straight or broken lines. This enables one to determine by extrapolation the creep limit in 100,000 hours based on short-time tests. At elevated temperatures and under large stresses, in many grades of steel with the lapse of time structural changes take place which worsen steel's properties. For this reason, now-a-days creep-rupture tests are carried out for longer periods, i.e. for 10 to 20 thousand hours and even more.

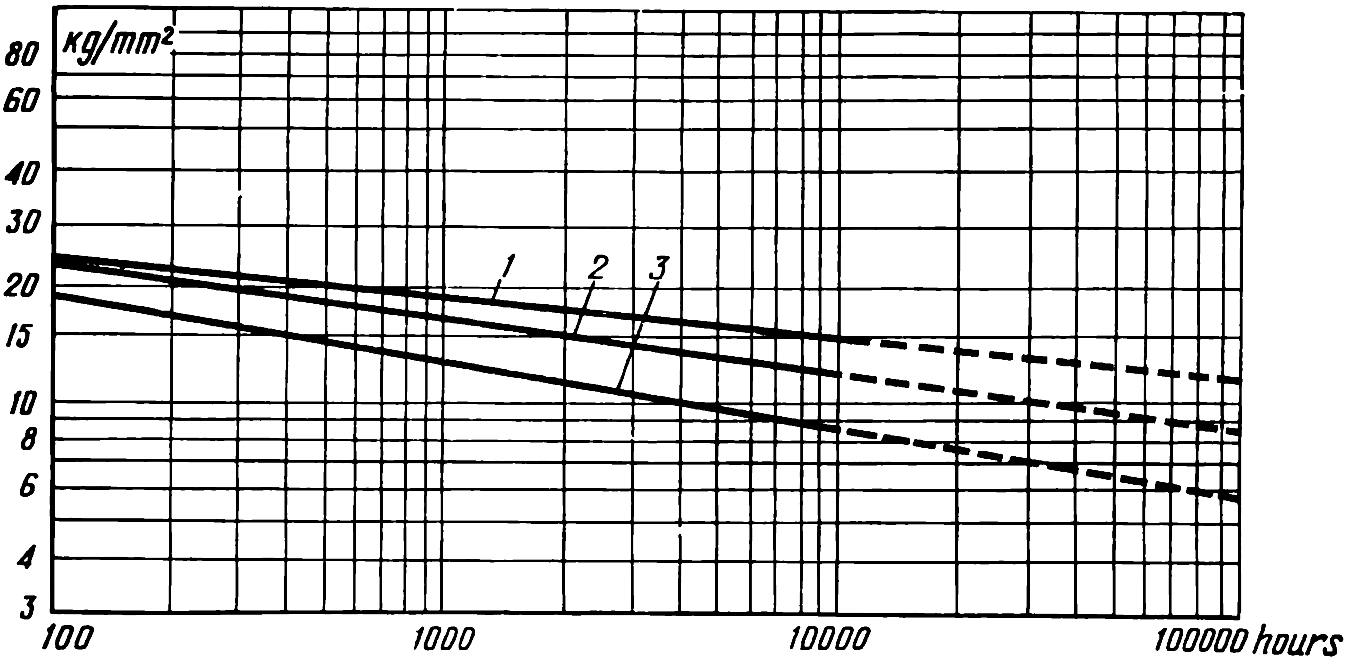

Fig. 3.4. Creep limit for steel 12XIMФ

1—at 560°C; *2*—at 580°C; *3*—at 600°C

The designation system for quality and alloy steels, standardized in the Soviet Union, utilizes a combination of Russian letters and numbers. The letters indicate the presence of a certain alloying element. Accordingly, X indicates chromium, H—nickel, M—molybdenum, Ф—vanadium, B—tungsten, T—titanium, Б—niobium, P—boron, Г—manganese, C—silicon. The number preceding the letter indicate the carbon content in hundredths of one per cent while the number after the letter indicates the approximate percentage of the alloying element, if its content equals or exceeds 1%. In case the content of the alloying element is less than 1% no number follows the letter. Since manganese and silicon enter into the composition of every steel, the letters Г and C, used in the designation of a steel, indicate a higher content of these elements.

For example, steel 12XIMФ contains about 0.12% carbon, 1% chromium (Cr = 0.9 to 1.2%), and less than 1% molybdenum and vanadium (Mo = 0.4 to 0.55% and V = 0.15 to 0.35%).

Besides the designation system for steels, accepted in the USSR Standard, GOST, the systems used by steel manufacturers are also practiced to designate various steels. For example, ЭИ-257, ЭИ-531, ЭП-17, ЭП-695-Р and so on.

The following steel grades are used for power plant piping:

Carbon steel Grade 20 (GOST 1050-60) is a quality steel, smelted in an open-hearth furnace. It is a killed steel with chemical composition and mechanical properties guaranteed. It contains approximately 0.20% carbon. Maximum allowable content of carbon for this steel amounts to 0.24%. Such a composition ensures good weldability without additional heat treatment. The cost of pipes made of steel Grade 20 and 10 is the same, but the value of allowable stresses for steel 20 is 15 to 20% higher than for steel 10, therefore the wall thickness of pipes made from steel 20 may be 13 to 17% less than for similar size pipes made of steel 10. At present seamless pipes up to a diameter of 465 mm are manufactured from steel 20. Pipes made of such steel can be used for steam lines carrying steam at a temperature of up to 450°C (40 atm 440°C) and feed pipelines at any pressure.

Carbon steel 10, of the same cost as steel 20, has a comparatively low strength. For this reason, it is advisable to use pipes made of steel 10 only when minimum pipe wall thickness satisfies strength requirements (in this case the pipe wall thickness is the same as for pipes made of steel 20). An example of such pipes are the pipes of 89 mm diameter and less operating at nominal pressure P_n 64 or less. For nominal pressures P_n 25 or less, pipes made from steel 10 with minimum wall thickness, including pipes of 426 mm diameter, can be employed. But, the use of similar size pipes, having different strengths, at one and the same erection site, generally speaking, is not desirable as it leads to the mistake of welding in high pressure pipelines pipes made of steel 10 which have low strength to withstand such high parameters.

Ordinary carbon steel, (GOST 380-60) Grades 3 and 2, is used to manufacture seamless pipelines operating at parameters up to 23 atm 300°C and for welded pipelines serving at a nominal pressure of P_n 16 or less and at a temperature of up to 300°C. Steel Grade 3 has almost the same mechanical properties as Grade 20, and steel Grade 2 has tensile strength close to that of Grade 10.

Steel 15ГС contains a higher content of manganese and silicon and is used to manufacture feed water pipelines for working pressures 185, 230 and 380 kg/cm^2, respectively. The value of allowable stresses for this steel is 25% higher than for steel Grade 20, and this fact permits, for a similar internal diameter, the pipeline weight to be decreased by 30% and pipeline rigidity lowered (equitorial moment of inertia of cross section) by 36%. The cost of pipelines manufactured from steel 15ГС is more by 120 to 140 roubles/ton than of pipelines made from steel Grade 20.

Heat resistant low-alloy pearlitic steels are used for manufacturing steam pipelines operating at 450-570°C. In the past, for standard steam temperature 510°C chromium-molybdenum steels 12MX and 15XM were used, but with the increase in steam temperature up to 540 and 565-570°C it became necessary to use chromium-molybdenum steels 12XIMФ and 15XIMIФ having more strength at elevated temperatures. Steel 12XIMФ is used for manufacturing 540 and 570°C steam pipelines with wall thickness up to

40 mm. The limitation on wall thickness is due to the fact that heat treatment in thick-walled pipelines does not produce desired results. In particular, it does not enable one to achieve the required toughness. At the present time, pipes of 45 mm wall thickness or more are manufactured from steel 15XIMIФ containing a higher content of molybdenum. Nominal permissible stresses for this steel are approximately 13% more than for steel 12XIMФ. Steel 15XIMIФ finds less application in industry and costs 1 1/2 times more than steel 12XIMФ. But, it is difficult to manufacture pipes with passage size more than 205 mm (wall thickness 60 mm) from steel 15XIMIФ for steam parameters 255 atm 565°C. Because of this, multirow pipelines are installed to meet the requirements of modern large power units. In this respect high chromium content steel ЭИ-756 (IX12B2MФ) is of interest, allowable stresses for which at a steam temperature of 565°C are more by 30% than for steel 15XIMIФ. This permits to manufacture pipes of passage size twice more, thus reducing the number of pipe runs to one half. Steel ЭИ-756 is used for manufacturing steam pipelines for separate installations so that data on the working of this steel under operating conditions could be collected.

High-alloy austenite steels have higher creep limits and creep resistances compared to low-alloy steels. The following austenitic steels X18H12T (ЭЯ1*T*), X16H16B2MБP (ЭП182) and others have been applied at different power units.

Austenitic steels have a high corrosion resistance, and because of this they are called stainless steels. At the same time austenitic steels cost much more than low-alloy steels, and require large amounts of scarce nickel. For this reason, it is wise to use such steels only for temperatures greater than 600°C and also when it is necessary to fight pipe corrosion, for example, in the primary circuit pipelines at atomic power stations.

Austenitic steels have a higher ductility and toughness, but the final creep deformation, at which the failure takes place, is very small in magnitude and many times less than in pearlitic steels. The reliability of austenitic pipelines is still an unknown factor. This is witnessed by the large number of papers published and dedicated to the problems of intercrystalline corrosion, formation of cracks, improvement in welding processes and other ways of increasing the pipeline reliability and that of superheat elements made of different grades of austenitic steels.

3.3. Wall Thickness Calculations

The pipe wall thickness is determined for the design pressure, other external loads (weight, wind loads, etc.) are not considered.

By design pressure we mean the maximum pressure which a pipeline withstands during operation. For piping equipped with pressure release safety valves (installed in the pipeline itself or in the equipment to which the pipeline is connected) the increase in pressure necessary to open the safety valve is not taken into account, if it does not exceed the value prescribed in the Gosgortekhnadzor (State Committee of the Council of Ministers for Supervision of Industrial Safety and for Mining Inspection) Standards. Depending upon the source of steam, the design pressure for pipelines is taken from the Table given below:

Source	Design pressure for pipelines
Boiler, steam generator	Nominal effective pressure of steam at the boiler outlet
Controlled extraction or back pressure	Maximum pressure in extraction or back pressure envisaged by technical specifications for turbine supply
Uncontrolled extraction	Highest possible pressure of steam in extraction line (for maximum discharge rate of steam in the stages following the extraction)
Reducing unit	Maximum effective pressure of reduced steam, taken in the design
Blow-off and drainage expanders	Effective pressure of expander

For pipelines, under pump pressure, the highest pressure of the pump from its characteristics is taken as the design pressure with allowances made for hydrostatic head in the suction pipe. In those cases, when safety valves are installed beyond the pump the installed pressure of the safety valves is taken as the design pressure, and to the pressure in the pipe between the pump and the point of safety valve installation must be added hydraulic pressure losses.

For feed pumps equipped with turbopumps or electric motors, fitted with variable speed gear, the design pressure is taken as 1.05 times the nominal pressure.

For drainage and blow-off pipelines the main pipeline pressure is taken as the design pressure.

In exhaust pipelines the pressure beyond the safety valve should be determined by performing hydraulic calculations. The design pressure for water pipes connected to a reservoir is taken equal to the hydrostatic water column pressure above the pipeline plus the steam pressure in the reservoir over the water surface.

The design temperature of pipe walls, according to paragraph 1.4.8 of the Standards, is equal to the highest temperature of the fluid flowing through them.

For steam pipelines the nominal temperature of steam after the steam reheater of boiler or steam generator is taken as the design temperature, however, according to paragraph 1.4.1 of the Standards, the deviation in steam temperatures from the nominal temperature within permissible limits, outlined in GOST 3619-59, are not taken into account.

The maximum temperature of steam, received from extractions or back pressure of turbine, with allowance made for the peculiarities of turbine control systems is taken as steam design temperature. The steam has the highest temperature in controlled extractions when the steam flow rate through the turbine is small for duties when the first valve is used to throttle the steam flow rate. In uncontrolled extractions of condensing turbines the steam attains its highest temperature when the steam flow rate through the turbine is maximum and the heat drop at the adjustable stage is minimum.

To manufacture station pipelines, pipes are selected from the ranges contained in Inter-Branch Standards to match the limiting parameters listed in Tables. To determine wall thickness for parameters not listed in the MBH Standards and also for solving problems of using other pipes not covered by assortment specifications it is necessary to use design formulas.

The nominal wall thickness of seamless pipes is determined from the condition:

$$s \geqslant \frac{D_n p}{200\sigma_{al} + p} + c_1 \text{ mm} \tag{3.1}$$

in which D_n—nominal outside pipe diameter, mm; c_1—addition to design wall thickness, mm; p—design hydraulic pressure, kg/cm^2; σ_{al}—allowable stresses, kg/mm^2.

Formula (3.1) holds true, if

$$\frac{s - c_1}{D_n} \leqslant 0.25 \tag{3.2}$$

The design formula is obtained from the third strength theory by substituting the mean values of the maximum and minimum principal stresses along the pipe's wall:

$$\sigma_{al} \geqslant \sigma_{\max} - \sigma_{\min} = \frac{D_n - 2s}{200s} p - \left(-\frac{p}{200} \right) \text{ kg/mm}^2$$

The 0.25 wall thickness limitation to design formula (3.2) is to avoid large plastic deformations at the inner wall surface.

The amount to be added to the wall thickness is determined from the relation:

$$c_1 = A(s - c_1) = \frac{A}{1 + A} s \geqslant 0.5 \text{ mm} \tag{3.3}$$

The value of coefficients A and $\frac{A}{1+A}$, depending upon the negative tolerance value to the wall thickness and bend radius is found in Table 3.1. For pipelines, the radii of bends more than 3.5 D_n are covered by Inter-Branch Standards.

The addition to the wall thickness, in all cases, must not be less than 0.5 mm. The wall thickness determined by formula (3.1) is rounded off to the next higher standard thickness available in the range. Rounding-off to a smaller thickness is limited to not more than 3% of the nominal thickness.

The nominal wall thickness of welded pipes is determined from the condition:

$$s \geqslant \frac{D_n p}{200\varphi\sigma_{al} + p} + c_1 \text{ mm} \tag{3.4}$$

Table 3.1

Parameters	Maximum negative tolerance along wall thickness, %				
	15	12.5	10	5	0
Coefficient A:					
for straight pipes	0.18	0.14	0.11	0.05	—
for bent pipes of radius $R > 3.5\,D_n$	0.18	0.15	0.12	0.06	0.03
for bent pipes of radius $1.9\,D_n \leqslant R \leqslant 3.5\,D_n$ . . .	0.20	0.17	0.15	0.10	0.08
Coefficient $A/(1+A)$:					
for straight pipes	0.15	0.125	0.10	0.05	—
for bent pipes of radius $R > 3.5\,D_n$	0.15	0.13	0.11	0.056	0.03
for bent pipes of radius $1.9\,D_n \leqslant R \leqslant 3.5\,D_n$ . . .	0.17	0.145	0.13	0.09	0.075

in which φ—strength coefficient of the longitudinal or spiral welded seam. The remaining notations are the same as in formula (3.1).

The addition c_1 is taken equal to the maximum negative tolerance along the wall thickness contained in GOST for welded pipes or steel plate used to manufacture these pipes. For instance the range of the negative tolerances in millimeters goes as: 0.6 mm for steel plates of thickness 7 mm, 0.8 mm for plates of thickness ranging from 8 to 25 mm and so on.

For butt-welded pipes produced by any permissible automatic, semi-automatic or manual welding method ensuring complete welding along the thickness of the elements to be welded, provided that: (a) thermite treatment is carried out when necessary; (b) the seam quality along its total length is checked by non-destructive methods; the seam strength coefficient can be assumed (a) for carbon, low-alloy manganese and chromium-molybdenum steels and austenitic steel $\varphi = 1.0$ and (b) for chromium-molybdenum-vanadium steel and high chromium content steel $\varphi = 0.8$.

The value of the seam strength coefficient for carbon and low-alloy manganese steel (the quality of seams is checked by non-destructive methods along their total length) can be assumed with reference to the welding method: (a) for submerged two sided arc welding, electroslag welding, resistance welding, one side manual welding and submerged arc welding on underneath plate or by welding seam base, manual welding in carbon dioxide and argon-arc welding method $\varphi = 0.85$; (b) for other types of manual electric and gas welding methods, not listed above, $\varphi = 0.7$.

According to the above, the strength coefficient of a longitudinal welded seam for pipes supplied as per GOST 10704-63 and GOST 10706-63 with two sided seams, the quality of seams is checked along the total length by non-destructive methods, $\varphi = 1$. For pipes with single seam and physically checked not along the total seam length, $\varphi = 0.7$.

For pipes with two sided spiral seam, supplied as per GOST 8696-67 with a 25% nominal sheet thickness allowance for permissible edge displacements and hundred per cent seam quality control (physical inspection), $\varphi = 0.75$.

For known pipe sizes (D_n, s) and grade of steel, the permissible working pressure can be determined from:

$$p_{al} = \frac{200\,(s - c_1)\,\sigma_{al}\varphi}{D_n - (s - c_1)}\ \text{kg/cm}^2 \tag{3.5}$$

in which σ_{al}—allowable stress and is determined at a given design temperature; c_1—additional wall thickness tolerance stipulated in the terms of delivery.

Deviations in nominal wall thickness tolerances from the values listed in the Standards and Technical Specifications are presented in Appendix 21.

3.4. Calculation for Combined Action of Internal Pressure and Additional External Loads

It was pointed out (Sec 3.1) that to calculate the result of combined action of internal pressure, bending moment and torque, which are caused by additional external loads, formulas derived for the limiting condition, as per the Mesis plastic deformation condition, are given in the Standards (Fourth theory of strength).

The principal design formula giving the relationship between internal hydraulic pressure (design or permissible) and reduced pipe wall stresses (design or permissible) is:

$$p=\frac{(s-c_1)}{D_n-(s-c_1)}\,200\sigma_{red}=\frac{(s-c_1)}{D_n-(s-c_1)}\,230\cdot(0.87\sigma_{red})$$

in which σ_{red}—reduced stresses for internal pressure in accordance with the Saint-Venant Tresque condition, kg/mm^2.

The first formula satisfies the Saint-Venant Tresque plasticity requirement, and the second—Mises-Huber plasticity condition. A comparison of these formulas shows that they differ in the reduced design and allowable stresses. In the second formula, these stresses account for $\sqrt{3}/2 = 0.87$ of stresses used in the first formula. This fact is taken into account when determining permissible equivalent stresses in a pipeline caused by additional external loads.

When we talk of principal external load we mean internal hydraulic pressure which produces in pipe walls circular (diametrical) and longitudinal (axial) tensile stresses and radial compressive stresses. By additional loads we mean all external loads, *viz*: (a) weight loads, i.e. pipeline weight in its working condition and the weight of accessories connected to it; to the weight loads, which appear when the pipeline is cold, should be added the unbalanced forces of tension in spring hangers caused by the pipeline's weight and vertical displacements of the pipeline; (b) wind loads, i.e. loads caused by wind pressure on the thermal insulation of pipelines at wind exposed electric generating stations and laid on trestles; (c) loads resulting from hydraulic and hydrodynamic pressures in split pipelines (exhaust pipelines and portions with axial expansion compensators of bellows and sliding types).

All additional external loads produce bending and torsional moments in a pipeline and in certain portions, longitudinal tensile or compressive forces (for example, weight load on the supports). For general pipeline fastening diagrams the longitudinal forces produce very small tensile (or compressive) stresses (not more than 0.2 kg/mm^2) and these stresses, as a rule, are neglected in calculations.

Equivalent stresses caused by additional external loads, i.e. axial forces Q^{ext}, bending moment M_b^{ext}, kg·m and torque M_t^{ext}, kg·m are calculated in accordance with the accepted condition of plasticity by the formula:

$$\sigma_e^{ext} = \sqrt{(\sigma_t + 0.8\sigma_b)^2 + 3\tau^2} \text{ kg/mm}^2 \tag{3.6}$$

in which $\sigma_t = Q^{ext}/f$—additional tensile or compression stresses in pipe walls of cross section f; $\sigma_b = M_b^{ext}/\varphi_b W$—additional bending stresses; 0.8—coefficient that takes into account the relative decrease in stresses during plastic bending; $\tau = M_t^{ext}/2W$—additional torsional stress; W—nominal moment of flexural resistance, cm^3; φ_b—strength coefficient of a cross joint weld during pipe bending.

The coefficient of strength in bending φ_b is taken equal to: for rolled pearlitic steel pipes, 0.8; for forged and drilled pearlitic steel pipes, 0.9; for rolled austenitic pipes or pipes made of high content chromium steel, 0.6; for forged and drilled pipes made from austenitic and high content chromium steels, 0.7.

The value of permissible equivalent stresses due to additional external loads $[\sigma^{ext}]$ is determined by the formula that takes into account the Mises plasticity condition:

$$[\sigma^{ext}] = 0.87\sigma_{al} \sqrt{1.2 - \left(\frac{\sigma_{rd}}{\sigma_{al}}\right)^2} = 0.87 \sqrt{(1.095\sigma_{al})^2 - \sigma_{rd}^2} \tag{3.7}$$

in which σ_{rd}—reduced stress for internal pressure, and is determined by the formula given below:

$$\sigma_{rd} = \frac{D_n - (s - c_1)}{200\,(s - c_1)}\, p \tag{3.8}$$

From formula (3.7) it follows that for calculating the combined action of all external loads an increase in permissible stresses by 9.5%, compared to the value taken for calculating the action of internal pressure, is foreseen in the Standards. The minimum value of $[\sigma^{ext}]$ for $\sigma_{rd}/\sigma_{al} = 1.03$ (permitted in the Standards as a limiting case) equals $0.36\sigma_{al}$. In most cases the ratio σ_{rd}/σ_{al} for high pressure pipelines is approximately 0.95, and then $[\sigma^{ext}] = 0.47\sigma_{al}$. For low pressure pipelines the ratio σ_{rd}/σ_{al} decreases down to 0.3 or less and then $[\sigma^{ext}]$ increases to $0.9\sigma_{al}$, in the limit up to $0.95\sigma_{al}$.

In the Standards, no mention is made of the method to determine bending moments and torques caused by additional external loads, but it is mentioned there that calculations are performed for limit loads and, accordingly, the bending stresses are taken with a coefficient 0.8. This coefficient considers the ratio between the moment of resistance of a thin walled pipe during elastic and plastic bending $W_{el}: W_{pl} = 0.25\pi \approx 0.8$. For this reason, the value, corresponding to the limit load of a multispan continuous beam with rigid ends, is taken from the bending moments diagram [3-3]. The bending moments diagram for beam *1*, which is loaded with an evenly distributed load q along its length, is shown in Fig. 3.5 where, M_{n-1} and M_n are the bending moments at the supports (n-1) and n, which are dependent on the effect of neighbouring spans. For equal span length and flexible bending $M_{n-1} = M_n = -\frac{1}{12}\,ql^2$, and the moment in the middle of a span $M = \frac{1}{24}ql^2$, where, l—distance between two supports; q—load, kg/m. The bending moment in the middle of a span is half that of the moment at the supports. On increasing the load q (or the span length l), the ratio of moments throughout the span length will remain unchanged until plastic deformation appears in the highly stressed sections at the supports; for a further increase in q (or l) the bending moments at the supports will increase more slowly than the bending moments in the span and, finally, in the limiting case, the moments at the supports and

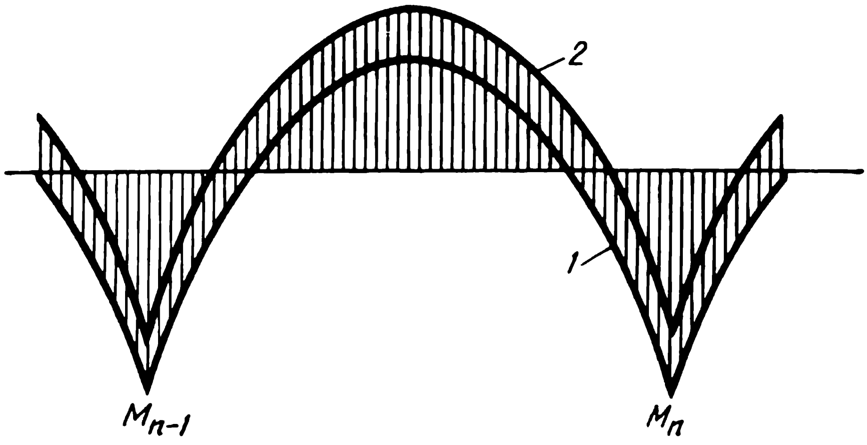

Fig. 3.5. Bending moment diagram for a solid beam
1—during elastic bending; *2*—during plastic bending

in the middle of the span will become equal to $\frac{1}{16}ql^2 = \frac{4}{\pi}W\sigma_s$, i.e. will attain their limiting value conforming to a plastic hinge. If with two plastic hinges (at the supports) the beam continues to offer resistance to bending, then with the formation of a third plastic hinge (in the span) the beams capacity to resist exhausts and this very condition is considered as the limiting case. Curve *2* of the bending moments diagram, shown in Fig. 3.5, corresponds to the limit load.

Now we calculate the safety factor for the values given in the Standards when calculating bending moments by formula $M = \frac{1}{16} ql^2$. The value (ql^2) is taken as the load parameter, and to simplify the calculation assume that the pipeline is not under pressure, i.e. $\sigma_{rd} = 0$ and consider only bending moments and stresses when $\sigma_t = 0$ and $\tau = 0$. In this case, as per formulas (3.6) and (3.7), we get $0.8\sigma_b = \sigma_e^{ext} = 0.87\sqrt{1.2\sigma_{al}}$ and, since $\sigma_{al} = \sigma_s/1.5$, we obtain the maximum allowable stresses $\sigma_b = 0.79\sigma_s$, where, σ_s—creep limit. Accordingly, the maximum permissible value of the parameter (ql^2)

$$[ql^2] = 16M_{al}^{ext} = 16 \cdot 0.79\sigma_s W = 12.7W\sigma_s$$

For the limiting load

$$(ql^2)_{lim} = 16M_{lim}^{ext} = 16\sigma_s \frac{4}{\pi} W = 20.4W\sigma_s$$

in which $\frac{4}{\pi} W$ is the moment of resistance of a thin walled pipe to plastic bending.

Thus, the safety factor calculated as per the limit loads method amounts to $n = 20.4 : 12.7 = 1.6$ which is quite sufficient (this safety factor exceeds the coefficient 1.5 taken for calculating thin walled pipes). If the bending moments were calculated by the flexible bending formula $M^{ext} = \frac{1}{12} ql^2$ the actual safety factor would have increased by another 33%, i.e. up to 2.13.

When calculating pipelines for combined action of all types of loads including moments caused by thermal expansion, the value of total equivalent stresses listed in the Standards is limited by the yield strength, i.e. by the limit that conforms to insignificant plastic deformations. Therefore, for determining moments caused by the combined action of external loads and thermal expansion the theory of elastic deformations (bending, torsion) should be applied. The above mentioned holds true for the initial operation period until relaxation of stresses, caused by deformations, becomes apparent.

As the stresses relax the bending moments at the supports decrease but cause the span moments to increase, and the bending moment diagram gradually starts approaching the limit load curve (curve *2*, Fig. 3.5).

Thus, (1) the determination of maximum allowable span length, i.e. distance between two supports should be based on the limit load calculation and the design bending moment calculated from the formula $M = 0.0625\, ql^2$; in doing so, it is not necessary to take into account the effect produced by neighbouring spans because the design formula is intended for the limiting case when plastic bending hinges are formed at the supports; (2) when determining total equivalent stresses due to additional external loads and self-compensation of thermal elongations, the bending and torsional moments for a pipeline in the initial operation period should be calculated on the basis of the flexure theory; (3) when calculating total equivalent stresses in the cold condition, with allowance made for complete relaxation of temperature stresses (self-compensation), the partial relaxation of stresses caused by weight may also be taken into account.

In conclusion, it may be pointed out that the procedures proposed in [3-12], similar to the method discussed in this section, was objected to in [3-7] for the reason that actual bending stresses exceeded 1.7 times the allowable stresses. This objection is not well founded. When calculating statically indefinable systems as per the limiting condition it is essential to take into account not only the increment in the moment of resistance to bending (1.27 times) but also the variation in the ultimate bending moments (1.33 times) as pointed out, for example, by N. M. Belyaev [3-3]. Thus, the coefficient 1.7 defines the total increment in allowable loads when calculating the pipeline for bending as per the limit condition compared to the calculation as per maximum flexural bending stresses. Maximum stresses calculated for elastic strains must not be compared, as done in [3-7], with allowable stresses which account for plastic deformations.

3.5. Self-Elongation of Pipelines

Before we present general information and formulas for check calculation of stresses appearing due to thermal elongations of pipelines, we shall first consider the self-elongation phenomenon of pipes. Self-elongation is the spontaneous decrease in self-compensation stresses caused by the pipeline hot condition. A decrease in the self-compensation stresses of a pipe in the hot condition leads to the appearance of self-compensation stresses of opposite sign on cooling. Thus, the self-elongation effect is similar to the effect due to erection negative tolerances in the cold condition.

The principal cause of self-elongation of pipelines is the relaxation of self-compensation temperature stresses. The other cause can be plastic bending under stresses exceeding the proportional limit. Stress relaxation is described as a decrease in stresses in the course of time as a result of the change from elastic strains to plastic deformations. The relaxation process can be considered as a creep process when stresses are produced by elastic deformations (fully or partially).

Appearance of plastic strain (creep) $d\varepsilon$ decreases elastic deformation by this value and lowers the stresses by $Ed\varepsilon$. If with the decrease of actual stresses in a specimen the creep velocity decreases, then the relaxation velocity gradually decreases. In the pure state (i.e. when constant stresses caused by external loads are absent) the relaxation process proceeds as shown in Fig. 3.6, curve *1*. In the first stage (conforming to creep stage I) a significant decrease in initial stresses is observed. In experiments conducted by Professor I. A. Oding with ring-shaped specimens the bending stresses decreased by 40 to 50% in a few hours. In stage II, the creep velocity varies and, approximately, follows the decreasing exponential curve. If for steady creep velocity, we assume the formula

$$v = \frac{d\varepsilon}{dT} = kA\sigma^n$$

then for relaxation velocity in stage II, we write

$$v_{rl} = \frac{d\sigma}{dT} = -kAE\sigma^n$$

where, A and n are constants depending upon material and temperature, respectively; k—coefficient, which depends upon the ratio of principal stresses.

The relaxation process continues, therefore, with a decreasing velocity, and completes only after infinite long time.

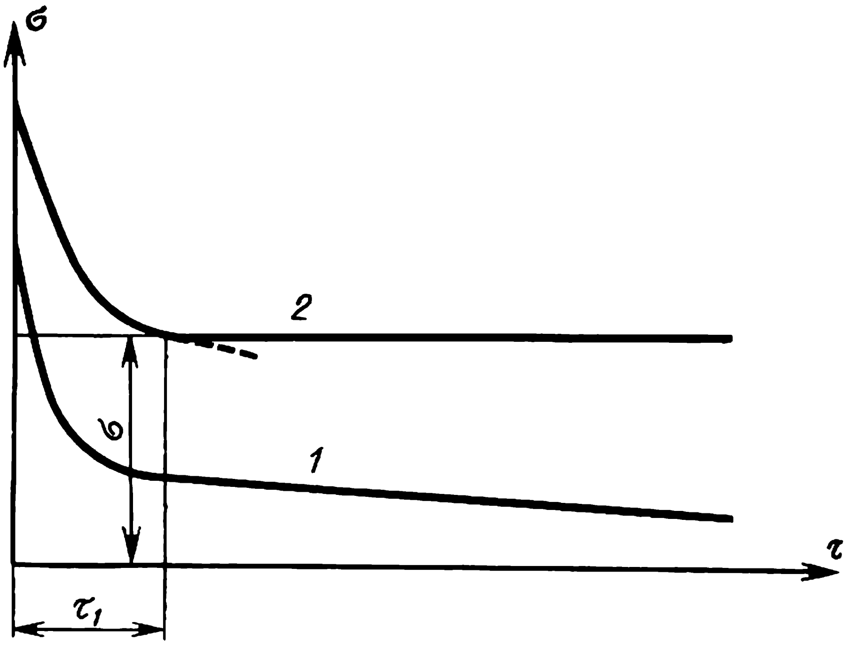

Fig. 3.6. Relaxation of stresses

1—in the pure state, i.e. without constant stresses; 2—with stresses due to external loads

In the general case, the initial stress comprises a constant stress due to external loads σ^{ext} and to an additional stress $\sigma_{add} = E\varepsilon_{add}$ coinciding with the constant stress and caused by initial deformations ε_{add}.

In this case, the creep velocity will, evidently, be determined by the total stress $\sigma = \sigma^{ext} + \sigma_{add}$, and the relaxation rate—by the relationship

$$v_{rl} = -kAE\left(\sigma^{ext} + \sigma_{add}\right)^n$$

The appearing creep deformation will result in a decrease of the initial elastic strain ε_{add} until the plastic strain attains value ε_{add} and the stress σ_{add} disappears completely. At this point the stress relaxation process completes and stresses equal to σ^{ext}, a value determined by external loads.

The relaxation process, for this case, is shown in Fig. 3.6, curve *2*. Here, the first two creep stages, by virtue of high stresses proceed at a very high rate than in the earlier discussed case, and the total relaxation process completes in a relatively short period.

At high metal temparature and significant loads, i.e. in conditions when creep velocity is appreciable (more than 10^{-7} to 10^{-8} mm in an hour), the relaxation process for the self-compensation stresses of thermal elongations proceed intensively and may complete in a few days. A significant decrease in self-compensation stresses—by 30% or more—causes the process to complete in a few hours. The studies [3-2] show that relaxation processes are observed also at moderate temperatures, down to 300°C and even 200°C, but they proceed very slowly.

In ships' steamlines working at steam temperatures of about 300°C, an increase in cold spring is noticed between repair periods. During repairs and dismantling the increase in cold spring is noticed particularly as flange joints are used in marine piping.

The relative plastic deformations appearing during relaxation of self-compensation temperature stresses are not equal to the initial relative elastic deformations in the same cross sections, because the relaxation velocity is not proportional to the stress σ but to the value σ^n, where $n > 1$. As a result the bending moments diagram for the relaxation process differs from the one for moments along the pipeline's length, and this causes that in the maximum bending moment section the final plastic strain ε_{pl} should be more than the initial elastic deformation in the same section. Complete elimination of plastic deformations caused by relaxation of self-compensation temperature stresses is possible by using hundred per cent initial cold spring for pipelines, i.e. 100% cold spring for temperature elongations in every direction.

Plastic strains due to bending are another reason which cause partial self-compensation of a pipeline. The bending plastic strains appear on increasing the proportionality limit which at high temperatures is much lower than the yield point (in carbon steel at $t \geqslant 400°C$ the proportionality limit is approximately half of the yield point). On increasing bending stresses up to the yield point and on further increasing the bending moments the load diagram for the pipe (beam) cross section takes the shape shown in Fig. 3.7; in this case, stresses attain the yield point practically throughout the beam cross section. The beam at such sections ceases to offer resistance to a further increase in bending deformations, and a so-called plastic hinge is formed. The moment of resistance to bending W_{pl} at the plastic hinge is twice the static moment of a half cross section of the pipe with respect to the diameter, i.e.

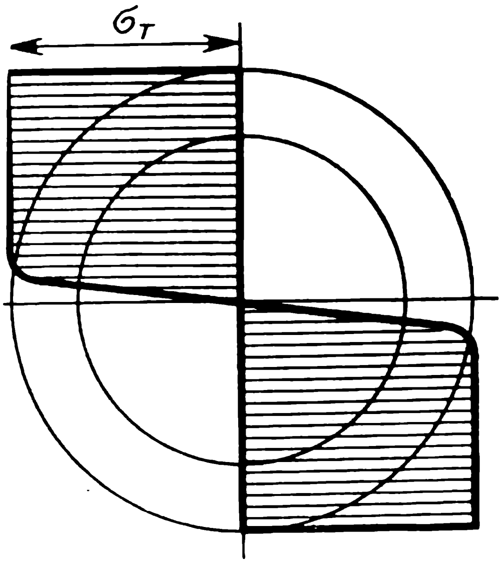

Fig. 3.7. Diagram of bending stresses in a pipe's cross section during plastic bending

$$W_{pl} = \frac{1}{6}[D_n^3 - (D_n - 2s)^3] \approx \frac{4}{\pi}\left(1 + \frac{s}{D_n}\right)W$$

The last expression offers sufficient accuracy when $s/D_n \leqslant 0.25$. For thin walled pipes $W_{pl} \approx 1.3\ W$, for pipes of wall thickness $s = 0.25\ D_n$ the moment of resistance to plastic bending increases to 1.59 W.

The limit bending moment, which can appear in a pipeline, is determined by its moment of resistance to plastic bending and stresses in metal at which (as per Mises) plastic bending on-sets:

$$M_{lim} = \frac{4}{\pi}\left(1 + \frac{s}{D_n}\right) W \sqrt{\sigma_{yield}^2 - (0.87\sigma_{lim})^2}$$

As an example we consider a steam pipeline designed for parameters 40 atm 440°C and made from 219 × 8 mm pipes, $W = 270\ \text{cm}^3$. The pipes are made of steel Grade 20 having a yield point $\sigma_{yield} = 12$ kg/mm^2 at 400°C. The pipeline has the configuration shown in Fig. 3.8 and lies in a horizontal plane. The bending moment in section B caused by weight load is equal to 1000 kg·m.

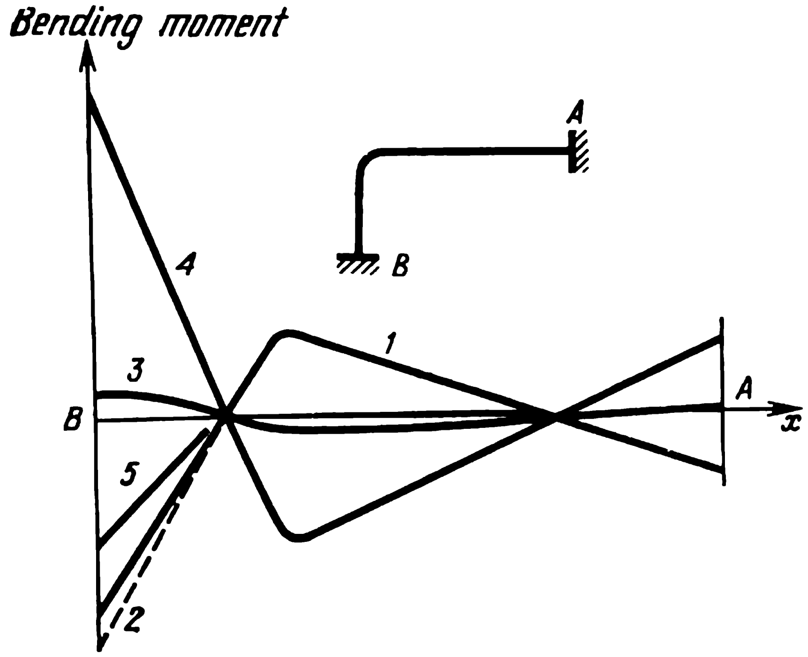

Fig. 3.8. Diagrams of bending stresses in a pipeline

1—during first heating and with the appearance of a plasticity hinge at the fixed end *B*; *2*—the same, during elastic bending; *3*—in the installed condition after first heating; *4*—in the installed condition after complete relaxation of temperature stresses; *5*—maximum allowable moment as per the Standards

The limit bending moment for reduced stresses $\sigma_{rd} = 5.15$ kg/mm^2 due to internal pressure equals

$$M_{lim} = \frac{4}{\pi}\left(1+\frac{8}{219}\right)270\sqrt{12.0^2-(0.87\times 5.15)^2} = 3980\ \text{kg}\cdot\text{m}$$

The limit bending moment due to self compensation

$$M_{lim}^{s\text{-}c} = \sqrt{M_{lim}^2-(M^{ext})^2} = \sqrt{3980^2-1000^2} = 3850\ \text{kg}\cdot\text{m}$$

The calculations show that for a constant Young's modulus $E = 1.645 \times 10^6$ kg/cm^2 the bending moment due to thermal elongations in section B should be as great as 4200 kg·m. Hence, a plastic hinge is formed in section B. At this hinge, the bending moment due to compensation equals 3850 kg·m. For this condition, the solution of the problem gives $P_x = 798$ kg, $P_y = 169$ kg, angle of rotation at the plastic hinge ≈ 0.001 radian or $\approx 0.06°$. Such a small angle of plastic bending cannot practically affect the pipeline strength. The bending moments diagrams for the pipeline are shown in Fig. 3.8. The appearance of plastic deformations in section *B* results in the appearance of bending moments to opposite sign in the cold pipeline (curve *3*), i.e. the pipeline's self-elongation of about 10%. Thereafter, self elongation takes place at the cost of stress relaxation. When stress relaxation process is complete, bending moments in the hot pipeline disappear, whereas, in the cold pipeline they increase up to the value represented by curve *4*; bending stresses, in this case, do not exceed permissible values for cold pipelines.

Maximum permissible bending moment due to self-compensation calculated for the given case as per strength calculation methods, amounts to only 2240 kg·m. To lower the stresses down to the value listed in the Standards, it is necessary to cold stretch the pipeline in direction x by 50 mm or 49%. In doing so, as is evident from the calculation results given above, the pipeline will not be damaged and its strength will not practically be reduced even if the pipeline is not cold stretched at all (this is totally inadmissible from the view point of fulfilling the project design requirements).

The appearance of plastic deformations during self-elongation is considered as an undesirable phenomenon. For certain types of high-alloy steels such deformations are sometimes considered to be responsible for the appearance of cracks during subsequent operation.

3.6. Check Calculation of Stresses Caused by Compensating for Thermal Elongations

The stresses appearing during thermal elongations compensation are thermal stresses. They are the result of limited strains, and can not cause failure of a pipeline, unless it has abrupt local weaknesses, for a small number of repeated loads (start-ups and shut downs). As mentioned in (Sec. 3.5), in a pipeline under pressure large bending moments can cause plastic bending, but plastic strains, in this case, are insignificant in the circumferential and radial directions (increase in diameter, decrease in wall thickness) and are not followed by a significant decrease in pipe strength with respect to internal pressure.

It should be mentioned that actual bending moments and torques can significantly exceed design moments as a result of an unfavourable combination of tolerances for pipe wall thickness and diameter. The ratio of the maximum moment of inertia of a pipe's cross section to the minimum attains a value 1.39 for a wall thickness tolerance of $\pm 12.5\%$ and diameter tolerance of $\pm 1.25\%$. Therefore, if a section of a pipe has maximum negative tolerances in the cross section where bending moments are maximum, and the remaining pipeline is made from pipes having maximum positive tolerances, then the actual self-compensation stresses may exceed the design stresses by 20 to 30%. In this case, a plasticity hinge appears in the most loaded cross section and the pipeline will self elongate (as discussed in the previous paragraph), but no damage will be caused to the pipeline. The capacity of steel pipelines to withstand plastic deformations permits the minimum safety factor to be used in the self-compensation calculations.

As per the Standards, the check calculation of stresses due to thermal expansion self-compensation is performed as follows. Equivalent stresses due to loads caused by pipeline's thermal elongation is determined from the formula:

$$\sigma_e^{s-c} = \sqrt{(\sigma_t^{s-c} + 0.8\sigma_b^{s-c})^2 + 3\tau^2} \text{ kg/mm}^2 \qquad (3.9)$$

in which $\sigma_t^{s-c} = \frac{Q^{s-c}}{f}$ —additional tensile or compression stresses caused by longitudinal force Q^{s-c} (reactions of rigid supports, forces of friction); $\sigma_b^{s-c} = \frac{M_b^{s-c}}{\varphi w}$ —stresses due to bending moment M_b^{s-c} appearing during self-compensation; $\tau = \frac{M_t^{s-c}}{2w}$ —stresses due to torque M_t^{s-c} appearing during self-compensation; φ—strength coefficient of circumferential weld; for rolled pearlitic steel pipes it equals 0.8, for forged and drilled pipes—0.9; for austenitic or high chromium content steel rolled pipes—0.6 and for forged and drilled pipes—0.7.

It may be mentioned that in the expression used to determine bending stresses, the stresses intensification coefficient for curved portions of pipes has not been introduced. Consideration of this coefficient would have been necessary, if stresses within elastic deformations had been considered. In the Standards plastic bending is considered as limit bending at which the bending stresses throughout the pipes cross section attain their limit value (yield point) and become equal.

The value of equivalent stresses due to self-compensation of thermal elongations calculated from formula (3.9) must, as per Standards, satisfy the condition:

$$\sigma_e^{s\text{-}c} \leqslant 0.87\sigma_{al}\sqrt{2-\left(\frac{\sigma_{rd}}{\sigma_{al}}\right)^2}-\sigma_e^{ext}=$$

$$=[\sigma^{t.ad}]-\sigma_e^{ext}\ \text{kg/mm}^2 \qquad (3.10)$$

in which σ_{rd}—reduced stresses due to internal pressure; they are calculated from formula (3.8); σ_e^{ext}—equivalent stresses due to additional external loads; they are calculated from formula (3.6).

In formula (3.10), the value

$$[\sigma^{t.ad}]=0.87\sigma_{al}\sqrt{2-\left(\frac{\sigma_{rd}}{\sigma_{al}}\right)^2}\ \text{kg/mm}^2 \qquad (3.11)$$

presents total allowable equivalent stresses due to additional external loads and loads caused by thermal elongation of pipeline.

Expression (3.10) can be presented as an inequality

$$\sigma_e^{s\text{-}c}+\sigma_e^{ext}\leqslant[\sigma^{t.ad}] \qquad (3.10a)$$

whose left hand side represents total equivalent stresses due to self-compensation and additional external loads, which appear in one and the same cross section of the pipeline.

However, the inequality (3.10*a*), and hence, the one referred to in the Standards, is fully valid only in one, comparatively, rare case when a two dimensional pipeline is positioned in a vertical plane. In this case the bending moments due to weight loads and self-compensation act in the same direction (i.e. they are of the same sign).

In all spatial pipeline configurations and in two dimensional horizontal sections the resulting bending moments due to self-compensation do not lie in the plane of moments action, which are caused by weight loads, and, therefore, maximum stresses $\sigma_e^{s\text{-}c}$ and σ_e^{ext} appear at different points in the considered cross section. For this reason they can not be added or subtracted.

For a correct solution it is necessary to use the geometrical addition of moments caused by thermal elongations of pipeline, and moments due to external additional loads and calculate the total bending moment $M_b^{t.ad}$ and total torque $M_t^{t.ad}$. Then determined are the total stresses due to the combined action of all additional loads: bending stresses $\sigma_b^{t.ad} = M_b^{t.ad}/\varphi W$, torsional stresses $\tau^{t.ad} = M_t^{t.ad}/2W$ and elongation stresses $\sigma_{el}^{t.ad} = Q^{t.ad}/f$. After this the equivalent additional total stresses are determined:

$$\sigma_e^{t.ad} = \sqrt{(\sigma_{el}^{t.ad} + 0.8\sigma_b^{t.ad})^2 + 3(\tau^{t.ad})^2}\ \text{kg/mm}^2 \qquad (3.12)$$

which must satisfy the condition

$$\sigma_e^{t.ad} \leqslant [\sigma^{t.ad}] \qquad (3.12a)$$

in which $[\sigma^{t.ad}]$ — allowable stresses determined from the equation (3.11).

How significant will be the difference in the calculation of allowable stresses due to self compensation of thermal elongations from formulas (3.10) and (3.12) can be ascertained after examining a plane horizontal portion in which the bending stresses due to weight amount to 0.55 $[\sigma^{t.ad}]$. This corresponds to the ratio $\sigma_{rd}/\sigma_{al} = 0.9$.

The value of allowable self-compensation stresses calculated from formula (3.10) should not exceed 0.45 $[\sigma^{t.ad}]$. On geometrical adding the moments the value of equivalent self-compensation stresses may be increased to $\sqrt{1 - 0.55^2}$ $[\sigma^{t.ad}] = 0.83\ [\sigma^{t.ad}]$ or by 85%.

While determining bending and torsional moments due to additional loads for the working condition, all strains are taken as elastic and stress relaxation does not occur.

In addition to the calculation of total additional stresses, appearing in pipelines when in the working condition, a check calculation for pipelines in the cold condition should also be done, as required in the Standards. As suggested in the

Standards, such a calculation is performed taking account of (a) test pressure during hydraulic testing of a pipeline, (b) total self elongation of a pipeline due to relaxation of temperature stresses. The bending moments due to a pipeline's own weight should also be determined for the hydraulic testing conditions, i.e. for steam pipelines the bending moments should be calculated by taking account of the weight of water in pipeline and the springs compression arresting devices installed on hangers, and for hot water pipelines—by taking into account the variation in compression of spring supports due to vertical displacements of the pipeline's axis.

The stresses due to pipeline's weight, appearing in the working pipeline, also relax partially and this causes a decrease in bending moments over the supports and an increase in bending moments in spans. For an equal span structure the decrease in moments over the support due to relaxation amounts to 25%. Because of this, the bending moments over the supports, appearing due to pipeline's weight, should, strictly speaking, be calculated from the formula:

$$M_b^{ext} = M_{b\text{-}c}^{ext} - 0.25 M_{b\text{-}w}^{ext}$$

in which M_{b-c}^{ext} is the bending moment in the cold state during hydraulic testing of pipeline; M_{b-w}^{ext}—bending moment in the working condition of pipeline, in the initial stage of operation (i.e. before stress relaxation takes place).

As a rule, for stationary pipelines the distances between supports are moderate and the stresses due to the pipeline's weight are very small, 2 kg/mm^2; in such cases, the relaxation correction for the stresses due to pipeline's weight is not necessary.

The allowable value of total stresses due to self-compensation and additional external loads $[\sigma^{t.ad}]$ appreciably decreases with the increase in temperature from approximately 12 kg/mm^2 at 200°C to 5.5 kg/mm^2 at 570°C (for steels Grade 20 and 12 ХМФ used at these temperatures, and for reduced stresses due to internal pressure approximating allowable stresses). If the stresses due to weight loads are considered, then the permissible self-compensation stresses will amount to about 10 kg/mm^2 at 200°C and about 3 kg/mm^2

at 570°C. Because of the decrease in allowable self-compensation stresses with a simultaneous increase in thermal elongations, sometimes, it is difficult to ensure the required self-compensation when designing high-temperature pipelines. In such a case, the required self-compensation can be achieved in different ways: (1) by eliminating superfluous rigid supports; (2) by decreasing in the most loaded section the stresses due to pipeline's weight by installing an additional support that permits the self-compensation stresses to be increased; (3) by decreasing or increasing the cold spring with the purpose of decreasing self-compensation stresses in the hot condition.

To illustrate this, we consider a pipe 325 × 38 mm at 140 atm 570°C. The allowable total stress due to additional loads, as per formula (3.11), equals 5.52 kg/cm^2 in the hot condition and 20.4 kg/mm^2 in the cold condition. The stress due to pipe's weight in the hot condition amounts to 2.8 kg/mm^2 for a span length of 12 m, and in the cold condition (when filled with water)—3.14 kg/mm^2. If we assume that self-compensation bending moments in the horizontal and vertical planes are equal, then the self-compensation stresses in the hot condition can be taken equal to 3.2 kg/mm^2, and in the cold condition, 18.1 kg/mm^2, i.e. 4.7 times more with allowance made for the difference in Young's modulus.

A decrease in span length by 30% halves the stresses due to pipeline's weight, i.e. down to 1.4 kg/mm^2, and in this case, the self-compensation stresses in the hot pipeline may be as high as 4.4 kg/mm^2, i.e. may be more by 40%, and in the cold pipeline, 19 kg/mm^2; with the allowance made for the difference in Young's modulii, the cold spring, in this case, increases the compensating capacity by 3.6 times.

From this it follows that cold springing is an effective means to increase the compensating capacity of high temperature pipelines. The cold spring for pipelines working at not very high temperatures (for example, feed water pipelines) does not increase their compensating capacity, because the stresses $[\sigma^{t.ad}]$ in the cold condition, by taking into account pressure increases during hydraulic testing, are less than in the hot condition.

Certain design organizations do not favour the use of pre-erection cold springing in pipelines as the belief is held that cold spring will not be maintained during pipeline erection. This fact, to a certain extent, has been taken into account in the cautions recommendation given in the Standards, which suggests to use in calculations a cold spring equal to $^2/_3$ of the design value. However, all such beliefs are not well founded, because cases of pipeline failures in the initial period of operation due to nonfulfilment of required design cold spring are not known. In the subsequent period of operation self-elongation of steam pipelines takes place due to relaxation of temperature stresses.

If the refusal to use erection elongation does not involve a necessity to artificially increase pipeline flexibility or increase compensator clearances, then it will not cause any particular concern (although in this case the erection negative tolerance is useful in terms of decreasing the total value of plastic strains caused by relaxation). But, in many cases, the objection to use pre-erection cold springing complicates and necessitates lengthening of pipeline's track involving unjustified additional capital investment and extra operating costs (an increase in depreciation deductions, repair costs, pressure losses in pipelines and heat losses through thermal insulation).

Lengthening and complicating a steam line's run envisaged in the design for the sake of avoiding the use of erection cold springing is regarded as an incorrect solution both from the technical and economic viewpoint. Here, it may be mentioned that in the United States of America [3-15] only the self-compensation stress range is limited, the value of self-compensation stresses for pipelines in the working condition is not restricted by technical specifications or in other words self-elongation is permitted.

3.7. Flexure in Curved Pipes and Equivalent Stress Ranges

Subjecting curved pipes to bending generate forces which tend to deform pipe's cross section. Now we consider an element confined between two adjacent cross sections of a curved circular pipe bent in the plane of curvature by moments having directions as shown in Fig. 3.9. Since the stretching forces on the convex side and the compressive forces on the concave side of the curved element have components directed towards the pipe's axis, the initial circular cross section becomes elliptical with a minor axis in the plane of bend.

When the direction of bending moments is opposite to that shown in Fig. 3.9, the force components appear. These components are directed away from the pipe's axis, the cross section also deforms into an ellipse, but its major axis will, in this case, lie in the plane of bend. If the cross section of the curved pipe is not circular (i.e. initially it has an oval or ellipse-like shape), then the bending moments will also cause elastic deformation which increases the ellipticity when the moments act in the direction shown in Fig. 3.9, or decreases the initial ellipticity if the bending moments act in the opposite direction. If we denote the increase in angle of the element in question by $\Delta\, d\theta$ and the displacement of the extreme wall fibre by δ, then the elongation of this fibre will equal

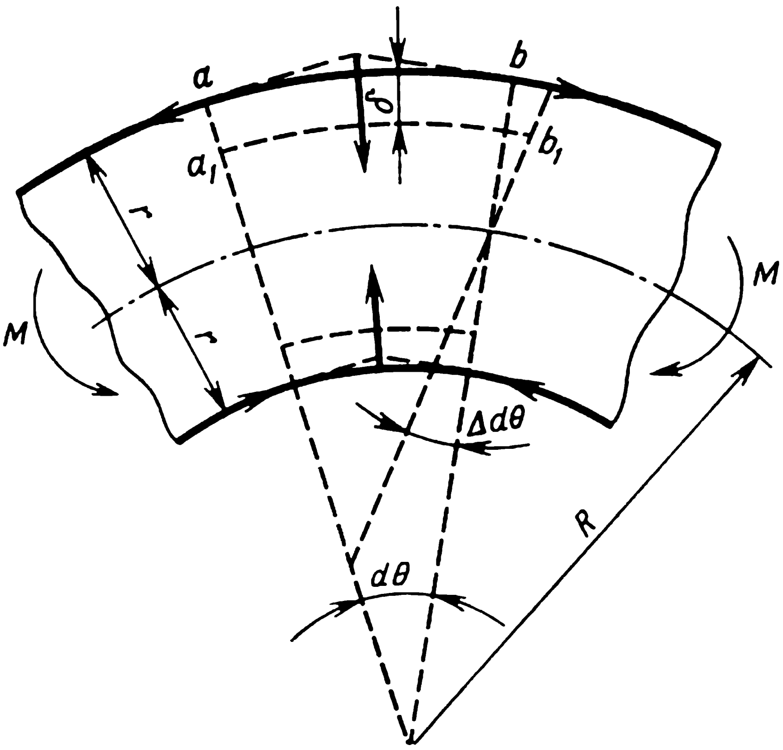

Fig. 3.9. Forces distorting the cross section of a circular curvilinear pipe during its bending

$$r\Delta\, d\theta - \delta\, d\theta$$

and the relative elongation

$$\varepsilon=\frac{r\Delta\, d\theta-\delta\, d\theta}{(R+r)\, d\theta}=\frac{r}{R+r}\frac{\Delta d\theta}{d\theta}-\frac{\delta}{R+r}$$

The first term of the right hand side of the expression represents relative elongation involved when bending solid bars, i.e. without taking into account the deformation of the cross section. The second term of the right hand side of the expression accounts for the flattening effect of the cross section. This effect may be large enough. Thus, when $\delta = 1$ mm, $R + r = 1500$ mm and $E = 20{,}000$ kg/mm^2 the flattening of the cross section will decrease the bending stresses in the extreme fibre by 13.3 kg/mm^2.

From this it follows that the farthest fibres from the neutral axis of the bent pipe do not resist bending so much as is clear from the general theory on the bending of a solid bar. This involves a relative increase in stresses in those parts of the pipe's wall which lie close to the neutral surface of bending, as a result the bending forces diagram takes the shape shown in Fig. 3.10 significantly differing from the usual diagram. This redistribution of bending stresses decreases the rigidity of a curved pipe far more than of a straight pipe and at the same time increases the maximum bending stresses. Besides, resilient flattening of the cross section is accompanied by the appearance of stresses due to pipe's wall bending. These bending stresses coincide in direction with circular stresses due to internal pressure (or are directed opposite to them) and are termed as circular or cross sectional bending stresses. The distribution of circular bending forces along the pipe's cross section is shown in Fig. 3.11 when bending takes place in the plane of curvature; the absolute value of these stresses has four maximums corresponding to the points of interaction of the pipe's wall and the major and minor axes of the ellipse. Stresses, appearing during bending in a plane normal to the plane of curvature, are shown in Figs. 3.12 and 3.13.

The flexibility of a curved axis pipe and the value of its longitudinal and transverse stresses depend upon the pipe's geometrical characteristics:

$$\lambda=\frac{R}{r_{aver}}\cdot\frac{s}{r_{aver}}=\frac{4sR}{(D_0-s)^2} \qquad (3.13)$$

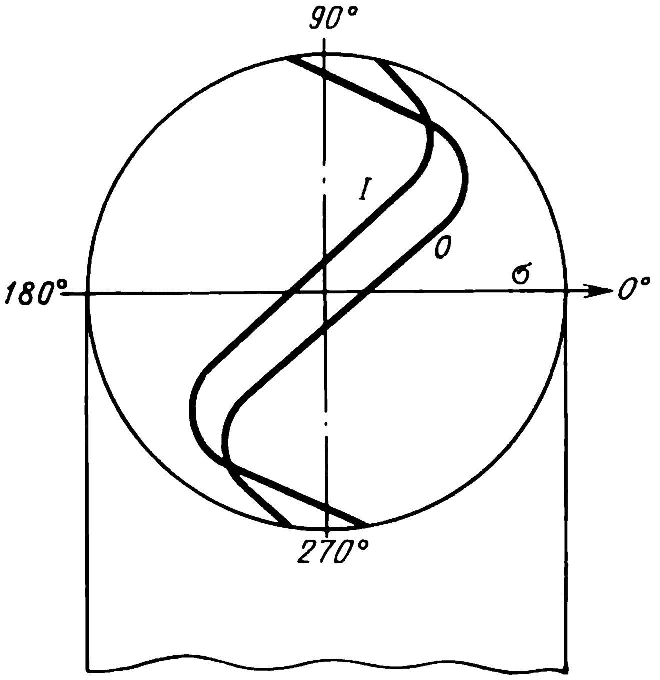

Fig. 3.10. Diagram of longitudinal bending stresses in a smooth elbow when the bending moment acts in the plane of curvature

0—on the outer surface; *I*—on the inner surface

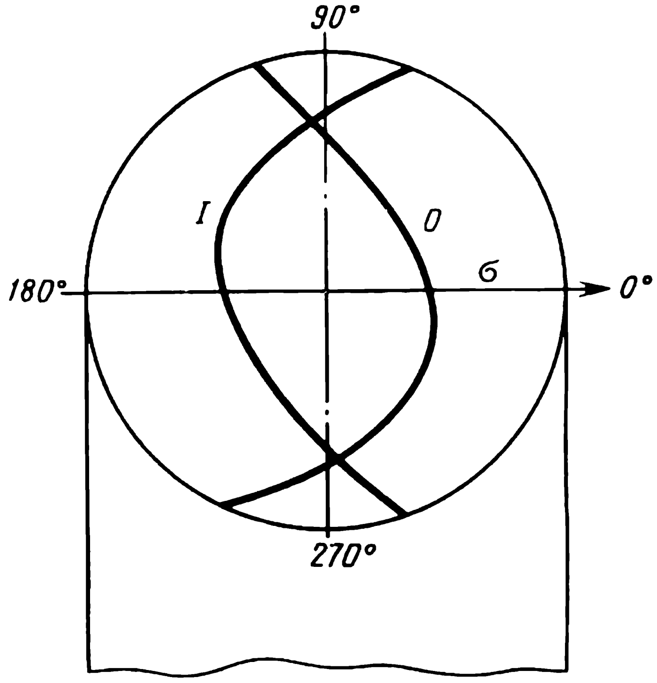

Fig. 3.11. Diagram of circumferential bending stresses present in the walls of a smooth elbow when the bending moment acts in the plane of curvature

0—on the outer surface; *I*—on the inner surface

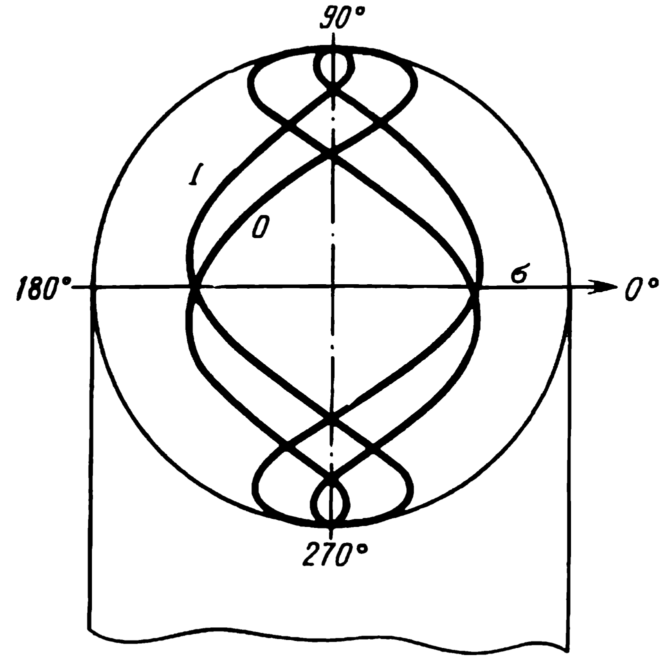

Fig. 3.12. Diagram of longitudinal bending stresses in a smooth elbow when the bending moment acts in the plane perpendicular to the plane of curvature

0—on the outer surface; *I*—on the inner surface

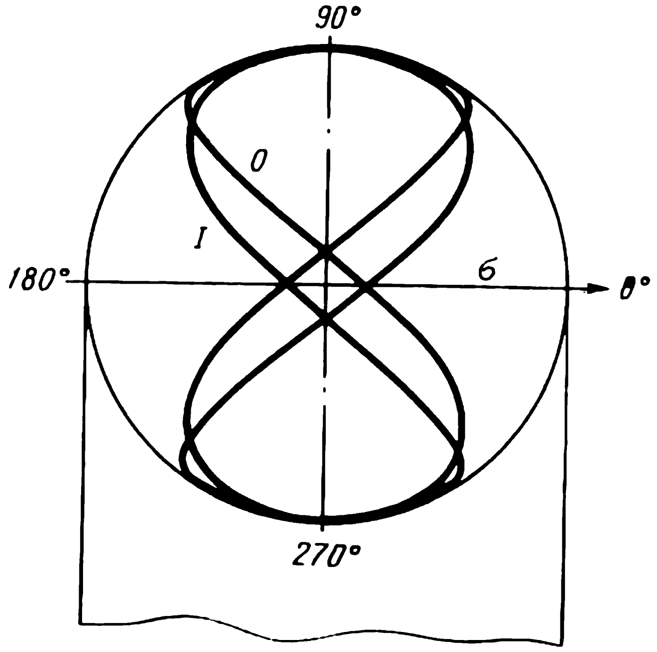

Fig. 3.13. Diagram of circumferential bending stresses in the walls of smooth elbow when the bending moment acts in the plane perpendicular to the plane of curvature

0—on the outside surface; *I*—on the inside surface

The flexibility coefficient K is determined from the ratio

$$EI\Delta\, d\theta = KM_bR\, d\theta = M_b\,(K\, dl)$$

in which $\Delta\, d\theta$ is the increment in the deflection angle; $Rd\theta = dl$—elementary length of arc; (Kdl)—elementary length of arc reduced to design rigidity EI of a straight pipe; M_b—bending moment.

Thus, the flexibility coefficient K shows by how many times the bending deformation of the arc element exceeds the deformation of a straight pipe of the same length.

From 1911 on, when Kármán [3-17] gave a theoretical explanation and basis for the increase in flexibility of curved pipes, many authors have been engaged in theoretical and experimental investigations on the flexibility coefficient. The history of this problem is covered comprehensively in the work by A. Kamerstein [3-8], and also in the handbook from Kellogg, M. W., Company [3-15]. When investigating the flexibility of pipes with curvilinear axis, Karman made certain assumptions, precisely, he assumed that the radius of pipe's cross section was many times less than the radius of curvature of the axis, wall thickness being small compared to the radius; the displacement of neutral axis during bending and the effect of Poisson coefficient were not considered. To solve this problem Kármán employed the energy method with a subsequent solution using the Ritz method. In design practice generally Kármán's first approximation is used, and the flexibility determined from

$$K = \frac{10 + 12\lambda^2}{1 + 12\lambda^2} \tag{3.14}$$

This formula gives satisfactory results at $\lambda > 0.3$, but does not ensure the required accuracy when $\lambda < 0.3$, and more so when $\lambda < 0.2$.

To solve the problem Clark and Reissner expanded the sought functions in a trigonometric series and by making assumptions, valid for the values of λ much less than unity, obtained simple finite equations. They solved the problem by making use of the thin-walled shell theory. The ultimate formula, which gives more accurate results for small values of λ than Kármán's formula, has a very simple form

$$K = \frac{1.65}{\lambda} \tag{3.15}$$

This formula, as proved by Clark and Reissner, holds true for $\lambda < 0.33$. The Kármán and Clark-Reissner formulae do not take into account the effect of internal pressure which by counteracting the flatting of cross section somewhat decreases the flexibility of a curved pipe. The flexibility of elbows and the stresses appearing in them, when subjected to internal pressure, were investigated by D. L. Kostovetskiy [3-9 and 3-10].

To determine the flexibility coefficient K_p for an elbow under pressure, the following formula is suggested by D. L. Kostovetskiy:

$$K_p = 1 + \frac{1.125}{a_1} \tag{3.16}$$

where a_1 is calculated from the formulae:

$$a_1 = 0.125 + \frac{3^2}{6}\lambda^2 + 3\omega - \frac{0.09766}{a_2}$$

$$a_2 = 1.0625 + \frac{15^2}{6}\lambda^2 + 15\omega - \frac{0.19141}{a_3}$$

$$a_3 = 1.0278 + \frac{35^2}{6}\lambda^2 + 35\omega - \frac{0.21973}{a_4}$$

$$a_4 = 1.01562 + \frac{63^2}{6}\lambda^2 + 63\omega - \frac{0.23160}{a_5}$$

$$a_5 = 1.0100 + \frac{99^2}{6}\lambda^2 + 99\omega$$

The parameter ω is a function of pressure:

$$\omega = \frac{2(1-\mu^2)}{E} \cdot \frac{2R^2}{(D_0-s)s}p = A\frac{p}{E} \tag{3.17}$$

in which $A = 3.64\frac{R^2}{(D_0 - s)s}$; p—working pressure, kg/cm^2; E — elastic modulus of steel, kg/cm^2; D_0—nominal outside diameter, mm; s—nominal pipe wall thickness, mm.

Formula (3.16) is given in a form which permits K_p to be calculated to the fifth approximation sometimes necessary when $\lambda < 0.03$. For $\lambda > 1.5$ the first approximation is sufficient, for $\lambda > 0.4$—the second, and for $\lambda > 0.1$—the third one.

For practical purposes, the graphs illustrating the relationship between λ and ω may be used. Such graphs are presented in Appendix 17.

It is clear from the graphs that internal pressure can decrease the flexibility coefficient by 10 to 15%, and to a maximum of 25% in normal radius elbows for $\lambda > 0.48$. In steep curved elbows ($\lambda < 0.23$), the internal pressure decreases the flexibility by not more than 12%. Practically, when $\sigma_{rd} < \sigma_{al}$, the decrease will be still less. Nevertheless, we consider it correct to take into account the internal pressure when determining flexibility coefficients. Using the graphs, it is not difficult to consider internal pressures, which helps avoid the regular error occurring when calculating elbow flexibility, an error which in certain cases can mount up to 33% with respect to the actual flexibility.

Maximum circumferential and longitudinal bending stresses in curved pipes are determined from the expressions:

$$\sigma_{b1} = \gamma \frac{M_b}{W}; \quad \sigma_{b2} = \beta \frac{M_b}{W} \text{ kg/mm}^2 \qquad (3.18)$$

in which σ_{b1}—maximum circumferential bending stresses (in the circular ring of the pipe's cross section); γ—intensification coefficient of circumferential bending stresses; σ_{b2}—maximum longitudinal bending stresses; β—intensification coefficient of bending stresses.

Here, and in other cases subscript 1 denotes circular (transverse) stresses, and subscript 2 denotes axial stresses.

The intensification coefficients γ and β depend upon the geometrical characteristic λ. For minimum values of $\lambda = 0.05$ encountered in practice these coefficients mount up to $\gamma = 13$, $\beta = 6.2$, i.e. maximum values of bending stresses can exceed the value M/W by many times. The values of stresses denoted by σ_{b1} and σ_{b2} do not determine the statical strength of elbows, i.e. their strength for one-loading as explained earlier. But during every pipeline start-up, i.e. when pressure and temperature are increased up to the working pressure and temperature, and then on subsequent shuts down with a decrease in pressure and pipe's walls temperature, the stresses in definite zones of elbows change abruptly. Such multiple variations in the stressed state can give rise to fatigue cracks after a relatively small number of operation cycles. The variation in the stressed state is convenient to measure from the equivalent stress range

$$\sigma_{range} = | \sigma_{e\text{-}h} - \sigma_{e\text{-}c} | \tag{3.19}$$

in which $\sigma_{e\text{-}h}$ and $\sigma_{e\text{-}c}$—equivalent stresses in the hot and cold states.

All stresses, having a constant value, for example, stresses due to the own weight, may not be taken into consideration in the calculation of $\sigma_{e\text{-}h}$ and $\sigma_{e\text{-}c}$. It is convenient to relate self-compensation stresses to the cold state, assuming complete relaxation of self-compensation stresses, and calculate them using the value of the elastic modulus for the metal in the cold condition. The stresses due to internal pressure should include not only circular stresses appearing in the circular ring, but also the stresses due to ovality of the pipe's cross section. Even in straight pipes, where ovality amounts to 1.2-1.5%, the transversal bending stresses can mount up to one half of the circumferential stresses. In curved elbows, where ovality up to 8% in high-pressure pipes, and to 10% in thin-walled pipes is permitted, the transversal bending stresses can mount up to $3\sigma_{rd}$. Here, σ_{rd}—reduced stresses due to internal pressure in a circular pipe. The total stress range in a bent pipe, having oval-shaped cross section, stresses being caused by internal pressure, can, therefore, mount up to $4\sigma_{rd}$ and has a decisive effect on the value of the stress range due to self-compensation of thermal elongations.

In steep bent and welded elbows ovality is insignificant and does not exceed the cross-sectional ovality of straight pipes. The internal pressure stress range can be taken equal to σ_{rd}.

According to flexure investigations made by Clark and Reissner in the plane of curvature

$$\gamma = 1.89\lambda^{-2/3}; \quad \beta = 0.84\lambda^{-2/3} \tag{3.20}$$

These coefficients do not consider internal pressure.

A method for calculating the coefficients β and γ with regard to internal pressure and the direction of action of bending moments (in the plane of curvature and perpendicular to it) has been suggested by D. L. Kostovetskiy. The intensification coefficients γ and β are functions of the dimensionless parameters λ and ω and their analytical determination requires lengthy calculations. Because of this, the graphs presented in Appendixes 19 and 20 should be used for practical purposes. When $\omega = 0$, i.e. at no pressure and for $\lambda < 0.4$ the appendixed data agrees with formula (3.20). Elbows used in practice are characterized by the following limiting parameters:

Table 3.2

Type of elbow	Ratio R/D_0	Minimum value of λ	Maximum possible value of ω
Normal	4-5	0.48	0.12
Steep bent	1.5	0.16	0.01
Welded	1.0	0.029	0.0045

From the comparison of γ and β values, it follows that in all the cases met in practice γ is always greater than β, i.e. $\sigma_{b1} > \sigma_{b2}$.

This difference is particularly large when ω is close to zero and γ exceeds β approximately twice. Since the transversal bending stresses range in elbows exceeds the longitudinal bending stresses range, the fatigue cracks may appear along the lines of maximum transversal bending stresses. Upon bending an elbow fatigue cracks appear in the plane of curvature along the elbow's neutral line of bend, where the transversal bending stresses are maximum, and the longitudinal stresses almost equal to zero. This is fully supported by the results of the experiments carried out by A. G. Kamerstein at the All-Union Scientific Research Institute for the Construction of Pipelines (ВНИИСТ).

Here, we may mention that very often calculations take into account the longitudinal stress intensification coefficient β, although this coefficient does not take account of neither the statical nor the fatigue strength of pipe bends. In the American Code the stress intensification coefficient for elbows is taken equal to $m = 0.90\lambda^{-2/3}$, a value which is 2.1 times less than the longitudinal bending stress intensification coefficient calculated from the Clark-Reissner formula $\gamma = 1.89\lambda^{-2/3}$. It can be explained by the fact that the stress intensification coefficient has been taken equal to 1.0 for straight runs of pipes, whereas the longitudinal stress intensification coefficient, as originally proposed by Markl [3-15], at fastening points and in welded joints mounts up to 1.5. The other factor being the different character of the stressed state. The circumferential stresses appearing in the elbow wall upon bending are the bending stresses in the wall; the neutral bending surface is located between the wall surfaces. The longitudinal stresses, which appear on bending a straight pipe in the most stressed zone, have the same sign throughout the wall thickness, and for reversal loads the wall in this zone is subjected to tension-compression conditions. But, as it is known, the fatigue limit during bending is about 1.4 times more than during tension-compression. Taking into account both the factors, the circumferential bending stresses in an elbow may be taken equal to $1.4 \times 1.5 = 2.1$ times more than in an ideal straight run of pipe with stress intensification coefficient equal to one. Accordingly, the values of allowable stresses, recommended in American Specifications for pipeline design, have been calculated for a low value of the stress intensification coefficient.

The rigidity of welded elbows, which are generally made of two or three sectors and have a radius 1-1.5 times the pipe diameter, is very often taken equal to the rigidity of straight pipes. Meanwhile flattening forces, similar to the forces acting in elbows with curvilinear axis, appear in conjugate planes upon bending the elbow (see Fig. 3.9), and therefore, the cross section becomes flat and rigidity decreases due to radial displacements of the walls. The difference between a smooth elbow and elbow made of welded sectors is that in the first case the flattening forces are distributed along the whole length of elbow, and in the second case these forces are concentrated along the ellipses of sector joints.

The problems of welded elbows flexibility and their strength were thoroughly investigated by A. G. Kamerstein

[3-7 and 3-8]. Based on experiments conducted on elbows from 219 mm to 720 mm in diameter, A. G. Kamerstein proved that the welded elbow flexibility coefficient should be determined from formula (3.15), i.e. from the curved pipe formulas.

The circular bending stresses are distributed along the circumference of the welded elbow in a slightly different manner than in bent elbows, particularly, between the neutral plane and the concave side of the elbow the circular bending stresses exceed the absolute stresses in a smooth elbow, but maximum circumferential bending stresses are 10 to 15% less than in a smooth elbow, and for this reason, quality-welded elbows prove to be stronger to withstand reversal loads than steep bent elbows having the same characteristic λ. Thus, the same formulas as used for steep curved elbows can be applied to the calculations of welded elbows for fatigue.

Now we consider another peculiarity of bent elbows. When bending elbows from straight pipes in bending machines their cross section becomes slightly elliptical (oval), the minor axis of the ellipse lies in the plane of elbow curvature. Here, by elliptical (oval) cross section is meant the difference between the maximum ($D_{\max}$) and minimum ($D_{\min}$) outside diameters referred to the nominal (or mean) outside diameter, i.e.

$$a = \frac{D_{\max} - D_{\min}}{D_0} 100\%$$

Ovality of up to 8% for bends $P_n \geqslant 200$ and to 10% for thin-walled pipes $P_n \leqslant 100$ is technically considered as the acceptable limit.

Under the action of internal hydraulic pressure the elliptical cross section tends to become a circular one, i.e. in the elliptical cross section deformations appear which result in the increase of ellipse's minor axis and the decrease in major axis at the same time. An increase in elbow diameter in its plane of curvature causes the elbow's radius of curvature to increase, and as a consequence the angle of elbow decreases by $\alpha\theta$. As proved by D. L. Kostovetskiy

[3-11], this angle

$$\alpha\theta = -\frac{aD_0}{200\,(D_0-s)}\,\theta K_\delta \text{ radians} \qquad (3.21)$$

in which a—ellipticity of elbow's cross section, %; θ—angle of elbow, radians; D_0—outside diameter, mm; s—wall thickness, mm; K_δ—coefficient depending upon the geometrical elbow characteristic λ and the dimensionless coefficient ω.

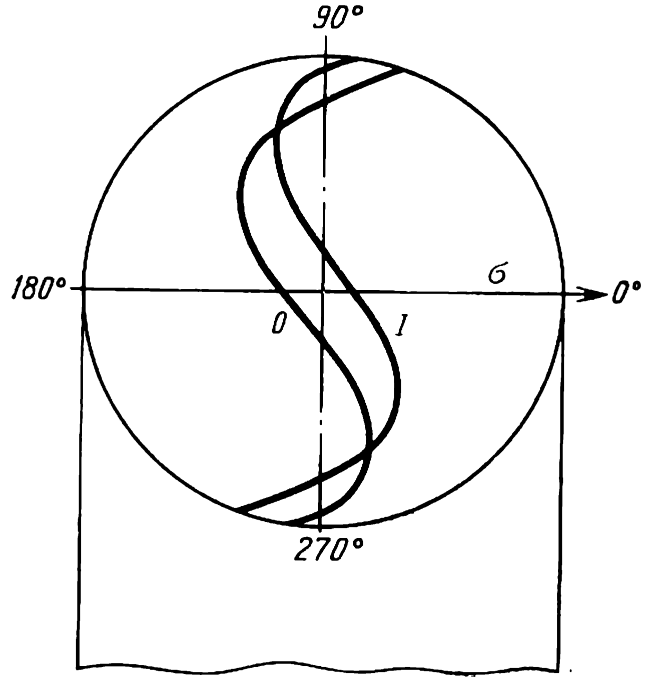

Fig. 3.14. Transversal bending stresses in an oval-shaped elbow due to internal pressure

0—on the outside surface; *I*—on the inside surface

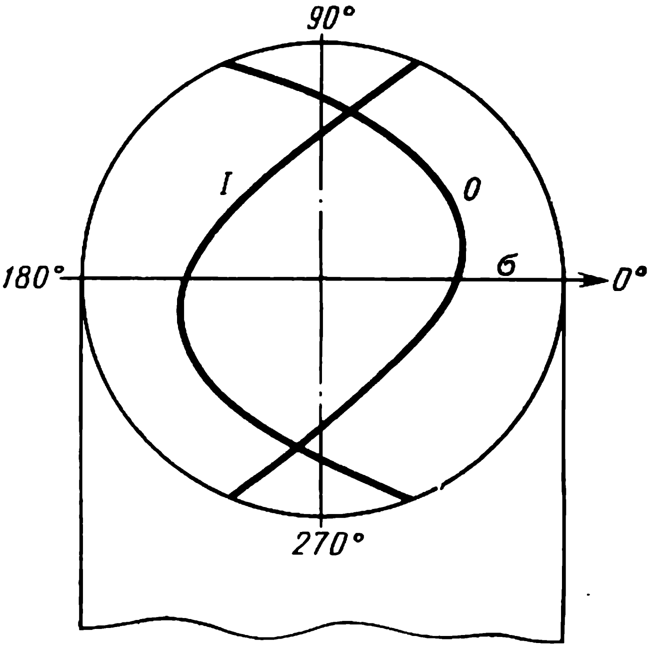

Fig. 3.15. Longitudinal bending stresses in an oval-shaped elbow due to internal pressure

0—on the outside surface; *I*—on the inside surface

The coefficient K_δ can be determined from Appendix 18 or calculated by the following formula:

$$K_\delta = \frac{18\omega}{1+12\lambda^2+24\omega} \qquad (3.22)$$

which although is the first approximation, but gives sufficiently accurate results for all practical calculations.

Bending stresses due to internal pressure appear in an elbow having oval-shaped cross section:

circumferential

$$\sigma_{b1}^{p} = p\frac{2RD_0}{(D_0 - s)\,s}\,a\cdot 10^{-4}\gamma\ \mathrm{kg/mm^2}$$

longitudinal

$$\sigma_{b2}^{p} = p\frac{2RD_0}{(D_0 - s)\,s}\,a\cdot 10^{-4}\beta\ \mathrm{kg/mm^2}$$

where p—pressure, kg/cm^2; R—radius of elbow, mm.

The remaining notations are the same as in formula (3.21).

The distribution of σ_{b1} and σ_{b2} stresses in the elbow cross section is similar to the distribution of stresses caused by bending moments acting in the plane of curvature, and is shown in Figs. 3.14 and 3.15. The bending stress intensification coefficients γ and β are similar to the intensification coefficients used in formula (3.18). So for determining total stresses in elbows having ovality, it is convenient to introduce the theoretical moment M_R^p acting in the plane of curvature and conforming to σ_{b1}^p and σ_{b2}^p stresses:

$$M_R^p = -pW\frac{2RD_0}{(D_0 - s)\,s}\,a\cdot 10^{-4}\ \mathrm{kg\cdot m} \tag{3.23}$$

Since σ_b^p stresses conform to bending strains of elbows (a decrease in the angle of elbow θ) and the thermal elongations in the pipeline cause an increase in angle θ (as a rule), the moment M_R^p is given a negative sign.

3.8. Check Calculation of Elbows for Cyclic Stress Ranges

The possible number of full stress cycles of varying magnitude for power station pipelines during anticipated life of 30 years is relatively small and lies between 1500 and 6000 cycles, and in expectionally rare cases it may reach 11,000 (when pipelines are heated from minimum to maximum temperature and back for 365 times in a year). The studies of metal fatigue limits for such a small number of cycles began fairly recently. At the present time the American Codes contain more reliable data on vessels of nuclear plants [3-16]. Figure 3.16 is based on this data, which is accepted by us as initial data for the proposed method of calculation. Graphs have been drawn for tension-compression cycles, i.e. for the worst circumstances, and are based on vast experimental data of special investigations. These investigations in particular showed that an increase in steel strength does not enhance its endurance strength and for this reason we could generalize data for all types of steels of a given Grade (pearlitic, austenitic). Curve *3* shown in Fig. 3.16 is based on bending test data of elbows made from steel Grade 20. The tests were conducted at 20°C and test data processed by Soviet scientists [3-8]. For a limited number of cycles start-up and shut down fatigue limits exceed the yield point of steel. Because of this, the limited fatigue strength is, generally, expressed in nominal stresses $\sigma = \varepsilon E$. Here, the elastic modulus of steel is taken to be constant irrespective of the magnitude of deformation ε. The conditionality of the value εE becomes already apparent when the technical yield point σ_s conforms to a residual deformation of 0.2%. Total deformation, including elastic strain, amounts to approximately 0.3% at the yield point, and, correspondingly, $\varepsilon E = 0.003E \approx 60$ kg/mm^2; this is two times in excess of the yield point.

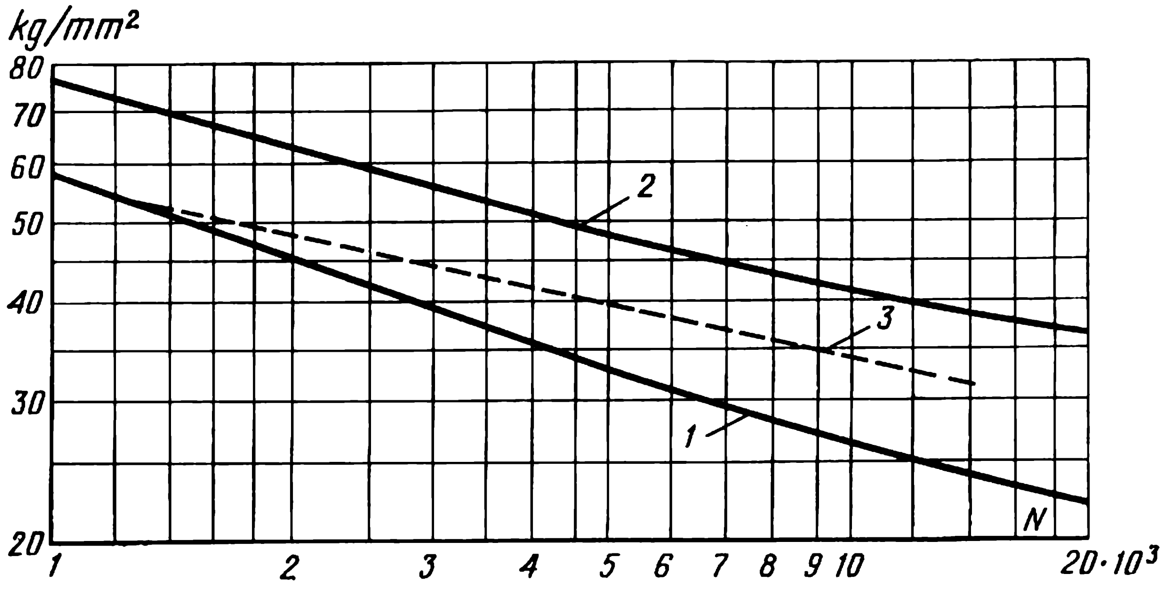

Fig. 3.16. Allowable amplitudes of elongation-compression cyclic stresses *versus* number of cycles

1—as per ASME for carbon steel at temperatures up to 370°C; *2*—as per ASME for austenitic chromium-nickel steel at temperatures up to 427°C; *3*—as per the test data obtained by ВНИИСТ (All-Union Scientific Research Institute for the Construction of Trunk Pipelines) taking the safety factor equal to 1.4

When the stress range exceeds total yield points of a pipeline in the hot and cold condition after a few initial transient cycles the nature of cycles start becoming symmetrical. This is illustrated in Fig. 3.17 where, numbers *0-1-2-3-4-2* indicate the variation in strains and stresses, and the letters *a-b* and *c-d*—the amplitudes of nominal stresses εE. The actual stressed state cycle in elbow walls differs from the symmetrical one, mainly, due to the change in metal properties (yield point, Young's modulus). This change is due to temperature variations in the operating and non-operating conditions of pipeline. But, these deviations from the cycle symmetry, caused by temperature changes, should not appreciably affect the limited endurance strength as one can see from American Codes [3-16] which suggest similar allowable stress amplitudes for carbon steels at all temperatures up to 370°C, and for austenitic steels at temperatures up to 427°C. The Standards envisage similar stresses at different temperatures, but as Young's modulus decreases with increasing temperature it will mean some increase in the allowable amplitude of strain ε with a rise in temperature.

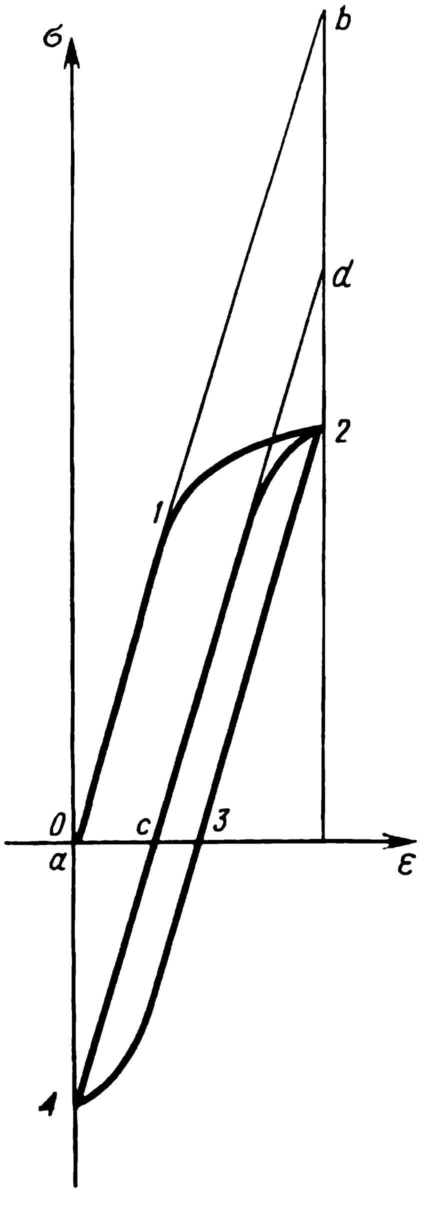

Fig. 3.17. Approximation of the asymmetrical cycles to symmetrical ones at large stress ranges

Considering the pipeline cycles as if they tend to become symmetrical, the allowable stress ranges for the above mentioned temperature limits (370 and 427°C) may be taken as twice the value of allowable amplitudes determined from Fig. 3.16.

Pipeline calculations can not be confined to these temperatures, therefore it is necessary to suggest a method for determining allowable stress ranges for higher temperatures. With the increase in temperature from the installed temperature to the operating one the stressed state of metal in the considered portion changes from one extreme to another, one conforming to tension strains and the other to compression strains. No-stress state in the considered portion corresponds to some intermediate temperature equalling approximately to one half the operating temperature. This intermediate temperature for steam (or gas) parameters now in use does not exceed 370°C for pearlitic steels and 427°C for austenitic steels. Hence, one half-cycle when the equivalent stress change from one extreme state to zero is completed for pearlitic steels up to temperatures of not exceeding 370°C, and 427°C for austenitic steels. The other half-cycle from zero to the other extreme state of equivalent stresses completes at higher temperatures. For this second half-cycle the allowable amplitude of stresses p_2 can be taken

$$p_2 = p_1 \frac{\sigma_{al\,1}}{\sigma_{al\,2}} \tag{3.24}$$

in which p_1—allowable amplitude determined from Fig. 3.16 at t_1°C; $\sigma_{a l1}$—nominal allowable stresses at t_1°C; $\sigma_{a l2}$—nominal allowable stresses at t_2°C; t_1—370°C for pearlitic and 427°C for austenitic steel Grades for which allowable stress amplitude curves are presented in Fig. 3.16; t_2—given (operating) temperature of pipeline, °C.

Correspondingly, the allowable stress range at a temperature of t_2 can be determined from the formula

$$[\sigma_{s\text{-}r2}] = k_t\,[\sigma_{s\text{-}r}] \tag{3.25}$$

in which

$$k_t = 0.5\left(1 + \frac{\sigma_{al\,1}}{\sigma_{al\,2}}\right)$$

$\sigma_{s\text{-}r}$—allowable stress range at a temperature of t_1.

The values of the coefficient k_t for the most commonly used steel Grades are given in Appendix 15. The value depends upon the expected number of start-up—shut-down cycles N, and is taken from data presented in Table 3.3.

Table 3.3

Total number of cycles during service life of pipelines	1500	3000	4500	6000	11,000
Allowable equivalent stress range, kg/mm^2:					
for pearlitic steels	100	78	68	62	51
for austenitic steels	136	112	100	93	81

As regards the design number of cycles the following should be noted:

1. Steam pipelines supplying industrial units and heat-and-power supply lines during their service life of 30 years are heated from minimum to maximum temperature and back for a few hundred times and, therefore, can be calculated for 1500 cycles.
2. Pipelines of large condensing units intended for taking the basal load, in the first years of operation, will have very few shut downs, however, in subsequent years with the introduction of more large capacity units the pipelines may be shut down at week ends, and in some months and seasons they may be shut down nightly. For such units the design number of cycles should not be taken less than 3000 for their service life.
3. Pipelines intended for heat-and-power supply units when used in summer for taking peak loads may have in a year up to 150 to 200 shut downs, and therefore, must be calculated for 4500-6000 cycles.
4. Steam-power plant pipelines intended for daily heating from minimum to maximum temperature and back (start-up—shut down) are calculated for 11,000 cycles (service life 30 years).

Temperature and pressure of certain pipelines, for example, condensate regenerative warming up and feed water systems and cold lines of steam reheat system vary with varying turbine load. In this category of pipelines besides complete cycles of stress ranges (when the unit is shut down) appear incomplete cycles of reduced stress range caused by turbine load variations. This fact should be taken into account when determining design number of cycles for such pipelines.

Elbow strength condition for cyclic stresses is written as

$$\sigma_{s\text{-}r} \leqslant [\sigma_{s\text{-}r}] \text{ kg/mm}^2 \qquad (3.26)$$

in which $\sigma_{s\text{-}r}$—allowable stress range for a stipulated number of cycles; $\sigma_{s\text{-}r}$—design equivalent stress range.

Maximum equivalent stresses in the operating condition are determined from superposed circumferential stresses due to internal pressure and bending and torsional stresses due to moments caused by pipeline elongation. In the course of time the self-compensation stresses relax fully or partially, then in the pipeline's operating condition the stresses in an elbow will be only due to internal pressure.

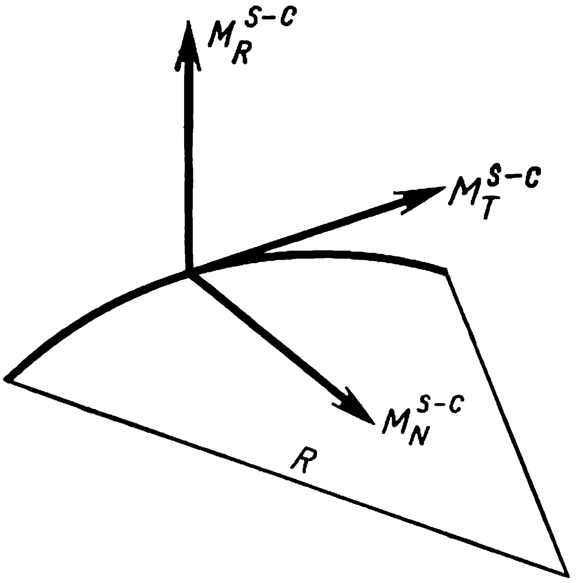

Fig. 3.18. Resolution of total self-compensation moment $M_{s\text{-}c}$ into components (the moment vectors perpendicular to the planes of their action are shown)

Maximum equivalent stresses in a cold pipeline are produced only by bending moments and torques appearing due to cold spring and self-elongation (relaxation of temperature stresses and plastic bending). The stresses appearing during hydraulic testing are not taken into account, because the number of such tests during the service life of pipeline is small. Stresses due to weight are also not considered as their value remains practically unchanged and have no effect on stress ranges. Since self-compensation stresses in the hot condition gradually decrease and in the cold condition increase, we determine the self-compensation stress range based on Young's modulus for the cold metal. Such an assumption somewhat increases the design stress range, and thereby ensures some additional strength.

To determine stresses in the considered section of an elbow, we shall resolve the total moment $M^{s\text{-}c}$ due to self-compensation into three components (Fig. 3.18):

$M_R^{s\text{-}c}$ = bending moment acting in the plane of curvature

$M_N^{s\text{-}c}$ = bending moment acting in a plane perpendicular to the plane of curvature

$M_t^{s\text{-}c}$ = torque

Besides this, the moment M_R^p, acting in the plane of curvature and accounting for the bending stresses in elbow due to internal pressure, should also be considered. Hence, the absolute value of total moment in the plane of curvature

$$M_R = |\, M_R^{s\text{-}c} + M_R^p \,| \tag{3.27}$$

Diagrams of bending stresses produced by moments $M_R^{s\text{-}c}$ and $M_N^{s\text{-}c}$ are shown in Figs. 3.10 through 3.15.

The design stress range should be determined as maximum variation of equivalent stresses. With this aim in view, it is convenient to follow the Saint-Venant Tresque theory and find such points on the inside and outside wall surfaces at which the difference between maximum normal circumferential and longitudinal bending stresses is maximum. It is evident that at these points the difference between maximum and minimum principal stresses with allowance made for tangential torsional stresses also attains its maximum. This problem can be solved with greater accuracy by calculating longitudinal and transversal stresses due to moments M_R and $M_N^{s\text{-}c}$, which appear on the inside and outside surfaces of walls (after every 5 to 10° of central angle), by adding these stresses with the corresponding circumferential and longitudinal stresses due to internal hydrostatic pressure, by determining the difference between normal circumferential and longitudinal stresses thus obtained, and by comparing the obtained differences in stresses to find the extreme value. This can be accomplished with the help of a digital computer. If a computer is not available the answer is confined to one or some other degree of accuracy.

From an analysis of possible combinations of stresses appearing on the inside and outside surfaces of elbow walls, D. L. Kostovetskiy suggested a simple method for determining maximum equivalent stresses. The design stress range to be used in this method equals maximum equivalent stresses determined from the following formulas:

$$\sigma_{s\text{-}r} = \sqrt{(\gamma\sigma_R + \beta\sigma_N^{s\text{-}c} + 0.5\sigma_{rd})^2 + 4(\tau^{s\text{-}c})^2} \tag{3.28}$$

$$\sigma_{s\text{-}r} = \sqrt{(\gamma\sigma_R + \sigma_{rd})^2 + 4(\tau^{s\text{-}c})^2} \tag{3.29}$$

$$\sigma_{s\text{-}r} = \sqrt{(\beta\sigma_R + \gamma\sigma_N^{s\text{-}c} + 0.5\sigma_{rd})^2 + 4(\tau^{s\text{-}c})^2} \tag{3.30}$$

$$\sigma_{s\text{-}r} = \sqrt{(\gamma\sigma_N^{s\text{-}c} + \sigma_{rd})^2 + 4(\tau^{s\text{-}c})^2} \tag{3.31}$$

In these formulae the intensification coefficients γ and β take account of internal pressure, and are determined from graphs of Appendixes 19 and 20. The reduced stresses σ_{rd} are determined from formula (3.8) and the remaining stresses, which appear in these formulae, are determined from the expressions:

$$\sigma_R = \frac{M_R}{W}; \quad \sigma_N^{s\text{-}c} = \frac{M_N^{s\text{-}c}}{W}; \quad \tau^{s\text{-}c} = \frac{M_t^{s\text{-}c}}{2W} \text{ kg/mm}^2$$

The selection of design formula (out of the four given above) is made easier by the fact that $\gamma > \beta$ practically throughout the range of our interest. For this reason, when selecting design formula we should be guided by the following:

1. If $\sigma_R > \sigma_N^{s\text{-}c}$ and in this case:

(a) $\beta\sigma_N^{s\text{-}c} > 0.5\sigma_{rd}$, then formula (3.28) should be used;

(b) $\beta\sigma_N^{s\text{-}c} < 0.5\sigma_{rd}$, then formula (3.29) is used.

2. If $\sigma_R < \sigma_N^{s\text{-}c}$ and in this case:

(a) $\beta\sigma_R > 0.5\sigma_{rd}$, then formula (3.30) is used;

(b) $\beta\sigma_R < 0.5\sigma_{rd}$, then formula (3.31) is employed

In flat portions $M_N^{s\text{-}c} = 0$ and the stress range is calculated by the formula

$$\sigma_{s\text{-}r} = \gamma\sigma_R + \sigma_{rd} \tag{3.32}$$

Example. Determine the stress range in a bent elbow with ovality $a = 10\%$. Elbow dimensions are: 426×11 mm, $W = 1451$ cm^3, $R = 1370$ mm, characteristics $\lambda = 0.43$, $A = 2300$. Pipeline parameters are: 25 atm, 340°C. The self-compensation bending moments at 340°C are: $M_R^{s\text{-}c} = -4400$ kg·m, $M_T^{s\text{-}c} = 8100$ kg·m, torque $M_T^{s\text{-}c} =$

$=3000$ kg·m. Since the stress range should be determined for $E = 2.1 \cdot 10^6$ kg/cm², the given self-compensation moments must be recalculated by multiplying with ratio 2.1 : 1.87 = 1.2, i.e. the following values of moments should be used in calculation:

$$M_R^{s\text{-}c} = -4920 \text{ kg}\cdot\text{m}, \quad M_N^{s\text{-}c} = 9050 \text{ kg}\cdot\text{m},$$

$$M_T^{s\text{-}c} = 3360 \text{ kg}\cdot\text{m}$$

The moment conforming to stresses in an ovalized elbow due to internal pressure is calculated from formula (3.23)

$$M_R^p = -1451 \times 24 \frac{2 \times 1370 \times 426}{(426-11)\,11} 10 \times 10^{-4} = -8900 \text{ kg}\cdot\text{m}$$

and the resultant moment in the plane of curvature

$$M_R = |-8900 - 4920| = 13{,}820 \text{ kg}\cdot\text{m}$$

Stresses in the pipeline are:

$$\sigma_R = 9.5 \text{ kg/mm}^2, \quad \sigma_N^{s\text{-}c} = 6.25 \text{ kg/mm}^2, \quad \tau^{s\text{-}c} = 1.15 \text{ kg/mm}^2$$

The reduced stresses $\sigma_{rd} = 5.38$ kg/mm² due to internal pressure. The parameter

$$\omega = \frac{p}{E} A = \frac{24}{2.1 \times 10^6} 2300 = 0.0263$$

and the stress intensification coefficients $\gamma = 2.6$ and $\beta = 1.9$ are determined from the graphs of Appendixes 19 and 20.

Since $\sigma_R > \sigma_N^{s\text{-}c}$ and $\beta\sigma_N^{s\text{-}c} = 1.9 \times 6.25 > 0.5\sigma_{rd} = 2.69$ kg/mm², the stress range is determined from formula (3.28), i.e.

$$\sigma_{s\text{-}r} = \sqrt{(2.6 \times 9.5 + 1.9 \times 6.25 + 2.69)^2 + 4 \times 1.15^2} = 39.6 \text{ kg/mm}^2$$

which is less than the allowable stresses, 62 kg/mm², for 6000 cycles.

First of all, we determine the stress range for elbows without ovalization (i.e. for forged, steep bent and welded elbows). For these elbows $M_R^p = 0$ and only one component $M_R = M_R^{s\text{-}c}$ of the self-compensation moment acts in the plane of curvature. The stress range is calculated from the deduced formulae, and the sign of the moment $M_R^{s\text{-}c}$, in this case, as follows from (3.27), does not play any role. However, when calculating elbows having ovalized cross sections (bent), the direction of the component of the self-compensation moment is considered because $M_R^p < 0$. Here, it may be mentioned that the positive sign has been taken

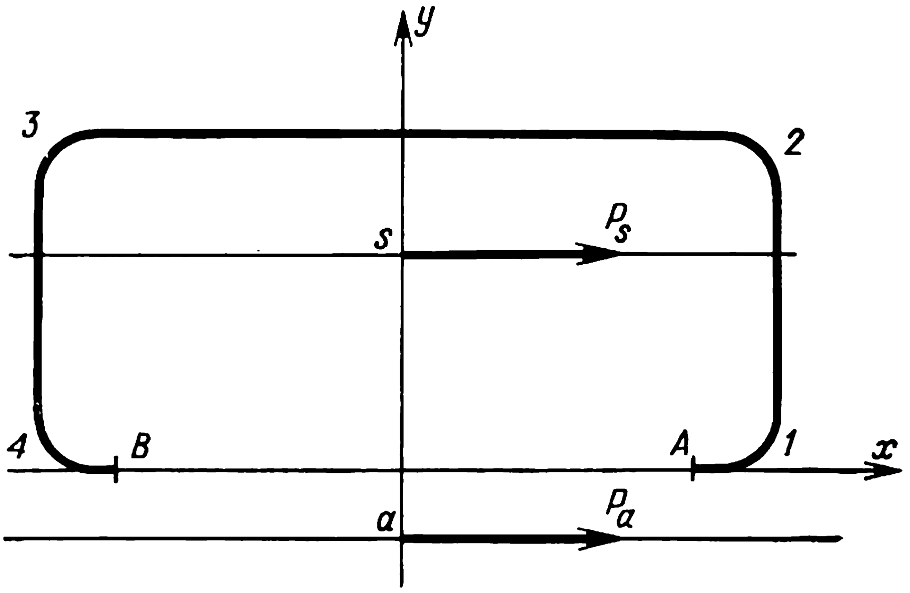

Fig. 3.19. Pipeline with negative self-compensation moments in elbows *1* and *4* having circular cross section

for moments which increase the central angle θ of elbow and negative for the moments decreasing this angle.

In those configurations where self-compensation takes place and which are encountered when designing electric generating stations and heating networks, the thermal elongations in pipelines always increase the angle θ of the elbow, i.e. $M_R^{s\text{-}c}$ is positive. Configurations may be encountered in which $M_R^{s\text{-}c}$ is negative. This is possible only when the elbow has no ovality. A portion shown in Fig. 3.19 can serve as example illustrating the above. If elbows have cylindrical cross sections and the angle θ does not change with pressure, then the line of action of forces P_s (line of zero moments) passes through point *s*. As end *A* was taken as fixed in determining the force P_s, then the force P_s tends to bend the elbows *1* and *4*, i.e. in these elbows $M_R^{s\text{-}c} < 0$. If in the same pipeline such elbows are replaced by ovalized elbows and the decrease in angle by $\alpha\theta$ for each elbow is considered, then, as proved by the calculation, the moments, in this case, will be determined from force P_a applied at point a. All these moments will be positive. The increase in moments up to their positive values is, in this case, due to the appearance of additional moments M_{ad} of reactive forces at fixed ends A and B. These moments restrict the rotation of pipe's end to angle $4\alpha\theta = 2\alpha\pi$.

When considering every possible configurations of simple parts, we did not find any configuration, containing bent elbows, in which the negative moment $M_R^{s\text{-}c}$ appeared on heating the pipeline. Thus one can assume that in simple parts (without any branching points) of constant diameter $M_R^{s\text{-}c}$ is always greater than zero. But for curved elbows of complex parts (with some fixed and branching points) $M_R^{s\text{-}c} < 0$ generally holds true, and the cases when $M_R^{s\text{-}c}$ is less than 0 must be regarded as exceptional cases. Thus, the appearance of M_R^p moments decreases the resulting moments in bent elbows. When steam pipelines are heated or cooled, i.e. when the walls are heated almost up to the nominal temperature and pressure in pipelines is small or equal to zero, $M_R^p = 0$ and $M_R = M_R^{s\text{-}c}$, i.e. more than for the steam pipeline under pressure. Besides this, under no pressure the intensification coefficients γ and β increase. As shown by calculations, in these conditions bent elbows are subject to the stresses higher than in the condition when the pipeline is under pressure.

The value of self-compensation moments in elbows is restricted by (1) conditions (3.12) and (3.12*a*) which limit total moments in an elbow during statical loading; (2) condition (3.26) restricting equivalent stress ranges with regard to stress intensification coefficients. A comparison of self-compensation moments determined by these conditions has shown that if $N \leqslant 6000$ and $M_R^{s\text{-}c} \geqslant 0$, then the second condition enables one to take large moments for no pressure and pressure regimes and, therefore, it is not the limiting condition.

Thus, the moments in normal radii bent elbows are limited by condition (3.12) and check calculation is not necessary for stress ranges when $N \leqslant 6000$ and $M_R^{s\text{-}c} \geqslant 0$. A check of stress ranges in bent elbows is necessary in exceptional cases, when $M_R^{s\text{-}c} < 0$. A check of stress ranges in steep bent and welded elbows is a must and is carried out with the use of aforementioned formulae, and for such elbows is taken $\sigma_R = \sigma_R^{s\text{-}c}$.

3.9. Hydrodynamic Forces in Pipelines

Some problems related to the hydrodynamic effect of the flowing fluid on pipelines have not been correctly interpreted in journals and some textbooks. Especially problems concerning the appearance of significant bending moments in pipes due to the flow reaction effect in elbows or due to fluid frictional forces acting on pipe walls [3-4 and 3-13].

Now we consider the law of linear momentum (impulse law), which for hydrodynamics can be expressed as:

$$\mathbf{N}_d = \frac{Q\mathbf{w}}{g} = \int^{F} \frac{m^2 v}{g}\, dF = 2\mathbf{p}_d F \cdot 10^4 \text{ kg} \qquad (3.33)$$

where $\mathbf{N}_d$—hydrodynamic force acting on the vessel (pipeline); Q—amount of liquid entering into pipeline, kg/sec; $\mathbf{w}$—mean velocity, m/sec; m—mass velocity, kg/(m^2·sec); v—specific volume, m^3/kg; F—pipe's cross section area, m^2; $\mathbf{p}_d$—hydrodynamic pressure, kg/cm^2.

The direction of the force $\mathbf{N}_d$ coincides with that of vectors $\mathbf{w}$ and $\mathbf{p}_d$ when liquid flows into a pipeline, and is directed opposite to $\mathbf{w}$ and $\mathbf{p}_d$ when liquid flows out of the pipeline. Thus, the vector $\mathbf{N}_d$ is always directed towards the vessel (pipeline). From equation (3.33) follows that the effect of a hydrodynamic force can be represented as twice the hydrodynamic pressure acting on the area F. Now we consider the forces appearing in the cross section *1-1* of a straight or curved pipe (Fig. 3.20). For the accepted flow direction the fluid flows out from the left-hand side of pipe and enters from the right, and therefore, a force $\mathbf{N}_d$ directed towards the left will act on the left-hand portion and the one directed towards the right—on the right-hand portion. The piezometric pressure also acts in the same manner.

Thus, acting in the cross section *1-1* are forces

$$\mathbf{N} = (\mathbf{p}_1 + 2\mathbf{p}_{d1}) F_1 \cdot 10^4 \text{ kg}$$

which tend to rupture the section. In a straight pipe the vector of the resultant force **N** coincides with the pipe's axis, and therefore, only tension stresses can appear in it. In [3-3] it was assumed that in curved pipes the force $\mathbf{N}_d$ also coincides with the hole axis of elbow. But, if the elbow has uniform wall thickness, then only tensile stresses can appear in it, and no bending moments due to the force $\mathbf{N}_d$ will appear*. If the vector of the resultant force **N** happens to be displaced with respect to the center of gravity of the cross section by a fraction *a* of diameter, then a bending moment *aDN* will appear. This moment is small, many times less than the moment due to internal pressure in bends having oval-shaped cross section.

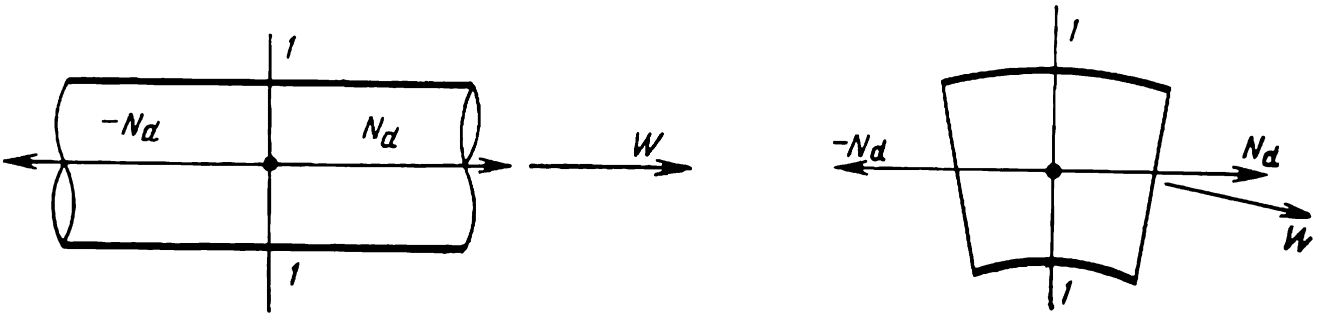

Fig. 3.20. Axial forces caused by hydrodynamic and piezometric pressures in a straight and curved pipe

To understand the effect of friction forces, we consider a model representing a suspended closed pipeline with a pump installed in it (Fig. 3.21). The pipeline may be of a variable cross section and may have different hydrodynamic resistances. As the pump operates the liquid will flow through the circuit, hydrodynamic pressure will develop and friction forces will appear. If the liquid does not flow away from the circuit there will be no external forces, and if the liquid is incompressible the center of mass does not change its position and the contour will be in equilibrium (if filled with compressible liquid equilibrium establishes in the steady state). This is possible only when for every element of the circuit is met the condition

---

* A. A. Voloshin in his work published in "Energomashinostroenie", 1965, No. 2 made an attempt to show on an example of calculating symmetrical pipelines that bending moments appear due to hydrodynamic forces. But, in the calculations given therein the reaction forces in the direction of *Y* a priori were taken equal to zero. As a result of this the sum of projections of forces on the *Y* axis was not equal to zero and the elementary conditions of equilibrium were not fulfilled. This lead to an incorrect result.

$$N_1 - N_2 + N_f = 0 \quad (3.34)$$

where N_1—force produced by hydraulic and hydrodynamic pressures acting in the flow direction; N_2—similar force acting opposite to the flow direction; N_f—wall friction force acting in the flow direction.

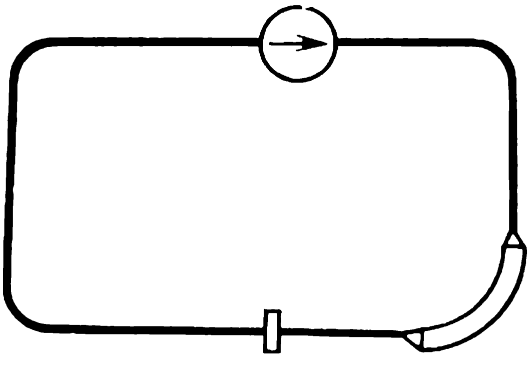

Fig. 3.21. Schematic diagram illustrating equilibrium of axial forces in pipelines

Condition (3.34) holds true for any element with smooth or sudden increase in passage area, for throttling devices, etc. Therefore, friction forces are balanced by the pressure difference between piezometric and doubled hydrodynamic pressures, and they can not produce any moments. Hydrodynamic forces in the same way as the hydrostatic pressure cause only axial tensile forces and do not produce any bending moments in long pipelines (if small moments produced by elastic elongation of pipeline under pressure are not considered).

In split pipelines (with bellows expansion joints without tightening devices, and with slip joints) the axial forces can not be transmitted from one rotation to another through pipe walls, and for this reason some design changes are necessary to exclude the appearance of large bending moments due to unbalanced axial forces. The last section of exhaust steam pipelines is also a split pipe, so the exhaust pipes should be designed with regard to unbalanced forces.

The reaction of an exhaust pipeline is determined by hydrodynamic and piezometric pressures (P_2, P_{d2}) in the exit section, and for 1 atm air pressure

$$N = (p_2 - 1 + 2p_{d2}) F_2 \cdot 10^4 \text{ kg} \qquad (3.35)$$

In his article [3-5] E. M. Zalkind suggested a method for calculating exhaust pipeline reactions, in which, erroneously proposed to add to the exhaust reaction another force equal to flow momentum per second after the last bend; this results in an increase in the reaction forces by approximately two times.

Chapter Four

Pipeline Thermal Elongation Compensation and Its Calculation

4.1. Methods of Compensating Thermal Elongations

On heating or cooling the length of pipelines changes by 1.2 to 1.8 mm per linear meter for every 100°C change in temperature. This necessitates the use of special measures to compensate for length variations between rigid supports or equipment. They are required to limit stresses appearing in pipelines, and also to restrict the level of moments and forces transferred to the equipment.

The most reliable and the only possible method for pressures over 16 to 25 kg/cm^2 is compensation of pipeline elongations at the cost of bending and torsional elastic strains, known as thermal elongation self-compensation. To achieve self-compensation it is necessary that a section of pipeline must have some (not less than two) arms located at an angle to each other. The minimum necessary length of the arms forming the shape of the self-compensating section is proportional to the pipeline's diameter and its relative thermal elongation. The arms of the hot sections of the steam reheat system require maximum length, and for these pipelines, in the layout schemes of electricity generating stations, good conditions are created for self-compensation without any artificial increase in the route.

In low pressure (up to 7 atm) large diameter pipelines used for steam extraction from turbines, circulating water lines, etc., bellows-type expansion joints are used. Bellows-type expansion joints can be used (1) to take axial displacements, i.e. for compensating elongations of straight sections subjected to tension—compression; (2) to create an elastic hinge for thermal elongation compensations. When using bellows-type expansion joints for axial compensation it is necessary to take into account large hydraulic thrust forces acting at rigid supports. The elastic hinge, on the contrary, enables to reduce the reaction forces acting from the side of the pipelines onto rigid supports and equipment to their minimum value, that is much less than the reactions during self-compensation.

Sliding joints are used in long and straight portions of pipelines operating at pressures up to 16-20 kg/cm^2. These joints have the following advantages: small size, large compensating capacity, small hydraulic resistance, the disadvantages being large hydraulic thrust and friction forces in compensators (expansion joints). For this reason, their location on trestles is ruled out. They require periodic inspection and maintenance to ensure required tightness of the packing. Sliding joints are widely used in combined heat-and-power supply lines and rarely in pipelines for other purposes.

4.2. Self-Compensation Problem and Methods of Its Solution

The problem of calculating forces and stresses appearing on a pipeline as its temperature varies is similar to the problem of determining forces and stresses from given deformations of the system, i.e. by its nature it is a statically indeterminate problem. Problems of this kind present no fundamental difficulties at the present time. A number of methods are known which enable one, when designing civil structures, to determine stresses in complex three dimensional frames with large number of joints. The solution of such problems, requiring lengthy calculations, present no difficulties now-a-days because of computers.

The calculation of pipelines for self-compensation has some specific peculiarities, i.e. absence of external loads, extended length and complex configuration, presence of curvilinear sections, rigid ends. Because of this it is advisable to develop special calculation methods, to have standard calculation procedures suitable not only for computers but also for desk calculators using slide rulers and arithmometers. The use of standard calculation procedures not only saves computation time, but also helps to a great extent perform calculations without errors.

The self-compensation calculation has in view the following: (1) to calculate reactions; (2) to determine maximum equivalent stresses due to self-compensation and external forces; (3) to determine maximum range of local bending stresses in curved elements of piping systems; (4) to determine the vertical, if necessary, horizontal displacements of pipelines at the fastening points. The amount of labour consumed in calculating a pipeline section, primarily, depends upon the order of static indeterminancy of the system and to a less extent on the number of bends in the piping system. This determines the total number of design elements involved in the system.

The most simple case is a plane pipeline with two rigid supports. To solve this system it is necessary to determine three reactions (two forces and a moment) at one of these rigid supports. The calculation of a three dimensional simple section is a six fold indeterminate problem, because in this case at one of the rigid supports six reactions, i.e. three components of the force and three components of the moment are determined. A two-dimensional section of pipeline is also a sixfold statically indeterminate system which calls for the determination of moments and components of reactions at both the rigid supports.

Generally, for a complex three-dimensional section with n rigid anchors the order of static indeterminancy equals 6 (n-1). It is quite evident that such problems can be solved only by taking recourse to the use of computers or by modelling. It should be noted that the order of the system of equations, which are solved to evaluate static indeterminancy, can be considerably lowered by choosing optimum computation procedure. Thus, at a rigid support lying at the center of an elastic system the moment of reaction is equal to zero. Therefore, by shifting the supports to the resilience center the moments acting at these supports can be taken equal to zero. In this case, for calculating a simple two-dimensional pipeline it is necessary to solve a system of equations of the second order (two equations with two unknowns) and for calculating a simple three-dimensional pipeline a system of the third order equations (instead of the system of the sixth order) is solved. If recourse is taken to the use of computers, then it is not necessary to reduce the order of equations even for systems having any appreciable degree of complexity.

The following assumptions are made to calculate self-compensation:

1. All rigid supports are considered as absolutely fixed ends which do not permit deflections and displacements. This assumption fully holds true only for those supports at which equal and opposite moments and forces act on both left-hand and right-hand sides. In all other cases, when the resulting moments and forces act on the support, the support proper and the structural elements connected to it will offer resistance to moments and forces only if there are some elastic strains in the elements of the support and the structure. Therefore, all fixed points are conditionally fixed supports, but in actual practice they are elastic ones. This assumption makes it possible to calculate every section separately, irrespective of adjoining section. This considerably simplifies self-compensation calculations. At the same time, the rated moments and forces calculated by making the aforementioned assumption are found to be slightly higher, and hence, this assumption increases the safety factor.

2. The displacements of a heated pipeline's axis are very small and do not affect the value of the bending moments and torques in the pipeline. As a rule this assumption holds true. Adjustments can only be required when calculating U-shaped compensators with a long back, whose displacement can be great enough as compared to the compensator stretch value. Adjustments can be introduced into calculations by way of consecutive approximations.

3. Only the bending and torsional strains are taken into account in the calculations. The effect of the axial stresses due to reactions and shearing forces is neglected.

4. The resistance of pipeline supports to displacements is insignificant and it may be neglected.

For the above mentioned assumptions, the self-compensation calculations of simple two-dimensional section do not present much difficulty and no computing machines are required. The calculations of simple three-dimensional sections can also be performed manually by making some additional simplifying assumptions. However, the use of a computer increases accuracy and saves time. For this reason, calculations of even simple three-dimensional sections should be done manually only when a computer is not available.

No discussion is given here of the methods for computer calculation, since they are described in other literature [4-1], journals [4-6] and manuals. This chapter deals only with the general theory for calculating pipelines for self-compensation. The knowledge of this theory as well as of the material presented in chapter three of this book is necessary to facilitate design and calculation work. Here, a simplified method has also been described which is employed only when computers are not available for calculation work.

4.3. Coordinate System and Determination of Displacements to Be Compensated

The orthogonal system of coordinates is used for self-compensation calculation. The Y axis is directed upwards, as already accepted in computer calculation practice. The direction of X and Z axes is selected in such a manner that the main (longest) straight parts of the pipeline are in planes parallel to the coordinate planes.

We denote the coordinate planes by the index of the axis to which this plane is perpendicular, i.e. plane $x = 0$ will be denoted by the index x and so on. The same index will be used for the components of force moments and torsion angles in the planes parallel to the coordinate planes. Hence, M_x and ψ_x denote force moment and torsion angle in the plane $x = \text{const}$ which is parallel to the plane $x = 0$. The vector of the moment M_x coincides in direction with the X axis. The positive directions of the force components and linear displacements are taken as positive directions of corresponding axis of coordinates. The positive direction of the components of a moment and also of angles are taken as the directions from the positive semi-axis of coordinates, termed as first, to the positive semi-axis, termed as second, precisely, in the plane x from Y axis to Z axis; in the y plane from Z axis to X axis; in the z plane from X axis to Y axis.

Thus, the positive directions of angles are determined by the law of circular permutation of indexes x, y, z located in alphabetic order (Fig. 4.1). The law of circular permutation of indexes permit the formulas obtained for any plane to be extended to other planes by changing indexes as per this rule. While solving problems, one end of a pipeline denoted by A (Fig. 4.2) is considered as the rigid end and the other end B is freed from the anchor. When a pipeline

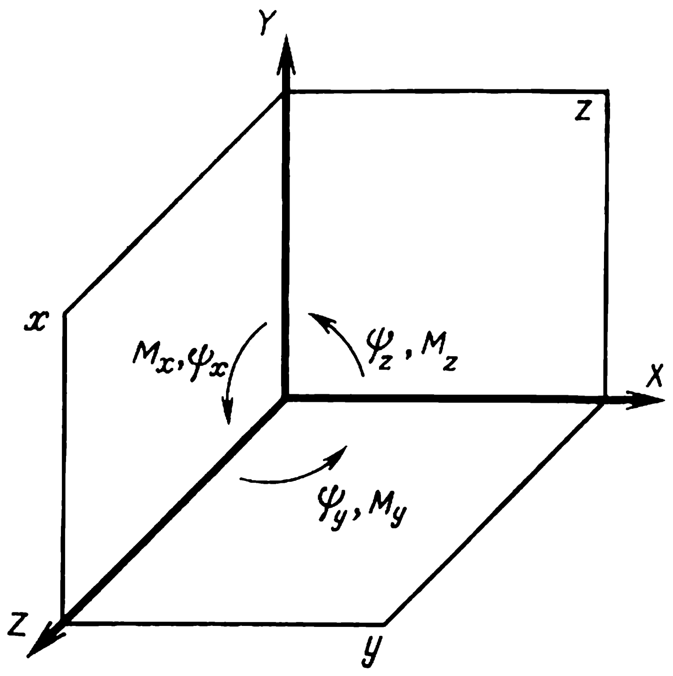

Fig. 4.1. Coordinate system, symbols of planes and positive directions of angles and moments

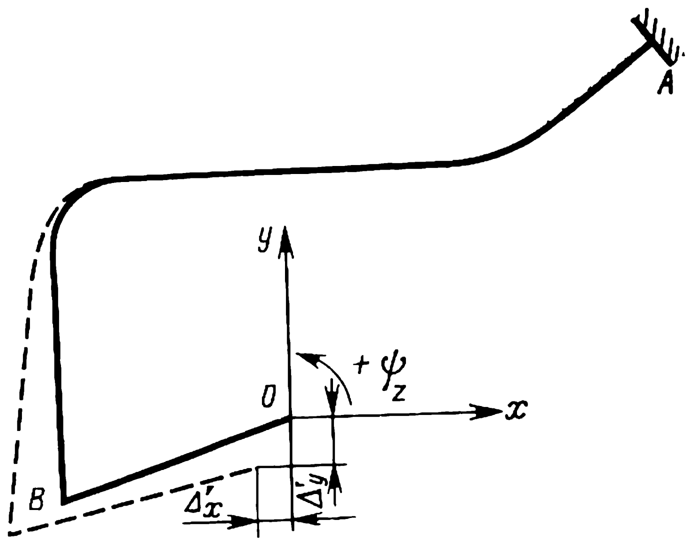

Fig. 4.2. Displacements of the cut free end B and the rigidly fixed to it origin of coordinates 0

is heated from the idle to the operating condition it elongates and the torsion angles of elbows (having ovality) vary, and as a result of this the end *B* undergoes deflections, displacements being Δ' and torsion angles ψ'. The aim of this calculation is to find the forces and moments whose action on end *B* would compel this free end to return to its initial position, and end *B* in this case will have elastic displacements $\Delta = -\Delta'$ and $\psi = -\psi'$. These elastic displacements should be accounted for when forming the deformation equations for a pipeline.

To have freedom in the selection of origin of coordinates and to simplify the expressions of coefficients in deformation equations we shall consider instead of the pipeline *AB* the system *ABO* in which section *B* is combined with the origin *O* by an absolutely rigid undeformable connection (Fig. 4.2). The torsion angles ψ at point *O* are equal to the torsion angles at point *B*, but the linear displacements, in this case, vary by $\pm\psi v_B$, where ψ—torsion angle, v_B—corresponding coordinate of point *B*. The displacements corrected in this manner should be taken into account for calculating the system *ABO*. When determining rated elastic displacements the following displacements and deformations must be taken into account:

1. The elongation caused by thermal expansion $\delta_t = \alpha(t - t_e)\cdot 10^2$ cm/m, where t_e—erection temperature, which is generally taken equal to 0°C. δ_t and α are determined from Appendixes 11, 12 and 13. However, when determining stresses in a cold pipeline (assuming complete relaxation of stresses in the hot pipeline) the relative thermal elongation should be taken as negative because in this case are considered the forces and stresses appearing on cooling.

2. Elastic elongation of pipes under internal pressure. The condition to keep pipes cross sections flat give rise to the ratio $\sigma_2 = 0.5\,(\sigma_1 + \sigma_3)$, where σ_2—axial stresses, σ_1 and σ_3—circumferential and radial stresses in pipe walls. This relationship for Poisson's ratio $\mu = 0.3$ leads to the following formula for determining relative longitudinal elongation of pipes under internal pressure p:

$$\delta_p = \frac{10p}{E}\left(\frac{D_n}{s} - 3\right) \text{ cm/m} \qquad (4.1)$$

where for the operating condition of pipeline Young's modulus E is taken corresponding to the operating temperature; for checking stresses in the cold condition pressure p is taken equal to the test hydraulic pressure and the elastic modulus E at 20°C.

For standard parameters of steam and feed water, the total-elongations both for the operating condition and the cold condition, i.e. during hydraulic testing with allowances made for elastic elongation are given in Appendix 13. As is clear from the values listed in this Appendix, elastic elongations in feed pipelines due to thermal expansion amount to 4-5% and must be taken into account. In pipelines of non-standard parameters the elastic elongations generally do not exceed 1% and may be ignored.

3. Variations in the angles of curved elbows, having oval-shaped cross section, due to internal pressure. For the present permissible limit of ovality, 8 to 10%, the variations in the angles of elbows reach 0.003 radians in high-pressure pipelines and in low-pressure pipelines they mount up to 0.018 radians (for elbows with central angle 90°). The displacements of the free end, in this case, can mount up to a few tens of centimeters and, therefore, must be added to the thermal elongation displacements of end B. The variation of angle is calculated from formula (3.21).

4. Inherent displacements of fastening points of pipelines, serving the equipment, due to equipment temperature variations.

The torsion and deflection angles taken by the free end of the system ABO, when it returns to its initial position under the action of forces and moments applied at the origin of coordinates, are determined from the following formulas:

$$\psi_x = \sum_A^B \alpha\theta \cos\beta_x; \quad \psi_y = \sum_A^B \alpha\theta \cos\beta_y; \quad \psi_z = \sum_A^B \alpha\theta \cos\beta_z \tag{4.2}$$

$$\left.\begin{aligned} \Delta_x &= \delta\,(x_A - x_B) + (\Delta_x^B - \Delta_x^A) + \Delta_x^{\alpha z} - \Delta_x^{\alpha y} - \Delta_x^b \text{ cm} \\ \Delta_y &= \delta\,(y_A - y_B) + (\Delta_y^B - \Delta_y^A) + \Delta_y^{\alpha x} - \Delta_y^{\alpha z} - \Delta_y^b \text{ cm} \\ \Delta_z &= \delta\,(z_A - z_B) + (\Delta_x^B - \Delta_z^A) + \Delta_z^{\alpha y} - \Delta_z^{\alpha x} - \Delta_z^b \text{ cm} \end{aligned}\right\} \tag{4.3}$$

In (4.3) the values Δ^{α}, representing displacements at the origin caused by variations in elbow angles, are equal to

$$\Delta_x^{\alpha z}=\sum_A^B y_k\alpha\theta\cos\beta_z\cdot 10^2;\quad \Delta_x^{\alpha y}=\sum_A^B z_k\alpha\theta\cos\beta_y\cdot 10^2$$

$$\Delta_y^{\alpha x}=\sum_A^B z_k\alpha\theta\cos\beta_x\cdot 10^2;\quad \Delta_y^{\alpha z}=\sum_A^B x_k\alpha\theta\cos\beta_z\cdot 10^2$$

$$\Delta_z^{\alpha y}=\sum_A^B x_k\alpha\theta\cos\beta_y\cdot 10^2;\quad \Delta_z^{\alpha x}=\sum_A^B y_k\alpha\theta\cos\beta_x\cdot 10^2 \quad (4.4)$$

where θ—central angle of elbow, radians; $\alpha = -\Delta\theta/\theta$—relative change in the angle of elbow due to internal pressure. This is taken with negative sign; β_x, β_y, β_z—acute dihedral angles between the plane of curvature of elbow and the coordinate plane; $\delta = \delta_t + \delta_p$—linear elongation of pipeline equal to the sum of thermal δ_t and elastic δ_p elongations, cm/m; x_A, y_A, z_A, x_B, y_B, z_B—coordinates of fastening ends A and B of pipeline, m; x_k, y_k, z_k—coordinates of the center of gravity of the arc of elbows axial line, m; Δ_x^A, Δ_z^A, Δ_z^A, Δ_x^B, Δ_y^B, Δ_z^B—inherent displacements of fastening points A and B, cm.

Value $\alpha\theta\cos\beta$ is the projection of the increment of angle $\alpha\theta$ on the appropriate coordinate plane, and is measured in the direction from the fixed end A towards the free end B. For bends coinciding with the accepted, for the considered plane, positive direction of angles this value is taken positive and for the non-coinciding as negative (Fig. 4.3).

The displacements of the free end of pipe caused by internal pressure (due to elastic elongation δ_p and the variation in the elbow angles Δ^{α}) have the same sign in the hot and cold conditions of pipeline under pressure. Thermal elongations are taken positive for the hot condition and negative when checking stresses in the cold condition (assuming that self enlongation of pipeline is complete). Similar results will be obtained if negative erection tolerances, equal to total thermal elongation, are taken for calculating displacements in the cold condition. For this reason, total elastic displacements for which self compensation stresses are checked in the cold condition can significantly differ from similar displacements in the hot condition even with no erection cold spring.

While calculating self-compensation using an approximate method, it is possible to simplify considerably the design

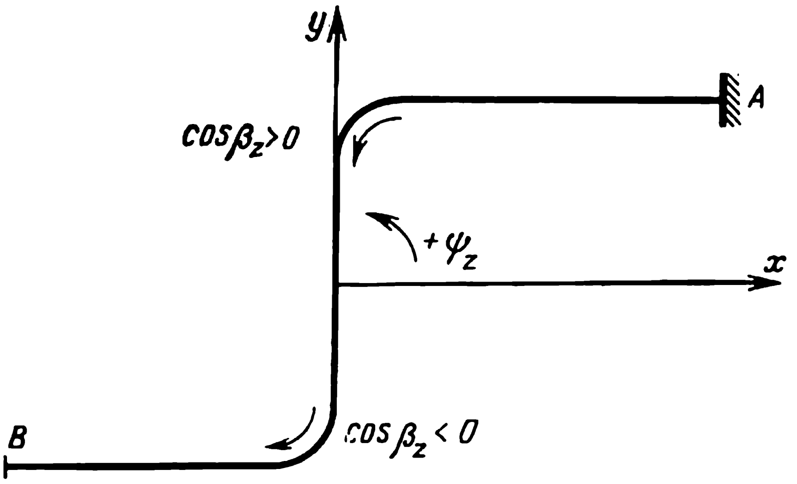

Fig. 4.3. Determination of the sign of $\alpha\theta \cos\beta$

formulas by shifting the coordinate axes to the center of elasticity. In this case the design elastic displacements must be taken equal to:

$$\begin{aligned} \Delta_{sx} &= \Delta_x - \psi_z y_s \cdot 10^2 + \psi_y z_s \cdot 10^2 \\ \Delta_{sy} &= \Delta_y - \psi_x z_s \cdot 10^2 + \psi_z x_s \cdot 10^2 \\ \Delta_{sz} &= \Delta_z - \psi_y x_s \cdot 10^2 + \psi_x y_s \cdot 10^2 \end{aligned} \tag{4.5}$$

where x_s, y_s, z_s—coordinates of the center of elasticity, m. Other notations have the same meaning as those in formulas (4.2) and (4.3).

The following formulas are used to determine design displacements at the center of elasticity of a plane (two-dimensional) section:

$$\begin{aligned} \Delta_{sx} &= \delta(x_A - x_B) + (\Delta_x^B - \Delta_x^A) + \Delta_x^{\alpha z} - \psi_z y_s \cdot 10^2 \\ \Delta_{sy} &= \delta(y_A - y_B) + (\Delta_y^B - \Delta_y^A) - \Delta_y^{\alpha z} + \psi_z x_s \cdot 10^2 \end{aligned} \tag{4.6}$$

where $\Delta_x^{\alpha z} = \sum_A^B y_k \alpha\theta \cdot 10^2$ and $\Delta_y^{\alpha z} = \sum_A^B x_k \alpha\theta \cdot 10^2$. All other symbols have the same meaning as those in formula (4.3).

4.4. General Theory of Pipeline Calculation for Self-Compensation

The compensation of pipeline elongations takes place at the expense of bending and torsional strains. The modulus of elasticity on elongation is greater than the modulus of elasticity in shear by $2(1+\mu)=2.6$ times. Here, $\mu = 0.3$ is Poisson ratio. The polar moment of inertia of a pipe is twice more than its equivalent moment of inertia. As a result the potential energy of strain on twisting is more than on bending by 2.6 : 2 = 1.3 times.

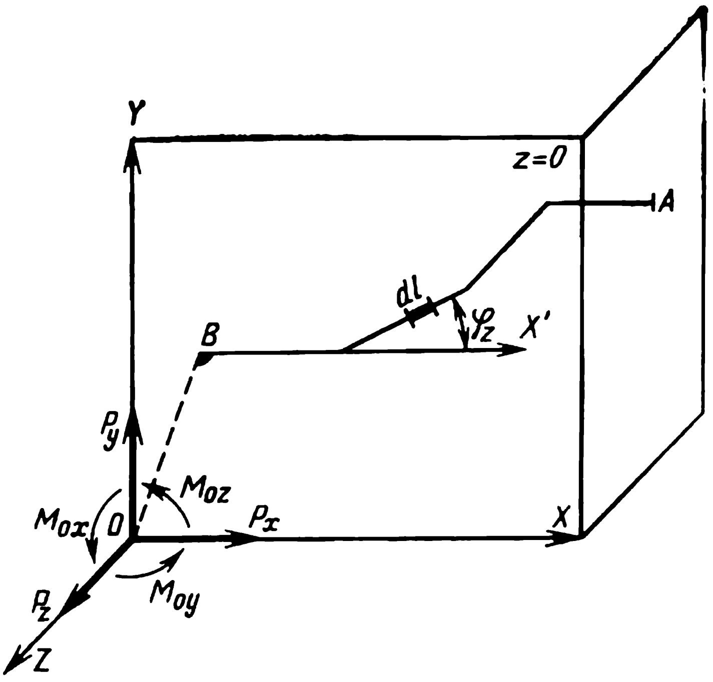

Fig. 4.4. Forces and moments acting on the length *dl* lying in plane $z = 0$

Total potential energy due to bending and twisting of section *AO*

$$U=\int_A^0 \frac{M_{b1}}{2EI}K_p j\,dl+\int_A^0 \frac{M_{b2}}{2EI}K_p j\,dl+\int_A^0 \frac{M_t}{2EI}1.3j\,dl$$

where M_{b1}, M_{b2}—components of bending moments in two mutually perpendicular planes; M_t—torque moment; K_p—coefficient of elbow flexibility on bending; EI—pipeline's rigidity, which is taken as design rigidity; $j = I : I'$—flexibility coefficient of elements having moment of inertia I' different from the design moment of inertia.

Now we examine a pipeline *AB* representing a three-dimensional elastic system (Fig. 4.4). Here, we assume that end *B* is connected to the origin O by an absolutely rigid and underformable coupling BO. The coordinate system is selected in such a manner that the observed elementary section dl lies in a plane parallel to the plane $z = 0$, and makes an angle φ with X axis. The loads applied at O will produce in section dl the following bending moments M_b and torsion moment M_t:

$$M_{b1} = M_{oz} + yP_x - xP_y$$

$$M_{b2} = (M_{oy} + xP_z - zP_x)\cos\varphi - (M_{ox} + zP_y - yP_z)\sin\varphi$$

$$M_t = (M_{ox} + zP_y - yP_z)\cos\varphi + (M_{oy} + xP_z - zP_x)\sin\varphi$$

Similar relationships can be obtained for elements of pipeline, which are located in other planes, provided every element is considered in any one plane. Total potential energy of deformation for the whole pipeline can be determined as the sum of potential energies for three planes. For the sake of simplicityc further we shall examine sections located in plane z.

The deflections and torsion angles at point O, the point of application of forces and moments, can be determined with the use of Castillano theorem. According to this theorem, the deflections are equal to the partial derivative of potential energy of deformation with respect to the applied force, and the torsion angles—partial derivative with respect to moment, i.e.

$$\Delta_x = \frac{\partial U}{\partial P_x}; \quad \psi_x = \frac{\partial U}{\partial M_x}, \text{ etc.}$$

Since the partial derivatives with respect to force (or moment M_0) of each integral, entering in the expression U, are equal

$$\frac{1}{EI}\int_A^0 M\frac{\partial M}{\partial P}K_p j\,dl \quad \text{or} \quad \frac{1}{EI}\int_A^0 M\frac{\partial M}{\partial M_0}K_p j\,dl$$

then for the determination of these derivatives it is necessary to find partial derivatives of moments M_{b1}, M_{b2} and

M_t with respect to each load acting at point O, i.e.

$$\frac{\partial M_{b1}}{\partial M_{oz}} = 1; \qquad \frac{\partial M_{b1}}{\partial P_x} = y; \qquad \frac{\partial M_{b1}}{\partial P_y} = -x$$

$$\frac{\partial M_{b2}}{\partial M_{oy}} = \cos\varphi; \qquad \frac{\partial M_{b2}}{\partial M_{ox}} = -\sin\varphi; \qquad \frac{\partial M_{b2}}{\partial P_x} = -z\cos\varphi$$

and so on.

After this we find $M\frac{\partial M}{\partial P}$ and $M\frac{\partial M}{\partial M_0}$ and expressions $\frac{\partial U}{\partial P}$ and $\frac{\partial U}{\partial M_0}$ representing deflections at point O produced by different components of forces and displacements. Each of the deflection components Δ_x, Δ_y, Δ_z and torsion angles ψ_x, ψ_y, ψ_z is a result of the combined action of all six components of loads applied at O. That is why for finding forces and moments conforming to given displacements, it is necessary to form a system of six equations of the type

$$EI\psi_1 = a_{11}M_1 + a_{12}M_2 + a_{13}M_3 + b_{11}P_1 + b_{12}P_2 + b_{13}P_3$$

$$EI\Delta_1 = b_{11}M_1 + b_{12}M_2 + b_{13}M_3 + c_{11}P_1 + c_{12}P_2 + c_{13}P_3$$

Each of the coefficients a, b, c represents

$$EI\frac{\partial U}{\partial P} = \int_A^B f(x, y, z, k, \varphi)\, j\, dl \quad \text{or} \quad EI\frac{\partial U}{\partial M_0} \int_A^B f(x, y, z, k, \varphi)\, j dl$$

Since the tie BO is thought to be absolutely rigid, then $j = 0$ and the upper limit of integration O can be replaced by B. The values of subintegrands determined by the earlier described method for each of the six equations are presented in Table 4.1.

The coefficients k entering in the subintegrands

$$k_1 = jK_p; \quad k_2 = j\,(1.3\cos^2\varphi + K_p\sin^2\varphi)$$

$$k_3 = j\,(K_p\cos^2\varphi + 1.3\sin^2\varphi); \quad k_4 = j\,(1.3 - K_p)\sin\varphi\cos\varphi$$

These coefficients can be regarded as flexibility or length reduction coefficients: k_1—for plane z; k_2—for plane x; k_3—for plane y; k_4—for sections lying outside the plane of moment action. Expressions of coefficients for sections lying in planes z = const are presented in Table 4.1; by

Table 4.1

Free terms	Integrands in the expressions of coefficients for unknown values of					
	M_x	M_y	M_z	P_x	P_y	P_z
$EI\psi_x$	k_2dl	k_4dl	0	$-zk_4dl$	zk_2dl	$-yk_2dl$ $+xk_4dl$
$EI\psi_y$	k_4dl	k_3dl	0	$-zk_3dl$	zk_4dl	xk_3dl $-yk_4dl$
$EI\psi_z$	0	0	k_1dl	yk_1dl	$-xk_1dl$	0
$EI\Delta_x$	$-zk_4dl$	$-zk_3dl$	yk_1dl	y^2k_1dl $+z^2k_3dl$	$-xyk_1dl$ $+z^2k_4dl$	zxk_3dl $+zyk_4dl$
$EI\Delta_y$	zk_2dl	zk_4dl	$-xk_1dl$	$-xyk_1dl$ $+z^2k_4dl$	x^2k_1dl $+z^2k_3dl$	$-zyk_2dl$ $+zxk_4dl$
$EI\Delta_z$	$-yk_2dl$ $+xk_4dl$	xk_3dl $-yk_4dl$	0	$-zxk_3dl$ $+zyk_4dl$	$-zyk_2dl$ $+zyk_4dl$	x^2k_3dl $+y^2k_2dl$

using method of circular permutation of indexes described in the previous paragraph, it is possible to obtain similar expressions for sections lying in planes y and z.

If the direction of the section is such that through it a plane parallel to one of the coordinate planes can not be drawn, then an auxiliary plane (a system of coordinates) is selected for calculation purposes. In this system the deflection coefficients are determined. And after this, appropriate coefficients are determined for the main system by using the system rotation rules. In the described method any one plane is taken for each element and all deflection coefficients are determined for this plane. Thereupon the coefficients in strain equations are calculated as sum of coefficients for different elements of pipeline.

The aforementioned method gives accurate results, but, as is clear from its description, it requires much time to calculate coefficients appearing in deformation equations. This method is applicable for computer-aided calculations. However, the knowledge of this method is of great utility for piping designers, but the use of this method without employing a computer involves much labour. For this reason, when under certain circumstances it is necessary to calculate manually, the appropriate simplified method of calculation should be employed.

Further simplification can be achieved by taking $k = 0$. In this case, as may be seen from Table 4.1, the torsion angles in the considered plane (ψ_x) will be determined only by moments (M_x) and forces (P_y, P_z) lying in the same plane or in a plane parallel to it, but the displacements (Δx) in any direction can be determined as sum of displacements due to moments and forces acting in planes (y, z) passing through the considered axis. However, while determining displacements of sections inclined to the coordinate axes, some problems arise due to the necessity of rotating the system of coordinates, and because of the displacements outside the planes of action of moments and forces. Further simplification can be obtained if we take $k = 1$ (instead of 1.3) for the flexibility coefficients of straight sections when twisted. In doing so, we get $k_1 = k_2 = k_3 = j$, $k_4 = 0$ (because for straight sections $K_p = 1$).

The flexibility coefficient of elbows in plane (two-dimensional) sections is taken equal to its actual value, i.e. K_p.

For arc elements of three-dimensional sections, the same value of flexibility coefficients can be taken for all directions, i.e. $k_1 = k_2 = k_3 = k_c$ and $k_4 = 0$, where

$$k_c = \left(\frac{1}{3}1.3 + \frac{2}{3}K_p\right) j = (0.43 + 0.67K_p)\, j \qquad (4.7)$$

Since in a three-dimensional section there are always some elbows oriented differently, the aforementioned assumption does not introduce appreciable error into the calculations. The calculations performed with this assumption give forces, moments and stresses enhanced by 10-15% (due to less flexibility taken for straight sections on torsion).

For the above mentioned assumptions, the coefficients where there are unknown quantities in the strain equations, as may be seen from Table 4.1, will have four different values: $\int k dl = L$; $\int kx dl = S_x$ and so on, $\int kx^2\, dl = J_x$, etc., $\int kxy dl = J_{xy}$ and so on. Here, L—equivalent length of the pipeline's axial-line, S_x, S_y, S_z—static moments, J_x, J_y, J_z—moments of inertia, J_{xy}, J_{yz}, J_{zx}—centrifugal moments of inertia of the axial line with respect to coordinate planes marked by indexes. Since the distance between the element dl and X-axis is equal to $\sqrt{y^2 + z^2}$, then $J_y + J_z = J_x$ represents the moment of inertia with respect to X-axis; the moments of inertia with respect to the Y and Z axes are determined in the same manner. If the coordinates and length of pipeline are expressed in meters and the rigidity in kg·cm², then the deformation equations, considering the earlier mentioned assumptions, can be rewritten as:

equations for angles of rotation

$$EI \cdot 10^{-4} \psi_x = S_z P_y - S_y P_z + L M_{ox}$$

equations for deflections at the origin of coordinates

$$EI \cdot 10^{-6} \Delta_x = (J_y + J_z)\, P_x - J_{xy} P_y - J_{xz} P_z + S_y M_{oz} - S_z M_{oy}$$

The remaining equations, which are not listed here, can be obtained by cyclic permutation of indexes.

From these equations, we get the following system which permit the unknown forces of reaction P to be found:

$$\left.\begin{aligned} EI \cdot 10^{-6} \Delta_{sx} &= (J_{sy} + J_{sz})\, P_x - J_{sxy} P_y - J_{szx} P_z \\ EI \cdot 10^{-6} \Delta_{sy} &= -J_{sxy} P_x + (J_{sz} + J_{sx})\, P_y - J_{syz} P_z \\ EI \cdot 10^{-6} \Delta_{sz} &= -J_{szx} P_x - J_{syz} P_y + (J_{sy} + J_{sx})\, P_z \end{aligned}\right\} \quad (4.8)$$

in which the coefficients J_s represent central moment of inertia, i.e. the moments with respect to the planes passing through the center of gravity (elasticity) of the system s, and the displacements Δ_s are determined from formula (4.5).

The coefficients J_s, m³, are determined from formulas:

$$\left.\begin{aligned} J_{sx} &= J_x - x_s S_x; & J_{sxy} &= J_{xy} - x_s S_y = J_{xy} - y_s S_x \\ J_{sy} &= J_y - y_s S_y; & J_{syz} &= J_{yz} - y_s S_z = J_{yz} - z_s S_y \\ J_{sz} &= J_z - z_s S_z; & J_{szx} &= J_{zx} - z_s S_x = J_{zx} - x_s S_z \end{aligned}\right\} \quad (4.9)$$

in which the moments of inertia J, m^3, with respect to the reference axes are equal to:

$$J_x=\int_A^B x^2k_c\,dl;\quad J_y=\int_A^B y^2k_c\,dl;\quad J_z=\int_A^B z^2k_c\,dl;$$

$$J_{xy}=\int_A^B xyk_c\,dl;\quad J_{yz}=\int_A^B yzk_c\,dl;\quad J_{zx}=\int_A^B zxk_c\,dl \tag{4.10}$$

and the static moments S, m^2, are equal to:

$$S_x=\int_A^B xk_c\,dl;\quad S_y=\int_A^B yk_c\,dl;\quad S_z=\int_A^B zk_c\,dl \tag{4.11}$$

Value $L=\int_A^B k_c\,dl$ is the equivalent length of pipeline.

The coordinates of the center of gravity are found from formulas:

$$x_s=\frac{S_x}{L};\quad y_s=\frac{S_y}{L};\quad z_s=\frac{S_z}{L} \tag{4.12}$$

The methods used to calculate all these coefficients are described in Sec. 4.6.

After determining the reactions P the moments M_0, kg·m, at the origin of coordinates can be found

$$\left.\begin{aligned}M_{ox}&=y_sP_{sz}-z_sP_y+\frac{EI\cdot 10^{-4}}{L}\psi_x\\ M_{oy}&=z_sP_x-x_sP_z+\frac{EI\cdot 10^{-4}}{L}\psi_y\\ M_{oz}&=x_sP_y-y_sP_x+\frac{EI\cdot 10^{-4}}{L}\psi_z\end{aligned}\right\} \tag{4.13}$$

and then the moments at any point having coordinates (x, y, z)

$$\left.\begin{aligned}M_x&=zP_y-yP_z+M_{ox}\\ M_y&=xP_z-zP_x+M_{oy}\\ M_z&=yP_x-xP_y+M_{oz}\end{aligned}\right\} \tag{4.14}$$

Equating the left-hand sides of these equations to zero, we get for each plane the equations of a line at which the moments are equal to zero. The coordinates of points through which lines of zero moments pass are easily determined in the following manner:

$$\left.\begin{array}{l}
\text{in plane } x \\
y_1=\dfrac{M_{ox}}{P_z};\quad z_1=0 \quad \text{and} \quad y_2=0;\quad z_2=\dfrac{-M_{ox}}{P_y} \\
\text{in plane } y \\
z_1=\dfrac{M_{oy}}{P_x};\quad x_1=0 \quad \text{and} \quad z_2=0;\quad x_2=\dfrac{-M_{oy}}{P_z} \\
\text{in plane } z \\
x_1=\dfrac{M_{oz}}{P_y};\quad y_1=0 \quad \text{and} \quad x_2=0;\quad y_2=\dfrac{-M_{oz}}{P_x}
\end{array}\right\} \quad (4.15)$$

If the torsion angles of the end which is cut free are equal to zero, then the lines of zero moments pass through the

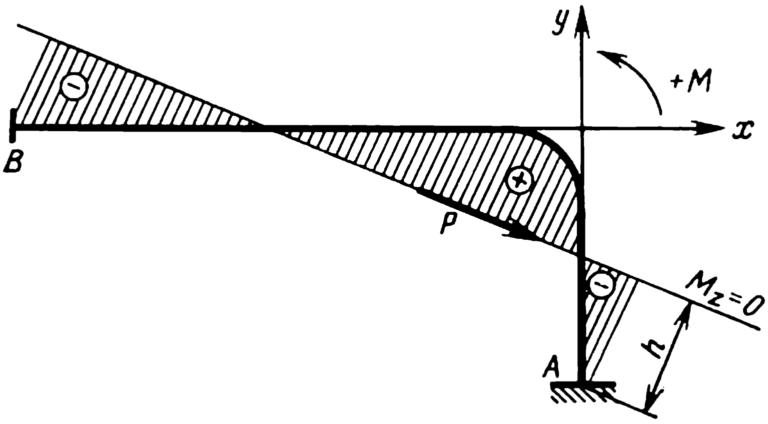

Fig. 4.5. Bending moments diagram drawn with the aid of lines of zero moments

center of elasticity. The lines of zero moments (Fig. 4.5) can be regarded as moment diagrams in the given plane, as the distance from any point on pipe's axis up to the line of zero moments represents the moment arm of the resultant force P in the given plane; this resultant force is directed along the line of zero moments. The signs of moments conform to the direction of force P (when end A is fixed and B is free) and the assumed positive direction of moments. Such moment diagrams reveal easily the most dangerous cross sections.

The bending moment $M_b^{s\text{-}c}$ and torque moment $M_t^{s\text{-}c}$ caused by self compensation are determined in the following manner. We denote the angles by α_x, α_y, α_z which are formed between the pipe's axis in the considered cross section and the corresponding planes of projections x, y, z. Then the bending moments caused by self compensation will accordingly be equal to $M_x^{s\text{-}c}\cos\alpha_x$, $M_y^{s\text{-}c}\cos\alpha_y$, $M_z^{s\text{-}c}\cos\alpha_z$, and the torsional moments—$M_x^{s\text{-}c}\sin\alpha_x$, $M_y^{s\text{-}c}\sin\alpha_y$, $M_z^{s\text{-}c}\sin\alpha_z$. As explained in Sec. 3.6, for finding equivalent stresses due to all additional loads, it is necessary to predetermine total bending and torsional moments with allowance made for the moments due to all additional external loads and self compensation.

The weight load results in bending moments M_x^{ext} and M_z^{ext} (moments acting in y plane are neglected).

Total bending moment

$$M_b = \sqrt{\begin{aligned}&(M_x^{s\text{-}c}\cos\alpha_x + M_x^{ext})^2 + (M_y^{s\text{-}c}\cos\alpha_y)^2 + \\ &\quad + (M_z^{s\text{-}c}\cos\alpha_z + M_z^{ext})\end{aligned}} \qquad (4.16)$$

and total torsional moment (neglecting torsional moments caused by weight)

$$M_t = \sqrt{(M_x^{s\text{-}c}\sin\alpha_x)^2 + (M_y^{s\text{-}c}\sin\alpha_y)^2 + (M_z^{s\text{-}c}\sin\alpha_z)^2} \qquad (4.17)$$

After checking the value of equivalent stresses caused by the combined action of self compensation and external loads, the vertical displacements h_y are calculated to select spring supports.

The resilient deflection of any point on the pipeline's axis with coordinates x_C, y_C, z_C can be determined as deflection of cantilever AC anchored at the origin of coordinates to which the earlier determined forces P and moments M_0 (Fig. 4.6) are applied. Resilient vertical displacements are calculated from the formula:

$$\begin{aligned}\Delta_{Cy}EI\cdot 10^{-6} = {} & (J_x + J_z - S_x x_C - S_z z_C)\,P_y - (J_{xy} - S_y x_C)\,P_x - \\ & - (J_{yz} - S_y z_C)\,P_z + (S_z - z_C L)\,M_{ox} - (S_x - x_C L)\,M_{oz}\ \text{cm}\end{aligned} \qquad (4.18)$$

The reactions are taken with signs for the end B, assumed free, and the moments S and J of the axial line and the length L of the axial line are calculated from the fixed end A up to the point C with respect to the reference system of coordinates.

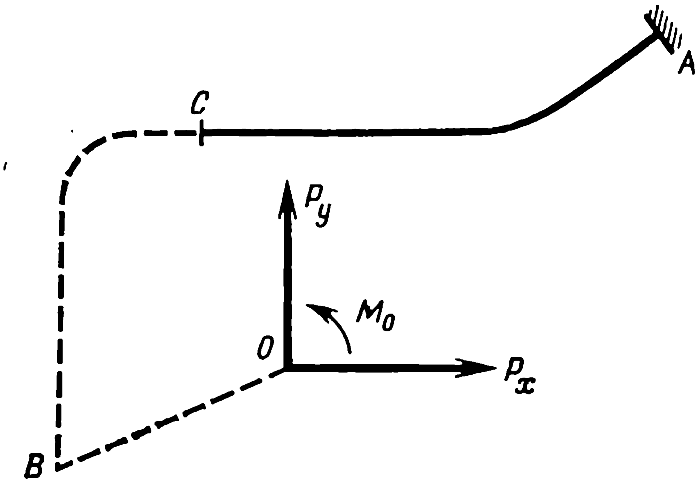

Fig. 4.6. Moments and forces acting on the intermediate cross section C of pipeline

Total vertical displacement is calculated from formula:

$$h_y = \Delta_{Cy} + \delta(y_C - y_A) + \Delta_y^A - \sum_A^C (z_k - z_C)(\alpha\theta \cos\beta_x) \cdot 10^2 + \\ + \sum_A^C (x_k - x_C)(\alpha\theta \cos\beta_z) \cdot 10^2 \text{ cm} \quad (4.19)$$

The notations used in this formula have the same meaning as those in formulas (4.3) and (4.4).

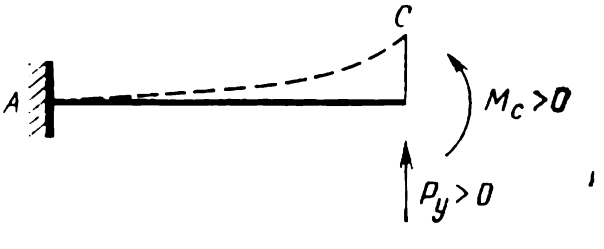

Fig. 4.7. Determination of deflections of straight section with one end fixed

For a horizontal straight section (Fig. 4.7), one end of which is anchored at A, the vertical displacements at point C can easily be calculated by the formula

$$h_y = \Delta_y^A + \left(\frac{l^3}{3} P_y + \frac{l^2}{2} M_C\right) \frac{10^6}{EI} \quad (4.20)$$

where l—distance between anchor A and the cross section C, m; M_C—bending moment in cross section C acting in the vertical plane which passes through points A and C. This moment is taken positive only when it bends the cantilever AC upwards and negative—when it bends AC downwards.

The obtained formulas are also suitable for calculating plane (two-dimensional) sections. If a two-dimensional section is considered in plane z in which all the coordinates $z = 0$, then the system of equations (4.8) takes the form:

$$\left.\begin{aligned} EI\cdot 10^{-6}\Delta_{sx} &= I_{sy}P_x - J_{sxy}P_y \\ EI\cdot 10^{-6}\Delta_{sy} &= -J_{sxy}P_x + J_{sy}P_y \end{aligned}\right\} \qquad (4.21)$$

where the subscript x does not denote a plane, but it denotes a line $x = 0$, and the subscript y, a line $y = 0$.

From Table 4.1 it follows that for plane z, in which the pipeline is located, the flexibility coefficient $k_1 = jK_p$. Equation (4.21) gives exact solution of a two-dimensional pipeline. Formulas (4.6) are used to determine design displacements. Formulas (4.18) and (4.19) are employed to calculate displacements at the intermediate point C. In these formulas S_z, J_z and all z coordinates should be taken equal to zero and $\cos \beta_z = 1$.

In the section symmetrical with respect to y axis $J_{sxy} = 0$ and $\Delta_{sy} = 0$, therefore,

$$P_x = \frac{EI\cdot 10^{-6}\Delta_{sx}}{J_{sy}}\ \text{kg};\quad P_y = 0 \qquad (4.22)$$

4.5. Determination of Bending Moments Due to Weight Load

At thermal power stations it is possible to locate fastenings at relatively small distances from each other, and therefore, the stresses due to weight are comparatively small. For this reason, it is not necessary to perform complicated and time-consuming calculations for the correct determination of moments due to evenly distributed and concentrated loads. If necessary, for example, when calculating austenitic steel pipelines, such calculations should be made with the use of computers employing one of the developed methods [4-1 and 4-5].

The equal span diagrams were considered earlier, but it is not possible always to obtain equal distances between the fastenings, and for this reason, it is necessary to investigate the effect of distance ratio between the considered and adjoining spans.

Fig. 4.8 presents a schematic diagram of a beam with anchored ends. Here, the distance between the supports, i.e. span length is equal to l, except for the middle span where it equals xl. Maximum bending moment due to evenly distributed weight can be calculated from formula:

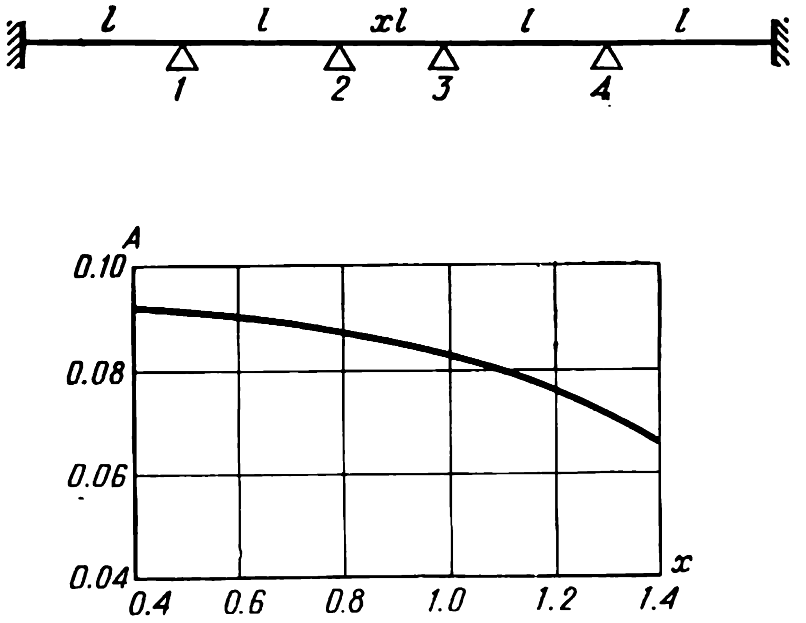

Fig. 4.8. Variation in coefficient *A* *versus* *x*

$$M = Aql_{\max}^2 \text{ kg}\cdot\text{m}$$

where $l_{\max}$—maximum span length, m; q—load intensity, kg/m; A—a coefficient, which depends upon the span ratio. The graph between A and x is presented in Fig. 4.8. For $x < 1$, the maximum distance between two supports is equal to l. Bending moments, in this case, are maximum at supports *1* and *4*, here $A = 0.092$ (when $x = 0.4$).

For $x > 1$, the maximum distance between the supports is equal to xl and the bending moments, in this case, are maximum at supports *2* and *3*. Here $A \leqslant 0.0833$.

The value of the coefficient A can safely be taken equal to 0.1, the same value can be taken for the span before a bend when the straight length of the cantilever $\approx {}^1/_3 l$. Therefore, when determining total equivalent stresses due to additional loads and self compensation, the bending moments due to weight appearing in the initial period of operation must be determined as per the flexure bending formula:

$$M_b^{ext} = 0.1 q l_{\max}^2 \text{ kg}\cdot\text{m} \tag{4.23}$$

where q—weight of pipeline in the operating condition, kg/m; $l_{\max}$—maximum distance between the supports close to the fixed end, the cross section of which is checked for self compensation stresses.

When checking total equivalent stresses in a cold pipeline, i.e. when it is subjected to hydraulic testing, the fact that moments due to weight at supports decrease by 25% as a result of relaxation may be taken into account, and, accordingly, these moments should be calculated by the formula:

$$M_b^{ext} = 0.1\,(q_x - 0.25q)\,l_{\max}^2 \text{ kg}\cdot\text{m} \tag{4.24}$$

where q_x—weight of pipeline when subjected to hydraulic testing, kg/m. The remaining notations have the same meaning as those in formula (4.23).

When spring hangers are correctly adjusted the weight of pipe length between two supports in its operating condition is taken by the supports; the fixed supports take 50% weight of extreme spans. In case common spring hangers are used, the pipeline on cooling displaces vertically, thereby, the spring compression and loads acting on fastenings vary. As a result of these displacements, in every spring hanger in its cold condition a force appears which is not balanced by pipeline's weight. All these unbalanced forces acting on the length between the anchors result in the appearance of not only reactions but also of significant bending moments which load the anchors in the installed condition of pipeline. To solve such a problem it is necessary to find a general equation for determining reactions due to concentrated forces.

For determining reactions, which result from the concentrated force P_{Cy} applied at point C with coordinates x_C, y_C, z_C, the system of equations (4.8) may be used. The free terms ($\Delta_{sx}EI \cdot 10^{-6}$, etc.) appearing in the system should, in this case, be replaced by the following:

$$\begin{aligned} D_{xy} &= (J^C_{xy} - x_C S^C_y - y_s S^C_x + x_C y_s L^C)\, P_{Cy} \\ D_{yy} &= [(-J^C_x - J^C_z + (x_C + x_s)\, S^C_x + (z_C + z_s)\, S^C_z - \\ &\qquad - (x_C x_s + z_C z_s)\, L^C)]\, P_{Cy} \\ D_{zy} &= (J^C_{yz} - z_C S^C_y - y_s S^C_z + z_C y_s L^C)\, P_{Cy} \qquad (4.25) \end{aligned}$$

in these formulas J^C, S^C, L^C—moments of inertia, static moments and equivalent length of section AC—from the support A up to the point of application of force P_{Cy}. All these values are calculated with respect to the reference coordinate axes. The coordinates x_s, y_s, z_s are the coordinates of the centre of elasticity of the whole system AB.

After determining the reactions P_x, P_y, P_z from the system of equations, the moments at the origin of coordinates can be calculated:

$$\begin{aligned} M_{ox} &= \frac{-S^C_z + z_C L^C}{L} P_{Cy} + y_s P_z - z_s P_y \\ M_{oz} &= \frac{S^C_x - x_C L^C}{L} P_{Cy} + x_s P_y - y_s P_x \text{ kg}\cdot\text{m} \qquad (4.26) \end{aligned}$$

The bending moments diagram is drawn in the usual way by drawing lines of zero moments, but in the section CA the moments due to force P_{Cy} must be taken into account.

If we assume that on cooling, a pipeline in every spring support develops an unbalanced force equal to 30% of the pipeline weight in the operating condition due to the weight of the pipeline span, then large bending moments and bending stresses will appear at the anchor due to the combined action of all spring supports present in the section.

For correct determination of unbalanced forces due to weight, which appear in the installed condition of a pipeline, the pipeline sags should be accounted for, as these forces depend upon these deflections [4-7].

4.6. Methods of Calculating Pipelines for Self-Compensation

The approximate method of calculating pipelines for self compensation as described here was used for several years by a number of piping design organisations. The principal features of this method are:

1. The first (S) and the second (J) orders axial-line moments of the considered section are determined as a sum of moments of different straight and arc sections forming the pipeline's configuration.

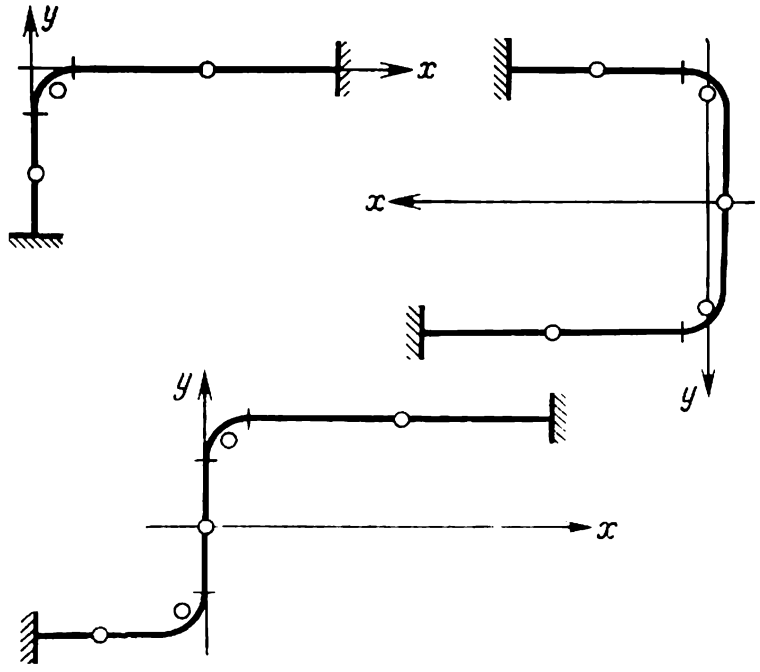

Fig. 4.9. Selection of coordinate system for typical configurations of pipelines

2. If the determination of displacements of some points forms a part of the problem, then these points are considered as ends of straight runs of pipeline.

3. The whole calculation is performed with respect to one reference system of coordinates which is so selected that minimum calculations will be required to determine the first and the second order moments. To achieve this the coordinate axis must be parallel to straight runs of pipeline and possibly pass through a greater number of centers of gravity of different elements (Figs. 4.9, 4.12 and 4.21).

4. The static moment for each element is calculated as the product of the reduced length of the elements and the coordinates of its center of gravity.

5. The second order moments for each element are calculated as the sum of two values: (a) product of the static moment and corresponding coordinate of the center of gravity of the element; (b) intrinsic moment of inertia of the section, i.e. intrinsic moment with respect to the coordinate axes parallel to the reference axis, but with the origin of coordinates lying at element's natural center of gravity.

6. To calculate inherent moments of inertia of elements the projection lengths of sections on the coordinate axis are used; this is convenient, as only the projections (not the angles of inclination) are given on the drawings.

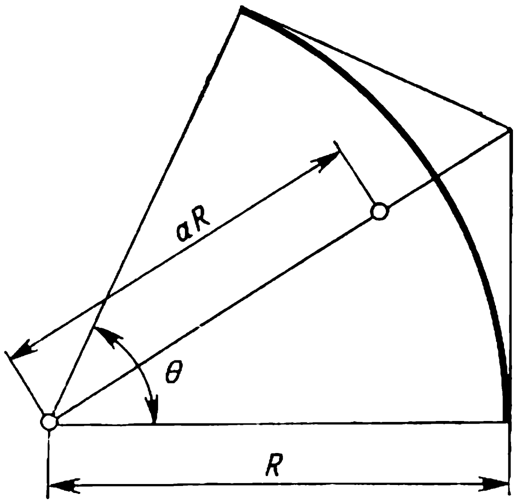

Fig. 4.10. Location of arc center of gravity

The center of gravity of arc element depends upon the radius R and the arc angle θ. The center of gravity (Fig. 4.10) lies on the bisector of the angle at a distance aR from the center of arc, where

$$a=\frac{\sin(0.5\theta)}{0.5\theta} \tag{4.27}$$

The values of the coefficient a are listed in Table 4.2.

Table 4.2

Arc angle	0°	30°	45°	60°	75°	90°
a	—	0.99	0.98	0.96	0.93	0.90
m	1	1	0.98	0.96	0.93	0.88
n	1	1	0.99	0.98	0.97	0.96

If the bisector of the 90° arc is inclined at 45° to the coordinate axes, then the coordinates v_i of arc's center of gravity are determined from the expression

$$v_i = v_C \pm 0.637R \tag{4.28}$$

where v_C —coordinate of the center of arc.

The intrinsic moments of inertia of both straight and curved sections are calculated from the following formulae:

with respect to planes (or axes for a plane section) $x = x_i$, $y = y_i$, $z = z_i$, where x_i, y_i, z_i —coordinates of the element's center of gravity

$$J'_x = \frac{l' l_x^2}{12m}; \quad J'_y = \frac{l' l_y^2}{12m}; \quad J'_z = \frac{l' l_z^2}{12m} \tag{4.29}$$

centrifugal moments with respect to two planes

$$J'_{xy} = \frac{l' l_x l_y}{12n}; \quad J'_{yz} = \frac{l' l_z l_y}{12n}; \quad J'_{zx} = \frac{l' l_z l_x}{12n} \tag{4.30}$$

where l'—reduced length of the element, m; l_x, l_y, l_z—element's length projections on X, Y, Z axes, m.

The values of coefficients m and n for different arc angles θ are taken from Table 4.2.

From the above given formulas and the data listed in the Table it follows that the intrinsic moments of inertia of arc section, arc angle less than 90°, are very close to the intrinsic moments of inertia of chords. The sign of intrinsic centrifugal moment of inertia is determined as follows: if both the coordinates of one end of an element are greater than both the coordinates of the other end of the same element, then the intrinsic centrifugal moment of inertia is positive, and negative otherwise. This rule can be formulated in the following manner: if a straight line drawn from the origin of coordinates is parallel to the considered straight section or chord or arc (Fig. 4.11) and passes through quadrants I and III (both the coordinates have the same sign in these quadrants), then $J'_{12} > 0$; if such a line passes through quadrants II and IV (both the coordinates have different signs in these quadrants), then $J'_{12} < 0$.

In the majority of cases, the intrinsic moments of inertia of arc sections, as well as of short straight sections can be neglected.

The moments of inertia are calculated with respect to the selected axes or planes of coordinates. Formulas (4.9) are used to determine centrifugal moments of inertia.

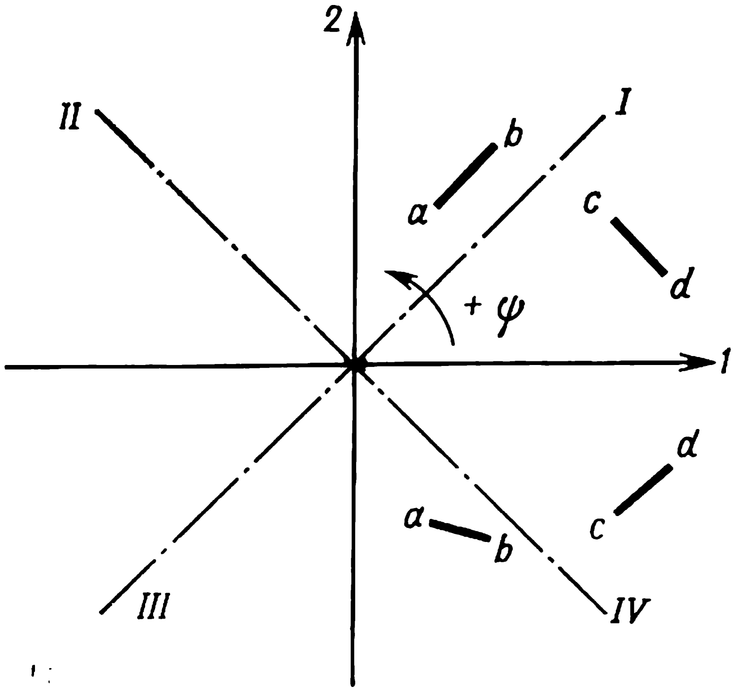

Fig. 4.11. Determination of the sign of intrinsic centrifugal moment of sections: for $abJ'_{12} > 0$, for $caJ'_{12} < 0$

Some necessary characteristics of pipes and elbows of conventional assortment in use at electrical generating stations are given in Appendix 16 for self compensation calculation.

If non-standard pipes are used, then the moment of inertia should be calculated by the formula

$$I = 0.3925s\,(D_0 - s)\,[(D_0 - s)^2 + s^2]\cdot 10^{-4}\ \text{cm}^4 \qquad (4.31)$$

which is a same degree equation.

To determine the coefficients K_p, K_δ, β, γ from the graphs of Appendixes 17, 18, 19 and 20, the dimensionless coefficient $\omega = \frac{p}{E}A$ and the geometrical characteristic λ of elbow (see Appendix 16) are predetermined.

If the rigidity EI' of an element differs from the accepted value of rigidity EI, then the reduced length of the element

$$l' = jl = \frac{EI}{EI'}\,l \qquad (4.32)$$

In the general case the flexibility coefficient of elbows for a two-dimensional section $k = jK_p$, and for a three-dimensional section when it is calculated in accordance with the approximate method, is determined from formula (4.7). The flexibility coefficient K_p of elbows, depending upon the ratio p/E, under hydraulic test conditions may differ slightly from the value of this coefficient at operating parameters. Since the difference between the values of K_p in the considered cases is insignificant, the minimum value of K_p (out of the two values) should be taken. In doing so we restrict ourself only to performing calculation of central moments of inertia and the coordinates of the section's center of elasticity. An example of the calculation of a two-dimensional section with hinged bellows-type expansion joints is presented in Sec. 4.8. This calculation is based on the principles of pipeline calculation for self compensation.

An example of the calculation of a three-dimensional section of a steam pipeline in the cold condition serving the intermediate superheat of a 200 MW unit (Fig. 4.12) is given below. First of all the axial line of steam pipeline in all three projections is drawn to scale, boundaries of different elements are marked and denoted by the points of the center of gravity of these elements. The same origin of coordinates and similar directions of axes should be used for all projections. The position of axes is so selected that the seven coordinates of the center of gravity of elements will equal to zero (see Table 4.4). This simplifies the calculations. The direction of the coordinate axes is so selected that all the coordinates of end A will be greater than the corresponding coordinates of end B. The rigid end of the collector of superheater (shown by dashed lines) is located along the boiler axis; at the end of the collector is provided a sliding guide A which for calculation purposes is taken as the fixed point with displacement $\Delta_x^A = 1.8$ cm; vertical displacement of point A is taken equal to zero (an increase in the safety factor).

Formulae (4.1), (3.21), (3.8) and (3.11) were used to complete the columns 14, 19, 21 and 23 of the initial data taken for the calculation of three-dimensional pipeline. Calculated in this example are the reaction forces along

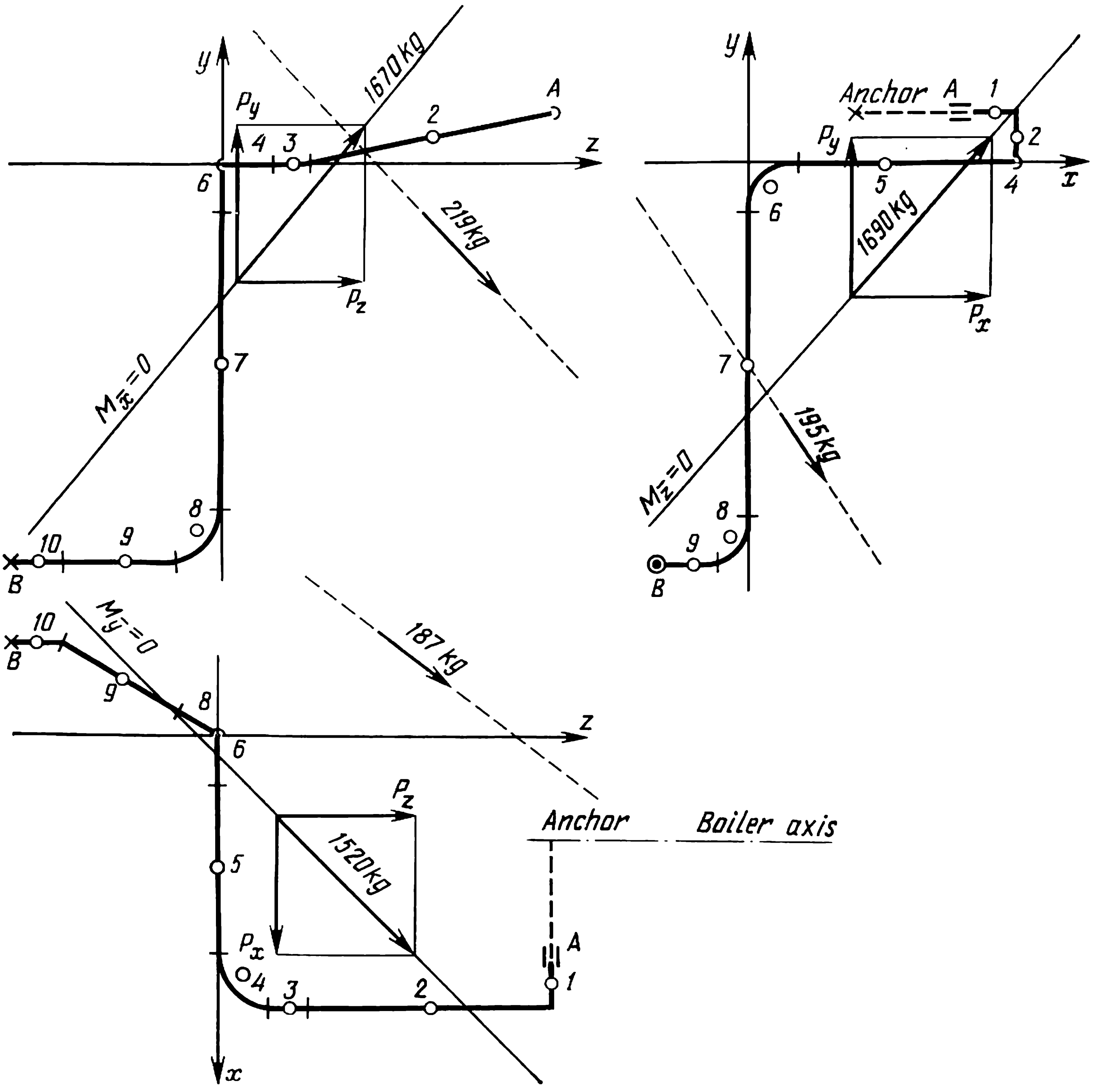

Fig. 4.12. Configuration of intermediate superheat steam pipeline for self-compensation calculation

with the vertical displacements at the end of element 6. For this reason, in the columns for moments *S* and *J* provision is made for subtotals.

The calculation of intrinsic moments of inertia is presented in Table 4.3; the value of intrinsic moments of inertia is calculated as the sum of a respective column of elements divided by 12. All intrinsic centrifugal moments, in accordance with the sign rule presented in Fig. 4.11, are taken positive. The indexes of intrinsic moments of inertia

Table 4.3

Serial number of elements	Reduced length l', m	Projections, m			Coefficients		$\frac{l'l_x^2}{m}$	$\frac{l'l_y^2}{m}$	$\frac{l'l_z^2}{m}$	$\frac{l'l_x l_y}{n}$	$\frac{l'l_y l_z}{n}$	$\frac{l'l_z l_x}{n}$
		l_x	l_y	l_z	m	n						
1	2	3	4	5	6	7	8	9	10	11	12	13
1	1.5	1.5	0	0	1	1	3	0	0	0	0	0
2	7.94	0	1.58	7.84	1	1	0	20	488	0	99	0
3	1.43	0	0	1.43	1	1	0	0	3	0	0	0
4	7.05	1.7	0	1.7	0.88	0.96	23	0	23	0	0	21
5	5.4	5.4	0	0	1	1	158	0	0	0	0	0
6	7.05	1.7	1.7	0	0.88	0.96	23	23	0	21	0	0
Σ_1^6	30.37	—	—	—	—	—	207	43	514	21	99	21
7	9.7	0	9.7	0	1	1	0	913	0	0	0	0
8	7.05	0.85	1.7	1.47	0.88	0.96	6	23	17	11	18	9
9	4.3	2.15	0	3.72	1	1	20	0	60	0	0	34
10	1.6	0	0	1.6	1	1	0	0	4	0	0	0
Σ_1^{10}	53.02	—	—	—	—	—	233	979	595	32	117	64
$\frac{1}{12}\Sigma_1^6$	—	—	—	—	—	—	17	4	43	2	8	2
$\frac{1}{12}\Sigma_1^{10}$	—	—	—	—	—	—	19	81	49	3	10	5

are determined by the indexes of projections appearing in the formula used for completing the appropriate column of the Table. Thus, the number in the lower line of column 9 (representing projection l_y) is the sum of moments of inertia J'_y, and the number in the lower line of column 13 (representing projections l_z, l_x) is the sum of moments J'_{zx}.

Table 4.4 is used to calculate central moments of inertia. The order of completing the columns is quite clear from the headlines of different columns. Here, it may be mentioned that the centrifugal moments of inertia can be calculated in two ways: (1) in the manner shown in the Table, and (2) as the product of static moments and the center of gravity coordinates, i.e. $J_{xy} = y_i S_x$, $J_{yz} = z_i S_y$; $J_{zx} = x_i S_z$, where x_i, y_i, z_i—coordinates of element's center of gravity. In the Table, the sums of the intrinsic inertia moments of the section elements, which were calculated in Table 4.3, are presented in a separate line. Shown under columns 3, 4 and 5 in the 10th line are the coordinates x_s, y_s, z_s of the center of elasticity of the whole section. These coordinates are calculated by dividing the appropriate static moment by the reduced length of the whole section. The corrections in the moments of inertia for the shift of axes to the center of elasticity are calculated from formulas (4.9). These corrections are listed in the last but one line, and the last line represents the central moments of inertia as the algebraic sum of the last but two lines.

Table 4.5 presents the calculation of free end displacements under the action of elbow deformations caused by pressure. As per the requirements of formula (4.2), the projections of angles $\alpha\theta \cos \beta$ are measured in the direction from end A, which is taken as fixed, towards the end B; these signs are listed in the Table as signs of $\cos \beta$ in 4, 5 and 6. Thus, elbow No. 8 in plane x turns in the clockwise direction, i.e. in the positive direction for this plane (from Y axis to Z axis); in z plane this elbow turns also in the clockwise direction, but the positive direction for this plane corresponds to anti-clockwise motion (from X axis to Y axis) and, therefore, $\cos \beta$ has a negative sign. The data for the cold condition are determined by multiplying the sum column for the hot condition with the ratio α_c/α_h.

Table 4.4

Serial No. of elements	Reduced length l', m	Coordinates of C. G., m			Static moments, m²			Moments of inertia, m³					
		x_i	y_i	z_i	$S_x = l' x_i$	$S_y = l' y_i$	$S_z = l' z_i$	$J_x = x_i S_x$	$J_y = y_i S_y$	$J_z = z_i S_z$	$J_{xy} = x_i S_y$	$J_{yz} = y_i S_z$	$J_{zx} = z_i S_x$
1	2	3	4	5	6	7	8	9	10	11	12	13	14
1	1.5	8.05	1.58	10.9	12.1	2.4	16.3	97	4	178	19	26	132
2	7.94	8.8	0.79	7.05	69.8	6.3	56.0	614	5	395	55	44	492
3	1.48	8.8	0	2.42	12.6	0	3.5	111	0	8	0	0	30
4	7.05	8.18	0	0.62	57.7	0	4.4	472	0	3	0	0	36
5	5.4	4.4	0	0	23.8	0	0	104	0	0	0	0	0
6	7.05	0.62	—0.62	0	4.4	—4.4	0	3	3	0	—3	0	0
Σ_1^6	30.37	—	—	—	180.4	+4.3	80.2	1401	12	584	71	70	690
7	9.7	0	—6.55	0	0	—63.5	0	0	416	0	0	0	0
8	7.05	—0.31	—12.48	—0.54	—2.2	—88.0	—3.8	1	1098	2	27	47	1
9	4.3	—1.93	—13.1	—3.33	—8.3	—56.3	—14.3	16	738	48	109	188	28
10	1.6	—3.0	—13.1	—6.0	—4.8	—21.0	—9.6	14	275	58	63	126	29
J'								19	81	49	3	10	5
Σ^{10}	53.02	3.11	—4.23	0.99	165.1	—224.5	52.5	1451	2620	741	273	441	753
ΔJ								—513	—950	—52	+698	+222	—163
J_s								938	1670	689	971	663	590

Table 4.5

Indexes and formulas	Calculation of displacements of the origin of coordinates for the				
	hot condition				cold condition
1. Serial number of elbow	4	6	8	Σ	Σ
2. Angle of elbow θ, radians	1.57	1.57	1.57	—	—
3. $\alpha_h\theta \cdot 10^2$	1.12	1.12	1.12	—	—
4. $\cos\beta_x$	0	0	0.87	—	—
5. $\cos\beta_y$	1	0	0	—	—
6. $\cos\beta_z$	0	1	—0.5	—	—
7. $\psi_x \cdot 10^2 = \alpha\theta\cos\beta_x\, 10^2$	0	0	0.97	0.97	1.04
8. $\psi_y \cdot 10^2 = \alpha\theta\cos\beta_y\, 10^2$	1.12	0	0	1.12	1.19
9. $\psi_z\, 10^2 = \alpha\theta\cos\beta_z\, 10^2$	0	1.12	—0.56	0.56	0.60
10. x_k	8.18	0.62	—0.31	—	—
11. $\Delta_y^{\alpha z} = x_k\psi_z\, 10^2$	0	0.69	0.18	0.87	0.92
12. $\Delta_z^{\alpha y} = x_k\psi_y\, 10^2$	9.15	0	0	9.15	9.72
13. y_k	0	—0.62	—12.48	—	—
14. $\Delta_z^{\alpha x} = y_k\psi_x 10^2$	0	0	—12.16	—12.16	—12.90
15. $\Delta_x^{\alpha z} = y_k\psi_z 10^2$	0	—0.69	6.99	6.30	6.68
16. z_k	0.62	0	—0.54	—	—
17. $\Delta_x^{\alpha y} = z_k\psi_y 10^2$	0.69	0	0	0.69	0.72
18. $\Delta_y^{\alpha x} = z_k\psi_k\, 10^2$	0	0	—0.53	—0.53	—0.56

Note. $\alpha_c/\alpha_h = 1.062$.

Thereafter, the elastic displacements taken by end *B* relative to the center of elasticity of the section are calculated from formula (4.5). These displacements are calculated (a) for the hot condition, and (b) for the cold condition after total relaxation of temperature stresses during hydrostatic tests. Then the system of strain equations (4.8) is formed for the hot and cold conditions. The solution of these equations gives reactions P at the support B. The lines of zero moments are drawn for each plane to form an opinion about the bending moments diagram (Fig. 4.12).

An example of the calculation of a three-dimensional pipeline.

I. Initial data

1. Medium and pressure—steam at 25 atm.
2. Design temperature 340°C.
3. Nominal pipe size 426 × 11 mm.
4. Negative tolerance for wall thickness 15%.
5. Design wall thickness $s\text{-}c_1 = 9.3$ mm.
6. Moment of inertia of pipe's cross section $I = 30{,}900$ cm^4.
7. Moment of resistance to bending $W = 1451$ cm^3.
8. Metal's cross sectional area $F = 14{,}300$ mm^2.
9. Characteristic of elbows:
   curved elbows with $R = 1700$ mm and ovality tolerance of 10%;
   geometric characteristic $\lambda = 0.43$;
   dimensionless coefficient $A = 2310$.
10. Pipe material and its properties.
    Steel Grade 20.
    Young's modulus at $t = 340°$C; $E = 1.87 \cdot 10^6$ kg/cm^2
    Young's modulus at $t = 20°$C, $E = 2.01 \cdot 10^6$ kg/cm^2.
    Thermal expansion from 0 to 340°C $\delta_t = 0.452$ cm/m.
11. Inherent displacements:
    of fixed point A $\Delta_x^A = +1.8$ cm; $\Delta_y^A = \Delta_z^A = 0$;
    of anchor B — nil.
12. Design number of start-up and shut-down cycles 6000.

II. Additional data

h—at the operating parameters;
c—during hydrostatic testing in the cold condition.

	hot	cold
13. Design rigidity EI, kg·cm^2....	$57{,}800 \cdot 10^6$	$65{,}000 \cdot 10^6$
14. Elastic elongation δ_p, cm/m...	0.005	0.006
15. Rated elongation $\delta = (\delta_t + \delta_p)$ cm/m . .	0.457	—0.446
16. Dimensionless parameter $\omega = \frac{p}{E} A$	0.0296	0.038
17. Flexibility coefficient of elbows K_p	3.32	3.3

18. Coefficient K_δ	0.139	0.148
19. Relative variation in elbow angle α due to pressure	—0.00712	—0.00757
20. Intensification coefficients for bending stresses:		
γ	2.5	2.5
β	1.9	1.9
21. Reduced stresses due to internal pressure, kg/mm²	5.38	6.72
22. Nominal allowable stresses, kg/mm²	10.9	14.7
23. Total allowable stresses due to self compensation and additional loads, kg/mm²	12.6	17.2
24. Allowable stress range, kg/mm²	62.0	62.0
25. Strength coefficient of butt welded joints . . .	0.8	0.8

The pipeline is made of similar size pipes, therefore, $j = 1$ and the reduced length of all straight elements is taken equal to their actual length. The mean flexibility coefficient of elbow $k_c = 0.43 + 0.67 \cdot 3.3 = 2.64$, and, hence, for an elbow of 90° the reduced length is taken equal to $l' = 2.64 \cdot 1.57 \cdot 1.7 = 7.05$ m. The reduced lengths of all elements are given in column 2 of Tables 4.3 and 4.4.

After the calculation of central moments of inertia (with respect to the planes $x = 3.11$ m, $y = -4.23$ m, $z = 0.99$ m) the moments of inertia with respect to the axes are calculated:

$$P_X = 1670 + 689 = 2359 \text{ m}^3$$

$$P_Y = 938 + 689 = 1627 \text{ m}^3$$

$$P_Z = 938 + 1670 = 2608 \text{ m}^3$$

The coordinates of ends A and B are: (7.3, 1.58, 10.9 m) and (—3.0, —13.1, —6.8 m), respectively. The displacements taken by end B relative to the center of elasticity s (3.11, —4.23, 0.99 m) are calculated from the formulas (4.5):

(a) displacements in the operating condition of the pipeline

$$\Delta_{sx} = \delta(x_A - x_B) + (\Delta_x^B - \Delta_x^A) + \Delta_x^{\alpha z} - \Delta_x^{\alpha y} - \\ - \psi_z y_s \cdot 10^2 + \psi_y z_s \cdot 10^2 = 0.457(7.3+3) - 1.8 + 6.30 - \\ - 0.69 - 0.56(-4.23) + 1.12 \cdot 0.99 = 11.97 \text{ cm}$$

in the same manner we get $\Delta_{sy} = 6.08$ cm, $\Delta_{sz} = 21.86$ cm;

(b) displacements in the cold condition of the pipeline at hydrostatic test pressure

$$\Delta_{sx} = -0.446(7.3+3) + 6.68 - 0.73 - 0.60(-4.23) = \\ = 1.19 \cdot 0.99 = 5.08 \text{ cm}$$

in the same manner we get $\Delta_{sy} = -7.18$ cm, $\Delta_{sz} = 6.63$ cm.

The reactions at the rigid support B are determined by solving the system of equations (4.8); the free terms appearing in these equations, for the operating condition of pipeline, are equal to the displacements multiplied by $E \cdot 10^{-6} = 57{,}800$ kg·cm².

$$6.93 \cdot 10^5 = 2359 P_x - 971 P_y - 590 P_z$$
$$3.52 \cdot 10^5 = -971 P_x + 1627 P_y - 663 P_z$$
$$12.65 \cdot 10^5 = -590 P_x - 663 P_y + 2608 P_z$$

By solving this system of equations, we get the reaction forces:

$$P_x = 1087 \text{ kg}; \quad P_y = 1294 \text{ kg}; \quad P_z = 1057 \text{ kg}$$

The equations for the cold condition are characterized by free terms which are determined from the displacements in the cold condition and the rigidity equalling $65{,}000 \times 10^6$ kg/cm². The solution of this system of equations gives the following forces:

$$P_x = 112 \text{ kg}; \quad P_y = -159 \text{ kg}; \quad P_z = 150 \text{ kg}$$

The comparison of obtained results for the hot and cold conditions shows that reactions in the latter case are many times less than in the former case. This is the cause of less design displacements Δ_s, in particular, of negative displacement Δ_{sy} in the cold condition. The reason for the decrease in design displacements is that the displacements caused by internal pressure and temperature to decrease have opposite directions in the second case, i.e. in the cold condition. First we determine moments and stresses in the operating condition.

The moments at the origin of coordinates

$$M_{ox} = y_s P_z - z_s P_y + \frac{EI \cdot 10^{-4}}{L} \psi_x = -4.23 \cdot 1057 -$$

$$-0.99 \cdot 1294 + \frac{57{,}800 \times 10^6 \times 10^{-4}}{53.02} 0.975 \times 10^{-2} = -4670 \text{ kg}\cdot\text{m}$$

Similarly, according to formula (4.13), we get

$$M_{oy} = -990 \text{ kg}\cdot\text{m}; \quad M_{oz} = +9235 \text{ kg}\cdot\text{m}$$

To draw the lines of zero moments we calculate from formula (4.15) the coordinates of the points of intersection of these lines with the coordinate axes:

in the plane x

$$y_1 = \frac{-4670}{1057} = -4.42 \text{ m} \quad \text{and} \quad z_1 = 0$$

$$y_2 = 0; \quad z_2 = -\frac{-4670}{1294} = +3.61 \text{ m}$$

In the same fashion we find for the plane y the coordinates (z; x) of the points of intersection (—0.91; 0) and (0; 0.94); for the plane z the coordinates (x; y) of the points (7.13; 0) and (0; 8.49).

In Fig. 4.12 the lines of zero moments are shown by thick lines, the direction of the resultant force of reaction in the given plane is shown by an arrow. The moment in any cross section is proportional to the distance from the considered cross section to the line of zero moments. It is seen from Fig. 4.12 that in section A for all projections the moments are greater than in section B, and it is necessary to perform check calculation for section A.

The moments in section A

$$M_{Ax} = z_A P_y - y_A P_z + M_{ox} =$$

$$= 10.9 \times 1294 - 1.58 \times 1057 - 4670 = 7790 \text{ kg}\cdot\text{m}$$

Similarly, we get

$$M_{Ay} = -5130 \text{ kg}\cdot\text{m} \quad \text{and} \quad M_{Az} = 1500 \text{ kg}\cdot\text{m}$$

In section A the pipeline's axis and the coordinate planes form the angles $\alpha_x = 90°$, $\alpha_y = \alpha_z = 0$, and hence, according to formula (4.17), the torsional moment is M_{Ax} and the bending moments are M_{Ay} and M_{Az}. Besides this, the negative moment due to weight acts in the plane z. This moment for the span of 4.0 m long and load intensity $q = 290$ kg·m is equal to $M_{zb}^{ext} = -0.1\ ql^2 = -0.1 \times 290 \times 4^2 = -464$ kg·m. Hence, in section A the total bending moment due to additional loads

$$M_b^{t\text{-}ad} = \sqrt{(-5130)^2 + (1500 - 464)^2} = 5225 \text{ kg}\cdot\text{m}$$

The torsional moment $M_t^{t\text{-}ad} = 7790$ kg·m.

The total equivalent stress is determined by the components:

$$\sigma_b^{t\text{-}ad} = \frac{M_b^{t\text{-}ad}}{\varphi W} = \frac{5225}{0.8 \cdot 1451} = 4.51 \text{ kg/mm}^2$$

$$\tau^{t\text{-}ad} = \frac{M_t^{t\text{-}ad}}{2W} = \frac{7790}{2 \cdot 1451} = 2.69 \text{ kg/mm}^2$$

$$\sigma_t^{t\text{-}ad} = \frac{P_x}{F} = \frac{1087}{14{,}300} = 0.08 \text{ kg/mm}^2$$

The equivalent stress

$$\sigma_e^{t\text{-}ad} = \sqrt{(0.08 + 0.8 \times 4.51)^2 + 3 \times 2.69^2} = 5.94 \text{ kg/mm}^2$$

this value is less than the allowable stress, i.e. $[\sigma_h^{t\text{-}ad}] = 12.6$ kg/mm². The lines of zero moments for the installed condition of pipelines are shown in Fig. 4.12 by dotted lines. The moment, in this case, is maximum at the fixed end B. The equivalent stress in this section amounts to 3.5 kg/mm², which is less than the allowable stress, i.e. 17.2 kg/mm².

In this case, it is not necessary to perform check calculation for the allowable stress range because: (1) the used elbows have normal radius of bend and (2) the self compensation bending moments in the plane of curvature tend to increase the angle in each elbow at the operating temperature of pipeline (see Sec 3.8).

Now we determine the vertical displacement of point C with coordinates (0; —1.7 m; 0) at the end of element 6 by using formulas (4.18) and (4.19).

From Tables 4.3 and 4.4, we take the following parameters of portion AC:

$$J_x^C = 1401 + 17 = 1418 \text{ m}^3; \quad J_z^C = 584 + 43 = 627 \text{ m}^3$$

$$J_{xy}^C = 71 + 2 = 73; \quad J_{yz}^C = 70 + 8 = 78 \text{ m}^3$$

$$S_x^C = 180.4 \text{ m}^2; \; S_y^C = 4.3 \text{ m}^2; \; S_z^C = 80.2 \text{ m}^2; \; L = 30.37 \text{ m}$$

Hence, the elastic displacement due to forces $P_x = 1087$ kg; $P_y = 1294$ kg, $P_z = 1057$ kg and moments $M_{ox} = -4670$ kg·m and $M_{oz} = +9235$ kg·m will amount to

$$\Delta_{Cy} = \frac{1}{57{,}800}[(1418 + 627 - 180.4 \times 0 - 80.2 \times 0)\,1294 - (73 - 4.3 \times 0)\,1087 - (78 - 4.3 \times 0)\,1057 + (80.2 - 0 \times 30.37)(-4670) - (180.4 - 0 \times 30.37)\,9235] = 7.6 \text{ cm}$$

In the portion AC, which includes elbows 4 and 6, the projections of the variations in angles are equal to $\alpha\theta \cos\beta = 0$ and $\alpha\theta \cos \beta z 10^2 = 1.12$. Taking this and $\Delta_y^A = 0$ into account, we get

$$h_y = 7.6 + 0.457(-1.7 - 1.58) + 0 + 0 + (0.62 - 0)\,1.12 = 6.8 \text{ cm}$$

4.7. Bellows-Type Expansion Joints and Their Use as Axial Expansion Joints

A corrugated or bellows-type expansion joint (Fig. 4.13) is a flexible element which accepts deformation along its axis. Welded in a pipeline it accepts the thermal expansion of the pipeline and ensures complete tightness. This makes bellows-type expansion joints better than slip joints. Corrugated expansion joints are fabricated from forged two piece corrugations and gas welded. The wall thickness of corrugations ranges between 2.5 and 4 mm depending upon pipeline pressure. The corrugated expansion joints fabricated as per the Standard MBH-195-63 with wall thickness 4 mm are used in stationary pipelines. To reduce hydraulic resistance the corrugated expansion joints used as axial expansion joints are manufactured with a special cylindrical inset known as a jacket.

The method suggested by Professor S. N. Sokolov [4-4] is used to calculate bellows-type expansion joints. The formulas with consideration for the latest corrections in the permissible sag value take the following form:

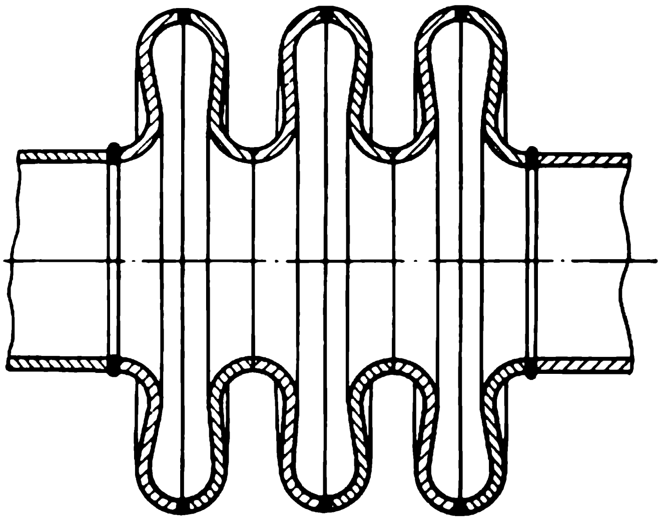

Fig. 4.13. Bellows-type compensator

Minimum wall thickness of the bellows

$$s=\frac{\lambda D_0}{100}\sqrt{\frac{K_h p_h}{\sigma_s}}\ \text{mm} \qquad (4.33)$$

Allowable axial deformation (sag) of one corrugation

$$\Delta_{al}=0.75\alpha\frac{\sigma_s D_0^2}{EsK}\ \text{mm} \qquad (4.34)$$

The force R_k corresponding to allowable sag

$$R_k=\frac{1.25\pi}{1-\beta}\cdot\frac{\sigma_s s^2}{K}\ \text{kg} \qquad (4.35)$$

The axial-pressure thrust

$$R_b=\varphi\frac{pD_0^2}{100K}\ \text{kg} \qquad (4.36)$$

In these formulas s is the corrugation wall thickness, mm; D_0—outside pipe diameter, mm; p—operating pressure, kg/cm^2; p_h—hydrostatic test pressure, kg/cm^2; σ_s—yield point of the metal used for the bellows, kg/mm^2; E—Young's modulus, kg/cm^2; K—safety factor at the operating temperature; K_h—safety factor for hydrostatic testing; Δ_{al}—allowable sag of corrugation, mm.

The dimensionless coefficients λ, α and φ depend upon the ratio $\beta = D_0/D_b$, where D_b—bellows diameter and is determined from the formulas:

$$\lambda = \frac{1}{2\beta} \sqrt{\frac{(1-\beta)(1-\beta^2)}{2(3+\beta)}} \qquad (4.37)$$

$$\alpha = \frac{6.9}{1-\beta} \left(\frac{1-\beta^2}{\beta^2} - \frac{4 \log^2 \beta}{1-\beta^2} \right) \qquad (4.38)$$

$$\varphi = \frac{\pi}{12} \frac{(1-\beta)(1+2\beta)}{\beta^2} \qquad (4.39)$$

For any pressure $K_h = 1.1$, for pressures less than $p < 6$ kg/cm^2, $K = 1.2$ and for $p = 6$ kg/cm^2, $K = 1.3$ are taken in the calculations.

The bellows-type expansion joints work in the elastoplastic range and their life is determined by their ability to stand a limited number of cycles. Under the normal operating conditions the pipelines (mostly low-pressure steamlines) fitted with corrugated expansion joints are called upon to act only quite infrequently (warming), and these expansion joints work satisfactorily. The use of prestressed bracing increases the compensating capacity of every corrugation approximately by two times, and correspondingly, the number of corrugations is reduced.

When compensating the thermal elongation of straight portions with the use of bellows-type expansion joints it is necessary to take into account large axial forces appearing in the considered pipeline configuration. The thrust of a bellows-type expansion joint

$$R = R_k + R_d \text{ kg} \qquad (4.40)$$

where R_k—force due to axial elastic deformation, kg; $R_d = R_b + 0.785 \left(\frac{D_0 - 2s}{10}\right)^2 p$—total force due to hydraulic pressure. This force is the sum of axial-pressure thrust acting on the bellows R_b and pressure forces acting on the blank flange, kg.

Given in the MBH Standards are force R_d^*—at a pressure equal to the nominal pressure P_n of the compensator, and force R_k^*=at an allowable sag of the compensator.

For pressure different from the nominal one pressure, R_d should be recalculated proportionally to the pressure

$$R_d = \frac{p}{P_n} R_d^* \tag{4.41}$$

where R_d is the thrust at an operating pressure p, kg. During the hydrostatic testing of a pipeline, the thrust

$$R_{d\text{-}h} = \frac{1.25p}{P_n} R_d^* \tag{4.42}$$

If the compensating capacity of an expansion joint is not utilized fully, then the elastic thrust force R_k^* is recalculated proportionally to axial deformation

$$R_k = \frac{\Delta p}{\Delta^*} R_k^* \tag{4.43}$$

where Δ_p—given axial deformation, mm; Δ^*—allowable axial deformation as per MBH, mm.

The axial-pressure thrust taken by a bellows joint in the operating conditions

$$R_t = R_d + R_k \text{ kg} \tag{4.44}$$

and during hydrostatic testing with allowance made for 50% cold spring

$$R_h = 1.25R_d - R_k \text{ kg} \tag{4.45}$$

In large diameter pipes the axial-pressure thrust can mount up to 10-20 tons and more. A maximum force appearing either under the operating or installed conditions, i.e. during the hydrostatic testing of a pipeline is taken as design force.

Tightening devices are provided to decrease forces acting on civil structures, platforms and equipment. In doing so, sometimes errors are made due to the assumption that such a tightening device completely relieves supports from transferring axial forces to the building, though for transferring a force the tightening device should have elastic deformation which in certain cases is commensurate to the thermal elongation of the pipeline.*

Besides this, the thermal elongation of tightening device which receives heat from the pipeline (through radiation and heat bridges of fastenings) should also be taken into account. Thus the use of tightening devices connecting the ends of the pipeline can not afford to keep the two ends in the same position. The variation of tightening device length, if we take its thermal elongation as 10% of the pipeline's elongation, can be determined from the formula

$$\Delta_{b\text{-}d} = \left(\frac{\sigma' - \sigma''}{E \cdot 10^{-5}} + \delta_t \right) L \text{ mm} \qquad (4.46)$$

where σ'—stress in the tightening device for the operating pipeline, kg/mm^2; σ''—stress in the tightening device for the cold pipeline, kg/mm^2; E—Young's modulus, kg/cm^2; δ_t—thermal elongation of the pipeline, mm/m; L—length of the tightening device, m.

When installing more than one bellows-type expansion joint on a pipeline, rigid supports for the tightening device are envisaged between every two expansion joints. These intermediate supports are designed to eliminate buckling in the compressed state and to ensure uniform deformation of all expansion joints (the actual rigidity of different expansion joints may vary). At the intermediate supports the hydraulic thrust on each side is mutually balanced.

Fixed supports mounted next to blank flanges, bends and stop valves serve as terminal supports and must be designed to take total thrust R_t or R_h.

Bracing is generally made as a combined support-tightening device designed to transmit tensile forces in the pipeline under the operating conditions, and compressive forces in the pipeline not under pressure, as well as to take the pipeline's weight. Due to the application of eccentric tensile and compressive forces the beams of the tightening device should be designed to take the bending moments caused by these forces.

---

* Thus, when a load of 16 kg/mm^2 acts on a tightening device, it elongates approximately 0.8 mm/m which is only half as much as thermal elongation of the pipeline at 2.5 atm.

The support-tightening device is fixed rigidly to the building at one point; if there are two or more rigid supports the support-tightening device is made of pieces which allow elongation of the tightening device beams. An example of calculating a pipeline with axial corrugated expansion joints is given below.

Example. Steam pipeline of size 630 × 9 mm operates at 2.5 atm, 160°C. Its thermal elongation is 0.197 cm/m. The pipeline is installed as per the diagram shown in Fig. 4.14.

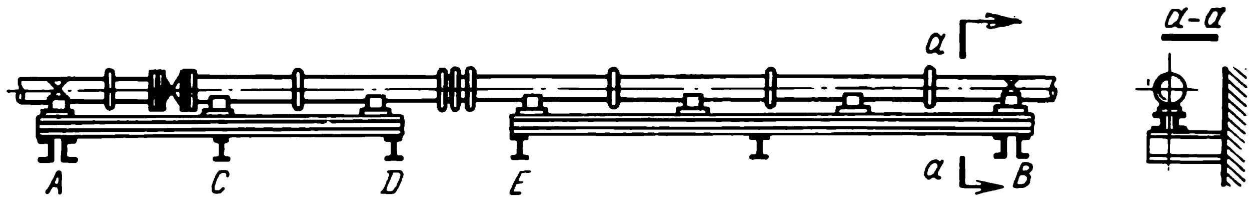

Fig. 4.14. Schematic diagram illustrating axial compensation of pipeline's thermal elongations by use of bellows-type expansion joints

The distance (total pipe length) between two end supports *A* and *B* is equal to 30 m. The distance between the intermediate supports equals 6 m. Steam is supplied through end *B*. Thermal elongation of the pipeline's section lying between the intermediate supports

$$\Delta_1 = 1.97 \times 6 = 11.8 \text{ mm}$$

The elongation of tie rods in this very section for a tensile stress of 3 kg/mm² and thermal elongation 0.2 mm/m

$$\Delta_c = \left(\frac{\sigma' - \sigma''}{E \cdot 10^{-5}} + 0.2\right) 6 = \left(\frac{3-0}{2 \times 10^6 \times 10^{-5}} + 0.2\right) 6 = 2.1 \text{ mm}$$

Here, we neglected the compressive stresses in the tie rods σ'' on the assumption that they are equal to zero. Each expansion joint (except the one installed between the supports *D* and *E*) must take axial deformation

$$\Delta = \Delta_1 - \Delta_c = 11.8 - 2.1 = 9.7 \text{ mm}$$

To accept this deformation it is sufficient to install one corrugation expansion joint of compensating capacity 10 mm. In this case, we take the negative tolerance as equal to 5 mm.

The expansion joint located between the supports D and E must take axial deformation 11.8 mm due to pipeline elongation, and, besides this, the elongation of the tie-rods in five spans, i.e.

$$\Delta = 11.8 + 5 \times 2.1 = 22.3 \text{ mm}$$

To accept this deformation the expansion joint must have three corrugations.

The expansion joints D_n600, as per the Standards, accept $R_k^* = 4600$ kg for sag of 5 mm; $R_d^* = 24{,}000$ kg at a 6 kg/cm^2 pressure.

Each straight portion of a pipeline at its end has either a bend or a blank flange. For this reason, hydraulic thrust forces will also act on supports A and B if the pipeline is under pressure 1.5 kg/cm^2:

$$R_d = \frac{1.5}{6.0} 24{,}000 = 6000 \text{ kg}$$

Furthemore, these supports will accept through tie rods a force R_k due to deformation of the expansion joint having three corrugations; taking the cold spring for this expansion joint equal to 12 mm, we find deformation in the hot condition, which equals 22.3—12 = 10.3 mm. The corresponding elastic force

$$R_k = \frac{10.3}{3 \times 5} 4600 = 3160 \text{ kg}$$

Total reaction of supports A and B in the operating condition of pipeline

$$R_p = R_d + R_k = 6000 + 3160 = 9160 \text{ kg}$$

Total reaction of supports A and B during hydrostatic testing of pipeline in the installed condition

$$R_h = 1.25 \times 6000 - \frac{12}{3 \times 5} 4600 = 3820 \text{ kg}$$

The forces acting on the remaining intermediate supports are absorbed by the tie rods and do not have any effect on the magnitude of forces at the supports A and B.

To determine the forces in the tightening device, it is necessary to draw a schematic diagram of all forces applied at the terminal and intermediate supports both for the open and closed valve positions.

4.8. Compensation of Pipelines Through the Use of Bellows-Type Expansion Joints as Elastic Hinges

In the sections of a low pressure pipeline, which are laid in a zig-zag manner, the corrugated expansion joints may be used as hinges. To transmit axial hydraulic thrust forces the pipe ends, between which a corrugated expansion joint is installed, are joined together with short tie rods permitting rotation in the plane perpendicular to the plane of tie rods (Fig. 4.15).

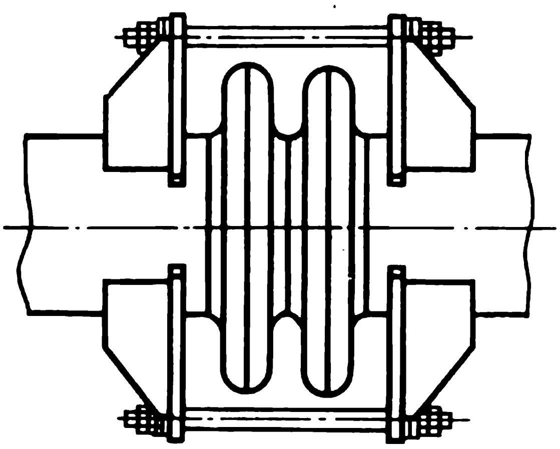

Fig. 4.15. Use of bellows-type expansion joint as a hinge

Compared with the schemes utilizing the axial deformation of corrugated expansion joints, the schemes in which bellows-type expansion joints work as hinges have significant advantages: (1) thrust forces are not transmitted to equipment and civil structures; (2) total compensation of thermal elongations is achieved; (3) less number of bellows are required to achieve compensation. The calculation of hinge schemes consists in determining the angles of rotation appearing in hinges, and the determination of required number of corrugations.

Maximum permissible angle of rotation in a corrugated expansion joint in the absence of axial deformation

$$\psi_{al} = \frac{2\Delta^*}{D_0 + D_c} \tag{4.47}$$

where Δ^*—allowable elongation (sag) as per the Standards, MBH, mm; D_0—outside pipe diameter, mm; D_c—diameter of corrugation, mm.

With axial deformation Δ_{ax} maximum permissible angle of rotation

$$\psi_{al} = 2\frac{\Delta^* - \Delta_{ax}}{D_0 + D_c} \qquad (4.48)$$

The moment, necessary to rotate the hinge by ψ_h, is

$$M_h = \frac{R_h^* (D_0 + D_c) D_0}{8\Delta^* \cdot 10^3} \psi_h \text{ kg} \cdot \text{m} \qquad (4.49)$$

where R_h^*—force, necessary to produce design sag Δ^*, kg.

The moment M_h is relatively small. Sometimes it is convenient to introduce a reduced length in the calculation, i.e. length of hinged expansion joint, whose flexibility is equivalent to the length of pipeline having moment of inertia of cross section I:

$$l_h' = \frac{EI \cdot 10^4 \psi_h}{M_h} = \frac{0.8\Delta^* EI}{R_h^* (D_0 + D_c) D_0} \text{ m} \qquad (4.50)$$

where E—Young's modulus for which determined is R_h^* ($E = 2.0 \times 10^6$ kg/cm^2).

The reduced lengths of hinged expansion joints are large. For example, the reduced length of an expansion joint diameter 1158 mm is equal to 183 m with respect to a pipe 920 × × 8 mm. So two-hinge and three-hinge compensation diagrams can be employed.

The two-hinge diagrams may have:

(a) short tie rods (Fig. 4.16) in which elongation in the direction x is compensated due to elastic deformation (bending) of arms, which do not have any expansion joints;

(b) long tie rods (Fig. 4.17) in which compensation in the direction x is achieved due to compression of corrugations, and in the direction y due to rotation in hinges; the expansion joints, in this case, take simultaneously the axial deformation and the bending moments. This diagram is applicable only for two-dimensional pipelines.

The three-hinge diagram (Fig. 4.18) is advantageous for short sections, when the use of a two-hinge diagram results in forces and moments the transmission of which to equipment can not be allowed.

The general method of calculation (Secs. 4.3, 4.4) may be used for calculating hinged schemes with short tie rods.

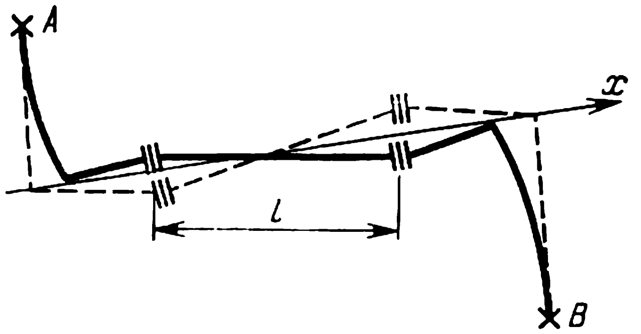

Fig. 4.16. Two-hinge compensating scheme with short tie rods

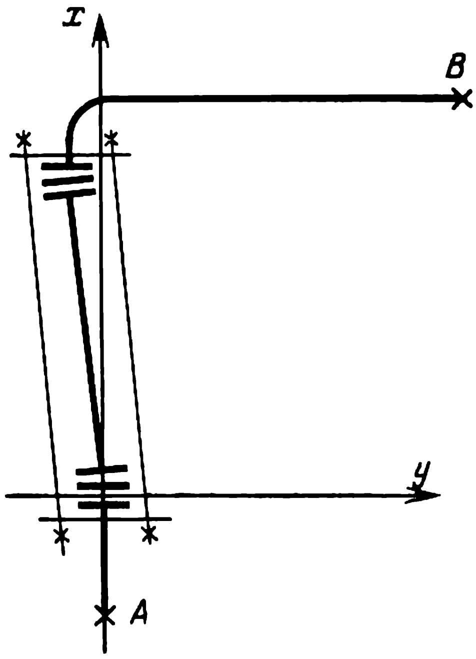

Fig. 4.17. Two-hinge compensating scheme with long tie rods

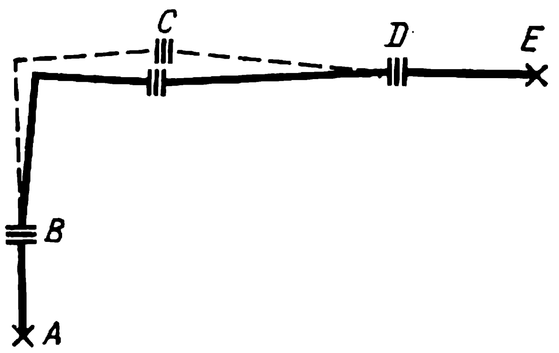

Fig. 4.18. Three-hinge scheme for thermal elongation compensation

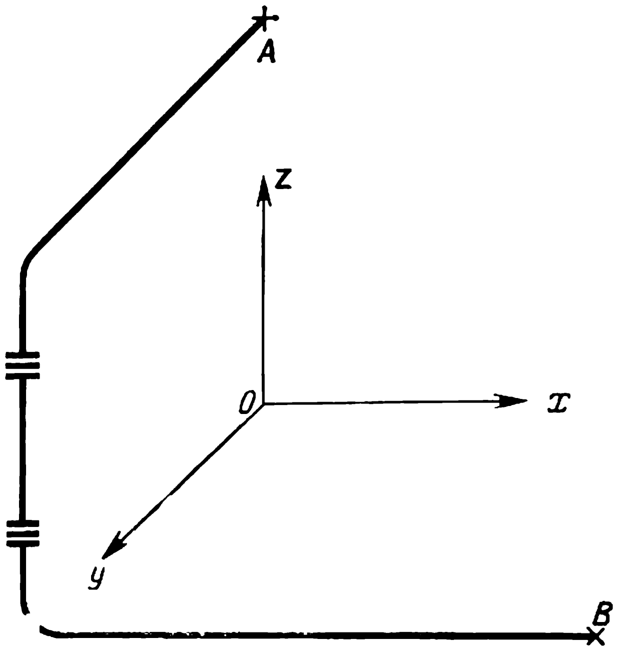

Fig. 4.19. Two-hinge three-dimensional pipeline (perspective geometry)

In these calculations hinged expansion joints are considered as points at which the reduced length calculated from formula (4.50) is concentrated. The angle of rotation in a hinge is easily calculated from the moment acting on the hinge:

$$\psi_h = \frac{M_h l'_h}{EI \cdot 10^{-4}} \qquad (4.51)$$

When calculating three-hinge schemes, which are used for short sections, the calculation can be simplified, as in this case the reduced length of all sections can be taken

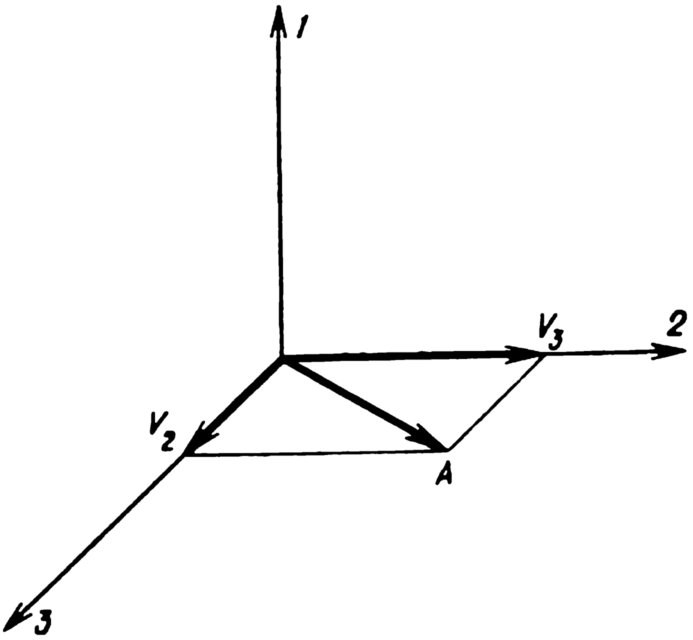

Fig. 4.20. Determination of angles of rotation and location of planes in which these angles lie

equal to zero, assuming that all deformations will be concentrated in hinges, and only the reduced length of these hinges should be taken for calculation purposes.

To increase the compensating capacity of hinged schemes the systems are pre-loaded, that is, in the hinges angles of rotation opposite in sign to the angles of rotation appearing in hot pipelines are produced in cold pipelines. If need be the systems may be cold sprung. This is achieved at the cost of bending of sections (arms). Such cold spring is desirable, in particular, to avoid gaps appearing in tightening devices of hot pipelines not under pressure.

Such pre-loadings can be easily achieved with the use of tightening devices. Hinged diagrams can be employed for three-dimensional sections of pipelines (Fig. 4.19). These sections are calculated on the same basis as two-dimensional sections, but in the calculation reduced length l'_h of elastic hinge is introduced. If the section (Fig. 4.20) containing hinged expansion joints is parallel to coordinate axis *1*, then in hinged expansion joints the angles of rotation appear in planes perpendicular to axes *2* and *3*. Since for small angles of rotation the tangents of angles are equal to the angles, the actual angle of rotation and the direction of the plane in which it appears are determined only by adding the vectors of angles. For this purpose, in plane *1* (perpendicular to axis *1*) we represent by vector V_2 the angle of rotation ψ_2 in plane *2*, directing this vector along the axis *3* (representing interaction of plane *2* with plane *1*); we represent the angle of rotation ψ_3 by vector V_3, directing it along the axis *2*. Vector A, which is the geometric sum of vectors V_2 and V_3, gives the magnitude of the angle and the direction of the plane in which this angle lies. The plane of location of tie rods should be perpendicular to the plane of the angle of rotation.

An example of calculating two-hinge scheme is given below.

Example. The schematic diagram and the dimensions of pipeline under 2.5 atm pressure are shown in Fig. 4.21. The

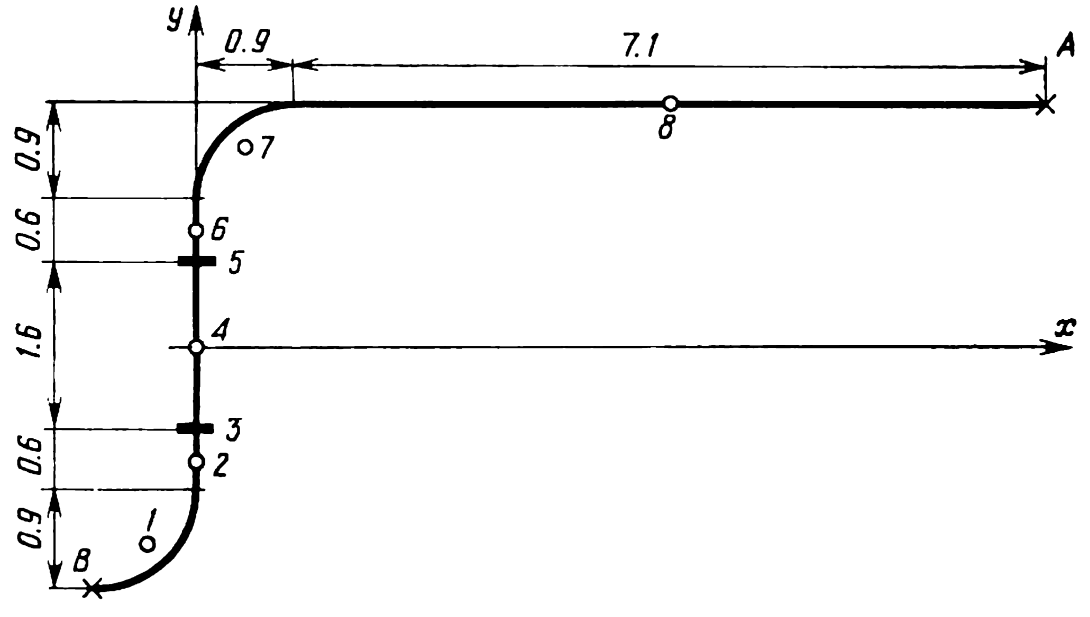

Fig. 4.21. Configuration of steamline containing two-hinge scheme for thermal elongation compensation

pipe size is 920 × 8 mm. $I = 238.5 \times 10^3$ cm^4, $W = 5185$ cm^3, thermal elongation—1.6 mm/m, $E_t = 2.02 \times 10^6$ kg/cm^2.

The characteristics of the welded elbow: $R = 900$ mm, $\lambda = 0.0346$,

$$\omega = \frac{1.5}{2.02 \times 10^6} \times 405 = 3 \times 10^{-4}, \quad K_p = 47.7, \quad \nu = 16$$

The characteristics of the bellows-type expansion joints D_n900: $D_c = 1158$ mm, $R_k^* = 6000$ kg for an elongation of 5.5 mm, allowable sag $\Delta^* = 4.5$ mm.

Reduced lengths:

of elbow $l_1' = l_7' = 1.57 \times 0.9 \times 47.7 = 67.5$ m, of corrugated expansion joint

$$l_3' = l_5' = \frac{0.8 \times 5.5 \times 238.5 \times 10^3 \times 2 \times 10^6}{6000\,(920 + 1158)\,920} = 183 \text{ m}$$

It is advantageous to take the origin of coordinates at the center of gravity of section *4* directing Y axis along the intermediate arm. For such a selection the x coordinates of portions *2*, *3*, *4*, *5*, *6* become equal to zero and the y coordinates of sections *1*, *2*, *3* will numerically be equal to the coordinates of portions *4*, *5*, *6*; this will decrease computational effort.

Displacements of end B:

$$\Delta_x = 0.16\,[8 - (-1)] = 1.44 \text{ cm}$$

$$\Delta_y = 0.16[2.3 - (-2.3)] = 0.736 \text{ cm}$$

The intrinsic moments of inertia of sections are given in Table 4.6, whereas the moments of short-length sections *2*, *4* and *6* due to their small value have not been included.

The central moments of inertia are listed in Table 4.7.

The (4.21) system of equations is used to calculate reactions. For solving this system first the coefficient

$$A = \frac{IE \cdot 10^{-6}}{J_{sx}J_{sy} - J_{sxy}^2}$$

is determined.

The reactions will be found from the following expressions

$$P_x = A\,(\Delta_x J_{sx} + \Delta_y J_{sxy}); \quad P_y = A\,(\Delta_y J_{sy} + \Delta_x J_{sxy})$$

Table 4.6

No.	Reduced length l', m	Length of projections, m		m	n	$\frac{l'l_x^2}{m}$	$\frac{l'l_y^2}{m}$	$\frac{l'l_x l_y}{n}$
		l_x	l_y					
1	67.5	0.9	0.9	0.88	0.96	62	62	—57
7	67.5	0.9	0.9	0.88	0.96	62	62	—57
8	7.1	7.1	0	1	1	356	0	0
$\sum$	—	—	—	—	—	480	124	—114
$\frac{1}{12}\sum$	—	—	—	—	—	40	10	—10

Table 4.7

Serial number of elements	Reduced length, l', m	Coordinates of C. G., m		Moments of force, m²		Moments of inertia, m³		
		x_i	y_i	S_x-$x_i l'$	S_y-$y_i l'$	J_x-$x_i S_x$	J_y-$y_i S_y$	J_{xy}-$x_i S_y$
1	67.5	—0.33	—1.97	—22.3	—133	7	262	+44
2	0.6	0	—1.1	0	—0.7	0	8	0
3	183	0	—0.8	0	—146.3	0	117	0
4	1.6	0	0	0	0	0	0	0
5	183	0	+0.8	0	+146.3	0	117	0
6	0.6	0	+1.1	0	+0.7	0	8	0
7	67.5	+0.33	+1.97	+22.3	+133	7	262	+44
8	7.1	+4.45	+2.30	+31.6	16.3	141	38	+73
J'	—	—	—	—	—	40	10	—10
$\sum$	510.9	+0.062	+0.032	31.6	16.3	195	822	151
ΔJ	—	—	—	—	—	—2	—0.5	—1
Js						193	821.5	150

In accordance with the problem requirements, we get

$$A=\frac{2.02\times 10^6\times 238.5\times 10^3\times 10^{-6}}{193\times 821.5-150^2}=3.54\ \text{kg/cm}^4$$

$$P_x=3.54\,(1.44\times 193+0.736\times 150)=1373\ \text{kg}$$

$$P_y=3.54\,(0.736\times 821.5+1.44\times 150)=2900\ \text{kg}$$

The moment at hinge *5*

$$M_5=(0.8-0.032)\,1373-(0-0.062)\,2900=1234\ \text{kg}\cdot\text{m}$$

The angle of rotation in the hinge (as per formula 4.51)

$$\psi_5=\frac{1234\times 183}{238.5\times 10^3\times 2.02\times 10^6\times 10^{-4}}=4.69\times 10^{-3}\ \text{radian}$$

The allowable angle of rotation

$$\psi_{al}=\frac{2\times 4.5}{1158+920}=4.32\times 10^{-3}\ \text{radian}$$

Since the appearing angle of rotation is more by 9% than the allowable angle of rotation, a 10% prestressed bracing will be sufficient.

The bending moment at point *A*

$$M_A=(2.3-0.032)\,1373-(8.0-0.062)\times$$
$$\times\, 2900=-19{,}910\ \text{kg}\cdot\text{m}$$

and the bending stresses

$$\sigma_b^{s\text{-}c}=\frac{19{,}910}{5185}=3.84\ \text{kg/mm}^2$$

are many time less than the allowable stresses.

The magnitudes of preliminary negative allowances in the directions x and y can be different. If we wish to decrease the reaction at the fixed end A by two times and at the same time to halve the angle of rotation in the hinge, then it is necessary to produce cold spring equal to 7 mm in the direction of x axis by shortening element *8* by this value, and in the y direction, 4 mm, by shortening each tie rod of hinged expansion joint by 2 mm.

4.9. Use of Electronic Digital Computing Machines for Calculating Self-Compensation of Pipelines

The steam-power-plant piping configurations are composed of mainly three-dimensional self-compensating sections the calculation of which, even with the use of simplified methods, requires considerable computational labour, in particular, if the calculations of vertical displacements necessary for the selection of spring hangers, and the calculation of unbalanced loads in the installed condition are performed.

The volume of self-compensation calculations of modern steam-power-plant piping is so large that for their manual computation the services of available design engineers in a design organization prove to be insufficient. This compelled to restrict only to the calculation of most important pipelines, that of main steamlines, the calculation of vertical displacements of these steamlines were performed using approximate sometimes not well founded methods. The feedwater pipelines and average and low-pressure steamlines were not calculated at all due to the shortage of desk-calculator operators.

As regards self-compensation calculation of heating systems and externally laid steamlines the situation was somewhat better, as these pipelines are composed of two-dimensional sections the calculation of which is not so complicated. Beside this, for typical *L*- and *Z*-shape configurations of pipelines and *U*-shape compensators are widely employed nomograms and charts. But all these charts and nomograms are drawn without taking into account the forces of friction acting at the sliding supports of pipelines, that does not ensure the required accuracy.

With the advent of high-speed electronic digital computers the engineers started making efforts to use the possibilities of the machines for performing complicated self-compensation calculations and for determining pipeline deformations due to concentrated and distributed external loads.

This became possible only after a number of years when computer programmes for the solution of piping-flexibility problem by use of high-speed electronic digital computing machines came into being.

The use of computers proved to be highly effective and enabled one (1) to make necessary calculations of all important configurations of pipeline which were not calculated earlier, (2) to solve displacements calculation problems and the problems associated with the selection and adjustment of spring hangers, (3) to use complicated piping configurations containing several movable and fixed points, the calculation of which without the use of computers were practically impossible, (4) to solve problems with allowance made for frictional forces at the sliding supports.

Nowadays for calculating steam-power-plant piping with the use of computers the programmes developed by the Urals branch of ВГПИ (All Union State Planning Institute) "Teploelektroproekt" [4-6] and the ЦКТИ (Central Research Planning and Design Boiler and Turbine Institute) [4-1] and [4-5] are used.

The programmes developed by the Urals branch of ТЭП (Teploelektroproekt) are based on the manual computation scheme for calculating pipelines which is described in [4-8]. These programmes are employed to calculate pipelines (1) for thermal elongations with allowance made for the displacements of the connected equipment and cold spring; (2) for external loads (uniformly distributed weight and reactions of intermediate supports); (3) for the combined action of forces and thermal elongations.

For the use of computer programmes, it is not necessary for piping designers to have any specific knowledge of computing machines. The designer simply fills in the data format sheets giving the following initial information on: pipe size and design wall thickness, pressure and temperature of the working medium pipe material (Young's modulus, coefficient of linear expansion, allowable stresses), uniformly distributed weight load, reaction of intermediate supports or characteristics of springs, as well as on pipeline route configuration, i.e. system geometry, including specification of coordinate system, dimensions and/or coordinates of all pipe items, and also the radii of bends of curved elements.

For this purpose pipeline is divided into elements. The point of conjugation of straight line and arc, the point of application of an external force or the rigidity variation point (i.e. changeover point from one diameter to another) serve as the boundary of the element.

The input data for computer calculations of the configuration shown in Fig. 4.12 are listed in Table 4.8.

Table 4.8

Nominal outside diameter D_0, mm	426
Nominal wall thickness s, mm	11
Design wall thickness s-c, mm	9.3
Design temperature t, °C	340
Young's modulus E, kg/cm^2	$1.87 \cdot 10^6$
Coefficient of linear expansion at the operating temperature, α	$13.3 \cdot 10^{-6}$
Allowable stress σ_{al}, kg/mm^2	10.9
Design internal pressure p, kg/cm^2	24
Uniformly distributed load q, kg/m	288
Displacement of the support A: Δx, m	+0.0177
Δy, m	0
Δz, m	0
Cold spring a_x, a_y, a_z, %	0

No.	Coordinates of elements end, m			R, m	Concentrated forces, kg		
	x	y	z		P_x	P_y	P_z
1	1.1	0	0	0	0	0	0
2	1.5	0.080	—0.392	0.4	0	0	0
3	1.5	1.58	—7.770	0	0	0	0
4	1.5	1.58	—8.00	0	0	—2100	0
5	1.5	1.58	—9.20	0	0	0	0
6	—0.20	1.58	—10.90	1.7	0	0	0
7	—2.90	1.58	—10.90	0	0	—2500	0
8	—5.60	1.58	—10.90	0	0	0	0
9	—7.30	3.28	—10.90	1.7	0	0	0
10	—7.30	8.68	—10.90	0	0	—3900	0
11	—7.30	12.98	—10.90	0	0	0	0
12	—8.15	14.68	—12.372	1.7	0	0	0
13	—10.30	14.68	—16.096	0	0	0	0
14	—10.30	14.68	—17.70	0	0	0	0

In case the pipeline configuration consists of a number of branches, then the main route, i.e. the section enclosed between any two fixed supports, and type I branches (branches from the main route) and type II branches (branches stemming from type I branches) and so on are marked out. Information about these branches is also included in data format sheets.

The computer programmes of the Urals Branch of Teploelektroproekt are used to calculate pipelines containing any type of branches, but the total number of fixed supports must not exceed 8 (i.e. the number of branches is restricted to 6). The total number of "pieces" in each branch should not exceed 80.

The programmes developed by the Central Scientific Research Planning and Design Boiler and Turbine Institute (ЦКТИ), which are based on matrix procedures coupled with the transformations method, are used to calculate pipelines for the following:

(1) heating temperatures with consideration for negative erection allowance;

(2) weight loads with allowance made for elastic resistance of intermediate supports and the working loads at the intermediate supports, which ensure minimum forces in pipeline in the operating condition, are calculated as well;

(3) the combined action of all loading factors;

(4) there is another possibility of calculating a pipeline subjected to nonuniform heating along pipe's cross section, and also of taking into account the ellipticity of bends.

For calculating a branched pipeline the trunk branch between any two fixed supports is marked out together with the branches stemming out of it (Fig. 4.22). The points where pipelines branch-off are known as branching points. The pipeline is divided into sections, i.e. portions of pipeline contained between two adjacent branching points or between a fixed support and a branching point; each section is divided into subsections. At the present time the programmes of ЦКТИ are used to calculate branched pipelines containing up to 10 branching points and 21 sections. The number of "pieces" in a section, in this case, should not exceed 40.

The programmes developed by ЦКТИ give a more complete analysis of the stresses in a pipeline: the calculation of stresses due to weight takes into account the flexible resistance of intermediate supports; there is a possibility to account for the sliding supports and rigid hangers in the calculation; the working loads on intermediate supports, which ensure minimum forces in the operating condition of pipeline, are calculated; the ellipticity of bends is taken into account in the calculations, and maximum equivalent stresses in bends are calculated with allowance made for the intensification of stresses.

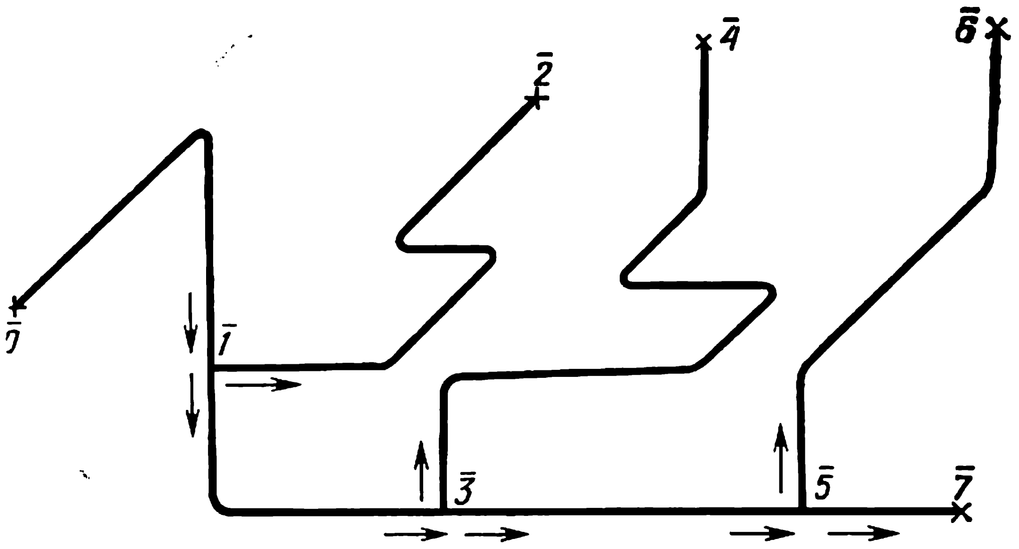

Fig. 4.22. Configuration of branched pipeline

4.10. Criterion for Calculating the Compensating Capacity of Pipelines

The self-compensation calculations of a pipeline, whether performed manually or by use of an electronic digital computer, are highly expensive because of high rates charged for each computer hour. This is mainly due to high depreciation costs of these machines. The self-compensation analysis of important pipelines is undoubtedly necessary, but such accurate calculations for evaluating the compensating capacity of preliminary routes are very costly. For this reason, attempts were made to have criteria permitting with minimum calculations to evaluate the compensating capacity of pipelines [4-8]. This problem has been studied in greater

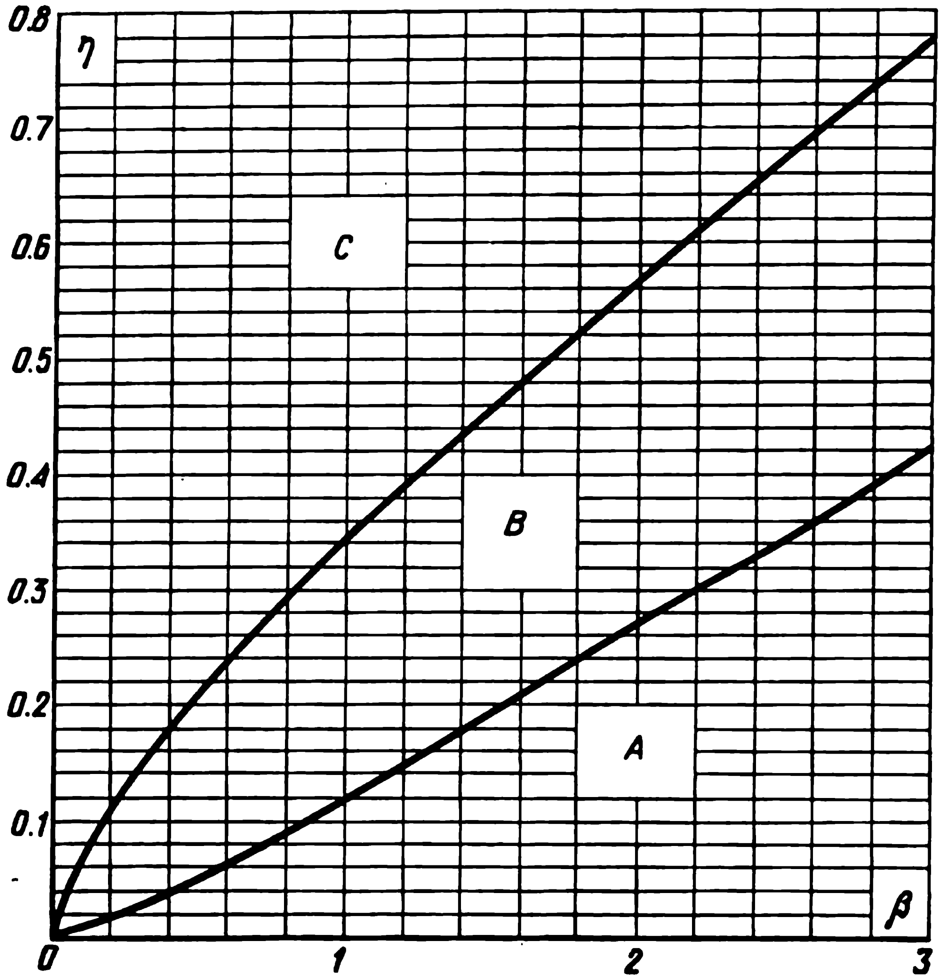

Fig. 4.23. Diagram for evaluating the compensating capacity of pipe line

detail by V. L. Blagonadezhin [4-2]. The proposed method of evaluating the compensating capacity is applicable to simple pipelines (without branching points). The knowledge of the following two parameters is necessary to evaluate the compensating capacity:

geometric parameter

$$\beta = \frac{L}{a} - 1 \tag{4.52}$$

and temperature parameter

$$\eta = \frac{ED_0 \,|\, \delta \,|\, 10^{-7}}{|\, \sigma^{s\text{-}c} \,| \cdot L} \tag{4.53}$$

where L—expanded length of pipeline section enclosed between fixed points, m; a—distance between the fixed supports, m; E—Young's modulus, kg/cm^2; D_0—outside pipe diameter, mm, $|\sigma^{s\text{-}c}|$ — allowable self-compensation stresses, kg/mm^2; $|\delta|$ — absolute thermal elongation, cm/m.

To determine the distance a it is necessary to take the origin of coordinates at the fixed support B, to determine the coordinates x_A, y_A, z_A of the fixed support A and calculate

$$a = \sqrt{x_A^2 + y_A^2 + z_A^2}$$

After calculating the parameters β and η, the area on Fig. 4.23 is determined in which the point having given parameters β and η is situated. Three cases are possible: (1) if the point lies in zone A, then the given thermal elongation δ is compensated for by the pipeline; (2) if the point lies in zone C, then the thermal elongation is not compensated for by the pipeline; (3) if the point lies in zone B the calculation should be rechecked.

The boundary lines have been drawn on the basis of analysis of eight types of plane and three-dimensional configurations of pipelines. Generally, $\beta \leqslant 1.5$ and $\eta \leqslant 0.4$. This very method may be employed to check the compensating capacity of pipeline in the installed condition at the hydrostatic test pressure.

From the graph, for the given parameter, may be determined the value of β lying on the lower boundary line and, therefore, not requiring through checking of self-compensation calculation. The value of η corresponding to this value of β is used in formula (4.53) to determine the thermal elongation δ_t, which may be taken by the pipeline. Thus, the value of the erection allowance $\frac{\delta - \delta_2}{\delta} 100[\%]$ is ascertained, for which there is no need to perform a detailed calculation. Such a method is suitable for pipelines lying in the horizontal plane, when there are no vertical displacements.

Appendices

Appendix 1.

Recommended Distance from the Axis of a Pipeline to the Wall

External pipe diameter, mm	Distance, mm					
	Without insulation	At the temperature of medium, °C				
		Up to 150	150-250	250-300	350-480	510-570
76	250	250	275	275	300	350
89	250	250	275	300	300	350
108	250	275	300	300	325	375
133	275	300	325	350	350	375
159	275	300	325	350	350	400
168	300	325	325	350	375	400
194	300	325	350	375	400	425
219	325	350	375	375	400	450
245	325	350	375	400	425	450
273	350	375	400	425	450	475
325	375	400	425	450	475	500
377	400	425	450	475	500	525
426	425	450	475	500	525	575
465	450	475	500	500	550	600
480	450	475	500	525	550	600
530	475	500	525	550	575	625
630	525	550	575	600	625	675
720	575	600	625	650	650	725
820	625	650	675	700	700	775
920	675	700	725	750	750	825
1020	725	750	775	800	—	—
1220	825	850	875	900	—	—
1420	925	950	975	1000	—	—

Note: To select the distance between the axis of a pipeline and the wall take into account the displacements of axis due to the compensation of thermal elongation and cold spring. For maximum displacement of the axis of a pipeline the distance between the insulation surface and the wall should not be less than 100 mm.

Appendix 2

Recommended Distances Between the Axis of a Pipeline and the Middle of the Gap Between the Insulation Surfaces ot Neighbouring Pipes

External pipe diameter, mm	Distance, mm					
	Pipes without insulation	At the temperature of medium, °C				
		Up to 150	150-250	250-300	350-450	510-570
76	150	175	200	200	225	250
89	150	175	200	225	225	250
108	150	200	225	225	250	275
133	175	225	250	275	275	300
159	180	225	250	275	275	300
168	180	250	250	275	300	325
194	200	250	275	300	325	350
219	225	275	300	300	350	375
245	225	275	300	325	350	375
273	250	300	325	350	375	400
325	275	325	350	375	400	425
377	300	350	375	400	425	450
426	325	375	400	425	450	500
465	350	400	425	450	475	525
480	350	400	425	450	475	525
530	375	425	450	475	500	550
630	425	475	500	525	550	625
720	475	525	550	575	600	675
820	525	575	600	625	650	725
920	575	625	650	675	700	775
1020	625	675	700	725	—	—
1220	725	775	800	825	—	—
1420	825	875	900	925	—	—

Note: The distances between the axis of pipes are equal to the sum total of distances up to the middle of the clearance. For example, the distance between the axis of pipes, size 273 mm at $t = 280$°C and size 325 mm at $t = 360$°C should be taken equal to $350+400=750$ mm. While selecting distances between the axis of neighbouring pipes the displacements of these axis of self-compensation of thermal expansion and cold spring should be taken into account. The distance between the surfaces of thermal insulation with allowances made for these displacements should not be less than 100 mm.

Appendix 3

Specific Coefficients of Hydrodynamic Resistance of Pipes

Relative passage size D_n, mm	Sizes of pipes, nominal $D_n \times s$, mm × mm	Internal, rated diameter d_p, m	Specific coefficient of resistance λ/d_p, 1/m
Seamless pipes for steam pipelines at 255 atm, 565°C Roughness $k_e = 0.2$ mm			
200	325×60	0.205	0.0951
150	245×45	0.1505	0.140
125	194×36	0.1184	0.189
100	150×30	0.0945	0.251
70	108×20	0.067	0.402
40	57×11	0.0345	0.922
20	28×5.5	0.017	2.38
Seamless pipes for steam pipelines at 140 atm, 570°C $P_n = 400$ Roughness $k_e = 0.2$ mm			
300	377×45	0.2803	0.0646
250	325×38	0.2433	0.0759
200	273×32	0.2042	0.0956
175	219×25	0.1652	0.1247
100	133×16	0.0978	0.241
50	76×10	0.055	0.502
20	28×3.5	0.021	1.790
Seamless pipes for steam pipelines at 100 atm, 540°C $P_n = 200$ Roughness $k_e = 0.2$ mm			
250	325×22	0.2778	0.0651
225	273×18	0.2343	0.0808
175	219×15	0.1868	0.1065
150	194×13	0.1661	0.1235
125	159×11	0.1354	0.160
100	133×9	0.1132	0.200
60	76×5	0.0648	0.405
20	28×2.5	0.023	1.580

(*Appendix 3. Cont.*)

Relative passage size D_n, mm	Sizes of pipes, nominal $D_n \times s$, mm × mm	Internal, rated diameter, d_p, m	Specific coefficient of resistance λ/d_p, 1/m
Seamless pipes for steam pipelines at 41 atm, 570°C $P_n = 100$		Roughness $k_e = 0.2$ mm	
500	550×25	0.4975	0.0320
450	465×19	0.4232	0.0389
400	426×18	0.3873	0.0434
350	377×17	0.3396	0.0510
250	273×11	0.2488	0.0748
150	159×7	0.1435	0.147
100	108×4.5	0.0986	0.238
50	57×3	0.0507	0.557
20	28×2.5	0.023	1.58
Seamless pipes for feed pipelines at 380 atm, 280°C		Roughness $k_e = 0.2$ mm	
300	377×45	0.2803	0.0646
250	325×40	0.2390	0.0786
200	273×32	0.2042	0.0956
150	194×22	0.1467	0.144
100	133×16	0.0978	0.241
50	57×7	0.0416	0.721
20	28×3	0.022	1.69
Seamless pipes for feed pipelines at 230 atm, 230°C $P_n = 250$		Roughness $k_e = 0.2$ mm	
300	377×28	0.317	0.0559
250	325×24	0.2735	0.0671
225	273×20	0.236	0.0833
175	219×16	0.1847	0.109
150	194×15	0.1618	0.129
100	133×10	0.1085	0.211
50	76×7.5	0.0606	0.442
20	28×3	0.022	1.69

(*Appendix 3. Cont.*)

Relative passage size D_n, mm	Sizes of pipes, nominal $D_n \times s$, mm × mm	Internal, rated diameter d_p, m	Specific coefficient of resistance λ/d_p, 1/m
Seamless pipes of pipelines $P_n = 100$			
		Roughness $k_e = 0.2$ mm	
400	426×14	0.398	0.0420
350	377×13	0.351	0.0490
300	325×13	0.299	0.0593
250	273×10	0.253	0.0730
200	219×9	0.201	0.0912
150	159×7	0.145	0.146
100	108×4	0.099	0.242
80	89×4	0.081	0.304
50	57×3.5	0.0501	0.566
32	38×3	0.032	1.01
20	38×3	0.022	1.67
Seamless pipes of pipelines at $P_n = 64$ and less			
		Roughness $k_e = 0.2$ mm	
400	426×11	0.4043	0.0412
350	377×10	0.3573	0.0479
300	325×8	0.3092	0.0572
250	273×8	0.2572	0.0718
200	219×7	0.2052	0.0950
150	159×4.5	0.1501	0.140
125	133×4	0.1251	0.176
100	108×4	0.100	0.239
80	89×3.5	0.081	0.301
70	76×3.5	0.069	0.375
50	57×3.5	0.050	0.566
40	45×2.5	0.040	0.757
30	38×2	0.036	0.936
25	32×2	0.028	1.207
20	25×2	0.021	1.773

(Appendix 3. Cont.)

Relative passage size D_n, mm	Sizes of pipes, nominal $D_n \times s$, mm × mm	Internal, rated diameter d_p, m	Specific coefficient of resistance λ/d_n, 1/m

Welded pipes of bigger diameters

$k_e = 0.3$ mm

1200	1220×11	1.198	0.0120
1200	1220×9	1.202	0.0119
1000	1020×10	1.000	0.0149
1000	1020×8	1.004	0.0149
900	920×9	0.902	0.0169
900	920×8	0.904	0.0169
800	820×9	0.802	0.0195
700	720×8	0.704	0.0229
600	630×7	0.616	0.0269
500	529×7	0.515	0.0335
450	478×7	0.464	0.0379
400	426×7	0.412	0.0441

Appendix 4

Coefficients of Local Hydrodynamic Resistance of Bends and Elbows

$\mathrm{Re} > 2\times 10^5$, $k_e = 0.2$ mm

Type of elbow	D_n	R/D_n	Coefficients of resistance for angles of bend				
			90°	60°	45°	30°	22.5°
Curved bends	—	> 3	0.2	0.15	0.12	0.09	0.07
Steep curved	—	1.5	0.25	0.2	0.16	—	—
Moulded	—	1	0.6	—	—	—	—
Welded	100	1.5	0.55	0.43	0.28	0.25	0.16
	125	1.5	0.48	0.37	0.24	0.22	0.14
	150	1.5	0.41	0.32	0.21	0.19	0.12
	200	1.5	0.35	0.27	0.18	0.16	0.10
	250—450	1.5	0.30	0.24	0.16	0.14	0.09
	500—1000	1.0	0.4	0.31	0.19	0.18	0.11

Appendix 5

Coefficients of Local Hydrodynamic Resistance of Welded T-joints

All the coefficients ξ_b and ξ_n hold true for the velocity w_c of the joint flow in the section *c-c*.

Legends: ξ_b—Coefficient of resistance of the side branch;
ξ_n —Coefficient of resistance of the straight flow passage;
$a = F_b/F_c$—ratio of areas of side flow F_b and straight (joints) F_c passages;
$q = Q_b/Q_c$—ratio of the discharge rates through branch Q_b and joint Q_c flows.

1. Merging of flows

ξ_b takes into account the resistance between sections *b* and *c*, ξ_n — takes into account the resistance between sections *n* and *c*.

$$\xi_b = A\left[1+\left(\frac{q}{a}\right)^2-2(1-q)^2\right]$$

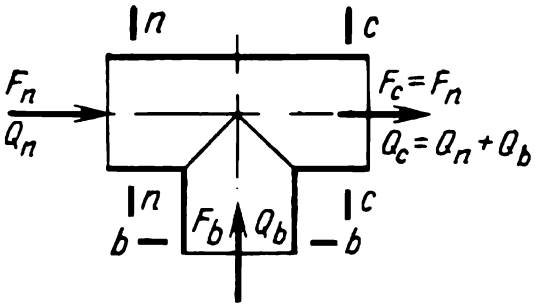

Fig. A5-1. Merging of flows

where *A* is taken from the table.

a	0-0.2	0.3-0.4	0.6	0.8	1
A	1	0.8	0.7	0.65	0.6

$$\xi_n = q\,(1.55-q)$$

(Appendix 5. Cont.)

Table for the Values of ξ

q	ξ_b for the values of a							ξ_n
	0.2	0.3	0.4	0.5	0.6	0.8	1.0	
0.2	0.7	0.1	0	—0.1	—0.1	—0.1	—0.2	0.27
0.3	2.3	0.7	0.4	0.3	0.2	0.1	0.07	0.38
0.4	4.3	1.5	1.0	0.7	0.5	0.4	0.26	0.46
0.5	6.7	2.4	1.5	1.1	0.8	0.6	0.46	0.53
0.6	9.7	3.5	2.2	1.5	1.2	0.8	0.62	0.57
0.7	13	4.7	2.9	2.0	1.5	1.0	0.78	0.59
0.8	17	5.9	3.7	2.5	1.9	1.2	0.94	0.60
0.9	—	7.3	4.6	3.1	2.2	1.5	1.08	0.59
1.0	—	8.9	5.4	3.6	2.7	1.7	1.2	0.55

2. Merging of Counter Flows

ξ_b—takes into account the resistance between sections *b* and *c*.

$$\xi_b = 1 + \frac{1}{a^2} + \frac{3}{a^2}(q^2 - q)$$

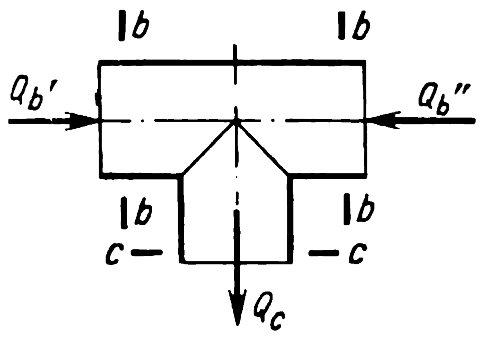

Fig. A5-2. Merging of head-on flows

Table ξ_b for $a = 1$

q	0.5	0.6	0.7	0.8	0.9	1
ξ_b	1.25	1.28	1.37	1.52	1.73	2.0

(Appendix 5. Cont.)

3. Separation of flows

ξ_b—takes into account the resistance between sections c and b.
ξ_n—takes into account the resistance between section c and n.

$$\xi_b = A'\left[1+\left(\frac{q}{a}\right)^2\right]$$

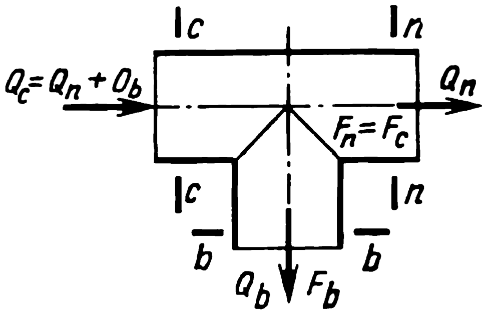

Fig. A5-3. Division of flows

where A' is taken equal to

$$\text{for} \quad \frac{q}{a} \leqslant 0.8 \quad A'=1$$

$$\frac{q}{a} > 0.8 \quad A'=0.9$$

$$\xi_n = 0.4q^2$$

Table for the Values of ξ

q	ξ_b for the values of a							ξ_n
	0.2	0.3	0.4	0.5	0.6	0.8	1.0	
0.2	1.8	1.4	1.3	1.2	1.1	1.05	1.04	0.02
0.3	2.9	1.8	1.6	1.4	1.2	1.14	1.09	0.04
0.4	4.5	2.5	1.8	1.6	1.4	1.25	1.16	0.06
0.5	6.5	3.4	2.3	1.8	1.5	1.4	1.25	0.10
0.6	9.0	4.5	2.9	2.2	1.8	1.6	1.36	0.14
0.7	—	5.8	3.7	2.7	2.1	1.6	1.49	0.20
0.8	—	7.3	4.5	3.2	2.5	1.8	1.64	0.26
0.9	—	9.0	5.5	3.8	2.9	2.0	1.62	0.32
1.0	—	—	6.5	4.5	3.4	2.3	1.8	0.40

(Appendix 5. Cont.)

4. Division into Diverging Flows

ξ_b—takes into account the resistance between sections *c* and *b*.

$$\xi_b = 1 + 0.3\left(\frac{q}{a}\right)^2$$

where ξ_b varies between 1.0 to 1.3.
For $a = 1$ and $q = 0.5$ $\xi_b = 1.075$

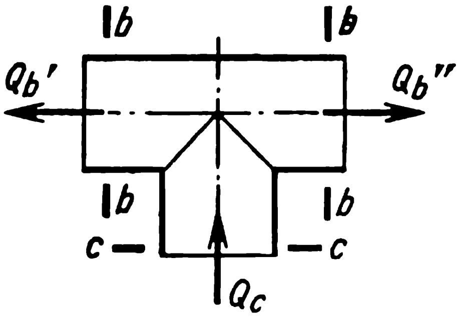

Fig. A5-4. Division of flows in opposite directions

Appendix 6

Coefficients of Hydrodynamic Resistance on Varying Passage Area

All the coefficients of resistance ξ hold true for the velocity in the section 1, which has smaller diameter *d*.

Legend: $a \left(\frac{d}{D}\right)^2$, where *d* is the smaller diameter; *D*—larger diameter of the reducer.

1. Conical Reducers.

The co-efficient ξ takes into account the friction over the length of reducer.

Table of Coefficients ξ

a	Change over to lesser diameter		Change over to larger diameter	
	$\varphi = 12°$	$\varphi = 15°$	$\varphi = 12°$	$\varphi = 15°$
0.8	0.05	0.04	0.03	0.04
0.7	0.065	0.05	0.04	0.05
0.6	0.08	0.06	0.05	0.07
0.5	0.095	0.07	0.07	0.09

(Appendix 6. Cont.)

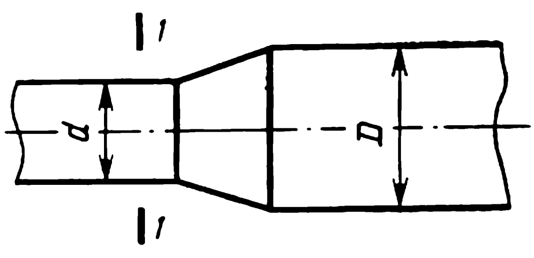

Fig. A6-1. Conical reducer

2. Sudden change in passage areas

(a) on decreasing the passage area ($Re > 10^4$) $\xi = 0.5\,(1 - a)$;

(b) on increasing the passage area ($Re > 4 \times 10^3$)

$$\xi = (1 - a)^2$$

On joining pipelines with tanks $a \approx 0$, we get:

(a) at the inlet to the pipe $\xi = 0.5$ (valid only if the pipe protrudes out of the wall to a distance not more than 0.1 times of its own diameter);

(b) at the exit from the pipe $\xi = 1$.

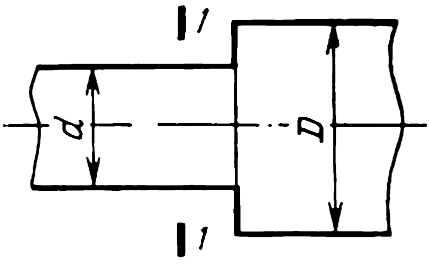

Fig. A6-2. Sudden variation in passage area

Appendix 7

Coefficients of Hydrodynamic Resistance of Orifice Plates

1. Orifice plates for incompressible fluids ($Re > 10^5$)

The coefficient of resistance ξ_0 holds true for the velocity w_0 in the orifice of the plate F_0 of diameter d_0.

Legends: F_1, F_2—Passage areas before and after the orifice plate

$$a = 1 - \frac{F_0}{F_1}; \qquad c = 1 - \frac{F_0}{F_2}$$

(Appendix 7. Cont.)

The coefficient of resistance equals to

$$\xi_0 = 0.5a + \tau\sqrt{ac} + c^2$$

When $F_1 = F_2$

$$\xi_0 = 0.5a + \tau\sqrt{a^3} + a^2$$

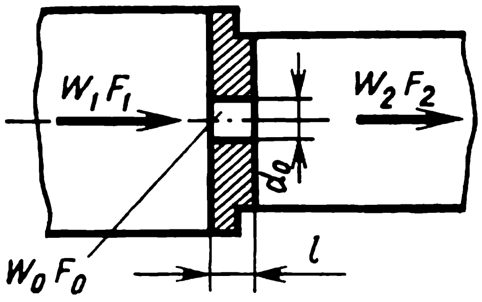

Fig. A7-1. Orifice plate

The values of τ are taken from the table:

l/d_0	0.1	0.15	0.2	0.3	0.4	0.6	0.8	1.0
τ	1.3	1.25	1.22	1.18	1.10	0.84	0.42	0.24

For successively arranged orifice plates the distance between them should not be less than 5 times the pipe diameter.

2. Orifice plates for steam ($k = 1.3$)

For selecting orifice diameter d_0 of an orifice plate the graph shown in Fig. A7.2 is used. The coefficient of resistance ξ holds true for the internal pipe diameter D and steam parameters before the orifice plate. The family of curves correspond to different ratios of pressure losses Δp_0 and the pressure p_1 before the orifice ($\Delta p_0/p_1 = 0.4$; 0.3; 0.2; 0.1 and 0). The graphs are valid for the length of straight portions not less than 10 D up to the orifice plate and 5 D beyond it.

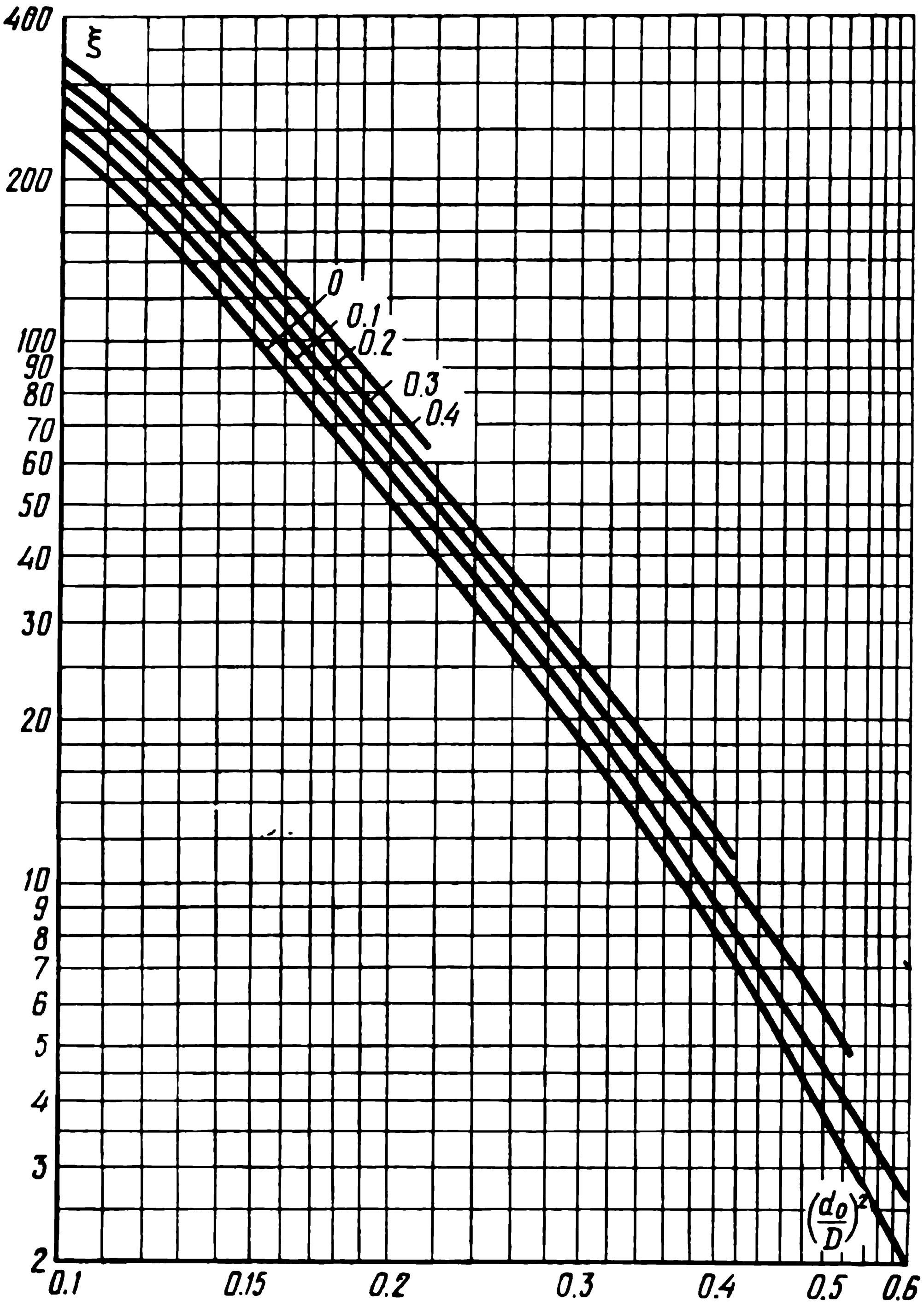

Fig. A 7-2. Graph for determining the coefficient of orifice plate hydrodynamic resistance ξ_1 related to pipe's passage area

Appendix 8

Coefficient of Hydrodynamic Resistance of Accessories and Expansion Joints.

Stop Gate Valves for Power Plants

P_n or operating parameters atm/°C	D_n	Code No.	ξ
$\frac{255}{565}$	100	B-505	0.42
	150	B-507	0.26
	200	B-509	0.38
$\frac{380}{280}$	100	B-605	0.7
	150	B-607	1.5
	200	B-609	0.95
	250	B-611	1.0
	300	B-612	2.0
400	100	B-305	0.6
	175	B-308	0.66
	225	B-310	0.4
	250	B-311	0.75
250	100	B-405	0.9
	175	B-408	1.1
	225	B-410	0.6
	250	B-411	1.4
	300	B-412	2.3
250	225	B-210	0.85
	250	B-211	2.0
100	150	B-707	0.95
	400	B-714	1.6
	450	B-715	1.05
	500	B-716	0.83
100	150	2c-9 2c-10	0.36
	200		1.2
	250		0.54
	300		1.22
64	150	2c-6 2c-7 2c-8	0.47
	200		1.63
	250		0.55
	300		1.03
	350		3.62

Accessories as per the catalogue of ЦКБА (Central Design Office for Pipe Fittings)

Name	P_n	D_n	Code number	ξ
Wedge plug	64	50	30c76	0.7
Parallel-connected gate valve	10	50-400	30ч6	0.2-0.25

(Appendix 8. Cont.)

Name	P_n	D_n	Code number	ξ
Shut-off valve flange type	64 16 16	15-40 25-50 70-200	15с27 15кч19 15ч14	4.8-7.2 4.5-5.0 5.2
Once through shut-off valve with lining	6 atm 100°C	25-200	15ч52	2-2.5
Once through shut-off valve	15.5 atm 225°C	80-100	15с58	1.35-2.5
Diaphragm type rubber-lined shut-off valve	6 atm 50°C	25-100	15ч60	1.5-2.0
Revolving reflux valve	10, 16	50-600	11ч16	0.8-9.4
Multidisc revolving reflux valve	10	800-1000	19ч18	1.8-1.9
Lifting reflux valve	10, 16	100	16ч6	6.4
Expansion joints (compensators)				
Slip joint	16	—	—	0.2
Bellows-type expansion joint	—	more than 200	—	0.2
Bellows-type expansion joint with a jacket	—	Same	—	0.1

Appendix 9

Tentative Cost of Pipelines for Power Station When Supplied with Parts

Steel grade	Parameters atm, °C	Type of pipes blank. ТУ. GOST (ТУ — Technical Specifications; GOST - All-Union State Standard)	Cost in Roubles/ton	
			Total	Ex-factory pipes supply
		Steam pipelines		
12Х1М1Ф	255/565	Forged ТУ	1780	1070
12Х1М1Ф	100/540	Rolled ТУ	1690	570

(*Appendix 9. Cont.*)

Steel grade	Parameters atm, °C	Type of pipes blank. ТУ. GOST (ТУ – Technical Specifications; GOST—All-Union State Standard)	Cost in Roubles/ton	
			Total	Ex-factory pipes supply
12Х1М1Ф	35/565	Rolled	1545	570
12Х1М1Ф	25/565	Same	1650	570
20	40/440	Same	1030	250
20	$\leqslant$16/300	GOST 8731-66	640	320
Feed water pipelines				
15ГС	$\geqslant$ 185/215	Forged ТУ	1320	750
15ГС	$\geqslant$ 185/215	Rolled, ТУ	950	370
Versatile purpose				
Various makes of steel	22 atm	—	600	220
Circulating water pipelines welded				
Steel 3	—	welded	400	165

Notes:
(1) in column No. 2 the pressure is shown in the numerator and the temperature in the denominator;
(2) in column No. 3 ТУ means Technical Specifications МРТУ-14-4-21-67;
(3) pipes of wall thickness more than 20 mm are manufactured from forged blank;
(4) this Table has been compiled from the data collected by the eastern branch of ВТИ (All Union Institute of Heat Engineering) with adjustments in ex-factory prices of pipes as per data of the Belgorod factory.

Appendix 10

Values of End Expendures for Fuel in the Major Regions of the Soviet Union, roubles/ton equivalent fuel in 1968-1973 (Teploenergetika, 1967, No. 8)

Regions and centres of fuel consumption	Natural gas	Fuel oil	Coal	Brown coal (lignite)
The Ukraine	19	18	14	13
Central Area	19.5	18.5	16	15
West	21	20	17.5	16

(Appendix 10. Cont.)

Regions and centres of fuel consumption	Natural gas	Fuel oil	Coal	Brown coal (lignite)
North-West	20	19	17	15.5
The Caucasus	18	17	15	—
The Urals	16	15	12.5	12
Western Siberia	14.5	13	8.5	4.5
Eastern Siberia	13.5	12	8	2
Volga region	17.5	16.5	14.5	14
Central Asia	13	13	10.5	9.5
Kazakhstan	16.5	14	10	7.5

Appendix 11

Physical Properties of Steel

Linear expansion α, $\frac{m}{m°\mathrm{C}}\cdot 10^6$

Young's Modulus E, kg/cm$^2\cdot 10^{-6}$

Steel grade	Symbols	Temperature, °C							
		20	100	200	300	400	500	600	700
10	α		11.6	12.6	13.0	13.6	14.2	—	—
	E	2.1	2.03	1.99	1.9	1.82	1.72	—	—
20	α	—	11.6	12.6	13.1	13.6	14.1	—	—
	E	2.1	2.03	1.99	1.9	1.82	1.72	—	—
15ГС	α	—	13.0	14.0	15.3	16.2	16.2	16.2	—
	E	2.1	2.07	2.04	1.98	—	—	—	—
15XM	α	—	11.9	12.6	13.2	13.7	14.0	14.3	—
	E	2.08	—	—	—	1.72*	—	—	—
12X1MФ	α	—	10.8	11.79	12.36	12.8	13.2	13.65	13.8
	E	2.13	2.1	2.06	2.01	1.93	1.83	1.69	—
15X1M1Ф	α	—	11.2	11.7	12.5	13.0	13.5	13.7	—
	E	2.14	2.08	2.01	1.94	1.87	1.77	1.69	1.60

(Appendix 11. Cont.)

Steel grade	Symbols	Temperature, °C							
		20	100	200	300	400	500	600	700
1X11B2MΦ	α E	— 2.13	10.7-10.8 2.08	— 2.03	12.6 1.95	— 1.86	— 1.73	13.3-14.0 1.64	— 1.51
1X18M12T 1B18H9T	α E	— 2.05	16.6 2.02	17.0 1.97	17.2 1.90	17.5 1.81	17.9 1.73	18.2 1.60	18.6 1.50

* At 450°C

Appendix 12

Linear Expansion $\sigma_t = \alpha\,(t\text{-}0)\,10^2$ cm/m and Young's modulus E, kg/cm^2 of carbon steel 10, 20, steel 2 and 3

t, °C	δ_t	$E \cdot 10^{-6}$	t, °C	δ_t	$E \cdot 10^{-6}$	t, °C	δ_t	$E \cdot 10^{-6}$
20	—	2.10						
70	0.081	2.06	200	0.252	1.99	330	0.437	1.88
80	0.093	2.05	210	0.266	1.98	340	0.452	1.87
90	0.104	2.04	220	0.280	1.97	350	0.467	1.86
100	0.116	2.03	230	0.293	1.96	360	0.482	1.85
110	0.129	2.03	240	0.307	1.95	370	0.497	1.84
120	0.141	2.02	250	0.321	1.95	380	0.513	1.84
130	0.155	2.02	260	0.335	1.94	390	0.527	1.83
140	0.168	2.01	270	0.349	1.93	400	0.544	1.82
150	0.181	2.01	280	0.364	1.92	410	0.560	1.81
160	0.195	2.01	290	0.379	1.91	420	0.575	1.80
170	0.209	2.00	300	0.393	1.90	430	0.591	1.79
180	0.223	2.00	310	0.407	1.89	440	0.607	1.78
190	0.237	1.99	320	0.422	1.88	450	0.623	1.77

Appendix 13

Total Linear Elongation and Young's Modulus of Pipelines of Standard Parameters

Linear expansion $\sigma_t = \alpha\,(t\text{-}0)\cdot 10^2$, cm/m
Totat elongation at operating parameters $(\delta_t + \delta_p)$, cm/m
Reduction in length under the conditions of total relaxation $(-\delta_t + \delta_p)$, cm/m

Steel grade	Parameters		δ_t, cm/m	$(\delta_t + \delta_p)$, cm/m	$(-\delta_t + \delta_p)$, cm/m	$E\cdot 10^{-6}$, kg/cm^2
	°C	atm				
20	20	—	—	—	—	2.10
	145	76	0.175	0.185	0.162	2.01
	215	185	0.230	0.240	0.219	1.98
	230	230	0.293	0.304	0.280	1.96
	440	40	0.607	0.613	0.601	1.78
15ГС	20	—	—	—	—	2.10
	215	185	0.305	0.315	0.293	2.04
	230	230	0.331	0.343	0.316	2.03
	280	380	0.421	0.431	0.409	2.00
12Х1МФ	20	—	—	—	—	2.13
	540	100	0.722	0.730	0.714	1.78
	565	255	0.762	0.765	0.759	1.74
	570	140	0.770	0.774	0.765	1.73
15Х1М1Ф	20	—	—	—	—	2.14
	565	255	0.770	0.773	0.767	1.72
	570	140	0.776	0.780	0.771	1.71
1Х11В2МФ	20	—	—	—	—	2.12
	565	255	0.770	—	—	1.67
	570	140	0.775	—	—	1.67

Appendix 14

Nominal Allowable Stresses in Pipelines at the Rated Temperature up to 300°C, kg/mm^2

Temperature, °C	Steel grade							
	Steel 2	Steel 3	10	20	25	16ГС (3Н) 09Г2С	10Г2С1 (МК)	15ГС
20	13.0	14.0	13.0	14.7	16.5	17.0	17.7	18.5
100	12.25	13.3	12.35	14.15	15.85	16.1	17.2	17.8
110	12.15	13.2	12.3	14.1	15.8	16.0	17.15	17.7
120	12.05	13.1	12.2	14.05	15.7	15.9	17.1	17.6
130	12.0	13.0	12.1	14.0	15.6	15.8	17.05	17.5
140	11.9	12.95	12.05	13.9	15.55	15.7	17.0	17.45
150	11.8	12.85	11.95	13.85	15.45	15.55	16.95	17.35
160	11.7	12.75	11.9	13.75	15.4	15.45	16.9	17.25
170	11.6	12.7	11.8	13.7	15.3	15.35	16.85	17.15
180	11.5	12.6	11.7	13.65	15.25	15.25	16.75	17.1
190	11.45	12.5	11.65	13.55	15.15	15.15	16.70	17.0
200	11.35	12.4	11.55	13.5	15.05	15.0	16.65	16.9
210	11.25	12.35	11.5	13.45	15.0	14.9	16.6	16.8
220	11.15	12.25	11.4	13.35	14.9	14.8	16.55	16.75
230	11.05	12.15	11.35	13.3	14.85	14.7	16.5	16.65
240	10.95	12.05	11.25	13.25	14.75	14.6	16.45	16.55
250	10.9	12.0	11.2	13.2	14.7	14.5	16.4	16.5
260	10.65	11.75	10.95	12.95	14.4	14.3	16.2	16.3
270	10.4	11.50	10.7	12.7	14.1	14.1	16.05	16.15
280	10.2	11.25	10.45	12.45	13.8	13.85	15.85	15.9
290	10.0	11.0	10.2	12.15	13.5	13.6	15.55	15.6
300	9.8	10.8	10.0	11.9	13.2	13.4	15.3	15.3

Appendix 15

Allowable Range of Equivalent Stresses in Pearlitic Steels

The allowable range of stresses at temperatures up to 370°C is taken according to the number of cycles N:

N	1500	3000	4500	6000	11,000
$[\sigma^{870}$ *times*], kg/mm^2	100	78	68	62	51

At temperatures more than 370°C the allowable range of equivalent stresses is calculated from the formula

$$[\sigma_{times}] = k_t\,[\sigma^{370}_{times}]$$

in which the lowering coefficient k_t is taken from the data given in the table below:

Carbon steel 20

t, °C	380	390	400	410	420	430	440	450
k_t	0.985	0.97	0.96	0.945	0.93	0.915	0.865	0.82

Heat resistant steels 12X1MФ and 15XIM1Ф

t, °C	460	480	500	510	520	530	540	550	560	570	580
k_t	0.95	0.94	0.92	0.89	0.85	0.81	0.78	0.75	0.72	0.70	0.68

Appendix 16

Moments of Inertia and Resistance of Pipelines and Characteristics of Elbows for Pipe Assortment of Power Stations

Pipe dimension D_n×S, mm	Moment of inertia I, cm^4	Moment of resistance W, cm^3	Area of cross section F, mm^2	Characteristic of curved pipes and elbows		
				radius of bend R, mm	geometrical characteristic, λ	coefficient A
108×4	177	32.8	1 310	600	0.89	3150
108×4.5	196	36.3	1 460	600	1.01	2815
108×5	215	39.8	1 620	150	0.28	160
108×20	563	104	5 530	600	6.20	745
108×22	585	108	5 941	600	7.14	693
133×4	337	50.8	1 620	600	0.58	2540
133×5	412	62.0	2 010	190	0.23	205
133×9	677	102	3 510	600	1.4	1170
133×10	736	110.6	3 860	600	1.59	1065

(Appendix 16. Cont.)

Pipe dimension D_n×S, mm	Moment of inertia I, cm^4	Moment of resistance W, cm^3	Area of cross section F, mm^2	Characteristic of curved pipes and elbows		
				radius of bend R, mm	geometrical characteristic, λ	coefficient A
133×16	1025	154	5 880	600	2.81	700
159×4.5	652	82	2 190	650	0.49	2455
159×6	845	106	2 880	225	0.23	200
159×7	907	115	3 350	650	0.79	8445
159×11	1408	177	5 120	650	1.30	943
159×30	2664	335	12 152	650	4.69	442
194×13	3043	314	7 390	750	1.19	870
194×15	3402	351	8 440	750	1.40	763
194×36	5863	604	17 860	750	4.33	360
219×7	2623	240	4 660	1000	0.62	2450
219×8	2956	270	5 300	300	0.22	194
219×9	3279	299	5 940	1000	0.815	1930
219×15	5028	459	9 610	850	1.23	860
219×16	5290	483	10 200	850	1.32	810
219×25	7310	666	15 200	850	2.26	543
245×45	14 880	1210	28 260	1000	4.5	367
273×8	5 853	429	6 660	1370	0.62	3220
273×9	6 512	477	7 460	375	0.19	216
273×10	7 154	524	8 260	1370	0.79	2600
273×11	7 784	570	9 050	1000	0.64	1260
273×18	11 780	863	14 400	1000	1.12	793
273×20	12 800	938	15 900	1000	1.25	720
273×25	15 310	1108	19 500	1000	1.63	587
273×32	17 891	1311	24 216	1000	2.20	472
325×8	10 010	616	7 970	1370	0.44	2690
325×10	12 290	756	9 900	300	0.12	104
325×13	15 530	956	12 700	1370	0.73	1680
325×22	24 150	1486	20 931	1370	1.31	1025
325×24	26 280	1618	22 700	1370	1.45	945
325×30	30 930	1853	27 800	1370	1.89	772
325×38	35 877	2208	34 246	1370	2.53	625
325×60	46 000	2830	49 926	1370	4.68	312
377×10	19 430	1031	11 500	1500	0.454	2235
377×10	19 430	1031	11 500	350	0.10	122
377×13	24 650	1308	14 800	1500	0.59	1730
377×17	31 280	1659	19 200	1500	0.79	1340
377×28	46 800	2485	30 731	1500	1.38	839
377×45	65 700	3485	46 912	1500	2.45	550
426×7	20 310	953	9 200	600	0.095	446

(*Appendix 16. Cont.*)

Pipe dimension $D_n \times S$, mm	Moment of inertia I, cm^4	Moment of resistance W, cm^3	Area of cross section F, mm^2	Characteristic of curved pipes and elbows		
				radius of bend R, mm	geometrical characteristic, λ	coefficient A
426×10	28 290	1328	13 000	400	0.093	140
426×11	30 900	1451	14 300	1700	0.43	2300
426×14	38 490	1807	18 100	1700	0.56	1830
426×18	48 110	2259	23 100	1700	0.735	1430
465×16	56 918	2448	22 558	2400	0.76	2415
465×19	66 280	2851	26 608	2100	0.805	1895
478×7	28 900	1210	10 200	675	0.0853	503
529×7	39 700	1500	11 800	500	0.0514	250
550×25	142 312	5175	41 213	2500	0.91	1735
630×7	66 700	2117	13 700	600	0.0433	300
630×17	153 800	4880	32 800	—	—	—
630×19	170 530	5420	36 420	1000	0.235	314
630×25	217 750	6900	48 100	—	—	—
630×36	296 950	9430	67 120	1000	0.408	170
720×8	113 500	3153	17 900	700	0.0442	314
820×9	188 600	4 600	22 900	800	0.0439	410
820×22	440 000	10 720	55 200	—	—	—
820×27	529 000	12 940	67 200	1000	0.172	170
920×9	267 240	5 810	25 800	900	0.0391	360
1020×10	404 640	7 934	31 700	1000	0.0391	360
1220×11	763 600	12 520	41 800	1200	0.0361	394

Appendix 17

Graphs for Determining the Flexibility Coefficient K_p of Elbows

Dimensionless parameter $\omega = Ap/E$, where p is the pressure in the pipeline; E—Young's modulus of elbow walls. Parameters λ and A—see Appendix 16 and formulas (3.13) and (3.17)

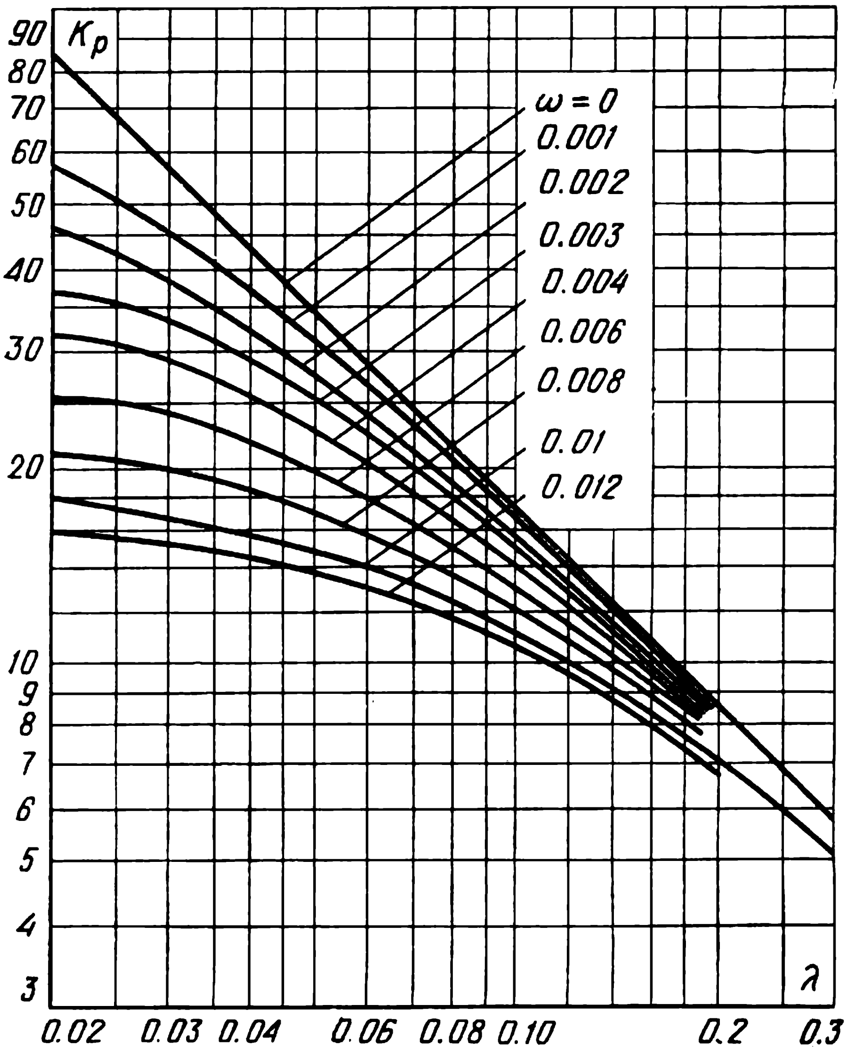

Fig. A17-1. Graph for determining coefficient K_p for $\lambda < 0.3$

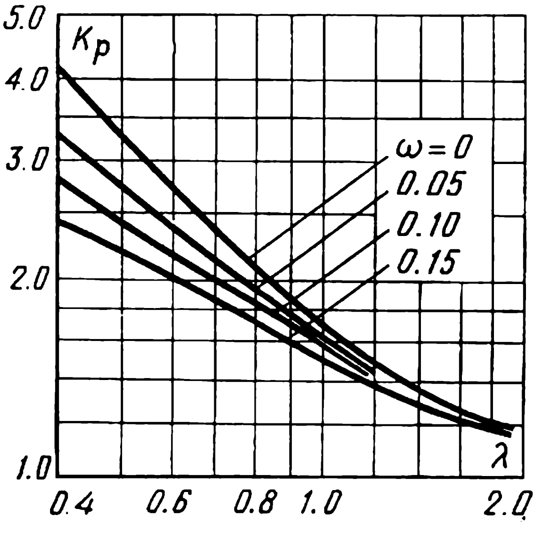

Fig. A17-2. Graph for determining coefficient K_p for $\lambda > 0.4$

Appendix 18

Graph for Determining the Coefficient K_δ Which Takes into Account the Initial Ellipticity of Elbows

Dimensionless parameter $\omega = Ap/F$ where p is the pressure in pipeline; E—Young's modulus of elbow walls. Parameters λ and A—see Appendix 16 and formulas (3.13) and (3.17).

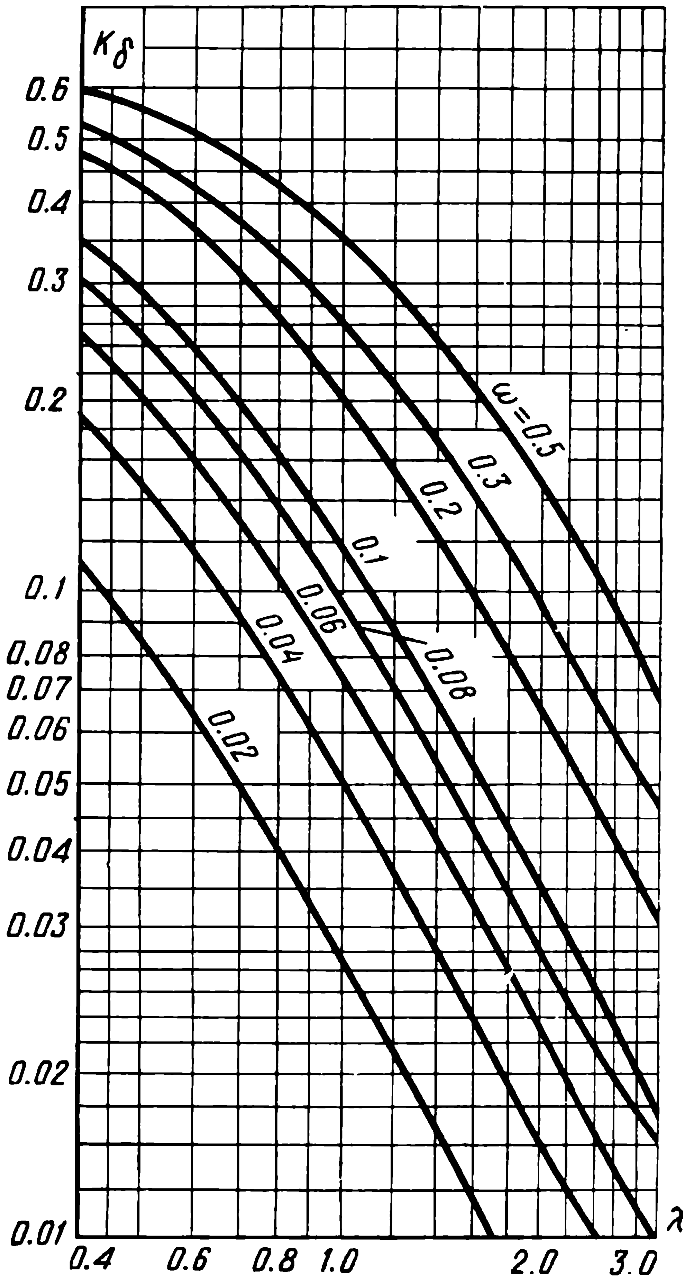

Fig. ***A18-1.*** Graph for determining coefficient K_δ

Appendix 19

Graphs for Determining the Coefficient β — intensification of Longitudinal Bending Stresses in Elbow

Dimensionless coefficient $\omega = Ap/E$ where p is the pressure in the pipeline; E—Young's modulus of elbow walls. Parameters λ and A—see Appendix 16 and formulas (3.13) and (3.17).

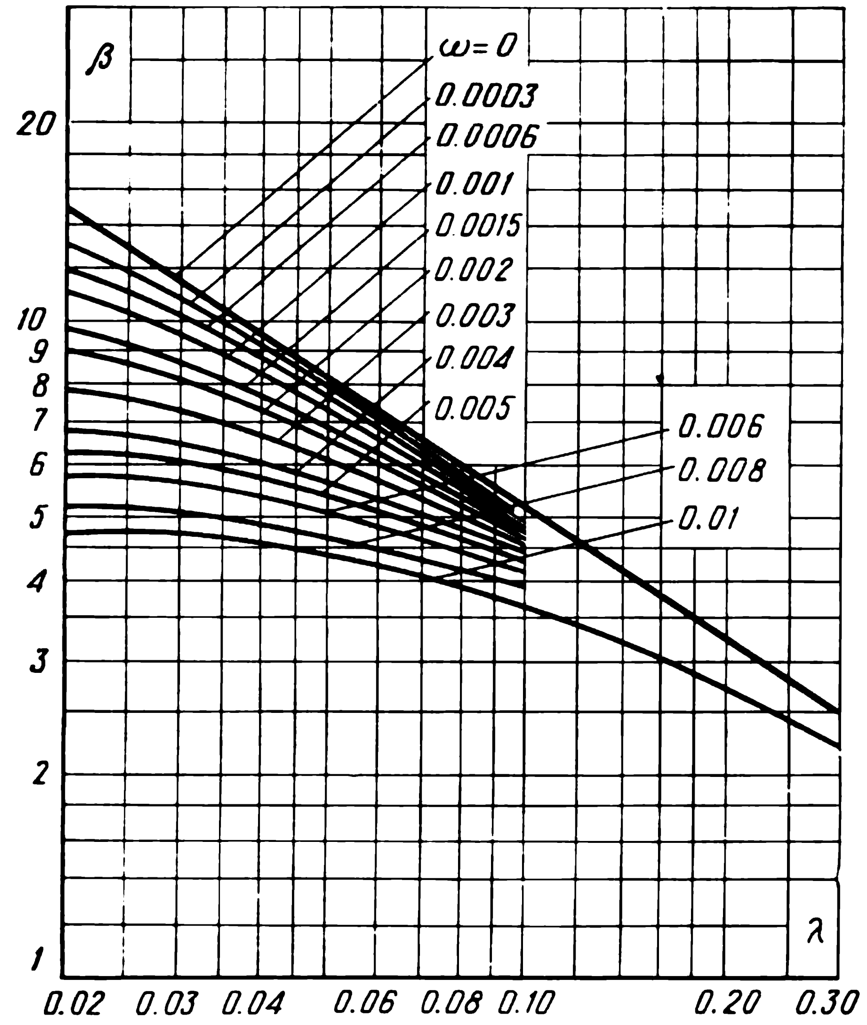

Fig. A19-1. Graph for determining coefficient β for $\lambda < 0.3$

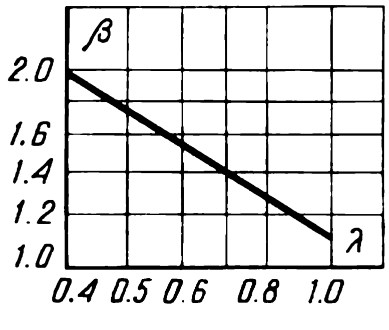

Fig. A19-2. Graph for determining coefficient β for $\lambda > 0.4$

Appendix 20

Graphs for determining the coefficient γ — intensification of cross-sectional bending stresses in elbow wall

Dimensionless parameter $\omega = Ap/E$ where p is the pressure in the pipeline; E—Young's modulus of elbow walls. Parameters λ and A—see Appendix 16 and formulas (3.13) and (3.17).

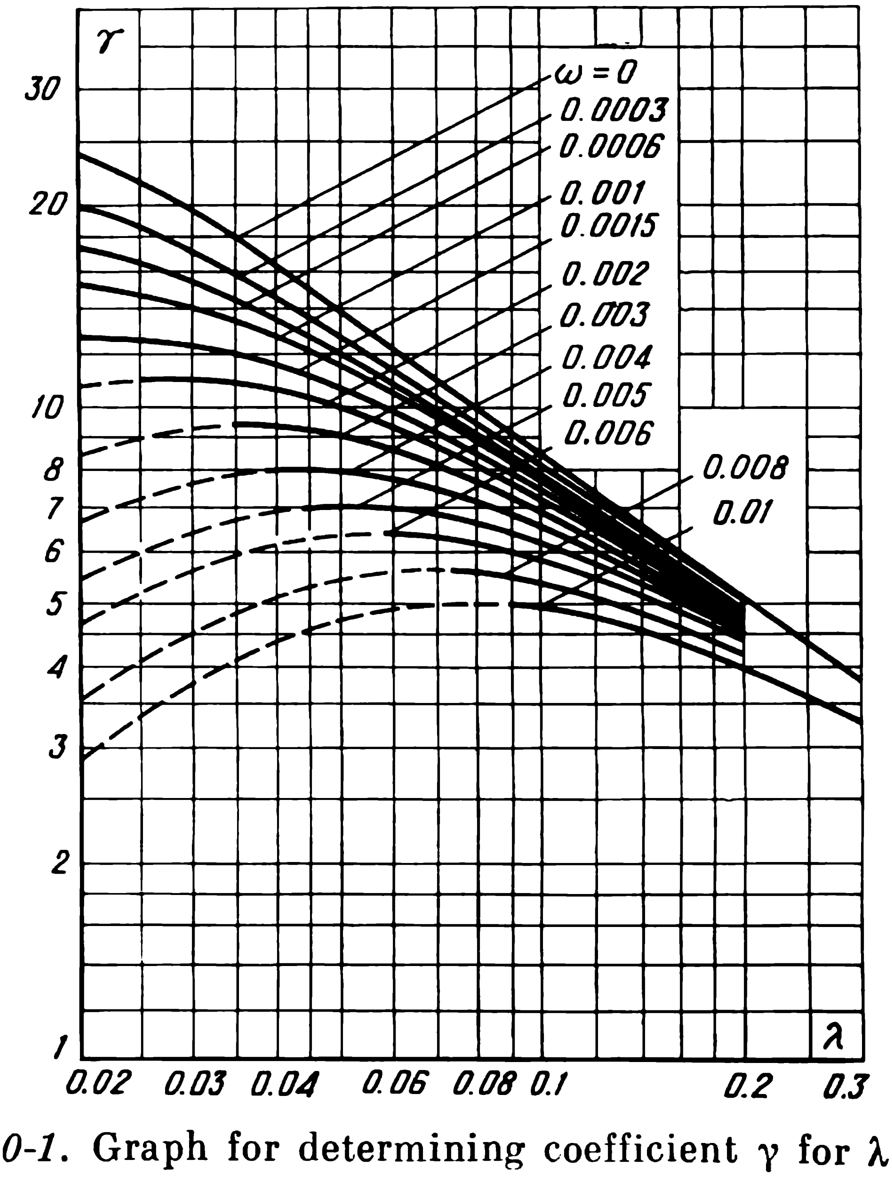

Fig. A20-1. Graph for determining coefficient γ for $\lambda < 0.3$

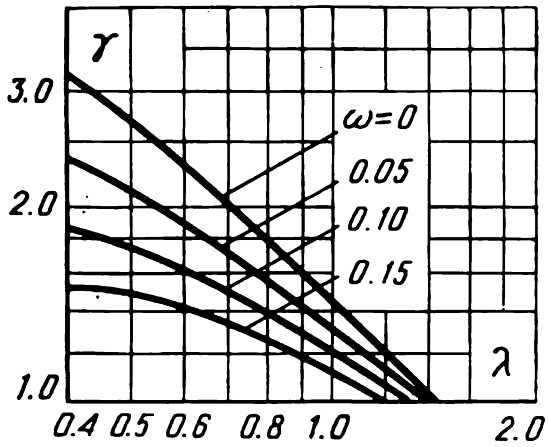

Fig. A20-2. **Graph for determining coefficient γ for $\lambda > 0.4$**

Appendix 21

Permissible Deviations from the Nominal Wall Thickness of Pipes

GOST or TY for pipes	External diameter, mm	Wall thickness, mm	Allowable deviations in wall thickness, %
Hot rolled as per GOST 8732-58	of no importance	Up to 15 incl.	+12.5 —15
	of no importance	More than 15	±12.5
Cold rolled as per GOST 8734-58	of no importance	More than 1 up to 5 incl.	±10
	of no importance	More than 5	±8
MPTY 14-4-21-67 hot rolled pipes from carbon and alloy steels (MPTY— Interrepublic Technical Specifications)	Up to 108	—	+15 —10
	More than 108	—	+20 —5
From high-alloy steel	Up to 140	—	+15 —10
	More than 140	—	+20 —5

Note: For electric welded pipes the negative allowance is determined from the deviation in plates thickness as per GOST 5681-57. Thus for a plate of 4 mm thick the allowance is 0.4 mm, for a plate of 5-5.5 mm thick—0.5 mm, for a plate of 6-7 mm thick—0.6 mm, for a plate of thickness 8-25 mm—0.8 mm.

References

1.1. Gurevich D. F. *Raschet i konstruirovanie promyshlennoi armatury* (Design of Industrial Equipment), Moscow, 1964.

1.2. Imbritskiy M. I., Nikitin A. P. *Spravochnik po truboprovodam i armature dlya elektricheskikh stantsiy* (Handbook on Pipelines and Fittings for Electric Power Stations), Gosenergoizdat, 1962.

1.3. Kostovetski D. L., Tokarskiy B. N. *O zatyazhke pruzhin uprugikh opor truboprovodov*. Trans. IsKTI, is. 67, 1966 (Tightening of Spring Resilient Supports of Pipelines).

1.4. Lovtski E. V. *Vybor promezhutochnikh opor truboprovodov i raschet zatyazhki pruzhin* (Selection of Intermediate Supports for Pipelines and Spring Tension Calculation), «Elektricheskiye Stantsii», 1966, No. 8.

1.5. Rudomino B. V. *O regulirovke pruzhinnykh krepleniy truboprovodov* (Adjustment of Spring Supports for Pipelines), «Electricheskiye Stantsii», 1962, No. 1.

1.6. *Pravila technicheskoy ekspluatatsii elektricheskikh stantsiy i setey* (Operation and Maintenance Rules for Electric Power Stations and Networks), Edition 12, «Energiya», 1968.

2.1. Vukalovich M. P., Novikov I. I. *Tekhnicheskaya termodinamika* (Engineering Thermodynamics), Gosenergoizdat, 1955.

2.2. Vukalovich M. P. *Tablitsy termodinamicheskikh svoistv para i vody* (Tables of Thermodynamic Properties of Steam and Water), Gozenergoizdat, 1963.

2.3. Gospitalnik G. L. *Tekhnico-ekonomicheskiye raschety v energetike* (Techno-Economical Calculations in Power Engineering), SZPI, 1961.

2.4. Dvornichenko V. V. *K voprosu o skorosti zvuka v dvukhfaznoy oblasti* (The Problem of Sound Velocity in a Two Phase Zone), «Teploenergetika», 1966, No. 10.

2.5. Deutsch M. E., Fillipov G. A., Stekolshchikov E. V. *Skorost zvuka v dvukhfasnykh sredakh* (Velocity of Sound in Two Phase Media), «Teploenergetika», 1964, No. 8.

2.6. Idelchik I. E. *Spravochnik po gidravlicheskim soprotivleniyam (koeffitsienty mestnykh soprotivlyeniy i soprotivlyenie treniya)* (Handbook on Hydraulic Coefficients) (Coefficients of Local Resistance and Force Friction), Gozenergoizdat, 1960.

2.7. Kamerstein A. G., Ruchimskiy M. N. *Raschet zavodskikh truboprovodov na prochnost* (Structural Design of Industrial Pipelines), Gostoptekhizdat, 1959.

2.8. Makarov A. N., Sherman M. Ya. *Raschet izmeritilnykh i reguliruyushchikh drosselnykh ustroistv* (Calculation of Measuring and Regulating Throttling Devices), Metallurgizdat, 1953.

2.9. Novikov I. I., *Pokazateli adiabaty nasyshchennogo i vlazhnogo para* (Adiabatic Indexes of Saturated and Wet Steam), USSR Academy of Sciences Reports, Vol. IX, No. 8, p. 1425, 1948.

2.10. Prandtl L. *Gidroaeromekhanika* (Hydro-Aero-Mechanics), Izdatelstvo Inostrannoy Literatury, 1951.

2.11. Semenov N. I., Kosterin S. I. *Resultaty issledovaniya skorosti zvuka v dvizhushchikhsya gazozhidkostnikh smesyakh* (Sound Velocity Study of Flowing Gas and Liquid Mixtures), «Teploenergetika», 1964, No. 6.

2.12. Taliyev V. N. *Raschyet mestnykh soprotivleniy troinikov* (Calculation of Local Resistances of T-joints), Gosstroiizdat, 1952.

2.13. Churakov S. V., Yurkina M. P. *O velichine gidravlicheskogo soprotivleniya linzovykh kompensatorov* (Hydraulic Resistance of Bellows Expansion Joints), «Energomashinostroyeniye», 1962, No. 8.

2.14. Benjamin and J. G. Miller. The flow of a Flashing Mixture of Water and Steam through Pipes, Trans. ASME, Vol. 64, 1942, p. 657.

3.1. *Normy rascheta elementov parovykh kotlov na prochnost* (Norms for Structural Design of Boiler Elements), TsKTI, 1965.

3.2. *Svoistva staley i splavov, primenyayemykh v kotloturbinostroyenii* (Steels and Alloys Used for Boilers and Turbine Engineering), TsKTI. *Rukovodyashchiye ukazaniya* (Guidelines), issue 16, part I and II, 1966.

3.3 Belyayev N. M. *Soprotivleniye materialov* (Strength of Materials), Gostekhizdat, 1951.

3.4. Voloshin A. A. *Raschet truboprovodov na vneshniye nagruzki* (Calculation of Pipelines for External Loads), «Energomashinostroyeniye», 1958, No. 3.

3.5. Zalkind E. M. *Opredeleniye reaktsiy pri rabote predokhranitelnykh klapanov* (Determination of Reactions for Safety Valves), «Elektricheskiye Stantsii», 1966, No. 4.

3.6. Zverkov B. V. *Predelnaya nagruzka truby pod deistviyem davleniya i izgiba* (Limiting Load on a Pipe under Pressure), «Energomashinostroyeniye», 1958, No. 3.

3.7. Kamerstein A. G., Ruchimskiy M. N. *Raschet zavodskikh truboprovodov na prochnost* (Structural Design of Industrial Pipelines), Gostoptekhizdat, 1959.

3.8. Kamerstein A. G. *Usloviye raboty stalnykh truboprovodov i rezervy ikh nesushchei sposobnosti* (Steel Pipelines Operating Conditions and Reserves of their Capacity), Gosstroiizdat, 1966.

3.9. Kostovetskiy D. L. *Ob izgibe krivoy tonkostennoy truby, sechenie kotoroy imeet formu, blizkuyu k krugovoy, pri nalichii vnutrennego i naruzhnogo davleniya* (Flexure of a Curved Thinwalled Pipe Whose Cross Section, under Internal and External Pressure, Is Almost Circular in Shape), USSR Academy of Sciences News. *Mekhanika i machinostroyeniye* (Mechanics and Engineering), OTN, 1959, No. 6.

3.10. Kostovetskiy D. L. *Raschet napryazheniy i peremeshcheniy v krivolineynom otrezke truby* (Calculation of Stresses and Displacements in the Curvilinear Portion of a Pipe), Trans. TsKTI, issue 67, 1966.

3.11. Kostovetskiy D. L. *Raschet truboprovodov na kompensatsiyu temperaturnikh rasshireniy s uchetom elliptichnosti krivolineinogo uchastka* (Calculation of Pipelines for Compensation of Thermal Elongations with Allowances Made for Ellipticity of Curved Portion), «Elektricheskiye stantsii», 1963, No. 3.

3.12. Kuznetsov L. A., Rudomino B. V. *Konstruirovaniye i raschet truboprovodov teplosilovykh ustanovok* (Design of Pipelines for Thermal Power Stations), Mashgiz, 1949.

3.13. Ratner A. V. and Aristov M. I. *O raschete paroprovodov sverkhvysokogo davleniya na prochnost* (Structural Design of Pipelines at Super High Pressure,) «Teploenergetika», 1960, No. 9.

3.14. Rudomino B. V. *O raschete truboprovodov na vneshniye nagruzki* (Calculation of Pipelines for External Loads), «Energomashinostroyeniye», 1962, No. 8.

3.15. *Raschet i konstruirovaniye sistem truboprovodov* (Calculation and Design of Pipelines. Handbook), (Translated from English), Gostoptekhizdat, 1961.

3.16. ASME, Boiler and Pressure Vessel Code, 1965, Section III, Nuclear Vessel.

3.17. Karman T. Über die Formänderung dünnwandiger Röhre ins besondere federndere Ausgleichrohre, VDI-Z, Bd 55, N-45

4.1. *Raschet truboprovodov na prochnost i zhestkost na ETsVM «Ural-2» po programme TsKTI* (Strength and Rigidity Calculation of Pipelines by Computer «Ural 2» as per the Programme of TsKTI) *Rukovodyashchie ukazaniya* (Guidelines), issue 10, TsKTI, 1965.

4.2. Blagonadezhin V. L. *Kriteriy dlya otsenki kompensiruyushchey sposobnosti stantsionnykh truboprovodov* (Criterium for Designability Evaluation of Station Pipelines), «Teploenergetika», 1965, No. 3.

4.3. Gurevich A. I. *Raschet truboprovodov na prochnost s uchetom vesovykh nagruzok* (Structural Design of Pipelines and Loads), «Elektricheskiye Stantsii», 1963, No. 1.

4.4. Kamerstein A. G. and Ruchimskiy M. N. *Raschet zavodskikh truboprovodov na prochnost* (Structural Design of Industrial Pipelines), Gostoptekhizdat, 1959.

4.5. Kostovetskiy D. L. and Tyntaryev E. M. *Sovershenstvovaniye proektirovaniya truboprovodov energoblokov na baze ispolzovaniya ETsVM* (Power Units Pipeline Design Using Computers), «Energeticheskoye stroitelstvo», 1967, No. 12.

4.6. Lovtskiy E. V., Skorodumova I. M. *Raschet razvetlennykh truboprovodov ne elektronnoi vychislityelnoy machine* (Multibranch Pipeline Design Using Computers), «Elektricheskiye stantsii», 1966, No. 10.

4.7. Rudomino B. V. *O regulirovke pruzhinnykh krepleniy truboprovodov* (Spring Supports Adjustments in Pipelines), «Elektricheskiye stantsii», 1962, No. 1.

4.8. *Raschet i proektirovanie sistem truboprovodov* (Calculation and Design of Pipelines. Handbook), (Translated from English), Gostoptekhizdat, 1961.

Subject Index

Anchors, rigid, 15
Austenitic steels, 127
Auxiliary high-pressure pipeline, 12

Box-header boilers, 9
Buckling, 219

Capacity, replaceable, 109
Coefficient of discharge, 48
Coefficient of hydraulic resistance, 40
Coefficient of local resistances, 56
Compensator, bellous-type, 215
Cold spring, 19
Computers, calculation of self-compensation with, 230
Condensate, drainege of, 20
Creep, 123
Creep curves. 123

Deaerator, 13
Deaerator tank, 17
Deformation, creep, 119
  elastic, 118
  plastic, 117, 143
  residual, 121
Degree of dryness, 89
Diaphragm, 18
Drainage of pipelines, 20

Elbows, curved, 57
  forged, 169
  steep curved, 57
  welded, 57, 169
Economizer, 13

Guides, 34

Hangers, spring, 24, 31
Hinge, plasticity, 119

Joints, bellous expansion, 25
  flange, 9
  sliding, 177
  slip, 25, 174
  U-shaped expansion, 25

Lines, circulating water, 12
  condensate, 11
  feed water, 11.
  fresh steam, 11
  live steam, 17
  main condensate, 12
  main steam, 9, 11
  reheat steam, 11, 17

Metal creep, 16
Moment of inertia, central, 191
  equitorial, 186
  polar, 186

Number, Reynolds, 52

Orifice plate, 59

Piping design, 8
  high-pressure, 11
  layout, 8
  low-pressure, 12

Platform, service, 14
Poisson ratio, 182
Proportionality limit, 123, 141

Rapids, 21
Risers, 21

Sag, 222
Sag, design, 223
Sign rule, 205
Stress, allowable, 122
  bending, 119, 143
  circumferential, 156
  circular, 151
  cylindrical, 121
  design, 118
  equivalent, 145
  local, 117
  longitudinal, 151
  resilient, 121
  rupture, 123
  self-compensation, 121
  shear, 120
  tensile, 120
  thermal, 143
Supports, anchor, 25
  fixed, 19
  guiding, 34
  pipeline, 24
  rigid, 25, 27
  roller, 27, 31
  sliding, 27, 30, 230
  spring, 24, 25
  swing, 27, 30
  variable, 25
System, ash-sluicing, 12
  cooling water, 12

Valve, gate, 35
  plug, 35
  regulating, 35
  safety, 35
  shut-off, 36
  restricting, 37

Yield point, 124

TO THE READER

Mir Publishers welcome your comments on the content, translation, and design of the book.

We would also be pleased to receive any suggestions you care to make about our future publications.

Our address is:
USSR, 129820, Moscow, I-110, GSP,
Pervy Rizhsky Pereulok, 2, Mir Publishers

Printed in the Union of Soviet Socialist Republics

ALSO FROM MIR PUBLISHERS

Nuclear Power Stations

by Prof. T. Margulova, D. Sc. (Tech.)
432 pp. 14 × 21.5

This textbook is based on lectures presented by the author for students specializing in nuclear engineering.
The book explains the theory of thermal electric power stations as applied to power plants using nuclear fuel. It covers the problems general for any thermal electric power station (conventional and nuclear) and specific, which are true for nuclear power plants only. The textbook was awarded a State prize for 1971.
Primarily the textbook is for university students and postgraduates and also for engineers specializing in design start-up and operation of nuclear power stations. It will also be of interest to every electrical or mechanical engineer whose work is associated with nuclear power plants.